Vectorisation des analogues de nucléosides pour le traitement des métastases

Roudayna Diab

N° Ordre 252- 2009 Année 2009

THESE

Présentée devant

L'UNIVERSITE CLAUDE BERNARD – LYON 1

pour l'obtention du

DIPLOME DE DOCTORAT

(Arrêté du 7 août 2006)

Présentée et soutenue publiquement le 02 décembre 2009

par

Roudayna DIAB

VECTORISATION DES ANALOGUES DE NUCLEOSIDES POUR LE TRAITEMENT DES METASTASES

Directeur de thèse : Pr. Hatem FESSI

JURY : M. FESSI Hatem, Directeur de thèse
M. OLIVIER Jean-Christophe, Rapporteur
M. KLEIN Jean-Paul, Examinateur
M. SKIBA Mohamed, Rapporteur
M. CHEVALIER Yves, Examinateur
M. MAINCENT Philipe, Examinateur

UNIVERSITE CLAUDE BERNARD - LYON 1

Président de l'Université	**M. le Professeur L. Collet**
Vice-président du Conseil Scientifique	M. le Professeur J-F. Mornex
Vice-président du Conseil d'Administration	M. le Professeur G. Annat
Vice-président du Conseil des Etudes et de la Vie Universitaire	M. le Professeur D. Simon
Secrétaire Général	M. G. Gay

COMPOSANTES SANTE

Faculté de Médecine Lyon Est – Claude Bernard	Directeur : M. le Professeur J. Etienne
Faculté de Médecine Lyon Sud – Charles Mérieux	Directeur : M. le Professeur F-N. Gilly
UFR d'Odontologie	Directeur : M. le Professeur D. Bourgeois
Institut des Sciences Pharmaceutiques et Biologiques	Directeur : M. le Professeur F. Locher
Institut des Sciences et Techniques de Réadaptation	Directeur : M. le Professeur Y. Matillon
Département de Formation et Centre de Recherche en Biologie Humaine	Directeur : M. le Professeur P. Farge

COMPOSANTES SCIENCES ET TECHNOLOGIE

Faculté des Sciences et Technologies	Directeur : M. Le Professeur F. Gieres
UFR Sciences et Techniques des Activités Physiques et Sportives	Directeur : M. C. Collignon
Observatoire de Lyon	Directeur : M. B. Guiderdoni
Institut des Sciences et des Techniques de l'Ingénieur de Lyon	Directeur : M. le Professeur J. Lieto
Institut Universitaire de Technologie A	Directeur : M. le Professeur C. Coulet
Institut Universitaire de Technologie B	Directeur : M. le Professeur R. Lamartine
Institut de Science Financière et d'Assurance	Directeur : M. le Professeur J-C. Augros
Institut Universitaire de Formation des Maîtres	Directeur : M R. Bernard

Remerciements

Monsieur Hatem FESSI

Je tiens à vous exprimer ma gratitude de m'avoir accueillie dans votre équipe et confiée un projet qui depuis me tient à cœur. Je vous suis reconnaissante de la liberté et la confiance que vous m'avez accordée et les moyens que vous m'avez assurés pour mener d'une façon autonome et idéale cette thèse.

Monsieur Yves CHEVALIER

Je vous remercie d'avoir accepté de siéger dans ce jury. Vos compétences en polymères et votre disponibilité m'ont été précieuses pour l'élaboration des copolymères.

Monsieur Jean-Christophe OLIVIER

Vous avez accepté de juger ce travail de thèse. Trouvez ici le témoignage de ma plus profonde gratitude.

Monsieur Jean-Paul KLEIN

Vous m'avez fait l'honneur de présider le jury. Soyez assuré de mon plus profond respect.

Monsieur Mohamed SKIBA

Vous avez accepté d'être rapporteur de ce travail. Trouvez ici l'expression de mes sincères remerciements.

Monsieur Philipe MAINCENT

Je vous remercie d'avoir accepté de siéger dans ce jury. Soyez assuré de mon plus profond respect.

J'adresse également mes remerciements à Monsieur Abdelhamid Elaissari, pour les corrections d'articles ainsi que pour ces conseils scientifiques.

Je tiens à exprimer ma reconnaissance à Olivier Boyron du laboratoire LCPP pour tout l'aide durant les manips de SEC et GC. Tu resteras pour toujours l'exemple d'un scientifique avec un esprit ouvert et collaboratif.

Mes vifs remerciements aux personnels du laboratoire Nadia, Olivier, Jean-Pierre et Serge pour leur disponibilité, sans oublier de remercier très chaleureusement mes collègues du laboratoire Chiraz, Emilie, Ahlem, Jaafar, Saïda, Mahboub, Misara et Nader...(liste non exhaustive) avec qui j'ai partagé la paillasse, les manips, des litres de café…

Mes hommages vont à ceux pour qui cette page est bien loin de suffire à exprimer toute ma reconnaissance. Mes parents et frères et sœurs que leur présence ne cesse d'illuminer le chemin de ma vie.

SOMMAIRE

Abréviations

AN	Analogues de Nucléosides
Ara-C	Cytarabine
AraC-SATE	Bis(*t*butyl-*S*-acyl-2-thioethyl)-cytidine monophosphate
BDP	Beclométhasone dipropionate
CLSM	Microscopie confocale à balayage laser « *Confocal Laser Scanning Microscopy* »
dCK	Déoxycytidine kinases
DCM	Dichlorométhane
DSC	Analyse thermique différentielle « *Differential Scanning Calorimetry* »
ε-CL	Epsilon-caprolactone
FPF	Fraction respirable « *Fine Particle Fraction* »
GC	Chromatographie phase gazeuse « *Gas Chromatography* »
HP-β-CD	Hydroxypropyl β-cyclodextrine
^{1}H RMN	Résonance magnétique du proton monodimensionnelle
IC 50	Concentration inhibant la croissance de 50% de la population cellulaire « *Inhibiting cell growth by 50%* »
IRTF	Spectroscopie infrarouge à transformée de Fourrier
MMAD	Diamètre aérodynamique massique médian « *mass median aerodynamic diameter* »
mPEG	Monométhoxy poly(ethylene glycol)
mPEG- PCL	Monométhoxy poly(ethylene glycol)- poly(ε-caprolactone)
MTT	Bromure de 3-(4,5-dimethylthiazol-2-yl)-2,5-diphenyl tetrazolium
PA	Principe actif
PCL	Poly(ε-caprolactone)
PLA	Poly(acide lactique)
PLGA	Poly(acide lactide) -co- (glycolique)
SEC–MALLS	Chromatographie d'exclusion stérique- diffusion de lumière multi-angle
$Sn(Oct)_2$	2-éthyle hexanoate d'étain

Introduction générale

Introduction générale

La conception de vecteurs galéniques colloïdaux a pris, au cours des dernières années, une importance considérable, car elle concerne pratiquement toutes les maladies et plus particulièrement, celles qui accablent l'Humanité (cancer, sida, maladies dégénératives, etc.). En cancérologie, les recherches actuelles s'orientent vers l'élaboration de traitements locaux, pour pallier le manque de spécificité des agents thérapeutiques actuels, ainsi que vers une détection précoce et précise des tumeurs. Ainsi, une amélioration significative de la thérapie des cancers viendra de la possibilité de véhiculer spécifiquement des drogues dans la tumeur primitive et surtout dans les métastases.

Les analogues de nucléosides, ont été parmi les premiers médicaments à être utilisés en chimiothérapie avec une activité potentielle dans le traitement d'hémopathies malignes et de certaines tumeurs solides. Le catabolisme rapide, la résistance cellulaire au traitement et le grand volume de distribution dans le corps limitent potentiellement l'efficacité thérapeutique des ces principes actifs. Le grand défi est de concentrer ces principes actifs dans le site d'action, tout en évitant leur distribution vers les tissus normaux. Un vecteur permettant un ciblage de ces molécules vers les tissus cancéreux, assurant son internalisation cellulaire et sa protection du milieu biologique serait le véhicule idéal pour aider à franchir tous ces obstacles. Néanmoins, l'encapsulation de ces molécules par les méthodes d'encapsulation traditionnelles, est pratiquement impossible, vue leur caractères hydrophiles n'ayant aucune affinité pour les polymères généralement utilisés dans ce type de procédés et leur poids moléculaire faible facilitant davantage leur fuite vers la phase aqueuse externe.

Notre objectif est de contribuer à l'amélioration de la chimiothérapie des cancers hématologiques et ses métastases en étudiant les possibilités de l'encapsulation de la cytarabine dans les systèmes vecteurs ainsi que les performances des vecteurs élaborés. Des méthodes adaptées ont été déployées pour la vectorisation de la cytarabine, dont l'encapsulation a été très peu étudiée parmi les analogues de nucléosides. Différents vecteurs moléculaires (complexe d'inclusion de cyclodextrines) et particulaires polymériques (microparticules) ou lipidiques (liposomes) ont été préparés et caractérisés.

Notre travail se divise en deux parties : une partie bibliographique et une partie expérimentale. La première partie comprend deux chapitres. Dans le premier chapitre nous présentons le concept de la vectorisation et les principaux types de vecteurs existants à l'heure actuelle. L'état d'avancement de la recherche en matière d'encapsulation des analogues de nucléosides en général est présenté dans une revue bibliographique qui constitue le second chapitre. Les travaux de thèse sont présentés dans la deuxième partie en trois chapitres. Le premier chapitre traite l'encapsulation de la cytarabine dans des microparticules à base d'un polymère biodégradable, la poly(ε-caprolactone), en utilisant comme surfactants des copolymères amphiphiles composés de blocs hydrophobes biodégradables de poly(ε-caprolactone) et de blocs hydrophiles bio-éliminables de polyéthylène glycol. Le second chapitre concerne l'encapsulation de la cytarabine dans des liposomes multilamellaires et l'évaluation de ces derniers comme un système de délivrance de la cytarabine par la voie pulmonaire pour le traitement des métastases au niveau de poumons. Le troisième chapitre est dédié à la préparation des complexes d'inclusion de cyclodextrines, où une inclusion moléculaire d'une nouvelle prodrogue la cytarabine (ayant un caractère lipophile) dans l'hydroxypropyle β-cyclodextrine a été réalisée et mise en évidence grâce aux différentes méthodes de caractérisation physico-chimiques.

Partie Bibliographique

Chapitre 1
Généralités sur les systèmes vecteurs & les procédés d'encapsulation

TABLE DES MATIERES

1. Introduction

Des centaines de nouvelles molécules intéressantes sur le plan thérapeutique sont abandonnées chaque année en raison de leurs propriétés physico-chimiques (hydrophilie, poids moléculaire, etc.) peu favorables à leur passage à travers les barrières biologiques, ou parce qu'elles manifestent des effets indésirables importants voire toxiques, ou encore parce qu'elles sont dégradées au cours leur acheminement vers leur cible thérapeutique. Dans ce contexte, l'utilisation des systèmes de délivrance susceptibles de véhiculer un médicament d'une manière sélective vers son site d'action est apparue indispensable et l'essor considérable des nanotechnologies a permis de proposer le concept de la vectorisation.

La vectorisation met en jeu des vecteurs, de type soit particulaires (nanoparticules, liposomes…), soit moléculaires (polymères conjugués, complexes d'inclusion des cyclodextrines, anticorps conjugués…), soit encore vivants (virus, bactéries, hématies), qui permettent de transporter des principes actifs (figure 1). La vectorisation inclut également l'évaluation de nouvelles formes galéniques qui, en plus d'influer sur les propriétés pharmacodynamiques, peuvent aboutir, à leur tour, à de nouvelles formes pharmaceutiques. Il s'agit donc d'un ensemble multidisciplinaire d'activités visant à mettre au point des vecteurs, de comprendre et de maîtriser les nombreux paramètres physiologiques et cellulaires permettant de piloter des molécules biologiquement actives vers leurs cibles ultimes. En effet, la faible taille des vecteurs, mais aussi la possibilité de moduler leurs caractéristiques de surface, leur permettent de franchir certaines barrières biologiques. Dès lors, il devient possible d'envisager différents niveaux de ciblage ; au niveau d'un organe (par exemple le foie), au niveau de cellules constitutives de cet organe (par exemple les cellules de Kupffer au niveau du foie) et enfin au niveau subcellulaire (lysosomes ou noyau par exemple). Ainsi, la distribution dans l'organisme ne dépend plus des propriétés de la molécule encapsulée elle-même, mais elle est soumise à celles du vecteur choisi en fonction de l'objectif envisagé.

Par ailleurs, le ciblage permet l'obtention de concentrations efficaces en thérapeutique des molécules encapsulées au niveau de leurs sites d'action et de diminuer potentiellement leur déperdition vers d'autres tissus ou cellules, ce qui va limiter leurs toxicités et améliorer leurs effets thérapeutiques à la fois.

Autre que l'adressage des molécules thérapeutiques vers leur cible, les caractéristiques particulières des systèmes vecteurs permettent d'atteindre d'autres objectifs, comme la protection des molécules encapsulées qui sont sensibles à la chaleur, l'humidité, l'oxygène ou

la lumière ou encore la protection de ces molécules contre de la dégradation enzymatique lors de leur transport dans l'organisme.

Le champ d'applications des systèmes vecteurs comprend aussi la libération différée ou prolongée dans le temps, et ceci est particulièrement vrai pour les systèmes microparticulaires, qui peuvent assurer un largage contrôlé du principe actif, à la dose voulue et selon une cinétique bien définie. La vectorisation constitue aujourd'hui un des axes majeurs de la recherche galénique dans l'industrie pharmaceutique pour la conception des nouveaux vecteurs particulaires, s'appuyant sur le développement de nouveaux matériaux (synthèse de nouveaux polymères par exemple), et sur de nouveaux concepts physico-chimiques. En général, ces vecteurs répondent à des besoins de s'affranchir de nombreux inconvénients pouvant émaner des propriétés intrinsèques des principes actifs (solubilité, poids moléculaires, interactions avec les différentes barrières biologiques, etc.) pour réaliser une plus grande maîtrise de l'index thérapeutique, de manière à réduire la toxicité des médicaments, ainsi que les effets secondaires ou simplement à améliorer leur efficacité.

En raison de la grande diversité et complexité des systèmes vecteurs, seuls les principaux types des vecteurs moléculaires (les complexes d'inclusion de cyclodextrines) et particulaires (micro- et nanoparticules et liposomes) seront présentés dans ce chapitre, ainsi que leurs méthodes de préparations et de caractérisation.

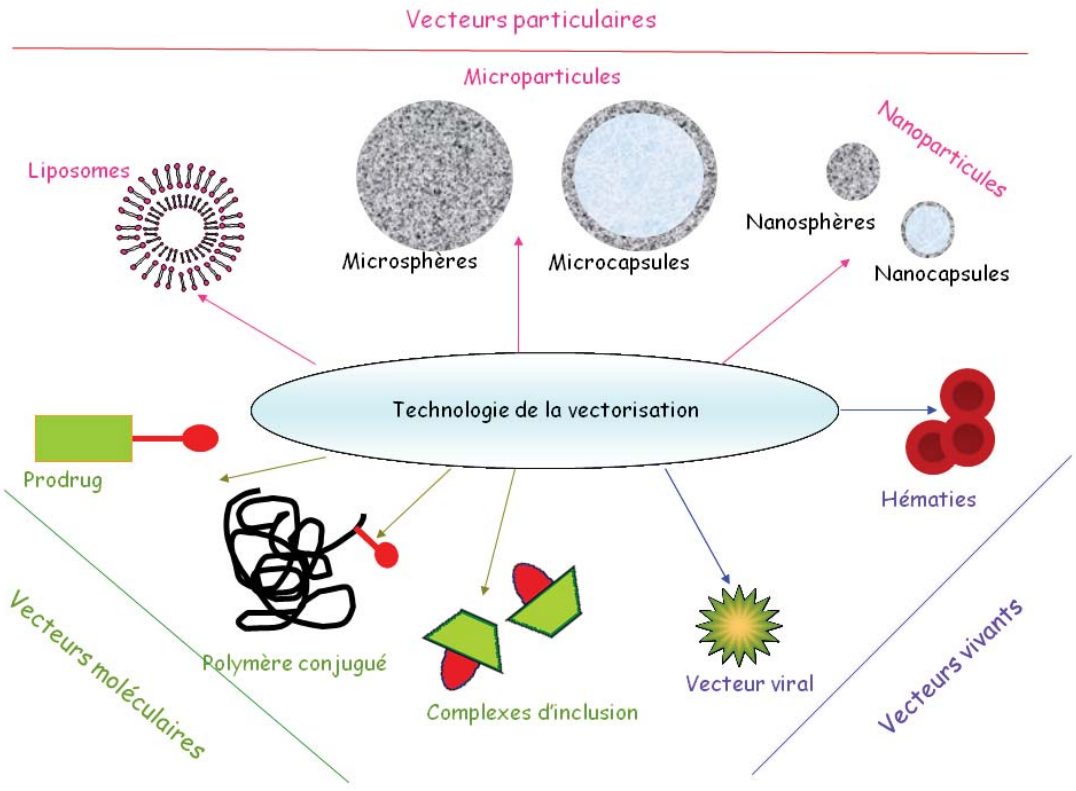

Figure 1. Schéma illustrant les différents types de vecteurs des médicaments.

2. Les cyclodextrines

Dans le domaine pharmaceutique, les cyclodextrines présentent un intérêt considérable, car l'encapsulation moléculaire des principes actifs conduit généralement à un changement de leurs propriétés physico-chimiques, telle que la solubilité, la vitesse de dissolution, la biodisponibilité, la stabilité chimique et les caractéristiques d'absorption (Mallick *et al.*, 2007), (Ansari *et al.*, 2009) , (Hirlekar *et al.*, 2009), (Sathigari *et al.*, 2009).

Les premières applications des cyclodextrines en pharmacie ont eu pour objet la protection vis-à-vis de l'oxydation de dérivés lipidiques de type prostaglandine (Uekama *et al.*, 1979). L'augmentation de solubilité associée à la protection du tractus digestif supérieur constitue une autre motivation pour l'inclusion moléculaire de certains principes actifs dans la β-cyclodextrine (Müller *et al.*, 1997). La suppression de l'amertume et l'amélioration des caractéristiques organoleptiques des médicaments est par ailleurs une autre indication de l'utilisation des cyclodextrines (Szejtli *et al.*, 2005). L'amélioration de la solubilité dans l'eau reste cependant une des principales motivations de l'utilisation des cyclodextrines en formulation.

2.1. Les cyclodextrines naturelles

Les cyclodextrines sont des oligosaccharides cycliques. Elles ont été isolées pour la première fois par Villiers en 1891 à partir de produits de dégradation de l'amidon puis caractérisées par Schardinger en 1904. Elles présentent la caractéristique originale de former des complexes d'inclusion avec de nombreuses molécules hydrophobes. Cette propriété est due à la structure particulière de ces molécules (Loftsson *et al.*, 2002).

Les cyclodextrines sont constituées par l'enchaînement de six, sept ou huit unités α-D-glucopyranosides (α-, β- et γ-cyclodextrine, respectivement) liées par des liaisons glucoside α-1,4 et cyclisées (figure 2). Les molécules de cyclodextrines sont toriques et présentent une forme tronconique dont la cavité interne est hydrophobe tandis que la surface externe est hydrophile. Cette asymétrie est due à l'arrangement particulier des groupements hydroxyles. Ainsi, les groupements hydroxyles primaires sont localisés au niveau de la section étroite du cône tandis que les hydroxyles secondaires le sont du côté large (figure 2). Les groupements hydroxyles confèrent une hydrophilie à l'extérieur de la molécule et assurent une certaine solubilité dans l'eau. La cavité centrale des cyclodextrines qui est constituée par les squelettes

carbonés et les ponts d'éther des résidus glucoside, est dotée d'un caractère hydrophobe. La présence d'un tel microenvironnement hydrophobe au sein de la molécule lui confère la capacité d'interagir avec d'autres molécules hydrophobes (Loftsson *et al.*, 1996), (Loftsson *et al.*, 2001). Ainsi, en fonction de leur taille et de leur polarité, des molécules hydrophobes ou des groupements chimiques hydrophobes pourront pénétrer dans la cavité et interagir avec la paroi interne de la cavité. Il en résulte la création d'un complexe d'inclusion. La possibilité d'inclusion dans la cavité dépend notamment de la taille de la molécule. D'une façon générale, les α-cyclodextrines présentent une cavité trop petite, tandis que les γ-cyclodextrines sont trop grandes (figure 2). La β-cyclodextrine se présente comme la plus appropriée, formant des complexes assez stables avec les molécules qui possèdent un poids moléculaire entre 200 et 800 g/mol (Loftsson *et al.*, 1996).

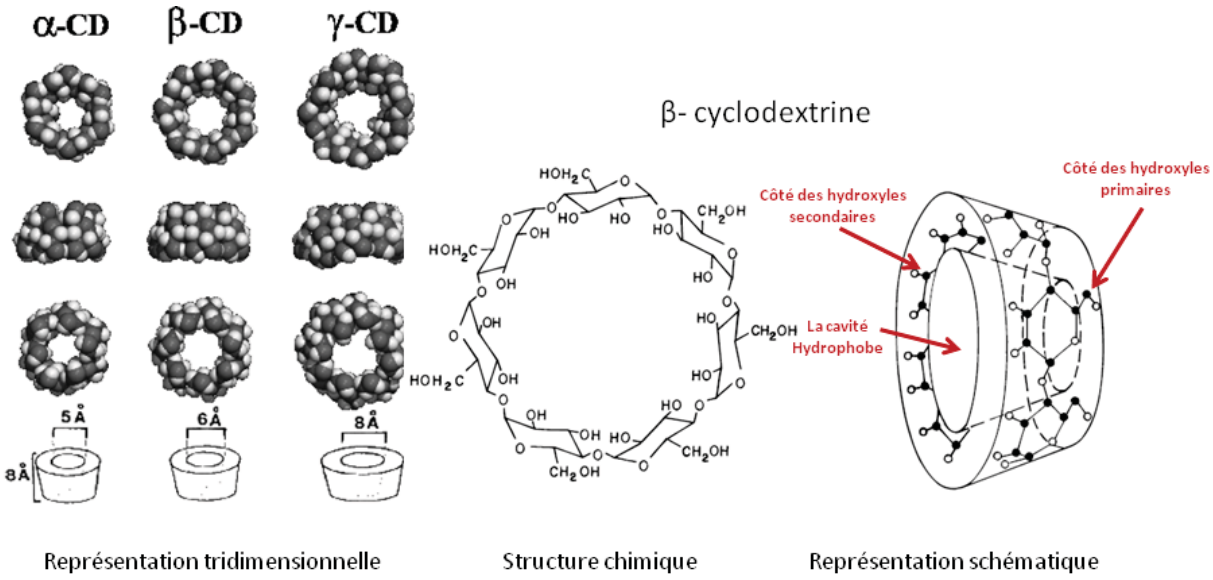

Figure 2. Une représentation tridimensionnelle des (α-, β- et γ- cyclodextrine) avec du haut en bas: une vue de la face des hydroxyles secondaires, une vue latérale et une vue de la face des hydroxyles primaires (à gauche). A droite, une représentation schématique de la forme tronconique de la β-cyclodextrine.

Les limitations des cyclodextrines naturelles ont amené au développement de dérivés synthétiques à la fois plus solubles et aussi plus sûrs sur le plan de leur toxicité.

2.2. Les cyclodextrines modifiées

Dans le but d'améliorer ou de changer certaines propriétés de cyclodextrines, et par conséquence, d'étendre leurs applications pharmaceutiques, la synthèse de nombreux dérivés de cyclodextrines a été entreprise. Le plus souvent, ces dérivés sont obtenus par substitution

d'un ou plusieurs atomes d'hydrogène des groupements hydroxyles primaires ou secondaires des unités de glucose. A l'heure actuelle, de très nombreux groupements chimiques ont été greffés sur ces molécules et notamment des groupements sulfure, alkyle, acyle, halogènes, etc. (Eastburn *et al.*, 1994). Le greffage de ces radicaux entraîne un changement de leurs propriétés physico-chimiques. Leur solubilité dans l'eau peut alors être modifiée considérablement. La recherche d'une solubilité accrue dans l'eau a ainsi été obtenue par le greffage de groupements hydroxypropyle ou sulfobutylether (Irie *et al.*, 1997). Par ailleurs, leur capacité à former des complexes avec d'autres molécules et la stabilité de ces complexes en est également affectée (Tongiani *et al.*, 2005).

2.3. Les cyclodextrines amphiphiles

Les cyclodextrines amphiphiles sont préparées par greffage de chaînes hydrocarbonées sur les groupements hydroxyles de l'α-, β- ou γ-cyclodextrines. Parmi ces dérivés amphiphiles de cyclodextrines, peut-on citer, les cyclodextrines dites « à bilboquet », les cyclodextrines dites « à bouquet » (figure 3), ou les cyclodextrines dites « à jupe ». Ces dernières, qui sont obtenues par estérification des groupements hydroxyles secondaires des cyclodextrines, sont potentiellement biodégradables par les estérases naturelles dans l'organisme (Duchêne *et al.*, 1999).

Les cyclodextrines amphiphiles possèdent des propriétés de tensioactifs et peuvent facilement donner naissance à des nanoparticules et en fonction de la technique de préparation, on peut obtenir au choix des nanosphères (Lemos-Senna *et al.*, 1998), (Lahiani-Skiba *et al.*, 2006) ou des nanocapsules.

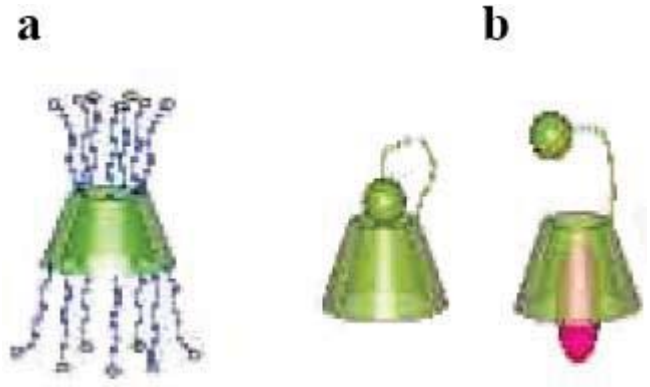

Figure 3. Représentation schématique de : a) cyclodextrines à bouquet b) cyclodextrines à bilboquet.

2 .4. Les propriétés physico-chimiques des cyclodextrines

2.4.1. Solubilité aqueuse

Grâce aux groupements hydroxyle qui sont exposés à la surface, les cyclodextrines naturelles varient de assez solubles à facilement solubles dans l'eau. En effet, la solubilité aqueuse des cyclodextrines naturelles est beaucoup plus faible que celle des saccharides acycliques comparables. Ceci est dû aux liaisons hydrogène intermoléculaires relativement fortes à l'état cristallin. Ainsi, la substitution d'un hydrogène de n'importe quel hydroxyle même par un groupement méthoxy entraîne une augmentation importante de leur solubilité aqueuse (Duchêne *et al.*, 1990). En conséquence, les dérivés de cyclodextrines naturelles possèdent des intérêts pharmaceutiques potentiels, comme par exemple, les dérivés hydroxypropyle de β- et γ- cyclodextrine, le dérivé méthylé de β-cyclodextrine, le sulfobutylether β-cyclodextrine et le glucosyl- β-cyclodextrine (Easton *et al.*, 1999).

2.4.2. Biodégradabilité et faible toxicité

Les cyclodextrines naturelles α- et β-cyclodextrine, contrairement à la γ-cyclodextrine, ne peuvent pas être hydrolysées par les amylases salivaires et pancréatiques humaines. En revanche, chacun de α- et β-cyclodextrine peut être fermentée par la microflore intestinale (Duchêne *et al.*, 1990). D'autre part, elles sont à la fois hydrophiles et possèdent un grand nombre de donneurs et accepteurs de protons et donc elles ne sont pas absorbés par le système gastro-intestinal à leur forme intacte. En conséquence, les cyclodextrines hydrophiles sont considérées non toxiques à des doses orales faibles voire modérées. Par contre, les dérivés lipophiles des cyclodextrines comme les dérivés méthylés, sont absorbés par le tractus gastro-intestinal vers la circulation sanguine et ont présenté des effets toxiques après une administration parentérale (Stella *et al.*, 2008).

2.4.3. Le phénomène d'inclusion

Dans les milieux aqueux, les cyclodextrines sont capables de former des complexes d'inclusion avec différentes molécules, en incluant la molécule entière ou plus souvent une partie de la molécule dans leur cavité centrale. En solution, la cavité hydrophobe de la cyclodextrine, constituée par la squelette carbonique et les ponts éthers des molécules de glucose, est occupée par des molécules d'eau ne pouvant pas former des liaisons hydrogène

avec elle. Il en résulte que le système est énergétiquement riche. En présence d'une molécule hydrophobe, les molécules d'eau vont être libérées de la cavité centrale pour céder la place à la molécule hydrophobe (figure 4), où il va y avoir des interactions hydrophobes et de type Van-Der-Waals (Connors, 1997). Aucune liaison covalente n'est formée ou rompue durant la formation du complexe et les molécules complexées sont en équilibre rapide avec les molécules libres dans la solution (Higuchi *et al.*, 1965).

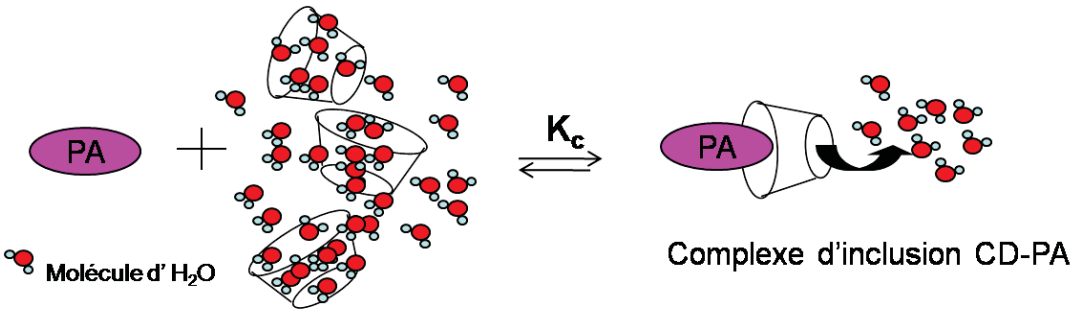

Figure 4. Le modèle conventionnel de la formation du complexe d'inclusion.

2.5. Les méthodes de préparation de complexes d'inclusion

Différentes techniques sont utilisées pour l'inclusion des molécules organiques dans les cyclodextrines. Cette inclusion peut ainsi avoir lieu en milieu solide, liquide ou biphasique. Les méthodes les plus utilisées sont les suivantes (Hedges, 1998), (Martin Del Valle, 2004) :

2.5.1. La co-précipitation

Cette méthode consiste à dissoudre la cyclodextrine dans l'eau. Le principe actif est ensuite ajouté à cette solution sous agitation et en chauffant, si nécessaire, jusqu'à sa dissolution complète. La précipitation du complexe d'inclusion est alors provoquée par refroidissement ou en ajoutant goutte à goutte un solvant organique dans lequel le complexe est peu soluble ou encore par modification du pH de la solution. Le complexe peut ensuite être isolé par décantation, centrifugation ou filtration et séché (Miller *et al.*, 2007), (Koontz *et al.*, 2009).

2.5.2. L'inclusion en milieux pâteux

C'est une technique qui ressemble à la granulation humide employée dans la compression des poudres. La cyclodextrine et le principe actif sont mélangés avec une faible

quantité d'eau (ou de solvant organique) dans un mortier ou dans un mélangeur planétaire lors de la production au niveau industriel. Le mélange est trituré et l'inclusion se fait petit à petit. Le complexe d'inclusion obtenu est ensuite lavé avec un solvant approprié pour éliminer la fraction du principe actif non incluse, puis récupéré et séché (Gan *et al.*, 2002).

2.5.3. L'inclusion par le chauffage

Dans ce cas la cyclodextrine et le principe actif sont mélangés puis introduits dans un récipient scellé. Le récipient est chauffé jusqu'à une température avoisinant les 100°C. Le complexe d'inclusion obtenu suite à ce chauffage est ensuite récupéré directement. Cette méthode nécessite un apport très important d'énergie et ne peut être utilisée qu'avec les principes actifs stables à très haute température (Cavallari *et al.*, 2002).

2.5.4. L'inclusion par extrusion

Il s'agit d'une variante continue de la méthode précédente où le mélange cyclodextrine-principe actif est passé à travers une extrudeuse tout en le chauffant. Le complexe d'inclusion est alors récupéré en continu à la sortie (Hedges, 1998).

2.5.5. Le Mélange à sec

Certaines molécules peuvent être incorporées dans les cyclodextrines par simple mélange avec cette dernière (Lin *et al.*, 1989). Il s'agit en particulier de certaines huiles et autres liquides. Le temps nécessaire pour l'inclusion est variable selon la substance en question (Lin *et al.*, 1988).

2.6. Les méthodes de caractérisation de complexes d'inclusion

Les propriétés physico-chimiques des molécules libres sont différentes de celles du complexe d'inclusion. Théoriquement, toute méthodologie employée pour observer les changements des propriétés physico-chimiques, peut être utilisée pour prouver la formation du complexe d'inclusion. Ceci comprend le changement de solubilité (Loftsson *et al.*, 2002), les changements de l'état physique de la molécule incluse (Koontz *et al.*, 2009), les changements des déplacements chimiques dans le spectre de RMN (Bernini *et al.*, 2004), les changements de la stabilité chimique (Connors, 1997) et les effets sur la perméabilité à travers

les membranes artificielles (Loftsson *et al.*, 2002). Néanmoins, les techniques les plus employées sont l'analyse thermique différentielle, la spectrophotométrie d'absorption en ultra-violet et la résonance magnétique nucléaire.

2.6.1. Analyse thermique différentielle

L'analyse thermique différentielle (DSC) est une méthode d'analyse qui mesure l'énergie consommée ou émise par un échantillon soumis à une variation bien déterminée de température. Elle permet donc de visualiser et d'étudier tous les phénomènes température-dépendants qui peuvent avoir lieu pour un composé donné : fusion, évaporation, transition vitreuse, dégradation. L'énergie échangée avec le milieu extérieur lors de ces phénomènes ainsi que la température à laquelle ils surviennent sont caractéristiques d'un système ou d'un composé donné et vont dépendre étroitement de sa structure moléculaire et en particulier des interactions intermoléculaires qui ont lieu au sein de l'échantillon. Dans le cadre particulier des cyclodextrines l'analyse thermique différentielle est une technique très utilisée pour caractériser le complexe à l'état solide (Giordano *et al.*, 2001), (Liu *et al.*, 2004).

Lors de la caractérisation du phénomène d'inclusion par DSC, le spectre DSC du complexe préparé est comparé avec les spectres de chacun de deux composés purs (le principe actif et la cyclodextrine) et également avec le spectre de leur mélange physique. Dans le cas où le principe actif se présente sous forme cristalline, on note la disparition du pic de fusion de ce dernier dans le spectre du complexe à analyser, indiquant la disparition du réseau cristallin du principe actif. L'échantillon analysé serait alors composé soit d'une dispersion du principe actif à l'état amorphe dans une matrice constituée par la cyclodextrine à l'état solide, soit d'un complexe d'inclusion, soit d'un mélange des deux (Giordano *et al.*, 1988).

2.6.2. Spectrophotométrie d'absorption en ultra-violet

Les molécules de cyclodextrines naturelles sont totalement transparentes dans l'UV. Il paraît donc possible d'étudier le complexe d'inclusion grâce au spectre d'absorption de la molécule incluse (Lu *et al.*, 1990). La spectrophotométrie d'absorption dans l'UV est très utilisée pour la détermination quantitative du principe actif total (libre et encapsulé) dans une solution mixte principe actif/cyclodextrine/complexe. Cette détermination est très utile en pharmacie étant donné que l'un des objectifs initiaux de l'inclusion dans les cyclodextrines est d'augmenter la solubilité apparente des principes actifs dans l'eau.

2.6.3. Résonance magnétique nucléaire RMN

La spectroscopie RMN consiste à soumettre les noyaux d'atomes de la molécule à un champ électromagnétique bien déterminé. Les noyaux résonneront alors à une fréquence qui dépend étroitement de leur environnement atomique, c'est à dire, les autres atomes auxquels ils sont liés. La RMN fournit des informations sur la structure de la molécule et donne une idée sur l'environnement immédiat de chaque proton ou carbone.

Pour les cyclodextrines, la RMN est une des méthodes les plus utilisées pour étudier les complexes d'inclusion et leur structure interne avec une grande précision (Ikeda *et al.*, 2004). En effet, l'inclusion de la molécule invitée dans la cavité de la cyclodextrine est systématiquement accompagnée d'une variation des pics de plusieurs protons de cyclodextrine et/ou de la molécule invitée (Ficarra *et al.*, 2000). Ainsi, la comparaison des spectres de RMN des produits purs avec le spectre du complexe d'inclusion permet de caractériser ce complexe et d'avoir une idée sur sa structure et sa conformation spatiale. D'une manière générale, nous obtenons des variations des pics des protons situés du côté interne de la cavité car c'est principalement cette partie qui est en contact avec la molécule. Dans certains cas, on peut observer des variations des pics des protons externes de la cyclodextrine. Ceci se produit quand la molécule encapsulée a une grande taille ou quand elle présente une ou plusieurs chaînes aliphatiques qui peuvent rester en dehors de la cavité et interagir avec les faces externes de la cyclodextrine (Bernini *et al.*, 2004).

3. Les vecteurs particulaires

Les vecteurs particulaires sont des systèmes d'encapsulation représentés par des particules sphériques à base de phospholipides (les liposomes) ou formées à partir des polymères biodégradables (les microparticules et les nanoparticules). Selon leur architecture interne, ils peuvent être classés en systèmes réservoirs (les capsules et les liposomes) ou matriciels (les sphères). Leur taille est comprise entre quelques nanomètres et un micron pour les nanoparticules, au-delà, on parle des microparticules.

En général, le choix du vecteur va se faire en fonction de la voie d'administration envisagée, mais aussi en fonction du profil de libération recherché.

3.1. Les liposomes

Les liposomes sont nés il y a plus de quarante ans où ils étaient conçus comme des modèles membranaires artificiels intéressants (Bangham *et al.*, 1965) et les premières recherches sur l'utilisation des liposomes pour l'encapsulation de principes actifs datent de plus de trente ans (Gregoriadis, 1977). Ils diffèrent des autres systèmes vecteurs (micro- ou nanoparticules) par leur taille, leur composition et leur architecture moléculaire.

Le terme de liposome ne s'applique qu'à l'entité comprenant une vésicule et une composition à base de phospholipides. En effet, il s'agit des vésicules constituées d'une ou plusieurs bicouches de nature phospholipidique entourant un espace interne aqueux (Torchilin, 2005) (figure 5). Les lipides utilisables sont des glycerophospholipides, naturels au synthétiques, saturés au insaturés ou des sphingolipides; des phospholipides chargés négativement ou positivement, ou encore du cholestérol (Gershkovich *et al.*, 2008). Les liposomes réalisés actuellement sont un mélange de phosphatidylcholine, de cholestérol et de différents lipides chargés comme la phosphatidylserine et le phophatidylglycerol. Un couplage avec des polymères tels que des polyéthylènes glycols (PEG) est possible et on parle alors de liposomes pégylés (Heger *et al.*, 2009).

Une variété étendue des principes actifs peuvent être incorporée dans des liposomes. Les lieux d'incorporation d'un principe actif au sein des liposomes dépendent essentiellement de ses propriétés physicochimiques : les molécules hydrosolubles seront localisés dans la phase interne aqueuse des liposomes (Hillerdal *et al.*, 2008) ; les molécules amphiphiles seront insérées dans la bicouche phospholipidique (Espuelas *et al.*, 2003), et les molécules liposolubles seront enchâssées dans la matrice hydrophobe de la paroi liposomale (Redziniak, 2003).

La morphologie des liposomes, la lamellarité en particulier, ainsi que leur répartition granulométrique dépendent des procédés de fabrication. Selon la taille et le nombre de lamelles, on distingue : les liposomes multilamellaires ou MLV (*multilamellar vesicles*), d'un diamètre > 0,5 µm ; les liposomes oligo-lamellaires, et les liposomes unilamellaires ou SUV (*small unilamellar vesicles*), d'une taille pouvant aller jusqu'a 20, voire 10 nm de diamètre. La méthode la plus simple pour préparer des MLV consiste à évaporer le solvant organique dans lequel sont dissous les lipides, puis à les remettre en suspension dans un solvant aqueux (Bangham *et al.*, 1965). Les SUV s'obtiennent le plus fréquemment en soumettant une suspension de MLV aux ultrasons (Lebed' *et al.*, 1989).

Les liposomes sont donc des vecteurs biocompatible, biodégradable et ils conviennent plusieurs voies d'administration comme la voie intravasculaire permettant de réaliser un ciblage d'organe, comme par exemple les liposomes à tropisme hépatique (Kim *et al.*, 2009). Les vecteurs liposomaux sont particulièrement intéressants pour la voie pulmonaire, pour le traitement de l'asthme (Konduri *et al.*, 2003), de la tuberculose (Vyas *et al.*, 2004) ou encore dans les métastases pulmonaires (Koshkina *et al.*, 2000). Dans la délivrance cutanée et transcutanée, les liposomes se présentent comme des véhicules de choix, non invasifs et non toxiques, pour les molécules hydrophobes et/ou hydrophiles, sans limitation de leur masse moléculaire, dans le cas d'applications dermatologiques (Banerjee, 2001) et cosmétiques (Werninghaus *et al.*, 1991). Certains types de liposomes peuvent être administrés par la voie orale comme les liposomes contenant des gangliosides type I et III et qui sont stables dans des différents milieux biologiques et peuvent survivre dans le tract gastro-intestinal (Taira *et al.*, 2004) ou encore les liposomes pégylés conçus pour l'administration des vaccins par la voie orale (Minato *et al.*, 2003).

Toutefois, en raison de la fluidité de la bicouche phospholipidique, les liposomes manifestent, une stabilité in vitro relativement faible, un taux d'encapsulation insatisfaisant avec une tendance à être perméables aux principes actifs pendant leur conservation (Clares *et al.*, 2009). Néanmoins, l'addition du cholestérol dans leur composition pourrait augmenter la rigidité de la membrane liposomale et la rendre moins perméable (Clares *et al.*, 2009). En outre, des problèmes de stabilité in vivo peuvent exister ; comme une déstabilisation dans le sang qui peut être occasionnée par l'échange des phospholipides avec les lipoprotéines sériques ce qui entraînera la libération du principe actif avant d'atteindre la cible (Constantinescu *et al.*, 2003). Par ailleurs, l'adsorption des opsonines (IgG, éléments du complément, fibronectine,..) sur leur surface hydrophobe (Wassef *et al.*, 1991), a pour conséquence de faciliter leur capture par les macrophages et leur élimination rapide de la circulation sanguine (Yan *et al.*, 2005). Cet inconvénient peut se transformer en un avantage majeur, si l'on envisage de cibler les cellules hépatiques, puisque les macrophages vont conduire les liposomes opsonisés vers le foie et plus précisément les cellules de Kupffer. Cette approche a été mise au profit pour traiter les métastases hépatiques par ciblage passif (Mayhew *et al.*, 1983).

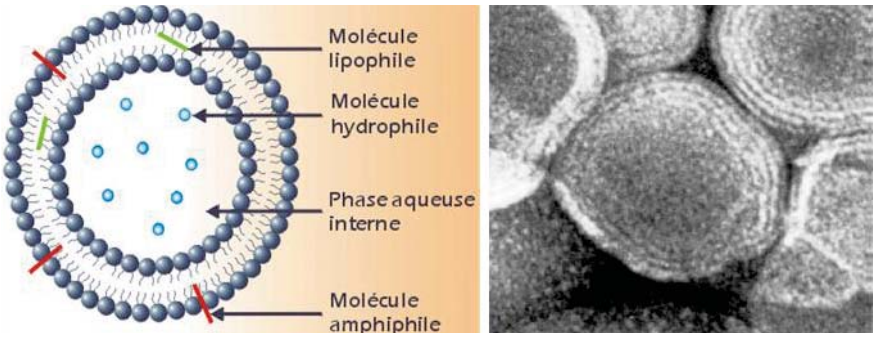

Figure 5. Représentation schématique et un micrographe des liposomes en microscopie électronique à transmission.

3.2. Les particules polymériques

Les particules polymériques ont été développées comme une alternative à l'utilisation de liposomes afin de contourner les problèmes de stabilité posés par ce type de vecteurs particulaires.

3.2.1. Les nanoparticules

Les nanoparticules sont définies comme étant des particules colloïdales ayant une taille comprise entre 10 et 1000 nm (Kreuter, 1983). Elles sont constituées de matériaux polymériques dans lesquels peuvent être dissous, piégés, encapsulés et/ou adsorbés ou encore greffés des principes actifs, des enzymes ou des antigènes. Cette définition inclut non seulement les particules présentant une structure matricielle, dénommées *nanosphères*, mais aussi les *nanocapsules*, constituées d'une fine paroi polymérique entourant une goutte d'huile où peuvent être dissous des principes actifs lipophiles (Allémann, 1993) (figure 6).

En raison de leurs propriétés physico-chimiques et leur faible taille inférieure à 1 micron, les nanoparticules peuvent être utilisées pratiquement dans toutes les voies d'administration pour des fins thérapeutiques ou diagnostiques (Veiseh *et al.*, 2005). En effet, ces systèmes attirent de plus en plus d'intérêt car ils permettent de cibler les organes, les tissus voire les cellules. Plus récemment, les nanoparticules ont trouvé leur place en thérapie génique comme un outil pour la délivrance intracellulaire d'acides nucléiques (Tahara *et al.*, 2008).

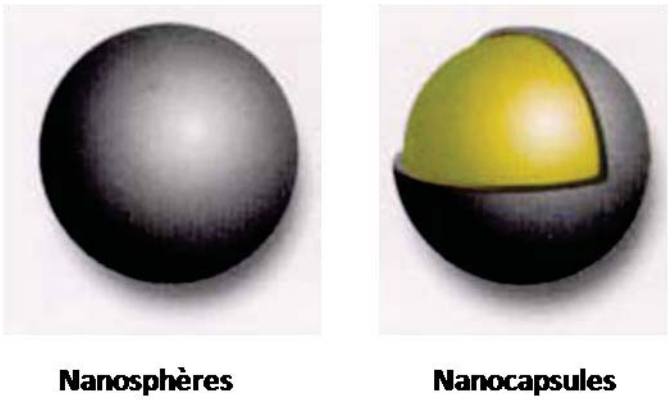

Figure 6. Représentation schématique des nanosphères et nanocapsules.

3.2.2. Les microparticules

Ce sont les vecteurs polymériques à libération prolongée, qui ont véritablement ouvert la voie aux thérapies locales. Ces systèmes sont basés sur l'emprisonnement des principes actifs au sein d'un réseau polymérique, dans le cas des microsphères, ou leurs dissolutions dans un cœur aqueux ou huileux délimité par une paroi polymérique, pour les microcapsules. Leur taille est comprise entre 1 et 1000 micromètres. Cette petite taille autorise leur injection dans des compartiments corporels par la voie sous-cutanée (Florindo *et al.*, 2008), intramusculaire (Zhang *et al.*, 2008), intraoculaire (Hachicha *et al.*, 2007), intratumorale (Hamoudeh *et al.*, 2008), intracérébrale (Menei *et al.*, 2005), intra péritonéale (Guerrero *et al.*, 2008), etc.

Lorsqu'elles se trouvent en contact avec les milieux biologiques, les microparticules libèrent leur principe actif encapsulé de façon contrôlée et prolongée par des phénomènes de diffusion et/ou érosion. Ces phénomènes sont dépendants de la vitesse de dégradation du polymère (Sanders *et al.*, 1984), de la taille du vecteur (Nicholas *et al.*, 2002) et de la solubilité aqueuse du PA encapsulé. La libération peut être observée sur une période définie allant de quelques heures (Hachicha *et al.*, 2006) à plusieurs semaines (Hamoudeh *et al.*, 2008). Le profil de cette libération peut être programmé et adapté à la situation. En théorie, toutes les cinétiques peuvent être obtenues, comme par exemple une cinétique de libération d'ordre zéro, en plateau ou diphasique (Lamprecht *et al.*, 2003).

3.3. Les polymères employés pour l'élaboration des nano- et microparticules biodégradables

Divers polymères sont employés dans l'encapsulation de principes actifs. Les premières particules polymériques ont été constituées essentiellement de polymères non biodégradables

comme les poly(acrylamides) et les poly(méthyl méthacrylates) (Birrenbach & Speiser, 1976). Cette absence de biodégradabilité a toutefois pour conséquence une toxicité par accumulation intracellulaire ou tissulaire lors de l'administration chronique de ce type de système, ce qui a limité considérablement leur utilisation. Actuellement, les polymères biodégradables sont les plus développés dans le domaine biomédical pour des raisons évidentes. Parmi eux, les polymères naturels, à savoir l'albumine humaine ou bovine, la gélatine, le collagène, l'alginate ou les chitosans, dérivés de carapace de crustacés, les polymères semi-synthétiques, comme les dérivés de cellulose, ainsi que les polymères synthétiques, comme les polyesters aliphatiques, qui sont actuellement les plus étudiés.

Nous nous contenterons d'étudier les polyesters aliphatiques, à savoir les polymères de l'acide polylactique, l'acide polyglycolique, et de la caprolactone, ainsi que les copolymères à base de poly(éthylène glycol), qui sont potentiellement utilisés dans la préparation des vecteurs particulaires. Ces polymères sont totalement biodégradables in vivo après interaction avec les fluides corporels, les cellules et les enzymes (Shive & Anderson, 1997). Les produits de dégradation peuvent être métabolisés par l'organisme (cas de l'acide lactique) ou éliminés (le poly(éthylène glycol < 20.000) (Coffin & McGinity, 1992).

D'une manière générale, lors de l'élaboration des vecteurs polymériques, le choix du polymère se fait en fonction des caractéristiques du principe actif à libérer, la durée et la cinétique de libération désirée.

3.3.1. Polycaprolactones (PCL)

C'est un polyester aliphatique synthétique, provenant de la polymérisation de l' ε-caprolactone (figure7). Il est semi-cristallin et hydrophobe. La cristallinité du PCL diminue avec l'augmentation de son poids moléculaire ; le polymère de 5000 est à 80% cristallin, par contre le PCL de 60.000 est à 45% cristallin.

D'une manière générale, la cristallinité du polymère et son poids moléculaire sont des facteurs importants influant sur sa vitesse de dégradation. Lorsque le polymère est semi-cristallin, l'hydrolyse commence dans les zones amorphes, puis se poursuit par l'attaque des zones cristallines. D'autre part, le bilan hydrophilicité/hydrophobicité influence l'hydrolyse et la libération du principe actif encapsulé car ces deux dernières dépendent de la capacité du polymère à absorber l'eau.

La dégradation du PCL se fait d'abord par hydrolyse non-enzymatique des liaisons esters, la baisse du degré de polymérisation étant conjointe à une augmentation de la

cristallinité. Cette réaction est auto-catalysée par les groupes terminaux d'acide carboxyliques du polymère (Ali *et al.*, 1993). Le clivage des liaisons esters produit des petits résidus polymériques qui peuvent diffuser hors de la matrice et sont phagocytés (Pektok *et al.*, 2008), (Silva-Cunha *et al.*, 2008).

Avec des systèmes réservoirs poreux de PCL, une libération médicamenteuse peut être obtenue sur plus de 250 jours avec une cinétique d'ordre zéro (Valmikinathan *et al.*, 2009), ils peuvent donc être utilisés pour des applications à long terme.

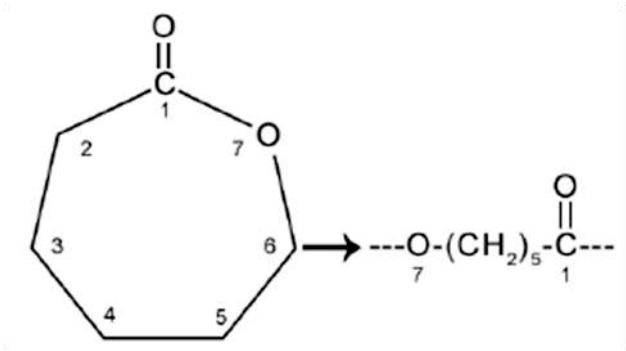

Figure 7. Synthèse de la polycaprolactone.

3.3.2. Acides poly(glycolique) (PGA), poly(lactique) (PLA), et poly(lactique-co-glycolique) (PLGA)

L'acide polyglycolique (PGA) suscite beaucoup d'intérêt du fait qu'il conduit à des produits de décomposition physiologiques chez l'homme. Il a été utilisé pour la première fois sous forme de sutures résorbables aux Etats Unis (Bender & Brouwer, 1975). Le PGA est semi-cristallin avec un taux de cristallinité de 50 % et hydrophile. Il est absorbé au bout de quelques mois du fait d'une bonne sensibilité hydrolytique.

L'acide poly(lactique) (PLA) est synthétisé à partir de l'acide lactique. Comme il existe deux énantiomères L et D de l'acide lactique, trois formes de PLA peuvent être obtenues, à savoir le poly(D- lactide) PDLA, le poly(L- lactide) PLLA et le poly(D,L- latide) PDLA. Les deux premières formes sont cristallines et la troisième est purement amorphe. Du fait du groupement méthyle qui confère un caractère hydrophobe au PLA, celui-ci se dégrade moins vite que le PGA (Brady *et al.*, 1973).

Afin d'obtenir une grande variété de polymères à différentes vitesses de dégradation et différents degrés de cristallinité, des copolymères de l'acide lactique et glycoliques ont été synthétisés. Ces copolymères se caractérisent par leurs poids moléculaires et par le taux relatif en acide lactique et acide glycolique, ce qui influence notablement la vitesse de dégradation et

par conséquence la cinétique de libération des principes actifs à partir des vecteurs particulaires. A titre d'exemple, Le copolymère 25/75 PLA/PGA se dégrade à 98 % à 120 jours, le copolymère 50/50 PLA/PGA à 100 % à 140 jours, le copolymère 75/25 PLA/PGA à 98 % à 180 jours (Miller *et al.*, 1977). Suite aux réactions d'hydrolyse, les vecteurs à base de PLA ou PLGA subissent une érosion massive occasionnant un *Burst* de libération des substances encapsulées (Vert *et al.*, 1994).

3.3.3. Les co-polymères à base de polyesters et poly(éthylene glycol)

En couplant, les polyesters avec les poly(éthylène glycol), une grande variété des copolymères biocompatibles peuvent être obtenus. Les copolymères résultant sont caractérisés par le poids moléculaire de chacun des blocs et le taux relatif d'un bloc par rapport à l'autre.

Dans le domaine de la vectorisation, les copolymères PEG-polyester sont généralement utilisés pour conférer un caractère hydrophile à la surface des vecteurs polymériques afin de limiter leurs reconnaissances par le système immunitaire et d'augmenter leurs rémanences dans la circulation sanguine. Le principe consiste à recouvrir les particules de chaînes des polymères hydrophiles et flexibles empêchant, par encombrement stérique, certaines protéines sanguines (appelées les opsonines) de se fixer à leur surface, ce qui va permettre aux particules d'échapper à la phagocytose par le système phagocytaire mononucléé (Gref *et al.*, 1997).

Les variations de composition et de poids moléculaire se traduisent par des propriétés différentes. En général, ce sont des produits amphiphiles et plus le rapport PEG/polyester est important, plus le copolymère est hydrophile. Pour un même rapport PEG/polyester, plus la chaîne PEG est courte, plus l'hydrophilicité augmente (Dobrzynski *et al.*, 2005). Par ailleurs, la cristallinité du copolymère dépend de la longueur de la chaîne du polyester qui est cristallin (comme le PLLA) ou semi-cristallin (comme le PCL et PLGA) (Li *et al.*, 2002).

La dégradation de copolymères PEG/polyester se fait par hydrolyse des liaisons esters et génère des chaînes de poly(éthylène glycol) de faible poids moléculaire (Li *et al.*, 2002), qui sont facilement excrétées et des oligomères du polyester qui continuent leur dégradation d'une manière telle que nous l' avons décrite précédemment.

3.4. Les techniques classiques de préparation des vecteurs particulaires

A l'heure actuelle plusieurs techniques de préparation sont au point. Une classification assez pratique décrite par (Allémann, 1993), divise les méthodes de production de nanoparticules en deux grandes catégories. La première catégorie est fondée sur la dispersion de polymères préformés tandis que la deuxième, elle rassemble les méthodes de préparation par polymérisation. En effet, selon la méthode de préparation, différentes caractéristiques physico-chimiques des vecteurs peuvent être obtenues, telles que la taille, l'efficacité d'encapsulation du principe actif et la porosité de surface des particules. Par ailleurs, le choix de la méthode elle-même est principalement déterminé par la solubilité du principe actif à encapsuler.

3.4.1. Méthodes de préparation par dispersion de polymères préformés

Les techniques les plus utilisées pour obtenir des particules à partir de polymères préformés sont : la technique d'émulsion-évaporation de solvant (Vanderhoff *et al.*, 1979), la technique de déplacement de solvant ou « la nanoprécipitation » brevetée par (Fessi *et al.*, 1992), la technique de désolvatation par les sels ou « salting-out », décrite par (Allémann *et al.*, 1993) et enfin la technique appelée « émulsification-diffusion » décrite et brevetée par (Leroux *et al.*, 1995). L'ensemble de ces méthodes consistent à solubiliser le polymère et le principe actif liposoluble dans un solvant organique dans un premier temps, puis à réaliser sa dispersion dans une phase externe continue dans laquelle le polymère est insoluble.

3.4.1.1. L'émulsion-évaporation de solvant

Dans cette méthode, le polymère et le principe actif liposoluble sont dissous dans un solvant organique volatil, non miscible à l'eau, comme le dichlorométhane ou le chloroforme (figure 8). Ensuite, la solution obtenue est émulsifiée dans une solution aqueuse, contenant un agent tensioactif. L'émulsion est alors cisaillée en l'exposant à une source d'énergie en utilisant l'agitation mécanique (Lemoine *et al.*, 1998) ou l'homogénéisation (Lamprecht *et al.*, 1999), afin de réduire la taille des gouttelettes. L'élimination du solvant organique, par la chaleur, le vide ou les deux, a pour conséquence la précipitation du polymère et la formation d'une suspension des nanoparticules (Tewes *et al.*, 2007) ou des microparticules (Hamoudeh

et al., 2008) selon l'importance de l'énergie de cisaillement appliquée à l'émulsion initiale et la taille des gouttelettes formées.

Une adaptation de cette technique a été mise au point pour l'encapsulation des principes actifs hydrosolubles ou partiellement hydrosolubles. Elle consiste à substituer la première étape de préparation par la réalisation d'une double émulsion (Eau/Huile/Eau). Le principe actif est alors dissous dans la phase aqueuse interne et une émulsion primaire est réalisée en émulsifiant cette dernière dans une phase organique contenant le polymère. L'émulsion primaire est ensuite émulsifiée dans une phase aqueuse externe contenant un agent tensioactif, pour former une émulsion secondaire. L'élimination du solvant, par évaporation (Nihant *et al.*, 1994) ou extraction (Péan *et al.*, 1998), conduit à la précipitation du polymère et la formation des nanoparticules ou des microparticules (Iwata *et al.*, 1992). Dans les particules obtenues, le principe actif hydrophile est piégé dans des nano-domaines plus ou moins hydratés situés à l'intérieur de la matrice polymérique.

La technique de double émulsion- évaporation de solvant a permis d'encapsuler une large variété des macromolécules hydrophile, comme les protéines (Fattal *et al.*, 2002), les macrolides (Lecaroz *et al.*, 2006) et certaines molécules de faible poids moléculaire ayant un caractère amphiphile (Ubrich *et al.*, 2004), avec une efficacité d'encapsulation satisfaisante.

Les différents paramètres de préparation, comme la concentration du polymère et de l'agent tensioactif, la charge initiale en principe actif, les volumes respectifs de la phase organique et la phase aqueuse (ou les deux phases aqueuses dans le cas de la double émulsion) ainsi que la vitesse d'agitation ou toute autre énergie appliquée à l'émulsion pour affiner la taille des gouttelettes, vont édicter les caractéristiques physico-chimiques des particules obtenus, comme entre autre, la taille, la morphologie, la porosité de surface des particules, et la cinétique de libération du principe actif encapsulé (Hachicha *et al.*, 2006), (Al Haushey *et al.*, 2007), (Mao *et al.*, 2007).

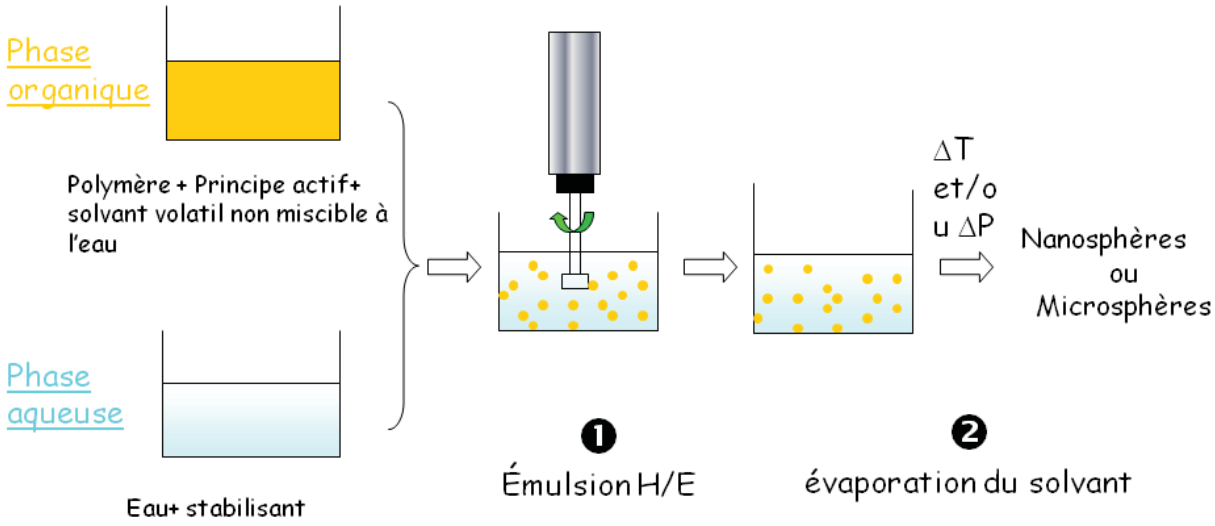

Figure 8. Schéma illustrant le principe du procédé de préparation des nano- ou microparticules par "émulsion-évaporation de solvant".

3.4.1.2. Le déplacement de solvant ou « la nanoprécipitation »

Dans cette méthode, le principe actif et le polymère sont dissous dans un solvant semi-polaire miscible à l'eau, comme l'acétone ou l'éthanol. Cette solution est alors injectée dans une solution aqueuse contenant un stabilisant sous une agitation magnétique (figure 9). Les nanoparticules sont formées instantanément par une diffusion rapide du solvant dans la phase aqueuse. Enfin, le solvant organique et une partie de l'eau sont évaporés sous pression réduite pour obtenir une suspension concentrée des nanosphères (Fessi *et al.*, 1992). L'addition d'une substance huileuse à la phase organique en faible quantité permet d'obtenir des nanocapsules (Fessi *et al.*, 1991).

Le mécanisme de formation des nanoparticules par ce procédé s'explique par la turbulence interfaciale transitoire due à la diffusion du solvant organique dans l'eau. Deux conditions contraignantes sont à respecter pour réaliser la nanoprécipitation ; la miscibilité mutuelle et totale entre la phase organique et la phase aqueuse, et le fait que le mélange des deux phases soit un non-solvant du polymère.

La simplicité et la rapidité de ce procédé de préparation des nanoparticules, qui peuvent être obtenues par une simple agitation magnétique sans avoir recours à un apport important d'énergie, constituent des avantages majeurs. Par contre, seuls les principes actifs liposolubles peuvent être encapsulés avec une efficacité d'encapsulation satisfaisante. D'autre part, cette méthode ne permet pas l'obtention des microparticules.

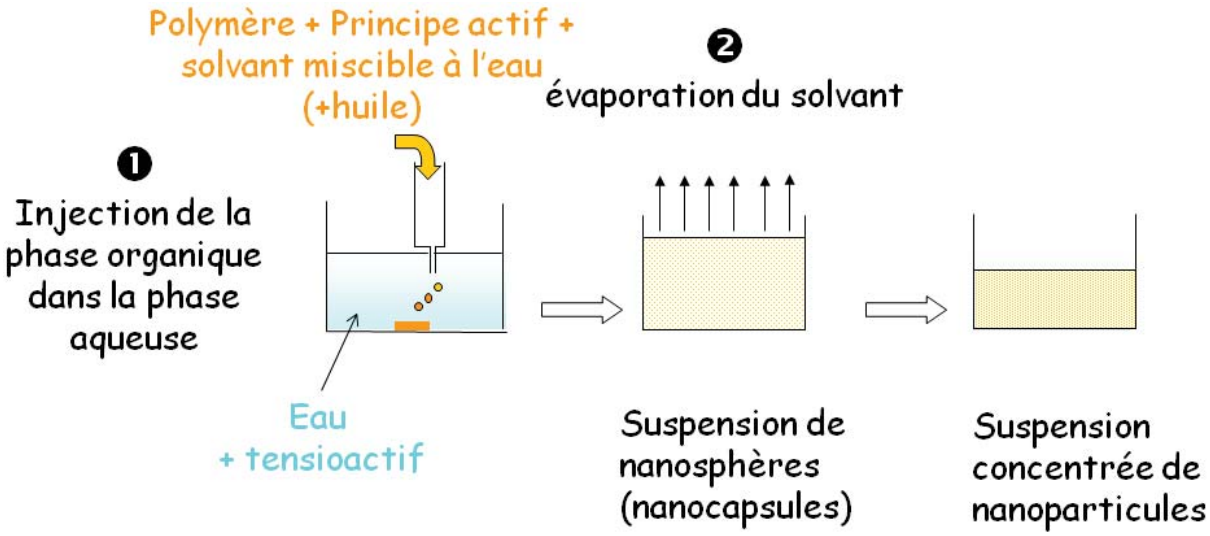

Figure 9. Schéma illustrant le principe de la nanoprécipitation.

3.4.1.3. La désolvatation ou « Salting-out »

Certains solvants miscibles à l'eau en toutes proportions permettent l'obtention de deux phases séparées s'ils sont ajoutés à une solution aqueuse saturée par un agent de désolvatation qui peut être un électrolyte comme le chlorure de magnésium, le chlorure de sodium ou un non-électrolyte comme le sucrose (Quintanar-Guerrero *et al.*, 1998). L'acétone est généralement choisie comme étant solvant miscible à l'eau en raison de sa séparation bien connue des solutions aqueuses par désolvatation par les électrolytes. Le polymère et le principe actif sont dissous dans l'acétone, ensuite cette solution est émulsifiée sous une agitation mécanique vigoureuse dans une phase aqueuse saturée en électrolytes et contenant un stabilisant. Une émulsion (huile/eau) est alors obtenue, l'acétone ne pouvant pas diffuser vers la phase aqueuse. L'émulsion formée est ensuite diluée avec un volume suffisant d'eau pour provoquer la diffusion de l'acétone vers la phase aqueuse, et donc provoquer la formation des nanoparticules (figure 10). Le solvant et l'agent de désolvatation seront ensuite éliminés par filtration tangentielle et plusieurs étapes de lavage.

Ce procédé permet l'obtention de nanoparticules monodispersées ayant une taille qui peut être ajustée en modulant les paramètres de préparation (Zweers *et al.*, 2003). Cependant, l'inconvénient de cette méthode est l'utilisation de fortes concentrations de sels, exigeant plusieurs étapes de purification minutieuse.

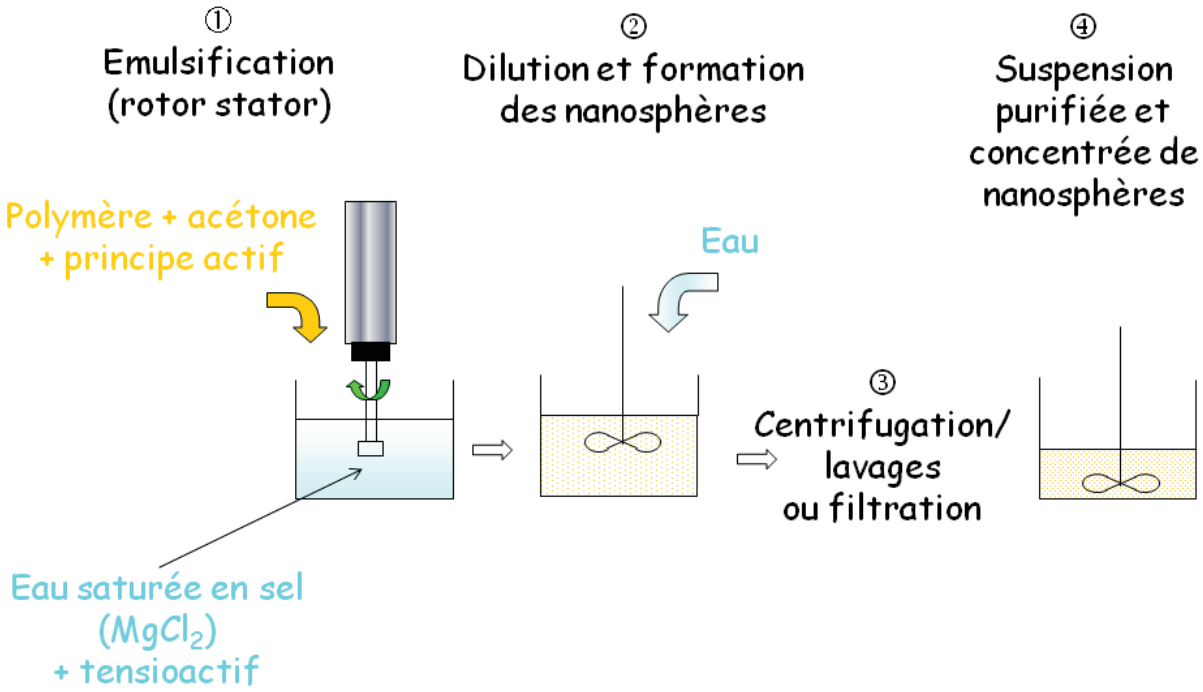

Figure 10. Schéma illustrant le principe de préparation des nanoparticules par salting-out.

3.4.1.4. L'émulsion-diffusion

Ce procédé est basé sur l'utilisation d'un solvant semi-miscible à l'eau, ce qui permet d'éviter l'utilisation des sels et les étapes de lavage intensif. Il comporte plusieurs étapes. Tout d'abord, la saturation mutuelle des deux solvants ; le solvant semi-miscible à l'eau comme l'acétate d'éthyle et l'eau. Ensuite, le polymère et le principe actif sont dissous dans le solvant semi-miscible saturé en eau. Un agent tensioactif est dissous dans l'eau saturée en solvant. Une émulsion (huile/eau) est préparée en ajoutant la phase organique dans la phase aqueuse sous agitation mécanique. L'addition suivante de l'eau au système entraîne la diffusion du solvant semi-miscible à l'eau dans la phase externe et la formation des nanoparticules. Enfin, l'acétate d'éthyle et une partie de l'eau seront éliminés pour obtenir une suspension concentrée de nanoparticules (figure 11).

Les avantages de cette méthode sont l'utilisation des solvants organiques acceptables pour la voie parentérale, et qui sont présents en très faibles quantités dans la préparation finale, l'efficacité d'encapsulation relativement élevée, la reproductibilité et la possibilité de la transposition d'échelle. Par contre, cette méthode a les inconvénients d'utiliser des grands volumes d'eau qui doivent être éliminés à la fin de la préparation et l'instabilité éventuelle des principes actifs dans la phase organique saturée en eau dans les premières étapes de la préparation.

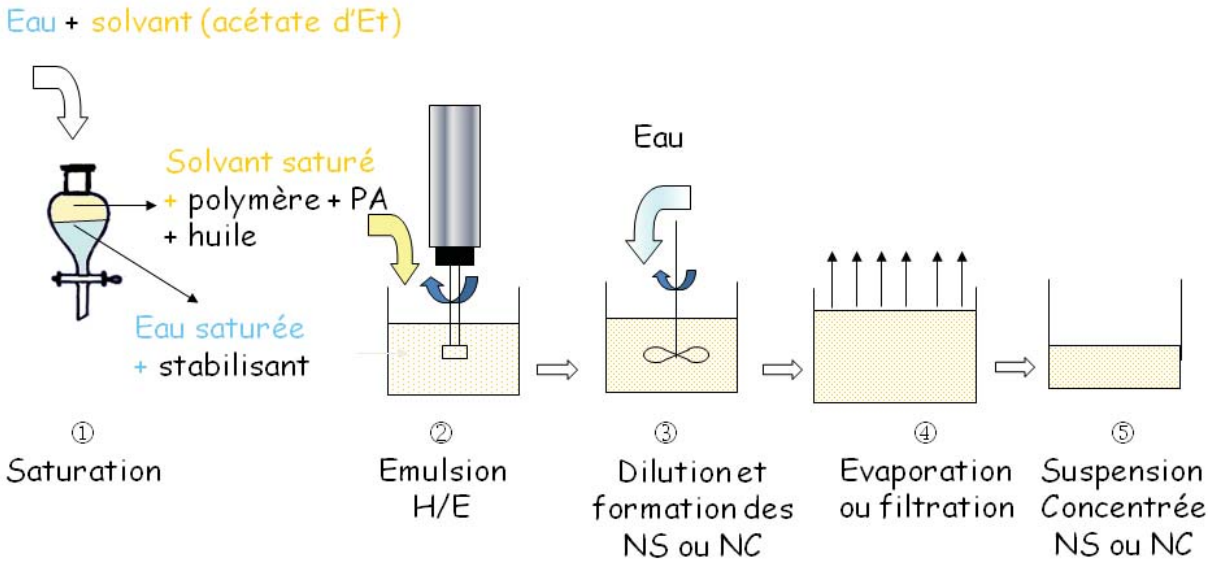

Figure 11. Les différentes étapes lors de la nanoencapsulation par émulsion-diffusion de solvant.

3.4.2. Méthodes de préparation par polymérisation

Les méthodes de préparation par polymérisation sont basées sur la formation in situ du polymère à partir soit d'un seul monomère ou de deux monomères différents. Lorsque la solution de monomères à polymériser est émulsifiée dans un non-solvant, on parle d'une polymérisation en émulsion (Couvreur *et al.*, 1982). Quand le monomère est dissous dans un solvant qui se comporte comme un non-solvant du polymère à obtenir, on parle d'une polymérisation en dispersion. Quand les micelles constitue le milieu principal de la polymérisation, on parle d'un polymérisation micellaire (Birrenbach *et al.*, 1976). Enfin, quand la polymérisation fait intervenir deux types de monomères qui sont dissous dans deux phases séparées et la réaction de polymérisation se fait à l'interface des deux phases, on parle d'une polymérisation interfaciale (Montasser *et al.*, 2000). En ajustant les paramètres de la préparation, les méthodes de polymérisation permettent l'obtention de nanoparticules et de microparticules (Munshi *et al.*, 1997).

3.4.2.1. La polymérisation en émulsion

Ce procédé consiste à émulsifier un monomère insoluble ou partiellement soluble dans le milieu de polymérisation, en utilisant un agent tensioactif. Le monomère est alors présent dans le mélange sous forme de gouttelettes et/ou sous forme de micelles, selon la concentration de l'agent tensioactif. L'induction de la polymérisation se fait par des initiateurs

physiques (irradiation), soit à l'aide d'un composé chimique, dit amorceur, ajouté au milieu réactionnel. L'amorceur étant soluble dans l'eau, et non soluble dans le monomère, va activer les monomères dispersés. Ces derniers réagissent en donnant des oligomères sur lesquels s'adsorberont soit les molécules de tensioactif soit les monomères dispersés. Ainsi, on assiste à la formation de nucléi stables, qui deviennent le lieu principal de la polymérisation par adsorption de nouvelles oligomères et monomères du milieu, pour donner naissance à des particules polymériques. Les particules croissent jusqu'à la consommation totale du monomère.

3.4.2.2. La polymérisation en dispersion

Ce procédé est basé sur la nucléation en phase continue aqueuse. Il consiste à dissoudre le monomère et le principe actif (qui sont hydrophiles) dans la phase continue. La polymérisation est amorcée par irradiation ou à l'aide d'un amorceur chimique, ce qui conduit à la formation d'oligomères. Ces derniers, lorsqu'elles atteignent une taille critique, elles précipitent pour former des particules primaires stabilisées par les molécules du tensioactif non ionique ajouté au milieu aqueux. Enfin, ces particules fusionnent pour former des nanoparticules (figure 12).

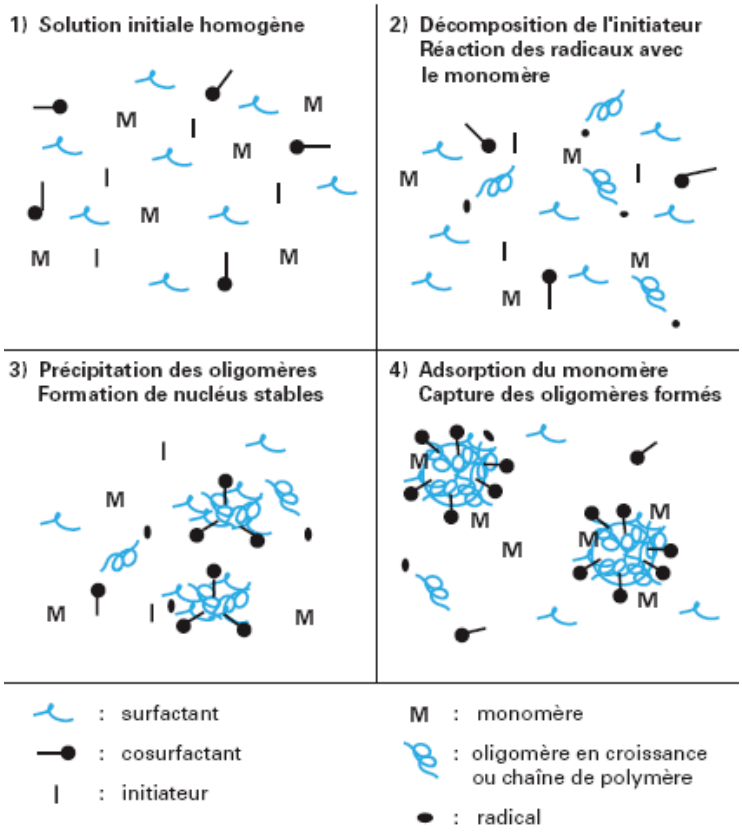

Figure 12. Le mécanisme de la polymérisation en dispersion.

3.4.2.3. La polymérisation en microémulsion-inverse « polymérisation micellaire »

Ce procédé consiste à dissoudre le principe actif hydrophile dans un petit volume d'eau ou d'un solvant organique hydrophile (méthanol). Cette solution est émulsifiée dans un solvant organique hydrophobe (hexane, cyclohexane, chloroforme) contenant des grandes quantités d'un agent tensioactif pour former des micelles aqueuses. Un monomère hydrophile est directement ajouté au mélange sous agitation continue. Ce dernier diffuse alors, à travers la phase organique vers l'intérieur de micelles, considérées comme le lieu principal de la polymérisation. La polymérisation est initiée par un amorceur physique ou chimique. Les oligomères formées conduisent à la formation des nanoparticules d'une faible taille.

3.4.2.4. La polymérisation interfaciale

Cette méthode repose sur la mise en contact d'une phase contenant la substance liquide à encapsuler et un ou plusieurs monomères, avec une autre phase non miscible à la première et contenant un autre ou plusieurs monomères susceptibles de réagir avec le(s) premier(s) pour donner un polymère. Lors de la mise en contact des deux phases, les deux composés réagissent à l'interface des phases et créent une paroi polymérique autour des gouttelettes de substances liquides (capsules). La combinaison de l'émulsification spontanée à la polymérisation interfaciale permet d'obtenir des nanocapsules (Montasser *et al.*, 2000). Le principe consiste à additionner une phase organique composée du monomère liposoluble, le principe actif, d'huile et un tensioactif dissous dans un solvant (ou mélange de solvants miscibles) à une phase aqueuse composé d'un monomère hydrosoluble, un tensioactif et d'un non-solvant (ou un mélange des non-solvants). Les nanocapsules se forment instantanément par réaction des deux monomères à l'interface liquide-liquide des gouttelettes (figure 13). La suspension est ensuite concentrée par évaporation sous vide puis filtrée.

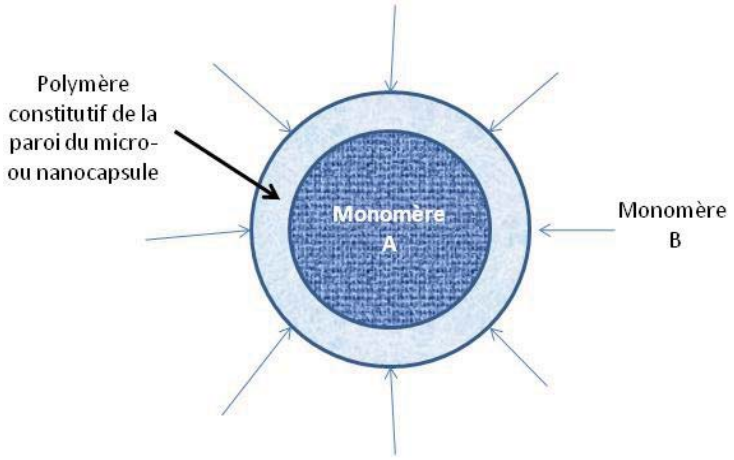

Figure 13. Le mécanisme de la polycondensation interfaciale.

3.5. Les méthodes de caractérisation des vecteurs particulaires

3.5.1. Taille

La taille d'un vecteur particulaire est une caractéristique fondamentale pour déterminer sa voie d'administration. De plus, le profil de libération d'un principe actif encapsulé est lié à la taille du vecteur qui le véhicule. La maîtrise de la taille des vecteurs, s'avère possible. Cela dépend du choix du procédé de préparation (Tewes *et al.*, 2007), des paramètres opératoires, notamment la vitesse et le temps d'agitation ou la puissance de sonication, et aussi les paramètres de formulation (Hachicha *et al.*, 2006), à savoir le type de polymère, son poids moléculaire et sa concentration dans la phase organique, le type de tensioactif et sa concentration dans la phase aqueuse, le type de solvant (ou mélange de solvants) organique, les volumes respectifs de la phase aqueuse et la phase organique (Esposito *et al.*, 1996).

Différentes méthodes sont employées pour déterminer la taille et la distribution de taille des particules. Les résultats d'une analyse granulométrique peuvent être exprimés sous la forme d'une taille moyenne et/ou d'une distribution de taille (histogramme présentant les pourcentages par classe granulométrique).

La granulométrie laser est la technique la plus utilisée et peut être utilisée pour déterminer la taille de plusieurs types de vecteurs, comme les nanoparticules, les liposomes et les microparticules. Elle est basée sur l'interaction d'un faisceau laser avec les particules dispersées. Lorsqu'une particule se trouve dans le trajet d'un faisceau de lumière monochromatique, l'énergie lumineuse peut être absorbée ou diffusée par cette particule selon la longueur d'onde de la lumière incidente et les propriétés optique de la particule. La lumière diffusée est la somme de trois composants ; la lumière réfractée, réfléchie, et diffractée. La méthode d'analyse repose sur deux théories fondamentales ; la théorie de Mie et celle de Fraunhofer. Lorsque le diamètre de la particule avoisine la longueur d'onde de la lumière incidente, c'est le cas des nanoparticules dont la taille est inférieure à un micron, les phénomènes de réflexion et de réfraction interviennent pour une part non négligeable dans l'intensité de la lumière diffusée en plus de la diffraction. Dans ce cas, la théorie de Mie, qui prend en considération les indices de réfraction de l'échantillon et du milieu dispersant, s'applique. En revanche, lorsque le diamètre des particules est largement supérieur à la longueur d'onde (> 3 µm), c'est le cas des microparticules, ou encore lorsque le matériau est très absorbant, l'effet de bord des particules contribue pour une part importante à l'intensité

de la lumière diffusée. L'interférence provient alors principalement de la diffraction créée par la courbure de la lumière à l'interface. Dans ce cas de figure, le modèle mathématique utilisé pour le calcul de la distribution de taille est celui de la théorie de Fraunhofer, une version restreinte de la théorie de Mie présentant l'intérêt de négliger totalement les propriétés optiques de l'échantillon et du milieu dispersant.

La technique de la diffusion dynamique de la lumière (DLS) convient de façon idéale à la détermination de la taille des particules dans la plage de tailles allant de 5 nm à quelques microns. Cette technique repose sur le mouvement brownien des nanoparticules en raison des collisions des particules se traduisant par des fluctuations d'intensité de la lumière diffusée. Le coefficient de diffusion, étant calculé à partir d'une fonction de corrélation, permet de déterminer la taille des particules grâce à l'équation de Stockes-Einstein.

3.5.2. Morphologie

La morphologie des vecteurs peut être examinée par diverses techniques microscopiques : la microscopie optique, la microscopie électronique à transmission, La microscopie électronique à balayage, microscopie électronique à balayage environnemental. Les nanoparticules ayant une taille inférieure à un micron, ne peuvent pas être visualisées qu'avec les microscopies électroniques. Dans certains cas, ces techniques permettent de déterminer la taille des particules et de vérifier l'homogénéité des préparations.

3.5.2.1. La microscopie électronique à transmission (MET)

C'est la technique la plus performante. Dans son principe, elle ressemble à la microscopie optique en lumière directe. Le faisceau d'électron est émis par un canon à électron, focalisé sur la préparation à l'aide de lentilles électromagnétiques et la traverse, ils sont plus ou moins absorbées (la préparation est dite plus ou moins dense aux électrons). L'image se forme derrière la préparation sur un écran fluorescent, donnant des informations sur l'architecture interne des particules observées.

3.5.2.2. La microscopie électronique à balayage (MEB)

Bien que de résolution plus faible que la précédente, cette technique donne des images absolument spectaculaires, en pseudo 3D. Lorsque le faisceau d'électrons bombarde la préparation, une partie des électrons la traverse, le reste est réémis pour former des électrons

secondaires du côté exposé de la préparation, ce sont eux qui serviront à construire l'image. Le résultat est une représentation de la surface de l'objet observée. Ainsi, cette technique permet d'avoir des informations sur les caractéristiques de surface des particules comme la porosité et la rugosité, qui sont extrêmement importantes ayant des conséquences sur le profil de libération du principe actif encapsulé (Sansdrap *et al.*, 1998), (Esposito *et al.*, 1996).

3.5.2.3. La microscopie électronique à balayage environnemental (MEBE)

L'échantillon ne peut pas être observée dans son état normal dans les deux techniques précédentes qui exigent une condition du vide poussé pour effectuer l'observation, en plus d'un traitement préalable de l'échantillon comme la métallisation dans le cas de la MEB ou l'ajout d'agent de contraste dans le cas de la MET. La microscopie électronique de balayage environnemental permet d'étudier l'échantillon dans son état normal ou dans des conditions environnementales normales sans préparation préalable pouvant produire des artéfacts dans l'échantillon.

Cette technique est rendue possible grâce à un système de pompage différentiel permet de maintenir le canon et le haut de la colonne sous un vide poussé, soit un vide de l'ordre de 10-7 Torrs. L'appareil est équipé d'un détecteur spécifique le GSED ou *Gaseous Secondary Electron Detector* qui peut détecter les électrons secondaires en utilisant l'environnement gazeux comme amplificateur, ce qui permet d'avoir une résolution identique à celle obtenue en mode conventionnel mais à 7 Torrs.

3.5.3. Charge de surface (potentiel zêta)

Le potentiel zêta d'une particule, qui est la charge globale que la particule acquiert dans le milieu liquide dans lequel elle est plongée. La valeur du potentiel zêta indique la force de répulsion présente entre les particules en suspension et permet de prédire la stabilité du système à long terme. Si toutes les particules en suspension ont un potentiel zêta négatif ou positif important, elles tendent à se repousser mutuellement et ne peuvent se rassembler (Merodio *et al.*, 2001). En revanche, si leur potentiel zêta est faible, aucune force ne les empêche de se rassembler et de floculer.

La charge de surface peut provenir de l'ionisation des groupes fonctionnels présents à la surface des particules ou de la substitution ou l'adsorption de tensioactifs ioniques. Par ailleurs, le pH, la concentration en additif ou la force ionique du milieu liquide sont des facteurs influant sur le potentiel zêta des particules dispersées.

La mesure du potentiel zêta est basée sur la mobilité électrophorétique des particules en suspension. Le principe consiste à appliquer un champ magnétique aux particules dispersées qui vont acquérir une mobilité en fonction de leur charge. La vitesse moyenne de déplacement des particules (μ) étant mesurée, le potentiel zêta (ξ) est alors calculé en employant différentes équations telle que celle de Smoluchowski pour de fortes concentrations ioniques $\mu = \varepsilon\xi / 4\pi\eta$ o u de celle de Huckel pour de fiables concentrations ioniques $\mu = \varepsilon\xi / 6\pi\eta$ avec ε le constant diélectrique du milieu et η la viscosité.

3.5.4. Efficacité d'encapsulation

L'efficacité d'encapsulation d'un principe actif dépend de son affinité vers le polymère constitutif des particules. Ceci est lié à la structure du polymère, son poids moléculaire et aux interactions principe actif-polymère (Olivier, 2005). La plupart des polymères employés dans la préparation des micro- et nanoparticules sont hydrophobes, par conséquent, les principes actifs liposolubles sont plus facilement encapsulés que les principes actifs hydrosolubles. Toutefois, le taux d'encapsulation des principes hydrosoluble peut être optimisé par différents moyens : le choix du procédé de préparation, l'optimisation du pH de la phase aqueuse, l'utilisation des additifs (Puglisi *et al.*, 1993).

La détermination de l'efficacité d'encapsulation nécessite au préalable la purification des particules par filtration, ultracentrifugation ou lavage afin d'éliminer la fraction non encapsulé du principe actif. Une fois, la purification est effectuée, l'efficacité d'encapsulation peut alors être calculée, après dosage du principe actif piégé à l'intérieur du vecteur ou adsorbé à sa surface, comme étant le pourcentage de la quantité dosée par rapport à la quantité théorique utilisée dans la formulation. La détermination de l'efficacité d'encapsulation peut être réalisée d'une manière indirecte par le dosage de la fraction non encapsulée du principe actif qui sera déduite de la quantité totale incorporée dans la préparation.

3.5.5. Cinétique de libération

La maîtrise de la cinétique de la libération du principe actif à partir des formes pharmaceutiques et celle de la durée d'action des médicaments est l'un des premiers défis ayant été proposés à la pharmacie galénique au cours des cinquante dernières années. La

conception des vecteurs particulaires, a permis l'obtention de deux types de libération du principe actif ; une libération déclenchée ou une libération continue, prolongée dans le temps.

En général, ce sont les systèmes réservoirs (les micro- et nanocapsules) qui permettent une libération brutale du principe actif qui peut être déclenchée par l'éclatement de leur paroi polymérique, suite à une variation du pH, de la température, de la pression osmotique ou sous l'effet d'un agent physique externe, comme par exemple l'ultrason.

Par ailleurs, la libération continue de l'actif peut être assurée par les systèmes matriciels (les nano- et microsphères). Les mécanismes mis en jeu sont la diffusion du principe actif et/ou la dégradation du polymère constitutif du vecteur. Ces deux phénomènes et par conséquence la cinétique de libération obtenue, dépendent de plusieurs facteurs. Le caractère hydrophile/lipophile du principe actif encapsulé et son poids moléculaire influent sur sa diffusion à travers la matrice polymérique vers le milieu de libération (Hombreiro Pérez *et al.*, 2000). Le type de polymère et son poids moléculaire se traduisent par des vitesses de dégradation différentes et donc par des profils différents de libération du principe actif (Ubrich *et al.*, 2004), (Lamprecht *et al.*, 2000). Les interactions principe actif-polymère qui va faire que l'actif est soluble dans le polymère sous forme amorphe ou dispersé à son état cristallin, sont aussi des facteurs importants pouvant influer la cinétique de libération (Karavas *et al.*, 2007). En plus, les propriétés de surface des vecteurs particulaires, comme la porosité et l'existence d'un block hydrophile comme le poly(éthylène glycol), va faciliter le mouillage de la surface des particules et la pénétration de l'eau à travers la matrice polymérique, ce qui va faciliter la libération du principe actif (Coombes *et al.*, 1997), (Klose *et al.*, 2006). D'autre part, la formulation (les types de tensio-actifs utilisés, la charge initiale en principe actif, le type de solvants et leurs proportions relatives), les paramètres du procédé de préparation et la méthode de séchage employé, peuvent avoir des conséquences sur la cinétique de libération (Weidenauer *et al.*, 2003), (Lagarce *et al.*, 2006).

Références

Al Haushey, L., Bolzinger, M. A., Bordes, C., Gauvrit, J. Y. & Briançon, S. (2007). Improvement of a bovine serum albumin microencapsulation process by screening design. *International journal of pharmaceutics*, *344*, 16-25.

Ali, S. A., Zhong, S. P., Doherty, P. J. & Williams, D.F. (1993). Mechanisms of polymer degradation in implantable devices. I. Poly(caprolactone). *Biomaterials*, *14*, 648-56.

Allémann, E., Gurny, R. & Doelker, E. (1993). Drug-loaded nanoparticles : preparation methods and drug targeting issues. *European journal of pharmaceutics and biopharmaceutics*, *39*, 173-191.

Allémann, E., Leroux, J. C., Gurny, R. & Doelker, E. (1993). In vitro extended-release properties of drug-loaded poly(DL-lactic acid) nanoparticles produced by a salting-out procedure. *Pharmaceutical research*, *10*, 1732-7.

Ansari, M. T., Iqbal, I. & Sunderland, V.B. (2009). Dihydroartemisinin-cyclodextrin complexation: solubility and stability. *Archives of pharmacal research*, *32*, 155-65.

Banerjee, R. (2001). Liposomes: applications in medicine. *Journal of biomaterials applications*, *16*, 3-21.

Bangham, A. D., Standish, M. M. & Miller, N. (1965). Cation permeability of phospholipid model membranes: effect of narcotics. *Nature*, *208*, 1295-7.

Bangham, A. D., Standish, M. M. & Watkins, J.C. (1965). Diffusion of univalent ions across the lamellae of swollen phospholipids. *Journal of molecular biology*, *13*, 238-52.

Bender, J. & Brouwer, J. (1975). Experience with the use of polyglycolic acid suture material (Dexon) in 500 surgical patients. *Archivum chirurgicum Neerlandicum*, *27*, 53-61.

Bernini, A., Spiga, O., Ciutti, A., Scarselli, M., Bottoni, G., Mascagni, P. & Niccolai, N. (2004). NMR studies of the inclusion complex between beta-cyclodextrin and paroxetine. *European journal of pharmaceutical sciences: official journal of the European Federation for Pharmaceutical Sciences*, *22*, 445-50.

Birrenbach, G. & Speiser, P.P. (1976). Polymerized micelles and their use as adjuvants in immunology. *Journal of pharmaceutical sciences*, *65*, 1763-6.

Brady, J. M., Cutright, D. E., Miller, R. A. & Barristone, G.C. (1973). Resorption rate, route, route of elimination, and ultrastructure of the implant site of polylactic acid in the abdominal wall of the rat. *Journal of biomedical materials research*, *7*, 155-66.

Cavallari, C., Albertini, B., González-Rodríguez, M. L. & Rodriguez, L. (2002). Improved dissolution behaviour of steam-granulated piroxicam. *European journal of*

pharmaceutics and biopharmaceutics : official journal of Arbeitsgemeinschaft fur Pharmazeutische Verfahrenstechnik e.V, *54*, 65-73.

Clares, B., Gallardo, V., Medina, M. & Ruiz, M.A. (2009). Multilamellar liposomes of triamcinolone acetonide: preparation, stability, and characterization. *Journal of liposome research*, 1-10.

Coffin, M. D. & McGinity, J.W. (1992). Biodegradable pseudolatexes: the chemical stability of poly(D,L-lactide) and poly(epsilon-caprolactone) nanoparticles in aqueous media. *Pharmaceutical research*, *9*, 200-5.

Connors, K. A. (1997). The Stability of Cyclodextrin Complexes in Solution. *Chemical reviews*, *97*, 1325-1358.

Constantinescu, I., Levin, E. & Gyongyossy-Issa, M. (2003). Liposomes and blood cells: a flow cytometric study. *Artificial cells, blood substitutes, and immobilization biotechnology*, *31*, 395-424.

Coombes, A. G., Tasker, S., Lindblad, M., Holmgren, J., Hoste, K., Toncheva, V., Schacht, E., Davies, M. C., Illum, L. & Davis, S.S. (1997). Biodegradable polymeric microparticles for drug delivery and vaccine formulation: the surface attachment of hydrophilic species using the concept of poly(ethylene glycol) anchoring segments. *Biomaterials*, *18*, 1153-61.

Couvreur, P., Kante, B., Grislain, L., Roland, M. & Speiser, P. (1982). Toxicity of polyalkylcyanoacrylate nanoparticles II: Doxorubicin-loaded nanoparticles. *Journal of pharmaceutical sciences*, *71*, 790-2.

Dobrzynski, P., Li, S., Kasperczyk, J., Bero, M., Gasc, F. & Vert, M. (2005). Structure-property relationships of copolymers obtained by ring-opening polymerization of glycolide and epsilon-caprolactone. Part 1. Synthesis and characterization. *Biomacromolecules*, *6*, 483-8.

Duchêne, D. & Wouessidjewe, D. (1990). Pharmaceutical uses of cyclodextrins and derivatives. *Drug Development and Industrial Pharmacy*, *16*, 2487-99.

Duchêne, D., Wouessidjewe, D. & Ponchel, G. (1999). Cyclodextrins and carrier systems. *Journal of controlled release : official journal of the Controlled Release Society*, *62*, 263-8.

Eastburn, S. D. & Tao, B.Y. (1994). Applications of modified cyclodextrins. *Biotechnology advances*, *12*, 325-39.

Easton, C. & Linclon, S. (1999). Modified Cyclodextrins: Scaffolds and Templates for Supramolecular Chemistry. London: Imperial College Press.

Esposito, E., Cortesi, R. & Nastruzzi, C. (1996). Gelatin microspheres: influence of preparation parameters and thermal treatment on chemico-physical and biopharmaceutical properties. *Biomaterials*, *17*, 2009-20.

Espuelas, S., Haller, P., Schuber, F. & Frisch, B. (2003). Synthesis of an amphiphilic tetraantennary mannosyl conjugate and incorporation into liposome carriers. *Bioorganic & medicinal chemistry letters*, *13*, 2557-60.

Fattal, E., Pecquet, S., Couvreur, P. & Andremont, A. (2002). Biodegradable microparticles for the mucosal delivery of antibacterial and dietary antigens. *International journal of pharmaceutics*, *242*, 15-24.

Fessi, H., Devissaguet, J. & Puisieux, F. (1991). Process for the preparation of dispersible colloidal systems of a substance in the form of nanocapsules. US patent 5 049 322 17.

Fessi, H., Devissaguet, J. & Puisieux, F. (1992). Process for the preparation of dispersible colloidal systems of a substance in the form of nanoparticles. US patent 5 118 528.

Ficarra, R., Ficarra, P., Di Bella, M. R., Raneri, D., Tommasini, S., Calabrò, M. L., Gamberini, M. C. & Rustichelli, C. (2000). Study of beta-blockers/beta-cyclodextrins inclusion complex by NMR, DSC, X-ray and SEM investigation. *Journal of pharmaceutical and biomedical analysis*, *23*, 33-40.

Florindo, H. F., Pandit, S., Gonçalves, L. M. D., Alpar, H. O. & Almeida, A.J. (2008). Streptococcus equi antigens adsorbed onto surface modified poly-epsilon-caprolactone microspheres induce humoral and cellular specific immune responses. *Vaccine*, *26*, 4168-77.

Gan, Y., Pan, W., Wei, M. & Zhang, R. (2002). Cyclodextrin complex osmotic tablet for glipizide delivery. *Drug development and industrial pharmacy*, *28*, 1015-21.

Gershkovich, P., Wasan, K. M. & Barta, C.A. (2008). A review of the application of lipid-based systems in systemic, dermal/ transdermal, and ocular drug delivery. *Critical reviews in therapeutic drug carrier systems*, *25*, 545-84.

Giordano, F., Novak, C. & Moyano, J. (2001). Thermal analysis of cyclodextrins and their inclusion compounds. *Thermochimica Acta*, *380*, 123-151.

Giordano, F., Pavan, M., La Manna, A., Bettinetti, G. P., Pavesi, L. & Bovis, G. (1988). Complexation behavior of vinburnine with beta and gamma cyclodextrins in aqueous solution and in the solid state. *Il Farmaco; edizione pratica*, *43*, 345-55.

Gref, R., Minamitake, Y., Peracchia, M. T., Domb, A., Trubetskoy, V., Torchilin, V. & Langer, R. (1997). Poly(ethylene glycol)-coated nanospheres: potential carriers for intravenous drug administration. *Pharmaceutical biotechnology*, *10*, 167-98.

Gregoriadis, G. (1977). Targeting of drugs. *Nature*, *265*, 407-11.

Guerrero, S., Muñíz, E., Teijón, C., Olmo, R., Teijón, J. M. & Blanco, M.D. (2008). Ketotifen-loaded microspheres prepared by spray-drying poly(D,L-lactide) and poly(D,L-lactide-co-glycolide) polymers: characterization and in vivo evaluation. *Journal of pharmaceutical sciences*, *97*, 3153-69.

Hachicha, W., Fessi, H., Casoli-Bergeron, E., Lee, M., Jaafar, C., Clayer-Montembault, A., Burillon, C., Freney, J. & Kodjikian, L. (2007). In vitro efficacy of newly designed vancomycin-based microparticles. *Journal of cataract and refractive surgery*, *33*, 702-8.

Hachicha, W., Kodjikian, L. & Fessi, H. (2006). Preparation of vancomycin microparticles: importance of preparation parameters. *International journal of pharmaceutics*, *324*, 176-84.

Hamoudeh, M., Diab, R., Fessi, H., Dumontet, C. & Cuchet, D. (2008). Paclitaxel-loaded microparticles for intratumoral administration via the TMT technique: preparation, characterization, and preliminary antitumoral evaluation. *Drug development and industrial pharmacy*, *34*, 698-707.

Hedges, A. R. (1998). Industrial Applications of Cyclodextrins. *Chemical reviews*, *98*, 2035-2044.

Heger, M., Salles, I. I., de Kroon, A. I. P. M. & Deckmyn, H. (2009). Platelets and PEGylated lecithin liposomes: when stealth is allegedly picked up on the radar (and eaten). *Microvascular research*.

Higuchi, T. & Connors, K. (1965). Phase-solubility techniques. *Advances in Analytical Chemisty and Instrumentation* , *4*, 117–212.

Hillerdal, G., Sorensen, J. B., Sundström, S., Riska, H., Vikström, A. & Hjerpe, A. (2008). Treatment of malignant pleural mesothelioma with carboplatin, liposomized doxorubicin, and gemcitabine: a phase II study. *Journal of Thoracic Oncology*, *3*, 1325-31.

Hirlekar, R. & Kadam, V. (2009). Preformulation study of the inclusion complex irbesartan-beta-cyclodextrin. *AAPS PharmSciTech*, *10*, 276-81.

Hombreiro Pérez, M., Zinutti, C., Lamprecht, A., Ubrich, N., Astier, A., Hoffman, M., Bodmeier, R. & Maincent, P. (2000). The preparation and evaluation of poly(epsilon-caprolactone) microparticles containing both a lipophilic and a hydrophilic drug. *Journal of controlled release : official journal of the Controlled Release Society*, *65*, 429-38.

Ikeda, Y., Hirayama, F., Arima, H., Uekama, K. & Yoshitake, Y. (2004). NMR spectroscopic characterization of Metoprolol/cyclodextrine complexes in aqueous solution: cavity size dependency. *Journal of Pharmaceutical Sciences*, *93*, 1659-71.

Irie, T. & Uekama, K. (1997). Pharmaceutical applications of cyclodextrins. III. Toxicological issues and safety evaluation. *Journal of pharmaceutical sciences*, *86*, 147-62.

Iwata, M. & McGinity, J.W. (1992). Preparation of multi-phase microspheres of poly(D,L-lactic acid) and poly(D,L-lactic-co-glycolic acid) containing a W/O emulsion by a multiple emulsion solvent evaporation technique. *Journal of microencapsulation*, *9*, 201-14.

Karavas, E., Georgarakis, E., Sigalas, M. P., Avgoustakis, K. & Bikiaris, D. (2007). Investigation of the release mechanism of a sparingly water-soluble drug from solid dispersions in hydrophilic carriers based on physical state of drug, particle size distribution and drug-polymer interactions. *European journal of pharmaceutics and biopharmaceutics: official journal of Arbeitsgemeinschaft fur Pharmazeutische Verfahrenstechnik e.V*, *66*, 334-47.

Kim, S. I., Shin, D., Lee, H., Ahn, B., Yoon, Y. & Kim, M. (2009). Targeted delivery of siRNA against hepatitis C virus by apolipoprotein A-I-bound cationic liposomes. *Journal of hepatology*, *50*, 479-88.

Klose, D., Siepmann, F., Elkharraz, K., Krenzlin, S. & Siepmann, J. (2006). How porosity and size affect the drug release mechanisms from PLGA-based microparticles. *International journal of pharmaceutics*, *314*, 198-206.

Konduri, K. S., Nandedkar, S., Düzgünes, N., Suzara, V., Artwohl, J., Bunte, R. & Gangadharam, P.R.J. (2003). Efficacy of liposomal budesonide in experimental asthma. *The Journal of allergy and clinical immunology*, *111*, 321-7.

Koontz, J. L., Marcy, J. E., O'Keefe, S. F. & Duncan, S.E. (2009). Cyclodextrin inclusion complex formation and solid-state characterization of the natural antioxidants alpha-tocopherol and quercetin. *Journal of agricultural and food chemistry*, *57*, 1162-71.

Koshkina, N. V., Kleinerman, E. S., Waidrep, C., Jia, S. F., Worth, L. L., Gilbert, B. E. & Knight, V. (2000). 9-Nitrocamptothecin liposome aerosol treatment of melanoma and osteosarcoma lung metastases in mice. *Clinical cancer research : an official journal of the American Association for Cancer Research*, *6*, 2876-80.

Kreuter, J. (1983). Evaluation of nanoparticles as drug-delivery systems. III: materials, stability, toxicity, possibilities of targeting, and use. *Pharmaceutica acta Helvetiae*, *58*, 242-50.

Lagarce, F., Garcion, E., Faisant, N., Thomas, O., Kanaujia, P., Menei, P. & Benoit, J.P. (2006). Development and characterization of interleukin-18-loaded biodegradable microspheres. *International journal of pharmaceutics*, *314*, 179-88.

Lahiani-Skiba, M., Bounoure, F., Shawky-Tous, S., Arnaud, P. & Skiba, M. (2006). Optimization of entrapment of metronidazole in amphiphilic beta-cyclodextrin nanospheres. *Journal of pharmaceutical and biomedical analysis*, *41*, 1017-21.

Lamprecht, A., Ubrich, N., Hombreiro Pérez, M., Lehr, C., Hoffman, M. & Maincent, P. (1999). Biodegradable monodispersed nanoparticles prepared by pressure homogenization-emulsification. *International journal of pharmaceutics*, *184*, 97-105.

Lamprecht, A., Ubrich, N., Hombreiro Pérez, M., Lehr, C., Hoffman, M. & Maincent, P. (2000). Influences of process parameters on nanoparticle preparation performed by a double emulsion pressure homogenization technique. *International journal of pharmaceutics*, *196*, 177-82.

Lamprecht, A., Yamamoto, H., Takeuchi, H. & Kawashima, Y. (2003). Microsphere design for the colonic delivery of 5-fluorouracil. *Journal of controlled release : official journal of the Controlled Release Society*, *90*, 313-22.

Lebed', O. I., Stefanov, A. V. & Primak, R.G. (1989). [Effect of the conditions of ultrasonic treatment on the characteristics of forming liposomes]. *Ukrains'kyi biokhimichnyi zhurnal*, *61*, 96-101.

Lecaroz, C., Gamazo, C., Renedo, M. J. & Blanco-Prieto, M.J. (2006). Biodegradable micro- and nanoparticles as long-term delivery vehicles for gentamicin. *Journal of microencapsulation*, *23*, 782-92.

Lemoine, D. & Préat, V. (1998). Polymeric nanoparticles as delivery system for influenza virus glycoproteins. *Journal of controlled release: official journal of the Controlled Release Society*, *54*, 15-27.

Lemos-Senna, E., Wouessidjewe, D., Lesieur, S., Puisieux, F., Couarraze, G. & Duchêne, D. (1998). Evaluation of the hydrophobic drug loading characteristics in nanoprecipitated amphiphilic cyclodextrin nanospheres. *Pharmaceutical development and technology*, *3*, 85-94.

Leroux, J., Allémann, E., Doelker, E. & Gurny, R. (1995). New approach for the preparation of nanoparticles by an emulsification-diffusion method. *European journal of pharmaceutics and biopharmaceutics*, *41*, 14-18.

Li, S., Garreau, H., Pauvert, B., McGrath, J., Toniolo, A. & Vert, M. (2002). Enzymatic degradation of block copolymers prepared from epsilon-caprolactone and poly(ethylene glycol). *Biomacromolecules*, *3*, 525-30.

Lin, S. & Kao, Y. (1989). Studies on drug interaction in pharmaceutical formulations. Part XII. Solid particulates of drug-b-cyclodextrin inclusion complexes directly prepared by a spray-drying technique.. *International Journal of Pharmaceutics*, *56*, 249-259.

Lin, S., Kao, Y. & Yang, J. (1988). Grinding effect on some pharmaceutical properties of drugs by adding b-cyclodextrin.. *Drug Developement and Industrial Pharmacy*, *14*, 99–118.

Liu, Y., Chen, G., Chen, Y., Cao, D., Ge, Z. & Yuan, Y. (2004). Inclusion complexes of paclitaxel and oligo(ethylenediamino) bridged bis(beta-cyclodextrin)s: solubilization and antitumor activity. *Bioorganic & medicinal chemistry*, *12*, 5767-75.

Loftsson, T. & Brewster, M.E. (1996). Pharmaceutical applications of cyclodextrins. 1. Drug solubilization and stabilization. *Journal of pharmaceutical sciences*, *85*, 1017-25.

Loftsson, T., Gudmundsdóttir, H., Sigurjónsdóttir, J. F., Sigurdsson, H. H., Sigfússon, S. D., Másson, M. & Stefánsson, E. (2001). Cyclodextrin solubilization of benzodiazepines: formulation of midazolam nasal spray. *International journal of pharmaceutics*, *212*, 29-40.

Loftsson, T., Magnúsdóttir, A., Másson, M. & Sigurjónsdóttir, J.F. (2002). Self-association and cyclodextrin solubilization of drugs. *Journal of pharmaceutical sciences*, *91*, 2307-16.

Loftsson, T., Másson, M. & Sigurdsson, H.H. (2002). Cyclodextrins and drug permeability through semi-permeable cellophane membranes. *International journal of pharmaceutics*, *232*, 35-43.

Lu, R., Wang, H. & Tong, L. (1990). Spectroscopic studies on inclusion complexes of MAQO and MPQO with cyclodextrins. *Materials Science and Engineering C*, *16*, 2487-99.

Mallick, S., Pattnaik, S., Swain, K. & De, P.K. (2007). Current perspectives of solubilization: potential for improved bioavailability. *Drug development and industrial pharmacy*, *33*, 865-73.

Mao, S., Xu, J., Cai, C., Germershaus, O., Schaper, A. & Kissel, T. (2007). Effect of WOW process parameters on morphology and burst release of FITC-dextran loaded PLGA microspheres. *International journal of pharmaceutics*, *334*, 137-48.

Martin Del Valle, E. (2004). Cyclodextrins and their uses: a review. *Process Biochemistry*, *39*, 1033-46.

Mayhew, E., Rustum, Y. & Vail, W.J. (1983). Inhibition of liver metastases of M 5076 tumor by liposome-entrapped adriamycin. *Cancer drug delivery*, *1*, 43-58.

Menei, P., Montero-Menei, C., Venier, M. & Benoit, J. (2005). Drug delivery into the brain using poly(lactide-co-glycolide) microspheres. *Expert opinion on drug delivery*, *2*, 363-76.

Merodio, M., Arnedo, A., Renedo, M. J. & Irache, J.M. (2001). Ganciclovir-loaded albumin nanoparticles: characterization and in vitro release properties. *European journal of pharmaceutical sciences : official journal of the European Federation for Pharmaceutical Sciences*, *12*, 251-9.

Miller, L. A., Carrier, R. L. & Ahmed, I. (2007). Practical considerations in development of solid dosage forms that contain cyclodextrin. *Journal of pharmaceutical sciences*, *96*, 1691-707.

Miller, R. A., Brady, J. M. & Cutright, D.E. (1977). Degradation rates of oral resorbable implants (polylactates and polyglycolates): rate modification with changes in PLA/PGA copolymer ratios. *Journal of biomedical materials research*, *11*, 711-9.

Minato, S., Iwanaga, K., Kakemi, M., Yamashita, S. & Oku, N. (2003). Application of polyethyleneglycol (PEG)-modified liposomes for oral vaccine: effect of lipid dose on systemic and mucosal immunity. *Journal of controlled release : official journal of the Controlled Release Society*, *89*, 189-97.

Montasser, I., Briançon, S., Fessi, H. & Lieto, J. (2000). Procédé de préparation de systèmes colloïdaux de type nanocapsule par polycondensation interfaciale. Brevet français 0003133.

Munshi, N., De, T. & Maitra, A. (1997). Size Modulation of Polymeric Nanoparticles under Controlled Dynamics of Microemulsion Droplets. *Journal of colloid and interface science*, *190*, 387-91.

Müller, P. & Simon, B. (1997). [Comparative endoscopic study of gastroduodenal tolerance of piroxicam-beta-cyclodextrin vs piroxicam]. *Zeitschrift fur Rheumatologie*, *56*, 76-9.

Nicholas, A. P., McInnis, C., Gupta, K. B., Snow, W. W., Love, D. F., Mason, D. W., Ferrell, T. M., Staas, J. K. & Tice, T.R. (2002). The fate of biodegradable microspheres injected into rat brain. *Neuroscience letters*, *323*, 85-8.

Nihant, N., Schugens, C., Grandfils, C., Jérôme, R. & Teyssié, P. (1994). Polylactide microparticles prepared by double emulsion/evaporation technique. I. Effect of primary emulsion stability. *Pharmaceutical research*, *11*, 1479-84.

Olivier, J-C (2005). Drug transport to brain with targeted nanoparticles. *NeuroRx : the journal of the American Society for Experimental NeuroTherapeutics*, *2*, 108-19.

Pektok, E., Nottelet, B., Tille, J., Gurny, R., Kalangos, A., Moeller, M. & Walpoth, B.H. (2008). Degradation and healing characteristics of small-diameter poly(epsilon-caprolactone) vascular grafts in the rat systemic arterial circulation. *Circulation*, *118*, 2563-70.

Puglisi, G., Giammona, G., Fresta, M., Carlisi, B., Micali, N. & Villari, A. (1993). Evaluation of polyalkylcyanoacrylate nanoparticles as a potential drug carrier: preparation, morphological characterization and loading capacity. *Journal of microencapsulation*, *10*, 353-66.

Péan, J. M., Venier-Julienne, M. C., Boury, F., Menei, P., Denizot, B. & Benoit, J.P. (1998). NGF release from poly(D,L-lactide-co-glycolide) microspheres. Effect of some formulation parameters on encapsulated NGF stability. *Journal of controlled release: official journal of the Controlled Release Society*, *56*, 175-87.

Quintanar-Guerrero, D., Allémann, E., Fessi, H. & Doelker, E. (1998). Preparation techniques and mechanisms of formation of biodegradable nanoparticles from preformed polymers. *Drug development and industrial pharmacy*, *24*, 1113-28.

Redziniak, G. (2003). Liposomes and skin: past, present, future. *Pathologie-biologie*, *51*, 279-81.

Sanders, L. M., Kent, J. S., McRae, G. I., Vickery, B. H., Tice, T. R. & Lewis, D.H. (1984). Controlled release of a luteinizing hormone-releasing hormone analogue from poly(d,l-lactide-co-glycolide) microspheres. *Journal of pharmaceutical sciences*, *73*, 1294-7.

Sansdrap, P. & Moës, A.J. (1998). Influence of additives on the release profile of nifedipine from poly(DL-lactide-co-glycolide) microspheres. *Journal of microencapsulation*, *15*, 545-53.

Sathigari, S., Chadha, G., Lee, Y. P., Wright, N., Parsons, D. L., Rangari, V. K., Fasina, O. & Babu, R.J. (2009). Physicochemical characterization of efavirenz-cyclodextrin inclusion complexes. *AAPS PharmSciTech*, *10*, 81-7.

Shive, M. & Anderson, J. (1997). Biodegradation and biocompatibility of PLA and PLGA microspheres. *Advanced drug delivery reviews*, *28*, 5-24.

Silva-Cunha, A., Fialho, S., Naud, M. & Behar-Cohen, F. (2008). Poly-epsilon-caprolactone intravitreal devices: in vivo study. *Investigative ophthalmology & visual science*, 0, iovs. 08-2969v1.

Stella, V. J. & He, Q. (2008). Cyclodextrins. *Toxicologic pathology*, *36*, 30-42.

Szejtli, J. & Szente, L. (2005). Elimination of bitter, disgusting tastes of drugs and foods by cyclodextrins. *European journal of pharmaceutics and biopharmaceutics : official journal of Arbeitsgemeinschaft fur Pharmazeutische Verfahrenstechnik e.V*, *61*, 115-25.

Tahara, K., Sakai, T., Yamamoto, H., Takeuchi, H. & Kawashima, Y. (2008). Establishing chitosan coated PLGA nanosphere platform loaded with wide variety of nucleic acid by complexation with cationic compound for gene delivery. *International journal of pharmaceutics*, *354*, 210-6.

Taira, M. C., Chiaramoni, N. S., Pecuch, K. M. & Alonso-Romanowski, S. (2004). Stability of liposomal formulations in physiological conditions for oral drug delivery. *Drug delivery*, *11*, 123-8.

Tewes, F., Munnier, E., Antoon, B., Ngaboni Okassa, L., Cohen-Jonathan, S., Marchais, H., Douziech-Eyrolles, L., Soucé, M., Dubois, P. & Chourpa, I. (2007). Comparative study of doxorubicin-loaded poly(lactide-co-glycolide) nanoparticles prepared by single and double emulsion methods. *European journal of pharmaceutics and biopharmaceutics : official journal of Arbeitsgemeinschaft fur Pharmazeutische Verfahrenstechnik e.V*, *66*, 488-92.

Tongiani, S., Velde, D. V., Ozeki, T. & Stella, V.J. (2005). Sulfoalkyl ether-alkyl ether cyclodextrin derivatives, their synthesis, NMR characterization, and binding of 6alpha-methylprednisolone. *Journal of pharmaceutical sciences*, *94*, 2380-92.

Torchilin, V. P. (2005). Recent advances with liposomes as pharmaceutical carriers. *Nature reviews. Drug discovery*, *4*, 145-60.

Ubrich, N., Bouillot, P., Pellerin, C., Hoffman, M. & Maincent, P. (2004). Preparation and characterization of propranolol hydrochloride nanoparticles: a comparative study. *Journal of controlled release : official journal of the Controlled Release Society*, *97*, 291-300.

Uekama, K., Hirayama, F., Yamada, Y., Inaba, K. & Ikeda, K. (1979). Improvements of dissolution characteristics and chemical stability of 16,16-dimethyl-trans-delta 2-prostaglandin E1 methyl ester by cyclodextrin complexation. *Journal of pharmaceutical sciences*, *68*, 1059-60.

Valmikinathan, C. M., Defroda, S. & Yu, X. (2009). Polycaprolactone and Bovine Serum Albumin Based Nanofibers for Controlled Release of Nerve Growth Factor. *Biomacromolecules*.

Vanderhoff, J., El-Aassar, M. & Ugelstad, J. (1979). Polymer emulsification process. US patent 4 177 177.

Veiseh, O., Sun, C., Gunn, J., Kohler, N., Gabikian, P., Lee, D., Bhattarai, N., Ellenbogen, R., Sze, R., Hallahan, A., Olson, J. & Zhang, M. (2005). Optical and MRI multifunctional nanoprobe for targeting gliomas. *Nano letters*, *5*, 1003-8.

Vert, M., Li, S. M. & Garreau, H. (1994). Attempts to map the structure and degradation characteristics of aliphatic polyesters derived from lactic and glycolic acids. *Journal of biomaterials science. Polymer edition*, *6*, 639-49.

Vyas, S. P., Kannan, M. E., Jain, S., Mishra, V. & Singh, P. (2004). Design of liposomal aerosols for improved delivery of rifampicin to alveolar macrophages. *International journal of pharmaceutics*, *269*, 37-49.

Wassef, N. M., Matyas, G. R. & Alving, C.R. (1991). Complement-dependent phagocytosis of liposomes by macrophages: suppressive effects of "stealth" lipids. *Biochemical and biophysical research communications*, *176*, 866-74.

Weidenauer, U., Bodmer, D. & Kissel, T. (2003). Microencapsulation of hydrophilic drug substances using biodegradable polyesters. Part I: evaluation of different techniques for the encapsulation of pamidronate di-sodium salt. *Journal of microencapsulation*, *20*, 509-24.

Werninghaus, K., Handjani, R. M. & Gilchrest, B.A. (1991). Protective effect of alpha-tocopherol in carrier liposomes on ultraviolet-mediated human epidermal cell damage in vitro. *Photodermatology, photoimmunology & photomedicine*, *8*, 236-42.

Yan, X., Scherphof, G. L. & Kamps, J.A.A.M. (2005). Liposome opsonization. *Journal of liposome research*, *15*, 109-39.

Zhang, Y., Yang, F., Yang, Y., Song, F. & Xu, A. (2008). Recombinant interferon-alpha2b poly(lactic-co-glycolic acid) microspheres: pharmacokinetics-pharmacodynamics study in rhesus monkeys following intramuscular administration. *Acta pharmacologica Sinica*, *29*, 1370-5.

Zweers, M. L. T., Grijpma, D. W., Engbers, G. H. M. & Feijen, J. (2003). The preparation of monodisperse biodegradable polyester nanoparticles with a controlled size. *Journal of biomedical materials research. Part B, Applied biomaterials*, *66*, 559-66.

Chapitre 2
Les systèmes de délivrance des analogues de nucléosides pour le traitement du cancer

Review

Expert Opinion

informa healthcare

Nucleoside analogue delivery systems in cancer therapy

Roudayna Diab, Ghania Degobert, Misara Hamoudeh, Charles Dumontet & Hatem Fessi†

†*Université Claude Bernard Lyon 1, Laboratoire d'Automatique et de Génie des Procédés (LAGEP), UMR-CNRS 5007 CPE Lyon, ISPB, 43, Boulevard du 11 Novembre 1918, 69622 Villeurbanne Cedex, France*

Nucleoside analogues (NAs) are important agents in the treatment of hematological malignancies. They are prodrugs that require activation by phosphorylation. Their rapid catabolism, cell resistance and overdistribution in the body jeopardize nucleoside analogue chemotherapy. Accordingly, therapeutic doses of NAs are particularly high and regularly have to be increased, resulting in severe toxicity and narrow therapeutic index. The major challenge is to concentrate the drug at the tumour site, avoiding its distribution to normal tissues. New drug carriers and biomaterials are being developed to overcome some of these obstacles. This review highlights novel NA delivery systems and discusses new technologies that could improve NA cancer therapy.

Keywords: DepoFoam™, dendrimers, inclusion complexes, liposomes, microparticles, nanoparticles, polymeric micelles, polyplex nanogels, Stealth® particles, vesicular phospholipid gel

Expert Opin. Drug Deliv. (2007) 4(5):513-531

1. Introduction

Nucleosides analogues (NAs) are critical components of anticancer, antiviral and immunosuppressive therapy. They are antimetabolites, a class of drugs that inhibit DNA synthesis either directly or through inhibition of DNA precursor synthesis on the *de novo* or salvage pathways [1,2]. The anticancer nucleosides include several analogues of physiological pyrimidine and purine nucleosides and nucleobases [1]. Among the presently available analogues of purine are cladribine, fludarabine and clofarabine, and those of pyrimidine are cytarabine and gemcitabine.

A major obstacle associated with the use of NA chemotherapeutic agents is the lack of selectivity toward cancerous cells. Consequently, the effective doses of NA anticancer agents are particularly high and have regularly to be increased. In this context, toxicity becomes the main limiting factor to the treatment. NA intracellular delivery is another major challenge, as these compounds are hydrophilic and therefore require facilitated transport to cross cellular membranes [3].

To exploit the specificity and potency of these drugs, several carrier systems, such as liposomes, nanoparticles, polyplex nanogels and polymeric micelles, have been developed as potential tools of tumour targeting, facilitating drug uptake by cancerous cells, and therefore increasing both safety and efficiency of NAs in cancer therapy.

In this paper, the authors overview the principal limitations of NAs and then present the presently available NA carriers and their role in NA tumour targeting.

2. The mechanism of action of nucleoside analogues

NAs mimic natural nucleosides. They are administered in forms that enter into the cells through nucleosides transporters before being phosphorylated to their active triphosphate form inside the cell by the kinases [4]. These agents can exert their

10.1517/17425247.4.5.513 © 2007 Informa UK Ltd ISSN 1742-5247

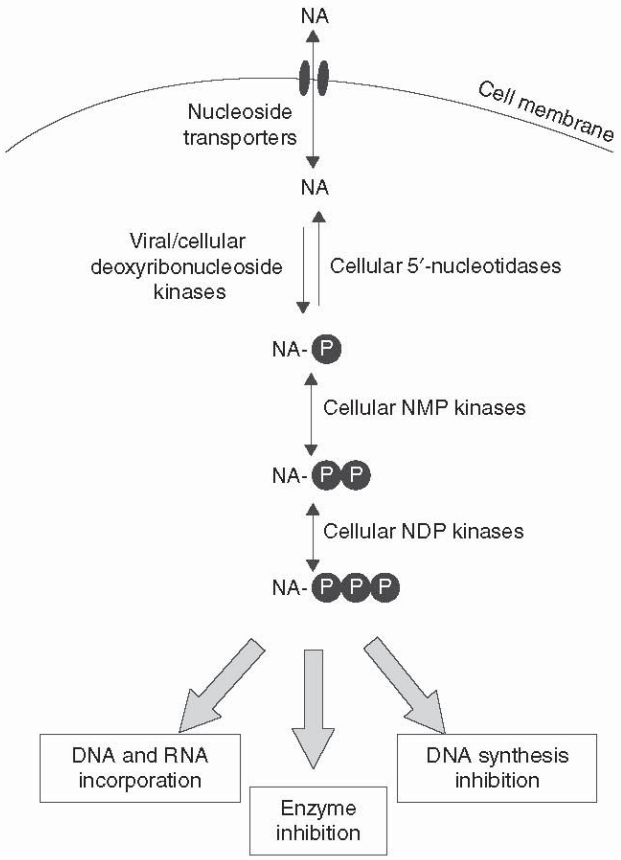

Figure 1. Nucleoside analogues require intracellular phosphorylation for pharmacological activity. The nucleoside analogues are transported across the cell membrane and phosphorylated by cellular kinases to their triphosphate form.
This figure was published in [4], Copyright Elsevier (2003).
NDP: Ribonuclotide diphosphate; NMP: Ribonuclotide monophosphate.

cytotoxic activity by being incorporated into and altering the DNA and RNA macromolecules themselves and/or by interfering with various enzymes involved in the nucleic acid synthesis, such as DNA polymerases and ribonucleotides reductases [1]. These actions result in the inhibition of DNA synthesis and the induction of apoptic cell death (**Figure 1**).

3. Physiological deoxyribonucleotide and ribonucleotide metabolism

Deoxyribonucleotides and ribonucleotides have to be synthesized within the cells because there is no carrier protein for them in the cell membrane. There are two synthesis pathways, called the *de novo* pathway and the salvage pathway [2,4].

Via the *de novo* pathway, ribonucleotides are synthesized from small molecules (amino acids, ribose-5′-phosphate and CO_2) to mononucleotides and then they undergo further phosphorylation (**Figure 2**). The 2′-OH group of the ribonuclotide diphosphate can be reduced to the corresponding 2′-deoxyribonucleotide diphosphate by ribonucleotide reductases.

In the salvage pathway, deoxyribonucleotides are synthesized from deoxyribonucleosides, catalyzed by the deoxyribonucleoside kinases, nucleoside monophosphate and diphosphate kinases. In addition, there are two salvage pathways for ribonucleotides. The first is from free bases, which undergo further phosphorylation through direct sugar phosphate transfer. The second salvage ribonuclotide pathway is from ribonucleosides, which are transformed by further phosphorylation to their triphosphate form [2,4]. Ribonucleosides and deoxyribonucleosides are imported into cells by nucleoside transport proteins that facilitate diffusion or actively transport nucleosides across the membrane.

In proliferating cells, the de novo deoxyribonucleotides synthesis is the main source for nuclear DNA replication [2,4] and takes place only in S phase of the cell cycle. Deoxyribonucleotides synthesized in the salvage pathway are believed to be important for DNA repair and this pathway is active throughout the cell cycle. The deoxyribonucleosides salvage pathway is of a particular interest to pharmacologists because NAs used to treat cancer are administered as prodrugs that are activated inside the cells by the salvage enzymes. Consequently, the rate of NA phosphorylation to the active triphosphate form may directly determine the therapeutic efficacy of these agents.

4. Limitations to nucleosides analogues

The chemotherapeutic treatment of tumours with NAs is potentially limited by their narrow therapeutic index, due to low anticancer activity and/or severe side effects. NAs are not naturally specific to tumour cells; hence they accumulate not only in tumours but also in healthy tissues. Furthermore, most NAs have only short half-lifes in the systemic circulation due their rapid enzymatic degradation; as a consequence, very high doses have to be given for efficient tumour treatment, leading to severe side effects.

4.1 Cytotoxicity and pronounced side effects

NAs are cytotoxic agents that can disturb the cellular metabolism, deregulating the physiological nucleoside/nucleotide pools in both normal and cancerous cells, due to the lack of their selectivity towards malignant cells. At conventional doses, NAs induce myelosuppression, hepatotoxicity (gemcitabine, fludarabine and cladribine) [1,5], renal toxicity (gemcitabine), leucopoenia, thrombocytopenia, mucositis and hair loss (cytarabine). Furthermore, NA high doses have commonly been associated with neurotoxicity and pericarditis (cytarabine and fluorouracil).

4.2 Emergence of drug resistance and low anticancer activity

There are three general mechanisms of resistance to NAs that have been described in cell lines and clinical samples:

- Insufficient intracellular concentrations of NA triphosphate, which might be due to inefficient cellular uptake caused by

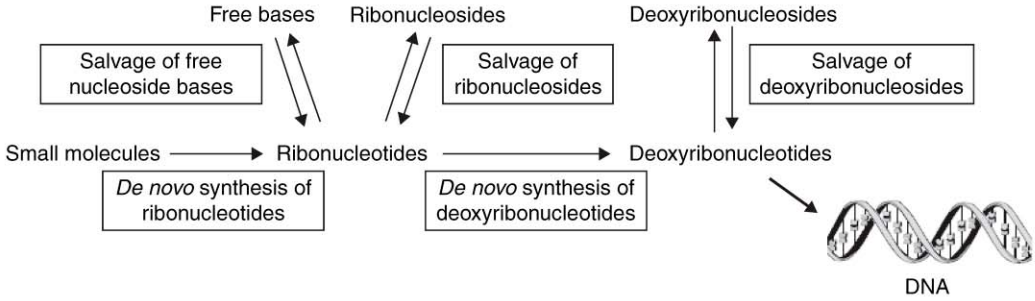

Figure 2. *De novo* and salvage synthesis of ribonucleotides and deoxyribonucleotides.
This figure was published in [4], Copyright Elsevier (2003).

deficiency in cellular membrane nucleoside transporters [3] or elevated levels of 5′-nucleotidases that remove the phosphate group from mononucleotides. The resulting nucleosides can be exported by nucleoside transporters outside of the cell [2], the levels of activating enzymes, such as nucleosides and deoxynucleoside kinases decrease [6], and catabolism caused by cellular over expression of 5′-nucleotidases [7] or deaminases increases [5,8].

- Inability to achieve sufficient alterations in DNA strands or deoxynucleotide triphosphate pools, which might result from altered interactions with DNA polymerases. This would reduce the affinity of these enzymes for NAs, reduce the inhibition of ribonucleotide reductases and cause expansion of deoxynucleotide triphosphate pools that may compete with NAs for incorporation into DNA [6].
- Defective induction of apoptosis. The key event of apoptosis is caspase activation, which may be a consequence of death triggering mitochondrial activation [9].

4.3 Hydrophilicity and low membrane permeability

NAs are hydrophilic polar molecules with low membrane permeability [5], and, thus, require specialised nucleoside transporter proteins to enter cells. Therefore, the abundance and tissue distribution of these transporters contributes to cellular specificity and sensitivity to nucleoside analogues [1]. On the other hand, there are no transporter proteins for ribonucleotides and deoxyribonucleotides in the cell membrane, and their negatively charged phosphate groups prevent their diffusion across the membrane [4].

4.4 Bioconversion *in vivo* drug catabolism and rapid clearance

The cytidine analogues, such as gemcitabine and cytarabine, undergo extensive degradation by cytidine deaminase to inactive metabolites (uracil arabinoside) in the liver and kidneys, which adversely affects their activities [5,8,10]. Consequently, these analogues have short circulation half-lifes of 10 – 20 min, and so they fail to maximize the intracellular accumulation of their active metabolites. After oral administration, although these drugs have shown to be stable at pH 1, and well-absorbed via the gastrointestinal tract, they are metabolized extensively in the first pass through the liver, as well as by the bacterial gut flora; as a consequence, they have poor oral bioavailability due to rapid hepatic deamination [11].

Purine analogues, such as cladribine, are unstable at low pH and are deglycosylated by bacterial gut flora purine nucleoside phosphorylases to chloroadenine, which has a lower cytotoxic effect [12]. Furthermore, cladribine can be cleaved in an enzymatic reaction to chloroadenine in the presence of the hepatic enzyme methylthioadenosine phosphorylase [12].

Given the previous limitations, a variety of novel drug delivery systems are presently being developed in an attempt to address some of the problems associated with the lack of NA stability and selectivity towards tumour tissues.

5. Nucleoside analogue delivery systems in cancer therapy

As previously mentioned, the efficacy of cancer chemotherapy is limited by the non-specificity of anticancer drugs, leading to severe systemic toxicity. The ideal scenario would be to sequester the drug in a package that would have minimal interactions with healthy cells, and to release drug at the appropriate time from the sequestering carrier at the tumour site.

Several drug delivery systems, namely liposomes, microparticles, nanoparticles, polymeric micelles, dendrimers, hydrogels, polyplex nanogels and cyclodextrin inclusion complexes, have been introduced in order to facilitate effective chemotherapy and to overcome some of the above limitations of NAs. The extended release of NA molecules has been made possible using microsized system, such as microparticles (e.g., DepoFoam™; SkyePharma), resulting in reduced toxicity and improved efficacy, especially for cell cycle-specific NAs. However, nano-sized carriers can either allow NAs to be passively targeted, as with long-circulating liposomes, or actively targeted, in the case of magnetic or pH-sensitive nanoparticles. Furthermore, polyplex nanogels seem to be an ideal carrier for NAs, by administering them in their active tri-phosphate form, avoiding the emergence of cellular

resistance related to the decreased activity of deoxycytidine kinase. Finally, their small size and the option to bind ligands to their surface resolve the relevant problems of NA poor cellular uptake and poor tumour cell selectivity, respectively.

The following sections cover the use of all these systems as carriers for NAs in detail.

5.1 Liposomal formulations

Liposomes are self-assembling vesicles with an inner aqueous compartment surrounded by a lipid bilayer, which consists of naturally occurring phospholipids as a main component [13]. Lipophilic and amphiphilic drugs can be incorporated into the liposomal bilayers, whereas hydrophilic drugs can be incorporated into the inner aqueous compartment. Thus, the systemic environment does not recognize the free drug. It recognizes only the liposomes and the drug pharmacokinetics become replaced by the pharmacokinetic behaviour of the liposomes..

Liposomes can be classified in two ways [14]:

- Classification according to structure and size (**Figure 3**):
  - Unilamellar liposomes, comprising one lipid bilayer and having diameters of 50 – 250 nm. They contain a large aqueous core and are used for the encapsulation of water-soluble drugs.
  - Multilamellar liposomes composed of several concentric lipid bilayers in an onion-skin arrangement and have diameters of 1 – 5 µm.
  - Multivesicular liposomes (MVLs, e.g., DepoFoam), consisting of numerous non-concentric lipid bilayers in a honey comb arrangement and have diameters of 1 – 100 µm.
- Classification according to a phylogenetic scheme:
  - Classical or conventional liposomes (simple mixtures of phospholipids and cholesterol) target the reticulo-endothelial system (RES) and are called RES-targeted liposomes. Vesicle size is inversely correlated with the amount of RES uptake.
  - Sterically stabilized liposomes, or surface-modified liposomes (by coating liposomes with polyethylene glycol; STEALTH® technology [ALZA]) escape from the RES uptake, allowing drug to target malignant tissues.

Liposomal formulations aim to reduce the toxic side effects of cytotoxic drugs without hampering their efficacy. This can be achieved by a selective drug accumulation in tumour tissues by means of active targeting (coating liposomes with antibodies or ligands in order to specifically recognize epitopes or receptors of malignant cells) [15,16], or by passive targeting due to the enhanced permeability and retention effect of sterically stabilized liposomes, due to differences in the vasculature between tumours and healthy organs or tissues [16].

5.1.1 Conventional liposomes

As most of NAs are polar (amphipathic at minimum) and water soluble, most early efforts in liposomal anticancer drug development focused on entrapping agents such as cytarabine in an attempt to improve its therapeutic index. However, significant protection from deamination and improvement of antitumour activity could not be achieved, mainly due to the drug leakage (initial burst) from liposomes, which is caused by their well-characterised instability and short half-life *in vivo*. The half-life of liposomes is generally influenced by their stability in serum [17] and their uptake by RES cells [18]. The uptake of liposomes by the RES is triggered by the binding of serum proteins to their phospholipid bilayer (opsonization). Once opsonized, liposomes can be rapidly recognized and phagocytosed. On the other hand, it is very difficult using presently available technologies to stably encapsulate water-soluble low molecular weight drugs such as NAs into conventional liposomes: these molecules diffuse rapidly through liposome bilayers. Thus, shortly after their preparation, rapid diffusion of the drug out of the liposomes occurs, limiting the shelf life and, therefore, the clinical use of conventional liposomes.

Much research work has tried to overcome the instability of liposomes in serum by optimizing their formulation. It was found that the addition of cholesterol in quantities of 35 – 50% mol of the cytarabine liposomal formulation stabilized membranes by reducing membrane fluidity and enhanced the encapsulation efficiency of cytarabine-loaded liposomes [19]. Furthermore, liposomal membranes consisting of glycerophospholipids with long hydrogenated fatty acid esters (e.g., synthetic phospholipids), such as distearoylphosphatidylcholine, have been shown to be more rigid than those consisting of glycerophospholipids made up of fatty acids of different lengths and saturation (e.g., egg lecithin, soya lecithin) [13,16]. As a consequence, these liposomal membranes are more stable against lipid exchange by serum proteins, as a rigid membrane decreases the efflux of drugs from liposomes and stabilizes the liposomes themselves.

5.1.2 Stealth liposomes

The modification of liposome composition with PEG-containing lipids greatly enhances their stability in the circulation. Components that sterically stabilize liposomes, such as PEG-phosphatidylethanolamine (Stealth components), lower the recognition and uptake by the RES by increasing the liposome hydrodynamic circumference (**Figure 4**). When gemcitabine was encapsulated in pegylated liposomes (Stealth liposomes), a significant antitumour effect was observed using lower drug concentrations and after an earlier exposure time [20]. Also, the cytotoxic activity of cytarabine encapsulated in long-circulating PEG liposomes (Stealth liposomes) was superior to that of other liposome formulations or of the free drug [21]. In fact, the increased permeability of the tumour endothelium allows liposomes to be extravasated, and the deficient lymphatic drainage lead to the drug being selectively accumulated in the site of action (enhanced permeability and retention effect) [22].

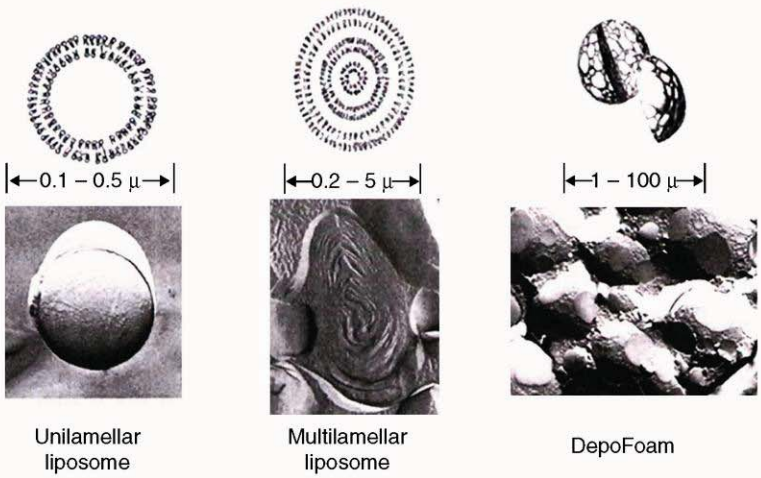

Figure 3. Stuctural differences between conventional liposomes and DepoFoam.
This figure was published in [23], Copyright Elsevier (2004).

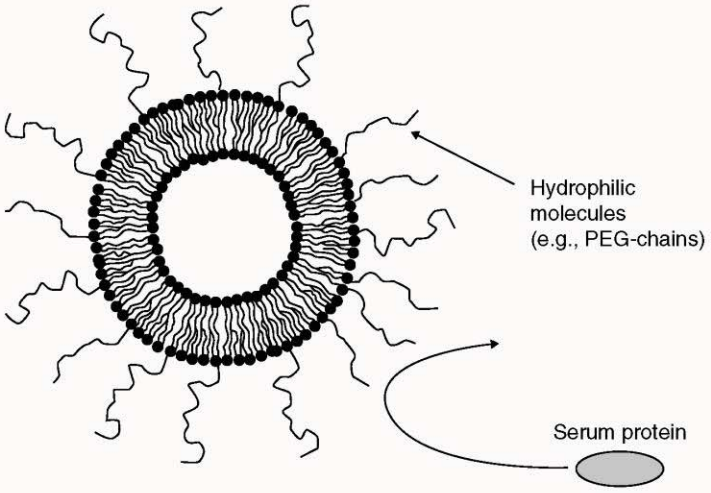

Figure 4. Sterically stabilized liposomes (Stealth liposomes): the interaction of serum proteins with the liposome bilayers is reduced by surrounding the liposomes with large hydrophilic molecules (e.g., PEG chains, pegylation of liposomes).
Reproduced with permission from [13].

More exciting results were obtained by sequestering the drug in multivesicular lipid-based particles using DepoFoam technology.

5.1.3 *Multivesicular liposomes (DepoFoam)*

The DepoFoam drug delivery system was developed to permit sustained release of water-soluble drugs, capable of delivering drugs for periods extending from a few days to a few weeks, from a depot after direct injection into a body compartment or a tissue [23].

DepoCyt® (cytarabine-loaded multivesicular liposomes; SkyePharma) is the first product based on the DepoFoam technology to be approved by the FDA. DepoCyt is an intrathecally injectable suspension of cytarabine encapsulated in DepoFoam particles (SkyePharma). Each particle has a diameter of ~ 3 – 30 µm and consists of numerous non-concentric vesicles in a honeycomb arrangement. The chambers are separated from each other by lipid bilayers consisting of dioleyl-phosphatidylcholine, dipalmitoyl-phosphatidylglycerol, cholesterol and triolein [21] (**Figure 5**).

The characteristic nonconcentric nature of a DepoFoam particle results in a higher aqueous/lipid ratio than for a concentric multilamellar liposomes, leading to greater encapsulation efficiencies for water-soluble drugs. Furthermore, the interconnection between the internal membranes gives rise to greater mechanical strength and stability than those known for traditional liposomes of equivalent size and aqueous content [14]. At a storage temperature of 2 – 8°C,

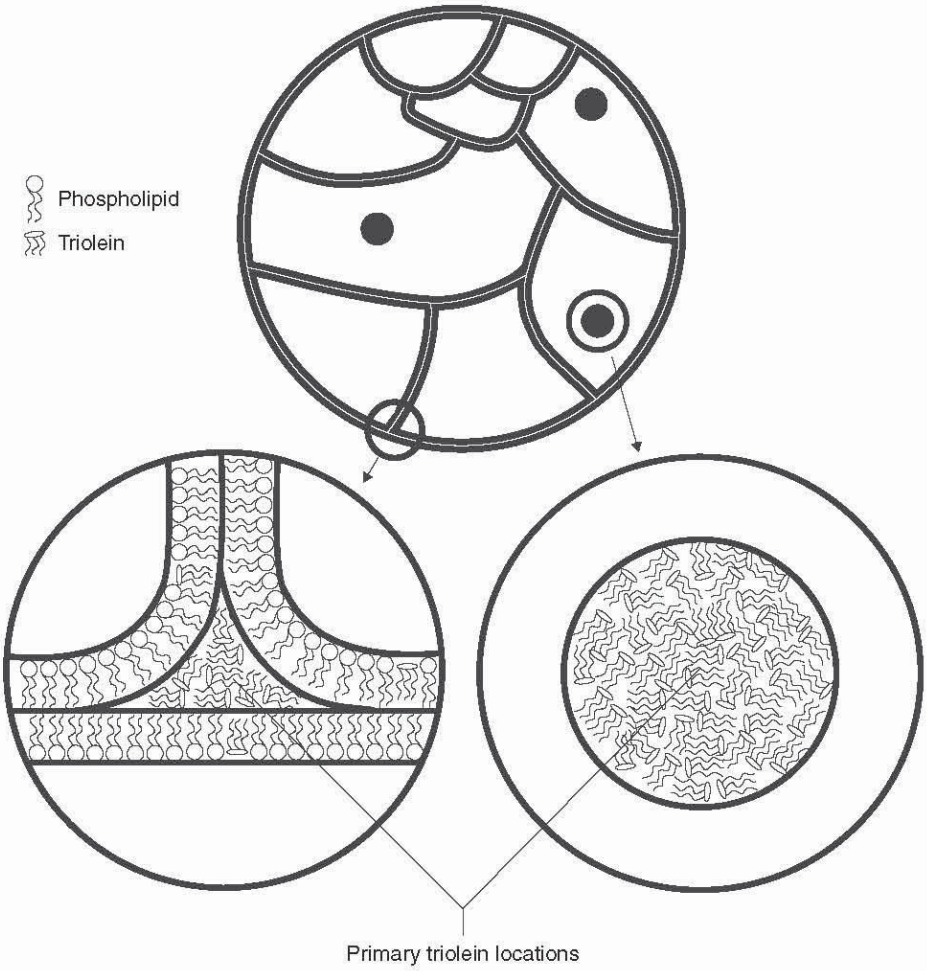

Figure 5. Schematic showing the location of triglycerides in DepoFoam.
This figure was published in [23], Copyright Elsevier (2004).

the particles are stable for 12 months. DepoCyt has a mean half-life of 130 – 277 h, compared with 3 – 4 h for free cytarabine [14].

Another NA that is an antiviral drug, acyclovir, was conditioned in MVLs in order to overcome the limitations of conventional liposomal therapies. The encapsulation efficiency in MVLs (45 – 82%) was found to be 3- to 6-times higher than that in conventional multilamellar vesicles. In addition, the *in vitro* release of acyclovir from MVLs was found to be in a sustained manner, and only 70% of drug was released in 96 h, whereas conventional multilamellar liposomes released 80% of drug in 16 h [24]. Moreover, formulations containing phosphatidylglycerol as negatively charged lipid showed better results because they increase the intralamellar distance between the successive bilayers of the MVL structure, which leads to a greater overall capture volume. Neutral oil is an integral structural component: it becomes a part of the corner or edges where membranes meet [24].

A more recent strategy to increase the shelf life of liposomal formulations is the encapsulation of small, hydrophilic molecules, such as NAs, into vesicular phospholipid gels (VPGs).

5.1.4 *Vesicular phospholipid gels*

VPGs are semisolid matrices of densely packed liposomes – mainly small unilamellar vesicles – which are prepared by high-pressure homogenization [25]. Due to their high lipid content, which leads to a considerably increased ratio of aqueous volume inside the vesicles compared with the surrounding aqueous volume, these formulations are suitable for entrapping water-soluble substances with high encapsulation efficiency compared with conventional liposomal formulations [26]. Moreover, due to their high lipid concentrations, these formulations have a semisolid or gel-like consistency. In contrast to conventional liposomal formulations, the non-encapsulated drug is not removed at the end of the preparation process, so that the drug is entrapped inside the liposomes and between them in the surrounding aqueous phase. This special characteristic leads to an increased shelf life and an increased encapsulation

efficiency of the drug-loaded VPG. This has been demonstrated for gemcitabine and 5-fluorouracil (5-FU)-loaded VPG formulations [27,28]. For gemcitabine, the drug still diffused through the liposomal bilayers, and thus its concentration was always in equilibrium between the inner and outer aqueous phases of the liposomes. As the volumes of the aqueous phases inside and outside the vesicles have the same magnitude, the concentration of the drug remained the same, resulting in a superior shelf life of gemcitabine-loaded VPG. Furthermore, the liposomal entrapment of gemcitabine in VPG was demonstrated to positively change its pharmacokinetics and pharmacodynamics and, hence, to enhance its antitumour activity [27] (**Figure 6**). This effect can be attributed to three reasons: i) prolonged circulation of the liposomally entrapped gemcitabine in blood and therefore prolonged drug exposure to the tumour; ii) protection of the drug against rapid metabolic inactivation; and iii) enhanced uptake and accumulation of the drug within the tumour by the enhanced permeability and retention effect [22].

The influence of the VPG lipid composition on the encapsulation efficiency was studied in 5-FU-loaded VPG [28], using mixtures of hydrogenated soy phosphatidylcholine and cholesterol with molar ratios ranging from 55/45 to 75/25. Interestingly, it was found that a decreasing amount of cholesterol correlated with an increasing encapsulation efficiency, which was probably due to a reduced amount of smaller vesicles and the number of lamellae.

5.2 Hydrogels

A hydrogel is a three-dimensional network of hydrophilic polymers swollen in water, being maintained in the form of an elastic solid. Hydrogels usually contain water accounting for at least 10% of the total weight [29]. They are divided into chemical and physical gels depending on the nature of the crosslinking. Chemical gels are those having covalently crosslinked networks. They can be prepared by two different approaches. First, they can be made by the polymerization of water-soluble monomers in the presence of bi- or multi-functional crosslinking agents (crosslinking polymerization). Second, chemical gels can be prepared by crosslinking water-soluble polymer molecules using typical organic chemical reactions that involve functional groups of the polymers. Physical gels are continuous disordered three-dimensional networks formed by noncovalent interactions such as hydrogen bonding, ionic association, hydrophobic interaction, stereocomplex formation and solvent complexation [29].

Hydrogel delivery systems can be administered by implantation into the tumour site, for topical, oral or rectal administrations. The drug release rate from hydrogel implants can be controlled by adjusting the crosslinking density and/or by adding water-soluble components. For example, the entrapment of 5-FU in poly(2-hydroxyethyl methacrylate-co-acrylamide) hydrogels allowed 5-FU to be included in the feed mixture of polymerization, up to 16 mg/disc, without any chemical drug alteration; it also made possible the control of its release over a wide range of times varying between 7 h and 9 days, just by modulating the crosslinking degree of the copolymer (**Figure 7**), as well as their comonomeric composition, maintaining sufficiently high hydrate degrees (66 ± 24 wt%) [30].

5.3 Polyplex nanogel formulations

The polyplex nanogels are hydrophilic nanosized particles consisting of crosslinked cationic polymers. Hydrophilic ionisable polymers are able to bind biomolecules of opposite charge, forming polyionic complexes or polyplexes, and deliver them into various biological environments [31]. This delivery system was studied to be a candidate for the vectorization of NA 5′-triphosphates [32]. In this study, a polycationic polymer polyethylenimine (PEI) was used to bind the active 5′-triphosphate form of fludarabine (FATP) to PEI's protonated amino groups. Subsequent compaction of the flexible nanogel network has resulted in the encapsulation of the FATP/PEI complex in a dense core surrounded by a hydrophilic PEG envelope. This structure has provided the sustained release of the drug, as well as an efficient protection of FATP against enzymatic degradation.

Cancer cell-targeting molecules, such as folate, can be easily attached to nanogels (**Figure 8**), and this modification has resulted in a strong 10-fold increase of the carrier's internalization in human breast carcinoma MCF-7 cells.

Tri-phosphorylated NAs (NTPs) are efficient terminators of nucleic acid synthesis in proliferating cancer cells, but they are considered to be unstable for direct use in cancer chemotherapy. The application of these delivery systems for NTP encapsulation and targeting offers hope to resolve many of the problems associated with this chemotherapy, especially the avoidance of the development of drug resistance due to decreased nucleoside kinase activity. In addition, they also protected the drug against the enzymatic degradation. These formulations allow lower doses of NAs to be administered, while maintaining strong anticancer efficacy.

This approach is very mild, efficient, and non-damaging to the NTP structure compared with their encapsulation into biodegradable nanoparticles or liposomes, for example. Drug-loaded nanogel formulations are easily dispersed in water, aggregationally stable, and of great importance from a pharmaceutical viewpoint, as they can be lyophilized and redissolved instantly at the moment of their administration. Lyophilized formulations maintain the same particle size and can be injected intravenously. The particle size of drug-loaded nanogels is ≤ 150 nm. This size is convenient for several reasons, for example: i) it allows the sterilization of drug–nanogel formulations by filtration; ii) particles can penetrate even small blood capillaries; and iii) can readily enter cells by endocytosis. The low buoyant density of nanogels makes them a unique type of drug carrier, with great potential for systemic administration.

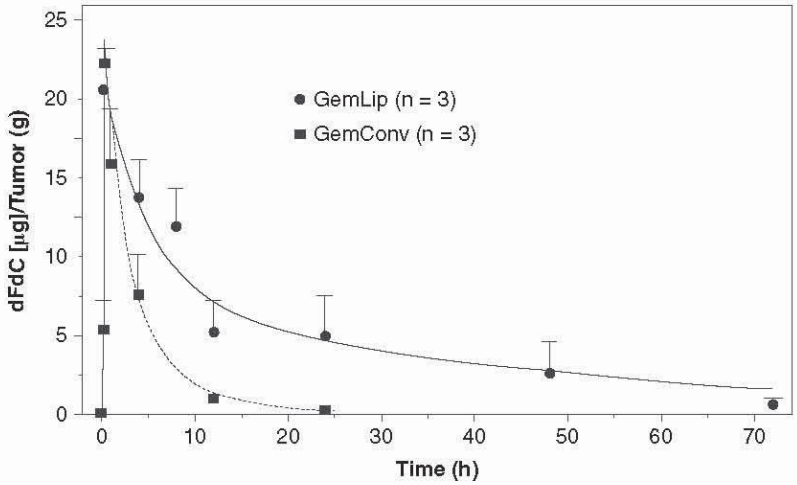

Figure 6. Accumulation of radiolabel presented as the amounts of FdC in tumors after administration of 14C-dFdC given as GemLip (vesicular phospholipid gels) or GemConv (6 mg dFdC/kg each).

This figure was published in [27], reproduced with kind permission of Springer and Business Media.
14C-dFdC: Radiolabeled gemcitabine hydrochloride; dFdC: Gemcitabine hydrochloride.

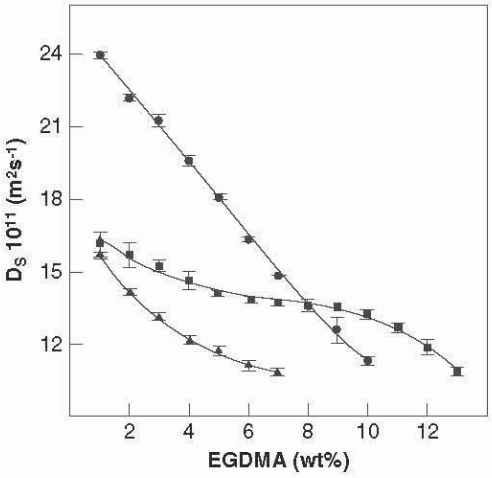

Figure 7. Variation of the apparent diffusion coefficient for saline solution uptake (Ds) in poly (2-hydroxyethyl methacrylate-co-acrylamide) (HEMA/A ± % EGDMA) hydrogels as a function of their percentage of EGDMA at 310 K: (●) 50 HEMA/50 A; (■) 75 HEMA/25 A; and (▲) 90 HEMA/10 A.

Reproduced with permission from [30].
EGDMA: Ethylene glycol dimethacrylate; HEMA: 2-Hydroxyethyl methacrylate.

Furthermore, the membranotropic properties of nanogels loaded with azidothymidine triphosphate, an antiviral NA, have been confirmed *in vitro* and have been clearly demonstrated by various microscopic methods [33]. Following interactions with membranes, drug-loaded nanogels actively release incorporated drug (**Figure 9**). A drug release mechanism triggered by the interaction of the drug-loaded nanogels with the phospholipid bilayer has been proposed and described [33].

5.4 Microparticles

Microparticles are spherical polymeric particles with sizes ranging from 1 to 2000 µm (ideally < 125 µm in diameter). They include microcapsules that are vesicular systems in which a drug can be confined to a cavity surrounded by a polymeric membrane; and microspheres that are matrix systems in which the drug is dispersed throughout the particle [34]. Biodegradable microparticles have been extensively used in pharmaceutical design to obtain delivery systems that allow drug to be released in a sustained manner. For NAs, it is essential to release them in efficient concentrations and for an extended period of time. In fact, most NAs are cell-cycle specific and, thus, their therapeutic efficacy is related to the exposure time of tumour cells to the active agent.

A major obstacle to the particulate formulation of NAs is their high water solubility and low molecular weight, resulting in rapid leakage of the small hydrophilic drug molecules through the thin polymer wall of the particle, giving rise to poor encapsulation efficiency and rapid drug release from microparticles.

Natural polymers such as gelatine [35], albumin [36], chitosan [37] and alginate [38] have been used as matrix materials for the preparation of NA microspheres. These hydrophilic polymers have been shown to efficiently entrap NA molecules. Entrapment efficiencies as high as 70.6 and 65% were obtained for cytarabine-loaded chitosan microspheres [37] and 5-FU-loaded gelatine microspheres [35], respectively. However, the release kinetics of hydrophilic polymer microspheres was characterized by a burst effect during the first hours, followed by a slower release rate. In an effort to resolve this problem, hydrophilic polymer microspheres were coated with a lipophilic polymer film such as poly(lactide-co-glycolide) (PLGA). The total release of cytarabine from chitosan microspheres *in vitro* was detected at

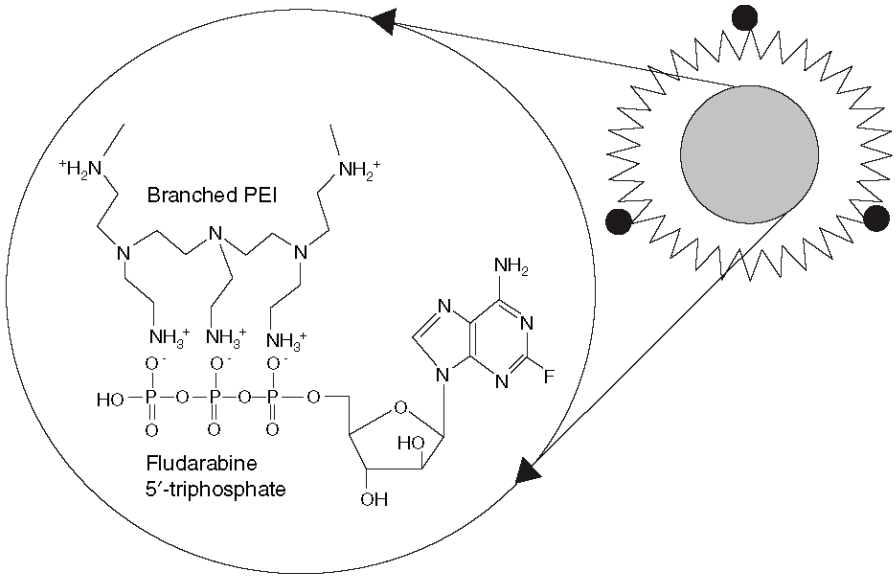

Figure 8. Schematic representation of a nucleoside analogue fludarabine triphosphate-loaded nanogel particle. The particle consists of a condensed core loaded with fludarabine triphosphate/polyethylenimine polyionic complex and a polymer envelope composed of PEG molecules, some of them with attached vector ligands.
This figure was published in [32], Copyright Elsevier (2005).
PEI: Polyethylenimine.

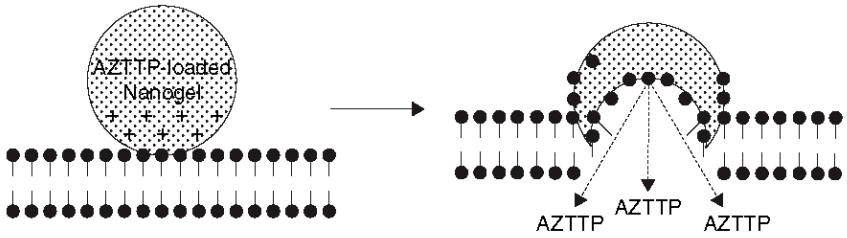

Figure 9. Graphic representation of nanogel fusion with the cellular membrane and substitution of the loaded drug azidodeoxythymidine triphosphate (AZTTP) with the anionic components of the phospholipid bilayer.
Reproduced with permission from [33].

48 h, compared with 80% of cytarabine released within 94.5 h from PLGA-coated chitosan microspheres (**Figure 10**) [37].

Several factors can affect the drug release process from hydrophilic polymer microspheres. Among the different factors, the degree of crosslinking plays an important role. An increase in the crosslinking agent concentration in the preparation of 5-FU-loaded gelatine microspheres produces smaller sized microspheres with lower degrees of swelling, a reduced 5-FU release rate and improved drug loading [35]. However, an increase in the mean diameter of 5-FU-loaded alginate microspheres was observed with an increase in the crosslinking concentration and time of crosslinking [38]. The polymer concentration is also an important factor influencing the morphology and size of microspheres: the lower the polymer concentration, the smaller the spheres produced and the better the microsphere surface obtained [35].

Hydrophobic polymers, such as poly(lactic acid; PLA) and PLGA, have also been used to create microparticles of NAs that are slightly soluble in water, such as 5-FU (~ 10 mg/ml), compared with the high water solubility of other NAs such as cytarabine (~ 148 mg/ml). In one study, 5-FU-loaded PLA-microparticles were prepared using a S/O/W emulsion method. These microparticles contained 5 – 15% w/w of 5-FU and released the drug *in vitro* over a period of 5 days [39]. There was a substantial burst (20 – 40%) of the encapsulated drug from these particles that increased with initial drug loading. To overcome this problem, another type of NA microparticle was prepared from PLGAs of high and low molecular weight, as well as a mixture of PLGAs of different molecular weights, using a S/O/W emulsion method [40]. The resulting microparticles were 50 – 60 µm in diameter, with encapsulation efficiency as high as 75%, and drug

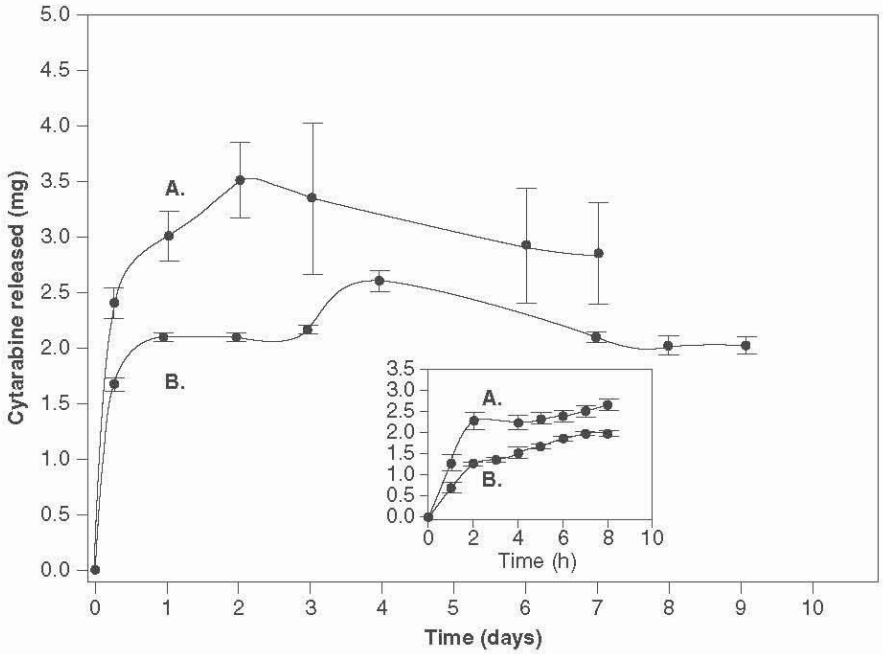

Figure 10. Cytarabine released from A. Chitosan microspheres and **B.** The comatrix, in phosphate buffer, 0.1 M, pH 7.4 at 37°C, by swelling as a function of time.
Reproduce with permission from [37].

loading of 25% by mass. In this case, the initial release was slow and sustained, with no burst, and remained ≥ 3 weeks depending on the PLGA molecular weight. Higher molecular weight polymers yielded formulations with a longer controlled-release duration. After polymer degradation, the remaining drug is released over a period of ~ 1 week. Thus, the release is controlled by both diffusion and polymer hydrolysis rates, resulting in a biphasic release profile.

Similar results have been obtained in a study comparing three types of 5-FU-loaded microparticles prepared from poly(lactide-co-caprolactone), PLA and PLGA, by a spray-drying method [41]. With PLGA microspheres, an increase in the lactide to glycolide ratio resulted in a progressive decrease in the 5-FU release rate from microspheres. Poly(lactide-co-caprolactone) microspheres released 5-FU more rapidly compared with PLGA systems. PLGA of a high lactide to glycolide ratio (85:15) was successfully used to entrap a combination of cytarabine and 5-FU into microspheres for slow drug delivery to ocular tissue [42]. A therapeutic concentration could be maintained for up to 48 h after a single intravitreal injection of these drugs. A lower concentration was maintained for up to 11 days.

In another study, a new material, poly(methylidene malonate 2.1.2), has been used to prepare 5-FU-loaded microparticles yielding a more prolonged release than PLGA microparticles due to its chemical structure (ester bonds in the side chains only) resulting in a long biodegradation time [43]. The authors reported that the percentage of 5-FU released within 24 h could be lowered to 65%, and microspheres were not significantly degraded *in vitro* after 43 days while the release was ongoing.

A pH-sensitive polymer, Eudragit® P-4135F (Degussa), was also used to prepare 5-FU-loaded microspheres by a simple o/w emulsification process. Eudragit P-4135F, pure or in a mixture, was found to retain the drug release at pH 6.8 lower than 35% within 6 h. At pH 7.4, almost immediate release (within 30 min) was observed for pure P-4135F, but mixtures with Eudragit RS100 enabled slightly prolonged release (**Figure 11**). A capsule-like structure, which was established by morphological analysis, caused only slight changes in the release kinetics after the RS100 addition. However, the formulation proved its applicability *in vitro* as a promising device for pH-dependent 5-FU colon delivery [44].

5.5 Nanoparticles

Nanoparticles are submicronic (< 1 µm) polymeric systems. According to the process used for their preparation, nanospheres or nanocapsules can be obtained. Nanospheres and nanocapsules are the morphological equivalents of microspheres and microcapsules, respectively [45]. Many processes can be used for the preparation of nanoparticles, including solvent evaporation, organic phase separation, interfacial polymerization, emulsion polymerization and spray drying. However, only a few are acceptable for NA formulation. As mentioned earlier, the high hydrophilicity and the low molecular weight of these molecules represent a major challenge to particulate formulation because most of

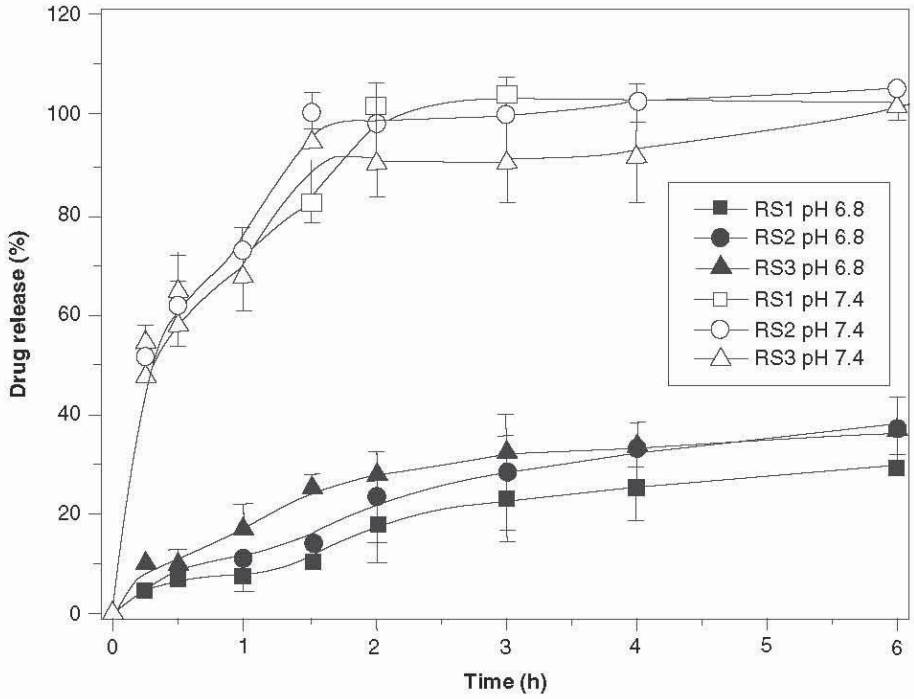

Figure 11. Cumulated 5-FU release versus time from microspheres composed of mixtures of Eudragit P4581F and Eudragit RS100, where RS1 represents the mixture 9:1, RS2 8:2, and RS3 7:3. All batches were tested in phosphate buffer systems of pH 6.8 and 7.4 (n = 3).
Reproduce with permission from [44].

the typical processes for nanoencapsulation are based on the affinity of the drug for the lipophilic phase of an emulsion or for the polymer.

Nanoparticle formulation of NAs offers numerous solutions to NA chemotherapeutic treatment problems. In particular, it provides NA sustained release, tumour targeting and improved cellular uptake because of their small size. Therefore, it would not only increase the NA therapeutic efficiency, but also would enable clinicians to reduce the amount of administered drug and hence minimize NA pronounced side effects [46,47].

Numerous polymers have been used or are available as matrices for nanoparticles. Most are biodegradable, for example polyesters such as poly(D,L-lactide), poly(D,L-lactide-co-glycolide), poly(orthoesters), polyanhydrides, poly(alkylcya noacrylates). Others are not-biodegradable, such as (methyl methacrylate), polystyrene and polyamide [48].

Most research performed on NA micro- and nanoencapsulation have been done with polyesters, especially PLGA. In fact, long experience of the use of co-polymers of lactic and glycolic acid has demonstrated their biocompatibility and biodegradation to toxicologically acceptable products. The second reason for their use for NA encapsulation is that particles of PLGA may be obtained by a solvent evaporation process, which is, in spite of some limitations, compatible with the handling of NAs. This has been demonstrated for 5-FU-loaded PLGA nanoparticles, which were prepared by a nanoprecipitation-solvent displacement technique [49]. Under optimized conditions, the encapsulation efficiency was as high as 78.30%, suggesting that 5-FU might be entrapped and adsorbed on the nanoparticle surface. *In vitro* drug release from the PLGA nanoparticles in phosphate buffered saline (pH 7.4) was suggested to be controlled by a combination of diffusion and slow and gradual erosion of the particles (**Figure 12**) [49].

In another study, efficient NA passive targeting to the intestinal mucosa, and a remarkably enhanced cellular uptake was possible using nanoparticulate systems prepared from poly(alkyl cyanoacrylate) by an emulsion-polymerization method. This is the case of poly(isohexylcyanoacrylate) nanospheres, which have been shown to be an efficient vector for the targeting of the antiviral NA, azidodeoxythymidine (AZT), to the gastrointestinal mucosa and the associated lymphoid tissues [50]. No similar example of anticancer NA-loaded nanoparticles is reported in the literature. In this study, the drug was added to the polymerization medium, resulting in encapsulation efficiency as high as 50%. The release profile was strongly dependant on the presence of esterases in the release medium. An initial burst release of 35% of loaded AZT was observed in water or in USP XIII simulated gastric medium, followed by a prolonged plateau

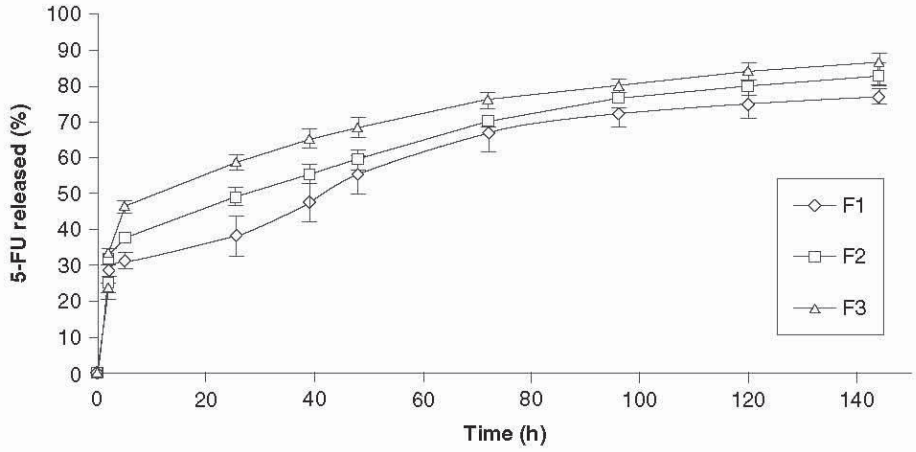

Figure 12. *In vitro* release of 5-FU from nanoparticles (n = 3).
Reproduced with permission from [49].

(40% released after 8 h). In the pancreatin-supplemented medium, AZT release was more progressive and reached almost 80% after 8 h, which could possibly be attributed to the progressive enzymatic degradation of the polymer by esterases contained in pancreatin [50].

Because of their specific affinity for the intestinal mucosa, poly(isohexylcyanoacrylate) nanospheres were able to concentrate at least 4.4- and 5.9-times more of AZT in the gastrointestinal tract compared with the free drug control solution after 30 and 90 min, respectively [50]. After oral administration, the poly(isohexylcyanoacrylate) particles were captured efficiently by the mucosa. This capture was due to the glycoproteic gel constituting the mucus, which acted as a porous adsorbent in which small nanospheres can diffuse and be immobilised until mucus renewal. In turn, because of immobilization, an increase in the contact time would result in an enhanced uptake.

In the emulsion polymerization method, less loading efficiency is generally obtained when the drug is added after the formation of nanoparticles, probably because only the surface of the polymer is available for drug adsorption. This was shown in the encapsulation of stavudine (an antiviral NA) in poly(butylcyanoacrylate) nanoparticles [51]. In this study, it was demonstrated that the larger the nanoparticles, the smaller the loading efficiency, as the specific surface area for stavudine loading of small particles is normally higher than that of large particles.

Magnetic nanoparticles represent very interesting carriers, allowing the active targeting of NAs to their site of action. Many attempts have been directed to this purpose. Gemcitabine-loaded magnetic nanocapsules have been successfully prepared, using poly(ethylcyanoacrylate) by an interfacial polymerization method [52]. The gemcitabine loading capacity was rather poor (9.37% w/w). An initial burst effect was observed in the early stage of the *in vitro* release study. This behaviour was probably due to the small amount of poorly encapsulated drug bound to the nanoparticle surface and/or to residual drug from manufacturing and handling. A smaller loading capacity for gemcitabine (7.6% w/w) has been achieved with poly(ε-caprolactone; PCL) magnetic nanospheres [53], even though similar release behaviour of gemcitabine from PCL nanospheres was observed.

NA tumour-targeting has also been approached, using pH-sensitive polymer nanoparticles because the environment of tumour cells shows a decreased pH value due to their hypoxic metabolism. Accordingly, pH-sensitive 5-FU nanoparticles were prepared to achieve selective drug release to tumour tissues [54]. These nanoparticles were synthesized from a polymer of amphiphilic nature (pullulan acetate/sulphonamide conjugate) by a diafiltration method. The nanoparticles showed good stability at pH 7.4, being equal to that of normal body fluid, but shrank and aggregated below pH 6.8, being close to tumour pH value. The release profile was heavily pH-dependent around physiological pH, and the release rate was significantly enhanced at pH values < 6.8.

5.6 Dendrimers

Dendrimers are emerging as a rather new class of polymeric nanosystems with increasing applications in drug delivery. These systems are built from a series of branches around an inner core, providing products of different generations, and offer intriguing possibilities in this regard. Dendrimers are synthesized from monomers using either convergent or divergent step growth polymerization. They can be synthesized from almost any core molecule and the branches are similarly constructed from any bi-functional molecule [55]. The distinctive architecture (star-shaped) of dendrimers has attracted interest in loading drug molecules to be either encapsulated into the interior of dendrimers or chemically attached or physically adsorbed onto the dendrimer surface, with the option to tailor the carrier properties to the specific needs of the active material and its therapeutic applications [56].

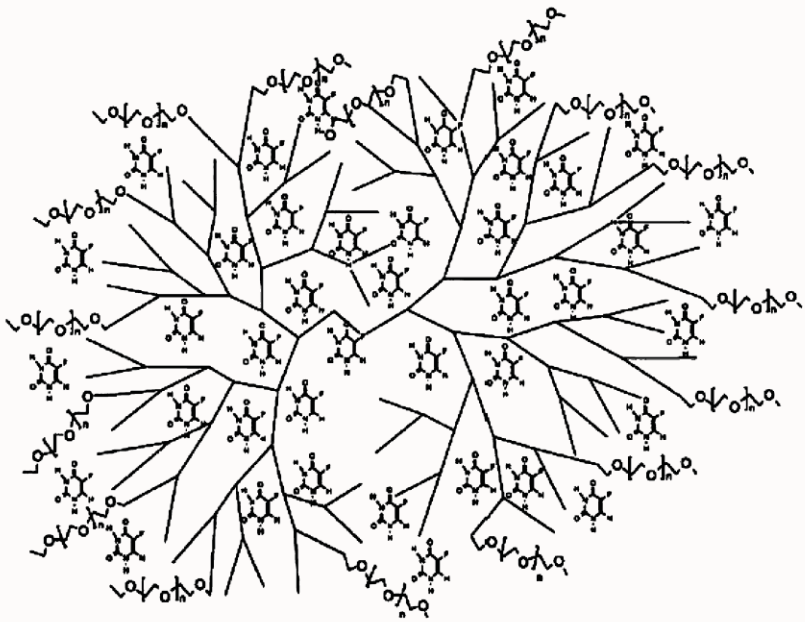

Figure 13. Schematic presentation of the encapsulation of 5-fluorouracil (right) into PEGylated third- and fourth-generation polyamidoamine dendrimers.
This figure was published in [59], Copyright Elsevier (2003).

Furthermore, the high density of surface groups allows the attachment of targeting groups, as well as groups that modify the solution behaviour or toxicity of dendrimers [57].

This technology was applied to NA delivery in an attempt to produce sustained release nanosystems. For this purpose, 5-FU was covalently attached to polyamidoamine dendrimers. Some of the NH_2 groups on the outer layer of dendrimers were acetylated. The acetylated dendrimers were then reacted with 1-bromoacetyl–5-FU to form dendrimer–5FU conjugates [58]. These conjugates release 5-FU on incubation in phosphate-buffered saline. This system may reduce 5-FU toxicity, due to slow release.

In a recent *in vivo* study, 5-FU was encapsulated into G4 polyamidoamine dendrimers with carboxymethyl PEG5000 surface chains (**Figure 13**). This system revealed reasonable drug loading, reduced release rate and hemolytic toxicity compared with the non-pegylated dendrimer [59].

In another study, cytarabine (Ara-C) was covalently linked to PEG. The hydroxyl functions of PEG were functionalised with a bicarboxylic amino acid, and Ara-C was conjugated directly to the peripheral carboxylic acid groups, providing the branching unit of the dendron [60]. This prodrug strategy was found to improve the blood residence time of the drug, to increase its stability towards degradation and to reduce the Ara-C toxicity when compared with the free drug.

Ara-C-loaded PEG–dendrimers hybrids can be synthesized in another way. The branching of termini can be accomplished via aspartic acid to form PEG–aspartic acid. Complete conjugation of dendritic acid with Ara-C has been achieved, via its amine group, by the use of spacers that allowed a greater separation of the branches to accommodate several large Ara-C molecules in proximity to one another [61]. Similar results were obtained for this Ara-C prodrug in terms of increased stability and reduced systemic toxicity, with one drawback: the low payload of the carried drug.

5.7 Polymeric micelles

Biodegradable colloidal nano-micelles are novel targeting drug delivery and controlled release systems, which could prolong the biological half-life and reduce the toxicity of NA anticancer agent, and offer acceptable biocompatibility [62].

5-FU has been entrapped into biodegradable nano-micelles formed from the amphiphilic copolymer polylactide-grafted dextrans (DEX-g-PLA), consisting of a hydrophobic block (PLA) and a hydrophilic block (DEX) [63]. Nano-micelles showed high stability both *in vitro* and *in vivo*. The encapsulating efficiency was ~ 9.3%. The 5-FU release from DEX-g-PLA nano-micelles was sustained for longer time than that of the naked drug. The *in vitro* inhibition rate of cell growth was similar in the 5-FU/DEX-g-PLA group and the naked 5-FU group; but interestingly, the *in vivo* inhibition rate of tumour growth was significantly higher in the 5-FU/DEX-g-PLA group than in the naked 5-FU group.

Drug release from nano-micelles is generally controlled by both drug diffusion and polymer degradation. Therefore, the molecular architecture of biodegradable polymers can be exploited to adjust polymer degradation and erosion rates. A series of four-armed block copolymers with different molecular weights and lactic acid/ethylene oxide ratio have been synthesized and evaluated as drug delivery nanocarriers for 5-FU and paclitaxel, and compared with nano-micelles derived from diblock and triblock copolymers [64]. The

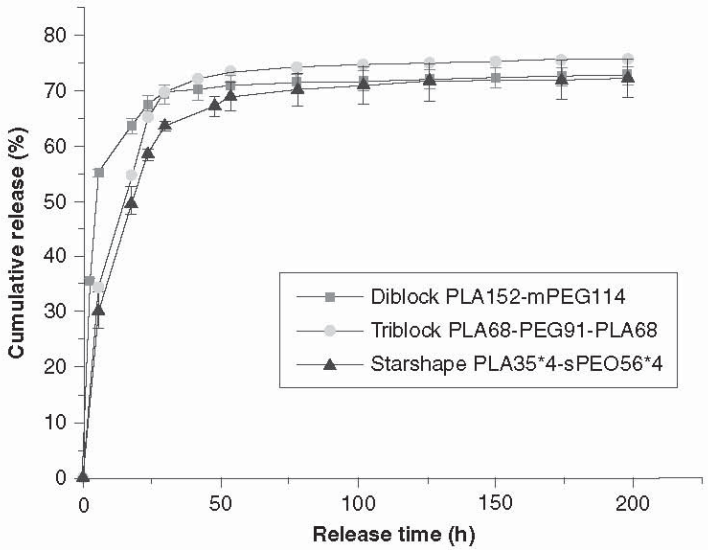

Figure 14. Release profile of 5-fluorouracil from nanoparticles of triblock PLA_{68}–PEG_{91}–PLA_{68}, diblock PLA_{152}–$mPEG_{114}$ and four-armed block copolymer PLA_{35*4}–$sPEO_{56*4}$ with a polymer:drug ratio of 10:2.
Reproduce with permission from [64].

micelles from the star-shaped branches showed more complete release of drug than the diblock copolymers; also, the lower hydrodynamic radius of star-shaped polymers may result in better clearance of the carrier polymer from the body. 5-FU was released *in vitro* over 300 h. Both diblock and star-shaped derived nano-micelles showed similar release patterns for 5-FU, with no control over the release (**Figure 14**).

5.8 Cyclodextrin – nucleoside analogue inclusion complexes

The ability of cyclodextrins to form inclusion complexes with many guest molecules by taking up a whole molecule, or some part of it, into their cavity places cyclodextrins in a unique class of encapsulation and controlled release techniques [65].

NA inclusion complexes are of interest in order to decrease the volume of the solution required for their administration and to improve their bioavailability, as with NAs with low water solubility, such as 5-FU (1% at room temperature) or NA hydrophobic prodrugs, and to increase their *in vitro* and *in vivo* stability. However, the complexation of NA molecules is difficult, as they lack hydrophobic groups that can interact with the cavity of cyclodextrin.

The preparation of inclusion complexes of 5-FU with β-cyclodextrin has been attempted, but no inclusion complex could be isolated, and the association constant was low [66]. However, 5-FU inclusion complex was successfully prepared using a cyclodextrin derivative bearing a free α-amino acid group [67]. The amino acid group might close the primary end of the cavity. Capping the primary alcohol side, or both sides, was shown in some cases to improve the inclusion property, explaining the possible inclusion of 5-FU. On the other hand, the preparation of inclusion complexes of NA hydrophobic prodrugs was easier. The inclusion complexes of a cytarabine mononucleotide prodrug were prepared, and their cytotoxic activities were investigated on leukemic murine cells [68]. Inclusion complexes exhibited more cyctotoxicity to leukemic cells resistant to Ara-C, compared with free Ara-C.

Table 1 shows an overall summary of the described NA delivery systems, with examples for each system.

6. Conclusion

The clinical use of nucleotide analogues in cancer treatment is limited by their poor stability in biological media, resulting in short half-lifes and low bioavailability. Furthermore, the important hydrophilic character of nucleotides also strongly limits their intracellular uptake, due to the low membrane permeability of these substances.

Many promising NA delivery systems are being developed, ranging from microcarriers, such as microparticles and DepoFoam particles, to nanocarriers, such as nanoparticles, liposomes, polyplex nanogel particles, dendrimers, polymeric micelles and cyclodextrin inclusion complexes. Exciting results can be obtained in terms of reduced systemic toxicity and improved efficiency, encouraging clinicians to investigate some of these systems in clinical trials, for example cytarabine-loaded DepoFoam particles (DepoCyt), which has been approved in several countries for the intrathecal treatment of lymphomatous meningitis. However, the problem of low drug loading still constitutes a major obstacle toward the clinical use of these NA-loaded carriers and, thus, requires more investigation in order to be overcome.

Table 1. Examples of recent research works in nucleoside analogue delivery systems.

Drug delivery system	Size	Nucleoside analogue molecule	Ref.	Advantages
Stealth® liposomes (ALZA)	50 – 250 nm	Gemcitabine Cytarabine	[20] [21]	Efficient encapsulation of all nucleoside analogue molecules (suitable for water-soluble drugs encapsulation); Effective reducing in system toxicity; Passive targeting
DepoFoam™ particles (SkyePharma)	1 – 100 µm	Cytarabine Fludarabine mono-phosphate	[23] [70]	Greater encapsulation efficiency than uni- and multi-lamellar liposomes; Greater stability *in vitro*; Sustained release for periods extending from a few days to a few weeks
Vesicular phospholipid gel	50 – 250 nm	Gemcitabine 5-Fluorouracil	[71] [72]	Higher stability *in vitro* than conventional liposomes
Polyplex nanogel particles	100 – 200 nm	Fludarabine tri-phosphate Azidothymidine tri-phosphate	[32] [33]	Encapsulation of tri-phosphate active form of nucleoside analogues; Overcome of drug resistance related to decreased nucleoside kinase activity
Microparticles	1 – 100 µm	5-Fluorouracil Cytarabine	[35] [36]	Sustain localized drug delivery for extended periods of time by controlling their size and porosity
Nanoparticles	< 1 µm	5-Fluorouracil Azidothymidine Stavudine Gemcitabine	[49] [50] [51] [52]	Sustained drug release, targeting the site of action, reduced toxicity, increased therapeutic efficacy
Dendrimers	< 10 nm	5-Fluorouracil Cytarabine	[59] [60]	Can be efficiently loaded by hydrophilic nucleoside analogue molecules, High density of surface groups allows attachment of targeting groups as well as groups that modify the solution behaviour or toxicity of dendrimers
Polymeric micelles	< 100 nm	5-Fluorouracil	[64]	Prolonged biological half-life, lightening of nucleoside analogue toxicity
Cyclodextrin inclusion complexes	< 10 nm	5-Fluorouracil	[67]	Controlled drug release; Higher *in vitro* and *in vivo* stability of the drug

7. Expert opinion

Despite the discovery of many new cytotoxic agents that are potential candidates for the treatment of cancer, this life-threatening disease still causes > 6 million deaths worldwide every year, and the number is growing.

Cytotoxic NAs and nucleobases were among the first chemotherapeutic agents to be introduced for the medical treatment of cancer, with potential activity in solid tumours and malignant disorders of the blood. However, various challenging problems with their clinical use have to be overcome. The most encountered difficulty toward an efficient clinical use of NAs is an adequate delivery of necessary therapeutic concentrations to the tumour target tissue. It is, therefore, of importance to develop novel micro- or nanocarrier technologies that can be used for targeted drug delivery to tumours and, thereby, improve the therapeutic index of the carried drugs.

In nearly all the carriers developed, researchers have been faced with general low NA-loading yields and an initial burst release effect (with the exception of DepoFoam particles), reaching a NA encapsulation efficiency of 82% and a prolonged release extending from few a days to a few weeks.

Several studies have approached NA targeting to cancerous tissues. Passive targeting using Stealth liposomes yielded a prolonged circulation time of these systems and thereby an enhanced cytotoxic activity. Active targeting using magnetic and pH-sensitive polymer nanoparticles achieved the selective delivery of NAs to targeted cancerous tissues and cells, respectively. Although promising results were obtained, many studies should be done to show the extent to which these delivery systems can be used for clinical applications.

From our point of view, an optimal NA carrier should meet the following criteria:

- Easy and efficient drug loading
- Safety, by excluding the use of toxic agents, such as monomers or crosslinkers of the formulation
- Nanoscale size, in order to facilitate an efficient NA transport into cells

- Efficient protection of encapsulated drug in biological media
- Possibility of vectorization of drug carriers for site-specific delivery
- Intracellular efficient drug release.

In this context, polyplex nanogels appear to be the most efficient NA carriers developed so far, allowing NAs to be administered in their active tri-phosphorylated form, thereby circumventing cellular resistance to NAs, being related to deoxycytidine kinase decreased activity. Their small size and the possibility to bind ligands to their surface should help solve the problem of poor cellular uptake and the poor tumour cell selectivity of NA, respectively. However, this developed system is based on the use of positively charged polymers, such as the polyethylenimine. The residence time of these positively charged complexes in the systemic circulation tends to be short, as interactions with plasma proteins lead to the formation of large polymer–protein aggregates, which are rapidly cleared from the bloodstream by phagocytosis.

DepoFoam particles constitute a safe NA carrier, with good drug loading, prolonged release and an efficient protection of the loaded drug, which is surrounded by numerous interconnected phospholipids bilayers. According to their large size, DepoFoam particles constitute a reservoir or a depot of NA and, thus, do not constitute a vector system capable of selectively targeting cancerous cells.

Nanoparticulate systems are vectors that could solve several problems related to NA treatments. More specifically, these systems provide NA tumour targeting and improved cellular uptake because of their small size. Therefore, they should not only increase the therapeutic efficiency of NAs, but also allow the amount of administered drugs to be reduced and, hence, minimize their side effects. Unfortunately, the important hydrophilic character of NA molecules and their low molecular weight result in poor drug loading and a burst release profile, as the nanoencapsulation process is based on the affinity of the drug for the lipophilic phase of the emulsion or for the polymer. Furthermore, nanoparticles prepared by an emulsion-polymerization method, although having good drug loading values, still contain traces of toxic initial monomers which are used in the preparation procedure, in spite of several steps of washing following nanoparticle preparation.

Other polymeric nano-sized systems, such as dendrimers and nano-micelles, are presently being developed on the basis of prodrug strategies and amphiphilic copolymers, respectively. Good results have been obtained in terms of increased stability and reduced systemic toxicity of the loaded NA. Nevertheless, the major limitation of this approach appears to be the low level of drug loading.

Although many of these carriers feature highly promising properties, only relatively few have been tested in clinical trials, and even fewer on the market. Clearly, this is because of the insufficient drug load, which might be sufficient for animal models, but certainly not for humans. Moreover, researchers should pay more attention to the fact that not all the animal studies performed, involving highly toxic anticancer agents, can be reliable to reflect expected drug responses in humans.

Nanoparticles prepared from biocompatible preformed polymers, such as PCL, PLA or PLGA could constitute an ideal NA delivery system, if the problems of poor drug loading and burst release are resolved. A few approaches are now available to circumvent these challenges. For example, the use of various water-soluble macromolecules in the formulation, such as dextran or chitosan, as with increasing the molecular weight of adjuvants, may retain NA small molecules within the aqueous compartment during nanoparticle preparation and thereby improve the encapsulation efficiency and slow drug release. This approach has been investigated by Hillaireau *et al.* [69]. In addition, polymeric micelles responsive to external stimuli, such as light, heat or ultrasound may exert the activity of the loaded drug in a site-directed manner, ensuring the effectiveness and safety of the nanocarrier-mediated targeting NA therapy, and thereby lower the necessary efficient doses and so the required drug loading. Thus, polymeric micelle-based nanocarriers could be promising, once applied to NA delivery. Furthermore, combining cancer imaging with targeted NA delivery would ultimately lead to a powerful system capable of identifying malignant cells, delivering necessary efficient NA therapeutic doses, and monitoring the extent of cell death in real time.

Clearly, the field of NA delivery systems is moving towards increasingly complex nanocarrier compositions, as well as sophisticated targeting and release devices, which many research teams, will undoubtedly pursue and hopefully achieve.

Acknowledgements

We would like to acknowledge the publishers, Elsevier, Springer Netherlands and ACS, as well as the authors who granted their permission to use previously published scientific data and schematics as referenced in the figure captions.

Bibliography

Papers of special note have been highlighted as either of interest (•) or of considerable interest (••) to readers.

1. GALMARINI CM, MACKEY JR, DUMONTET C: Nucleosides analogues and nucleobases in cancer treatment. *Lancet Oncol.* (2002) 3:415-424.
2. HUNSUCKER SA, MITCHELL BS, SPYCHALA J: The 5′-nucleotidases as regulators of nucleotides and drug metabolism. *Pharmacol. Ther.* (2005) 107:1-30.
3. MANGRAVITE LM, BADAGNANI I, GIACOMINI KM: Nucleoside transporters in the disposition and targeting of nucleoside analogs in the kidney. *Eur. J. Pharmacol.* (2003) 479:269-281.
4. VAN ROMPY AR, JOHANSSON M, KARLSSON A: Substrate specificity and phosphorylation of antiviral and anticancer nucleosides analogues by human deoxyribonucleoside kinanses and ribonucleoside kinases. *Pharmacol. Ther.* (2003) 100:119-139.

• A comprehensive and thorough study outlining the pathways of nucleoside and nucleoside analogue metabolism.

5. SONG X, LORENZI PL, LANDOWSKI CP, VIG BS: Amino acid ester prodrugs of the anticancer agent gemcitabine: synthesis, bioconversion, metabolic bioevasion, and hPEPT1-mediated transport. *Mol. Pharm.* (2005) 2(2):157-167.
6. MANSSON E, FLORDAL E, LILIEMARK *et al.*: Down-regulation of deoxycytidine kinase in human leukemic cell lines resistant to cladribine and clofarabine and increased ribonucleotides reductases activity contributes to fludarabine resistance. *Biochem. Pharmacol.* (2003) 65:237-247.
7. SÈVE P, MACKEY JR, ISAAC S *et al.*: CN-II expression predicts survival in patients receiving gemcitabine for advanced non-small cell lung cancer. *Lung Cancer* (2005) 49:363-370.
8. GALMARINI CM, THOMAS X, CALVO F *et al.*: Potential mechanisms of resistance to cytarabine in AML patients. *Leuk. Res.* (2002) 26:621-629.
9. GENINI D, ADACHI S, CHAO Q *et al.*: Deoxyadenosine analogs induce programmed cell death in chronic lymphocytic leukemia cells by damaging the DNA and by directly affecting the mitochondria. *Blood* (2000) 96(10):3537-3543.
10. SHIPLEY LA, BROWN TJ, CORNPROPST JD *et al.*: Metabolism and disposition of gemcitabine, and oncolytic deoxycytidine analog, in mice, rats, and dogs. *Drug Metab. Dispos.* (1992) 20(6):849-855.
11. HALE JT, BIGELOW JC, MATHEWS LA *et al.*: Analytical and pharmacokinetic studies with 5-chloro-2′-deoxycytidine. *Biochem. Pharmacol.* (2002) 64:1493-1502.
12. LINDEMALM S, LILIEMARK J, GUNNAR J *et al.*: Cytotoxicity and pharmacokinetics of cladribine metabolite, 2-chloroadenine in patients with leukaemia. *Cancer Lett.* (2004) 210:171-177.
13. MASSING U, FUXIUS S: Liposomal formulations of anticancer drugs: selectivity and effectiveness. *Drug Resist. Update* (2000) 3:171-177.
14. HOFHEINZ R, GNAD-VOGT SU, BEYER U *et al.*: Liposomal encapsulated anti-cancer drugs. *Anticancer Drugs* (2005) 16:691-707.
15. DRUMMOND DC, KIRPOTIN D, BENZ CC *et al.*: Liposomal drug delivery systems for cancer therapy. In: *Cancer Drug Discovery and Development. Drug Delivery Systems in Cancer Therapy.* Brown DM (Ed.), Humana Press, Inc., New Jersey (2004):191-213.
16. MAYER LD, KRISHNA R, BALLY MB: Liposomes for cancer therapy applications. In: *Polymeric Biomaterials,* 2nd Edition. DUMITRIU S (Ed.), Marcel Dekker, New York, NY (2001):823-841.
17. FUNATO K, YODA R, KIWADA H: Contribution of complement system on destabilization of liposomes of hydrogenated egg phosphatidylcholine in fresh rat plasma. *Biochim. Biophys. Acta* (1992) 1103:198-204.
18. PATEL HM: Serum opsonins and liposomes: their interaction opsonophagocytosis. *Crit. Rev. Ther. Drug* (1992) 9:39-90.
19. SUBRAMANIAN N, YAJNIK A, MURTHY RS: Artificial neural network as an alternative to multiple regression analysis in optimizing formulation parameters of cytarabine liposomes. *AAPS Pharm. Sci. Tech.* (2004) 5(1):E4.

• In this paper, the artificial neural network is applied to the pharmaceutical formulation prediction for the first time.

20. CELANO M, CALVAGNO MG, BULOTTA S *et al.*: Cytotoxic effects of gemcitabine-loaded liposomes in human anaplastic thyroid carcinoma cells. *BMC Cancer* (2004) 4:63.
21. HAMADA A, KAWAGUCHI T, NAKANO M: Clinical pharmacokinetics of cytarabine formulations. *Clin. Pharmacokinet.* (2002) 41(10):705-718.
22. ANDERSEN TL, JENSEN SS, JØRGENSEN K: Advanced strategies in liposomal cancer therapy: problems and prospects of active and tumor specific drug release. *Prog. Lipid Res.* (2005) 44:68-97.
23. MANTRIPRAGADA SB, HOWELL SB: Sustained-release drug delivery with DepoFoam. In: *Cancer Drug Discovery and Development. Drug Delivery Systems in Cancer Therapy.* Brown DM (Ed.), Humana Press, Inc., New Jersey (2004):247-262.

• In this paper, DepoFoam™ technology applied to cytarabine delivery (the unique cytarabine-loaded microcarrier existing on the market) is carefully highlighted.

24. JAIN SK, JAIN RK, CHOURASIA MK *et al.*: Design and development of multivesicular liposomal depot delivery system for controlled systemic delivery of acyclovir sodium. *AAPS Pharm. Sci. Tech.* (2005) 6(1):E35.
25. BRANDL M, BACHMANN D, DRECHSLER M *et al.*: Liposome preparation using high-pressure homogenizers. In: *Liposome Technology. 2nd Edition.* Gregoriadis G (Ed.), CRC (1993) 1:49-65.
26. BRANDL M, DRECHSLER M, BACHMANN D *et al.*: Morphology of semisolid aqueous phosphatidylcholine dispersions, a freeze fracture electron microscopy study. *Chem. Phys. Lipids* (1997A) 87:65-72.
27. MOOG R, BURGER AM, BRANDL M *et al.*: Change in pharmacokinetic and pharmacodynamic behaviour of gemcitabine in human tumor xenografts upon entrapment in vesicular phospholipid gels. *Cancer Chemother. Pharmacol.* (2002) 49:356-366.
28. KAISER N, KIMPFLER A, MASSING U *et al.*: 5-Fluorouracil in vesicular phospholipid gels for anticancer treatment: entrapment and release properties. *Int. J. Pharm.* (2003) 256:123-131.

29. HUWANG S, BAEK N, PARK H *et al.*: Hydrogels in cancer drug delivery systems. In: *Cancer Drug Discovery and Development. Drug Delivery Systems in Cancer Therapy.* Brown DM (Ed.), Humana Press, Inc., New Jersey (2004):97-115.
30. GARCIA O, BLANCO MD, MARTIN JA *et al.*: 5-Fluorouracil trapping in poly (2-hydroxyethyl methacrylate-co-acrylamide) hydrogels: *in vitro* drug delivery studies. *Eur. Polym. J.* (2000) 36:111-122.
31. ZHANG S, XU Y, WANG B *et al.*: Cationic compounds used in lipoplexes and polyplexes for gene delivery. *J. Control. Rel.* (2004) 100:165-180.
32. VINOGRADOV SV, ZEMAN AD, BATRAKOVA EV *et al.*: Polyplex nanogel formulations for drug delivery of cytotoxic nucleoside analogs. *J. Control. Rel.* (2005) 107:143-157.
33. VINOGRADOV SV, KHOLI E, ZEMAN AD: Cross-linked polymeric nanogel formulations of 5′-triphosphates of nucleoside analogues: role of the cellular membrane in drug release. *Mol. Pharm.* (2005) 2(6):449-461.
34. TICE TR, MASON DW, GILLEY RM: Clinical use and future of parenteral microsphere delivery systems. In: *Novel Drug Delivery and its Therapeutic Application.* Prescott LF and Nimmo WS (Eds), John Wiley & Sons, New York, NY (1989):223-235.
• A cellular-trafficking mechanism of the drug-loaded polyplex particles being triggered by their interaction with the negatively-charged phospholipids in the cellular membrane is proposed sand described.
35. MUVAFFAK A, GÜRHAN I, HASIRCI N: Cytotoxicity of 5-fluorouracil entrapped in gelatine microspheres. *J. Microencapsul.* (2004) 21(3):293-306.
36. GÖMEZ C, BLANCO MD, BERNARDO MV *et al.*: Cytarabine release from comatrices of albumin microspheres in a poly(lactide-co-glycolide) film: *in vitro* and *in vivo* studies. *Eur. J. Pharm. Biopharm.* (2004) 57(2):225-233.
37. BLANCO MD, GÖMEZ C, OLMO R *et al.*: Chitosan microspheres in PLG films as devices for cytarabine release. *Int. J. Pharm.* (2000) 202:29-39.
38. RAHMAN Z, KHOLI R, KHAR RK *et al.*: Characterization of 5-fluorouracil microspheres for colonic delivery. *AAPS Pharm. Sci. Tech.* (2006) 7(2):E47.
39. CIFTCI K, HINCAL AA, KAS HS *et al.*: Solid tumor chemotherapy and *in vivo* distribution of fluorouracil following administration in poly(L-lactic acid) microspheres. *Pharm. Dev. Technol.* (1997) 2:151-160.
40. BRINBAUM DT, BRANNON-PEPPAS L: Microparticle drug delivery systems. In: *Cancer Drug Discovery and Development. Drug Delivery Systems in Cancer Therapy.* Brown DM (Ed.), Humana Press, Inc., New Jersey (2004):117-135.
41. HITZMAN CJ, ELMQUIST WF, WATTENBERG LW, WIEDMANN TS: Development of a respirable, sustained release microcarrier for 5-fluorouracil: *in vitro* assessment of liposomes, microspheres, and lipid coated nanoparticles. *J. Pharm. Sci.* (2006) 95(5):1114-1126.
42. PEYMAN GA, CONWAY M, KHOOBEHI B, SOIKE K: Clearance of microsphere-entrapped 5-fluorouracil and cytosine arabinoside from the vitreous of primates. *Int. Ophthalmol.* (1992) 16:109-113.
43. FOURNIER E, PASSIRANI C, COLIN N, BRETON P, SAGODIRA S, BENOIT JP: Development of novel 5-FU-loaded poly(methylidene malonate 2.1.2.)-based microspheres for the treatment of brain cancers. *Eur. J. Pharm. Biopharm.* (2004) 57:189-197.
44. LAMPRECHT A, YAMAMOTO H, TAKEUCHI H, KAWASHIMA Y: Microsphere design for the colonic delivery of 5-fluorouracil. *J. Control. Rel.* (2003) 90:313-322.
45. DAVIS SS: Biomedical applications of nanotechnology – implications for drug targeting and gene therapy. *Trends Biotechnol.* (1997) 15:217-224.
46. KAWASAKI ES, PLAYER A: Nanotechnology, nanomedicine, and the development of new, effective therapies for cancer. *Nanomedicine* (2005) 1:101-109.
47. LIU Y, MIYOSHI H, NAKAMURA M: Nanomedicine for drug delivery and imaging: a promising avenue for cancer therapy and diagnosis using targeted functional nanoparticles. *Int. J. Cancer* (2007) 120(12):2527-2537.
•• An important review paper, showing the significance and recent advances of gene/drug delivery to cancer cells, and the molecular imaging and diagnosis of cancer by targeted functional nanoparticles.
48. SLOMKOWSKI S: Biodegradable nano- and microparticles as carriers of bioactive compounds. *Acta Pol. Pharm.* (2006) 63(5):351-358.
49. BOZKIR A, SAKA OM: Formulation and investigation of 5-FU nanoparticles with factorial design-based studies. *Il Farmaco* (2005) 60:840-846.
50. DEMBRI A, MONTISCI M, GANTIER JC, CHACUN H, PONCHEL J: Targeting of 3′-azido 3′-deoxythymidine (AZT)-loaded poly(isohexylcyanoacrylate) nanospheres to the gastrointestinal mucosa and associated lymphoid tissues. *Pharm. Res.* (2001) 18(4):467-473.
51. KUO Y: Loading efficiency of stavudine on polybutylcyanoacrylate and methyl methacrylate-sulfopropylmethacrylate copolymer nanoparticles. *Int. J. Pharm.* (2005) 290:161-172.
52. YANG J, LEE H, HYUNG W, PARK SB, HAAM S: Magnetic PECA nanoparticles as drug carriers for targeted delivery: synthesis and release characteristics. *J. Microencapsul.* (2006) 23(2):203-212.
53. YANG J, PARK SB, YOON HG, HUH YM, HAAM S: Preparation of poly ε-caprolactone nanoparticles containing magnetite for magnetic drug carrier. *Int. J. Pharm.* (2006) 324:185-190.
54. LIU L, JIN P, CHENG M, ZHANG G, ZHANG F: 5-Fluorouracil-loaded self-assembled pH-sensitive nanoparticles as novel drug carrier for treatment of malignant tumors. *Chinese J. Chem. Eng.* (2006) 14(3):377-382.
55. GILLIES ER, FRÉCHET JMJ: Dendrimers and dendritic polymers in drug delivery. *Drug Discov. Today* (2005) 10(1):35-43.
56. SVENSON S, TOMALIA DA: Dendrimers in biomedical applications-reflections on the field. *Adv. Drug Deliv. Rev.* (2005) 57:2106-2129.
57. KUKOWSKA-LATALLO JF, CANDIDO KA, CAO Z *et al.*: Nanoparticle targeting of anticancer drug improves therapeutic response in animal model of human epithelial cancer. *Cancer Res.* (2005) 65(12):5317-5324.
58. ZHUO RX, DU B, LU ZR: *In vitro* release of 5-fluorouracil with cyclic core

dendritic polymer. *J. Control. Rel.* (1999) 57:249-257.

59. BHADRA D, BHADRA S, JAIN S, JAIN NK: A PEGylated dendritic nanoparticulate carrier of fluorouracil. *Int. J. Pharm.* (2003) 257:111-124.
60. SCHIAVON O, PASUT G, MORO S, ORSOLINI P, GUIOTTO A, VERONESE FM: PEG-Ara-C conjugates for controlled release. *Eur. J. Med. Chem.* (2004) 39:123-133.
61. CHOE YH, CONOVER CD, WU D *et al.*: Anticancer drug delivery systems: multi-loaded N4-acyl poly(ethylene glycol) prodrugs of ara-C. II. Efficacy in ascites and solid tumors. *J. Control. Rel.* (2002) 79:55-70.
62. TORCHILIN VP: Micellar nanocarriers: pharmaceutical perspectives. *Pharm. Res.* (2007) 24(1):1-16.
63. ZHOU JJ, CHEN RF, TANG QB, ZHOU QB, LU HW, WANG J: Preparation of 5-fluorouracil encapsulated in amphiphilic polysaccharide nano-micelles and its killing effect on hepatocarcinoma cell line HepG2. *Chinese J. Cancer* (2006) 25(12):1459-1463.
64. JIE P, VENKATRAMAN SS, MIN F, FREDDY BY, HUAT GL: Micelle-like nanoparticles of star-branched PEO-PLA copolymers as chemotherapeutic carrier. *J. Control. Rel.* (2005) 110:20-33.
65. MARTIN DEL VALLE EM: Cyclodextrins and their uses: a review. *Process Biochem.* (2004) 39:1033-1046.
66. WEN JQ, CUI W: Studies on the composition and stability constant of inclusion complexes of β-cyclodextrin with fluorouracil and ftorafur by NMR. *Acta Pharm. Sin.* (1990) 25(5):345-348.
67. BAHADDI Y, LELIÉVRE F, GAREIL P, MAIGNAN J, GALONS H: Preparation and complexation ability of zwitterionic derivatives of cyclodextrins. *Carbohyd. Res.* (1997) 303:229-232.
68. JORDHEIM L, DEGOBERT G, FESSI H *et al.*: Solubilization of a nucleotide analogue prodrug by hydroxypropyl-β-cyclodextrin. *Proceedings of the 12th International Cyclodextrin Symposium*, Montpellier (2004):291-294.
69. HILLAIREAU H, LE DOAN T, CHACUN H, JANIN J, COUVREUR P: Encapsulation of mono- and oligo-nucleotides into aqueous-core nanocapsules in presence of various water-soluble polymers. *Int. J. Pharm.* (2007) 331:148-152.
70. PORT RE, SCHUSTER C, PORT CR, BACHERT P: Simultaneous sustained release of fludarabine monophosphate and Gd-DTPA from an interstitial liposome depot in rats: potential for indirect monitoring of drug release by magnetic resonance imaging. *Cancer Chemother. Pharmacol.* (2006) 58(5):607-617.
71. MOOG R, BURGER AM, BRANDL M *et al.*: Change in pharmacokinetic and pharmacodynamic behaviour of gemcitabine in human tumor xenografts upon entrapment in vesicular phospholipid gels. *Cancer Chemother. Pharmacol.* (2002) 49(5):356-366.
72. KAISER N, KIMPFLER A, MASSING U *et al.*: 5-Fluorouracil in vesicular phospholipid gels for anticancer treatment: entrapment and release properties. *Int. J. Pharm.* (2003) 256:123-131.

Affiliation

Roudayna Diab[1] Pharm MSc,
Ghania Degobert[2] PhD,
Misara Hamoudeh[3] Pharm MSc,
Charles Dumontet[4] MD PhD &
Hatem Fessi[†5] Pharm PhD
[†]Author for correspondence
[1]PhD Student, School of Pharmacy,
Université Lyon 1-ESCPE – UMR 5007,
Laboratoire d'Automatique et de Génie des Procédés, Bât. 308 G, 43,
Bd du 11 Novembre 1918,
69622 Villeurbanne Cedex, France
[2]Associate Professor at the School of Pharmacy,
Université Lyon 1-ESCPE – UMR 5007,
Laboratoire d'Automatique et de Génie des Procédés, Bât. 308 G, 43,
Bd du 11 Novembre 1918,
69622 Villeurbanne Cedex, France
[3]PhD Student, School of Pharmacy,
Université Lyon 1-ESCPE – UMR 5007,
Laboratoire d'Automatique et de Génie des Procédés, Bât. 308 G, 43,
Bd du 11 Novembre 1918,
69622 Villeurbanne Cedex, France
[4]Professor at the School of Medicine,
Laboratoire de Cytologie Analytique – Université Lyon 1, INSERM U590, 8 Avenue,
Rockefeller 69008 Lyon, France
[5]Professor at the School of Pharmacy,
Université Lyon 1-ESCPE – UMR 5007,
Laboratoire d'Automatique et de Génie des Procédés, Bât. 308 G, 43,
Bd du 11 Novembre 1918,
69622 Villeurbanne Cedex, France
Tel: +33 72 43 18 93; Fax: +33 72 43 16 82
E-mail: fessi@lagep.univ-lyon1.fr

Partie expérimentale

Chapitre 1
Microparticules de cytarabine à base de PCL/ mPEG-PCL

La micro-encapsulation de la cytarabine en utilisant des copolymères amphiphiles

Les microparticules constituent des vecteurs intéressants sur le plan pharmacotechnique permettant de réaliser des systèmes à libération prolongée qui peuvent avoir deux avantages directs ; améliorer le confort du patient en réduisant le nombre d'injections et réaliser un ciblage d'organe en les injectant directement dans un compartiment corporel donné. Néanmoins, en raison de sa solubilité aqueuse et de son faible poids moléculaire, l'encapsulation de la cytarabine est pratiquement impossible dans les particules à base de polyesters biodégradables comme le PLA, PCL et le PLGA. Les seuls essaies pour encapsuler la cytarabine ont consisté à utiliser des polymères hydrophiles ; le chitosan [1], et l'albumine [2] pour former des microparticules qui seront réticulés dans un second temps en utilisant des agents réticulants extrêmement toxiques, dont certaines traces persistent malgré les multiples étapes de lavage qui suivent le procédé de fabrication. Dans ce contexte, nous avons supposé que l'utilisation des copolymères amphiphiles à blocs hydrophobes biodégradables (polyesters) et blocs hydrophiles bio-éliminables (PEG $\leq$ 20.000 Da) pourrait apporter une solution convenable au problème d'encapsulation de la cytarabine.

Le copolymère à bloc se définit comme étant l'association d'au moins deux homopolymères A et B de nature chimique différente et liés par des liaisons covalentes. D'une manière générale, le mélange des deux homopolymères immiscibles conduit à une séparation de phases. Dans le cas des copolymères à blocs, la liaison chimique entre les différents blocs va limiter cette séparation de phases et conduire à des domaines de taille microscopique, on parle alors de micro-séparation de phases. Dans le cas d'un copolymère dibloc AB, la répulsion entre A et B les contraint à s'organiser pour minimiser ses contacts. Par conséquence, la liaison chimique va se localiser à l'interface entre les deux domaines, tandis que les blocs A et B vont tenter de s'en éloigner, en se déployant perpendiculairement à l'interface afin qu'elle soit la plus réduite possible. Cela va conduire à une morphologie

[1] Blanco, M. D., Gómez, C., Olmo, R., Muñiz, E. & Teijón, J.M. (2000). Chitosan microspheres in PLG films as devices for cytarabine release. *International journal of pharmaceutics 202*: 29-39.

[2] Gómez, C., Blanco, M. D., Bernardo, M. V., Olmo, R., Muñiz, E. & Teijón, J.M. (2004). Cytarabine release from comatrices of albumin microspheres in a poly(lactide-co-glycolide) film: in vitro and in vivo studies. *European journal of pharmaceutics and biopharmaceutics 57*: 225-33.

lamellaire si les blocs A et B sont symétriques, dans le cas contraire, l'interface entre les deux domaines va se courber (figure 1).

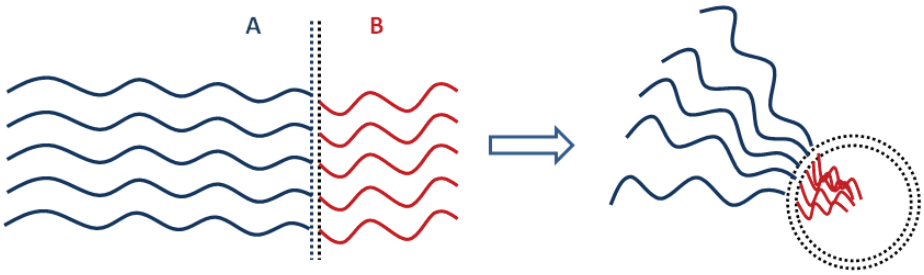

Figure1. Représentation schématique du phénomène de courbure dans les systèmes des copolymères dissymétriques.

L'utilisation des copolymères constitués des blocs de polyesters et de blocs de PEG a été étudiée depuis longtemps pour la conception des vecteurs pharmaceutiques dits « furtifs » à un temps de rémanence long dans la circulation générale, comme des systèmes de délivrance pour les molécules hydrophobes [3,4]. Toutefois, leur utilisation potentielle pour la délivrance des macromolécules hydrophiles (comme les peptides et les protéines) a été seulement reconnue au début des années 90[5]. En effet, la localisation de ces copolymères à l'interface entre la phase aqueuse et la phase organique pendant la préparation des micro- ou nanoparticules, limite considérablement l'interaction hydrophobe dénaturante entre la protéine et la phase organique[6]. D'autre part, grâce à leur caractère amphiphile, ces copolymères

[3] Gref, R., Domb, A., Quellec, P., Blunk, T., Muller, R. H., Verbavatz, J. & Langer, R. (1995). The controlled intravenous delivery of drugs using PEG-coated sterically stabilized nanospheres. *Advanced drug delivery reviews 16*: 215-233.

[4] Stolnik, S., Illum, L. & Davis, S. (1995). Long circulating microparticulate carriers. *Advanced Drug Delivery Reviews 16*: 195-214.

[5] Li, Y., Volland, C. & Kissel, T. (1994). In vitro degradation and bovine serum albumine release of the ABA triblock copolymers consisting of poly(L(+)lactic acid), or poly(L(+)lactic acid-co-glycolic acid) A-blocks attached to central polyoxyethylene B-blocks. *Journal of Controlled Release 32*: 121-128.

[6] Boury, F., Ivanova, T., Panaiotov, I., Proust, J., Bois, A. & Richou, J. (1995). Dilatational properties of adsorbed poly (DL-lactide) and BSA monolayers at the dichromethane/water interface. *Langmuir : the ACS journal of surfaces and colloids 11*: 1636-1644.

permettent d'améliorer l'efficacité d'encapsulation des principes actifs et de diminuer la quantité du tensioactif utilisé lors de la préparation des micro- ou nanoparticules[7].

Nous présentons dans ce chapitre l'élaboration d'un système microparticulaire à base de poly(ε-caprolactone) (figure 2). Les microparticules ont été préparées par la méthode de « double émulsion - évaporation de solvant » en utilisant comme surfactants des copolymères amphiphiles composés de blocs biodégradables de poly(ε-caprolactone) PCL et de blocs bio-éliminables de polyéthylène glycol PEG. Les blocs hydrophobes (PCL) permettent un ancrage dans les particules tandis que les blocs hydrophiles (PEG) qui sont exposés vers le milieu aqueux interne (dans les compartiments aqueux des microparticules) vont permettre de limiter la fuite de la cytarabine vers le milieu externe.

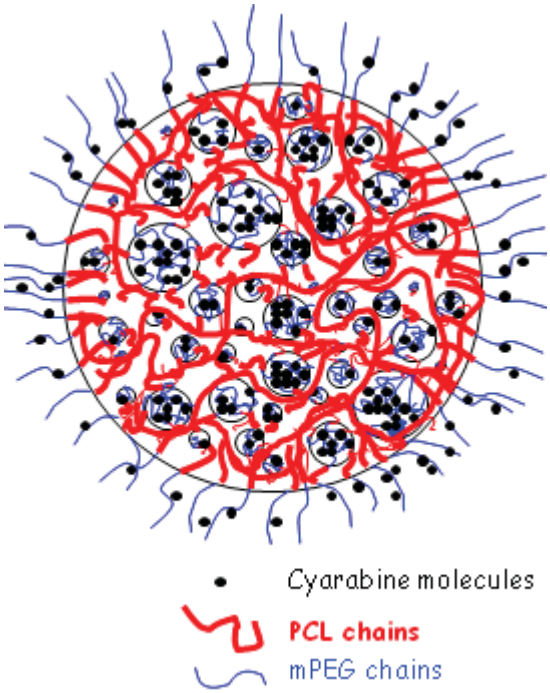

Figure 2. Illustration des microparticules de cytarabine à base de PCL/mPEG-PCL. Dans ce schéma, nous supposons que les chaînes de PEG sont orientées, à la fois, vers le milieu aqueux externe et le milieu aqueux des vésicules interne dans la matrice polymérique.

Dans ce travail une série de copolymères PCL-mPEG avec des blocs PCL de différents poids moléculaires a été synthétisée. La synthèse des copolymères constitués de blocs hydrophobes de PCL et de blocs hydrophiles de PEG s'est effectuée par polymérisation coordinative anionique en présence d'un catalyseur, 2-éthyle hexanoate d'étain $Sn(Oct)_2$, par ouverture de cycle de l' ε-caprolactone (ε-CL) à partir de la fonction hydroxyle disponible aux

[7] Deng, X., Zhou, S., Li, X., Zhao, J. & Yuan, M. (2001). In vitro degradation and release profiles for poly-dl-lactide-poly(ethylene glycol) microspheres containing human serum albumin. *Journal of controlled release 71*: 165-73.

extrémités terminales du PEG. Les copolymères obtenus ont été par la suite caractérisés par résonance magnétique nucléaire du proton, spectroscopie infrarouge et chromatographie d'exclusion stérique. Différents lots de microparticules ont été préparés et l'effet de la longueur de chaîne de PCL sur les caractéristiques physico-chimiques des particules a été étudié. Une efficacité d'encapsulation satisfaisante a pu être obtenue et qui a été dix fois plus importante que celle des microparticules de PCL préparées sans les copolymères.

C/e: KV C/e QA: LP

Drug Development and Industrial Pharmacy (2009) i*First*, 1–14

informa healthcare

ORIGINAL ARTICLE

Microencapsulation of cytarabine using poly(ethylene glycol)–poly(ε-caprolactone) diblock copolymers as surfactant agents

Roudayna Diab[1], Misara Hamoudeh[1], Olivier Boyron[2], Abdelhamid Elaissari[1] and Hatem Fessi[1]

[1]Pharmaceutical Technology Department, Laboratoire d'Automatique et de Génie de Procédés (LAGEP), Université Claude Bernard Lyon 1, ISPBL-Faculté de Pharmacie de Lyon, Villeurbanne, France and [2]Laboratoire de Chimie, Catalyse, Polymères et Procédés (C2P2), Equipe Chimie et Procédés de Polymérisation (LCPP), Université Claude Bernard Lyon 1, Villeurbanne, France

Abstract

Cytarabine-loaded microparticles (Ara-C MPs) were elaborated using poly(ε-caprolactone) (PCL) and monomethoxy poly(ethylene glycol) (mPEG)–PCL diblock copolymer as surfactant agents. For this purpose, a series of mPEG–PCL diblock copolymers, with different PCL block lengths, were synthesized. Compositions and molecular weights of obtained copolymers were characterized by Fourier transform infrared spectroscopy, nuclear magnetic resonance, size exclusion chromatography, and size exclusion chromatography-multiangle laser light scattering. Ara-C MPs were prepared by double emulsion–solvent evaporation method. The effects of varying PCL block lengths on microparticle encapsulation efficiency, size, and zeta potential were evaluated. Increasing the PCL block lengths of copolymers substantially increased the Ara-C encapsulation efficiency and the microparticle size, but it decreased their zeta potential. Microparticles were spherical in shape, with a smooth surface and composed of homogenously distributed Ara-C-containing aqueous domains in the polymer matrix. The in vitro drug release kinetics of the optimized microparticles showed a hyperbolic profile with an initial burst release. These results showed the important role of the amphiphilic diblock copolymers as stabilizing agent in the encapsulation of Ara-C in PCL microparticles, suggesting their potential use for the microparticulate formulations of other small hydrophilic bioactive molecules.

Key words: *Amphiphilic diblock copolymers; cytarabine; double emulsion; microparticles; poly(ε-caprolactone)*

Introduction

The clinical use of cytarabine (Ara-C) like other nucleoside analogues is potentially limited by its short half-life after intravenous administration and its narrow therapeutic index inducing severe side effects while maintaining a low anticancer activity[1,2]. Consequently, the minimum effective dose is high and has to be regularly increased. In this context, toxicity becomes the main limiting factor to the treatment[2]. Furthermore, the important hydrophilic character of Ara-C strongly limits its intracellular uptake, because of the low membrane permeability of this molecule[3]. On the other hand, its extensive degradation by cytidine deaminases in the liver and kidney and its poor stability in biological media adversely affect its anticancer activity and raise the question of improved formulation for better tumor targeting and drug stability[4–6].

Nano- and microparticulate systems prepared from biocompatible preformed polymers, such as poly(ε-caprolactone) (PCL), poly(lactic acid) (PLA), or poly(lactic-co-glycolic acid) (PLGA), could be promising carriers achieving both a controlled release and a good protection of encapsulated Ara-C from enzymatic degradation. Moreover, biodegradable microparticles could be particularly phagocytized by cancerous cells,[7–9] which make these drug vehicles suitable for the intraperitoneal[10],

Address for correspondence: Prof. Hatem Fessi, Pharmaceutical Technology Department, Laboratoire d'Automatique et de Génie de Procédés (LAGEP), UMR CNRS 5007, Université Claude Bernard Lyon 1, ISPBL-Faculté de Pharmacie de Lyon, Bat 308G, 43 Bd du 11 Novembre 1918, 69622 Villeurbanne Cedex, France. Tel: +33 472 431893, Fax: +33 472 431882. E-mail: fessi@lagep.univ-lyon1.fr

(Received 30 Jan 2009; accepted 14 Aug 2009)

ISSN 0363-9045 print/ISSN 1520-5762 online © Informa UK, Ltd.
DOI: 10.1080/03639040903261989

intratumoral,[11,12] or subcutaneous[13,14] anticancer drug delivery.

Unfortunately, the high water solubility and the low molecular weight of Ara-C are major obstacles against its particulate formulation, as a result of its low affinity to the commonly used hydrophobic polymers, such as PCL, PLA, or PLGA[15]. This generally induces the drug loss into the external aqueous phase during the emulsification and hardening of the microparticles[16], whereas the commonly used surfactant agents, such as poly(vinyl alcohol) (PVA) or pluronic, remain disabled to limit the drug migration to the external aqueous phase,[17] yielding low encapsulation efficiencies (EEs) of hydrophilic small molecules[18–20]. This is probably related to the fact that these surfactant agents do not contribute to the microparticle polymeric matrix formation during the solvent evaporation and the subsequent polymer precipitation.

To address this point resulting from the hydrophobic nature of homopolymers, we introduced a hydrophilic block, the monomethoxy poly(ethylene glycol) (mPEG), to form amphiphilic diblock copolymers mPEG–PCL to be used as surfactant agents for the preparation of Ara-C-loaded PCL microparticles.

In fact, diblock copolymers mPEG-polyester have been widely employed in the elaboration of stealth carriers[21,22] and for the encapsulation of some macromolecules such as proteins and peptides using the double emulsion technique[23].

Based on these considerations, we hypothesized that the use of surfactant agents with an anchor segment, such as mPEG–PCL copolymers, should potentially limit the drug partitioning to the continuous aqueous phase. These copolymers contributing to the microparticle polymeric matrix could sequester the small hydrophilic drug in the microparticles because of their hydrophilic segments (mPEG) increasing the hydrophilicity of the delivery system.

In this work, our objective was to elaborate a novel microparticulate system for Ara-C delivery. In this system, both of PCL and its diblock copolymer mPEG–PCL were employed (Figure 1). Indeed, as highlighted earlier, the use of a diblock copolymer composed of PCL and mPEG to encapsulate the Ara-C is of great interest, as it should increase the overall hydrophilicity of the polymeric matrix of the microparticles, leading to an improved EE of the hydrophilic small drug, whereas the homopolymer PCL chains could provide rigidity and a better in vitro stability of the microparticulate system[24]. To the best of our knowledge, no research work has already been reported on the encapsulation of Ara-C in micro- or nanoparticles based on PCL or other biodegradable polymers, such as PLA or PLGA, either with or without their corresponding PEG copolymers.

Having this goal in mind, we synthesized a series of mPEG–PCL diblock copolymers with different molecular weight (but with the same mPEG chain length). These copolymers were then used for the preparation of the microparticles using the double emulsion–solvent evaporation method, which has been generally applied to microencapsulate hydrophilic macromolecules, such as proteins and peptides[9,25,26].

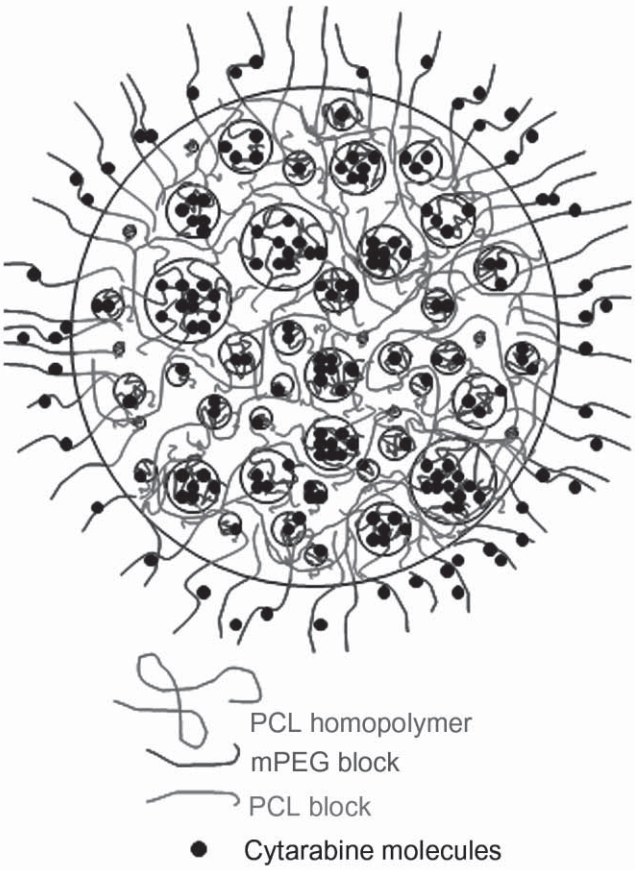

Figure 1. Illustration of PCL/mPEG–PCL composite microparticles loaded with cytarabine. In this schematic we suggest that mPEG blocks are oriented toward both the external aqueous medium and to the aqueous medium in the internal vesicles.

The different microparticle batches prepared from different corresponding copolymers were characterized for their size, morphology, and EE to select the appropriate diblock copolymer molecular weight for Ara-C encapsulation. Thereafter, the microparticles prepared with the selected diblock copolymer underwent further physicochemical characterizations and in vitro release studies.

Materials and methods

Synthesis of mPEG–PCL diblock copolymers

Epsilon-caprolactone (ε-CL) (Sigma-Aldrich, Saint Quentin Fallavier, France) was purified by vacuum distillation over CaH_2 (Acros Organics, Geel, Belgium). mPEG with a molecular weight of 5000 g/mol (Sigma-Aldrich) was

dried by an azeotropic distillation with anhydrous toluene (Sigma-Aldrich) under dry nitrogen atmosphere. Metal calcium was used as received. Stannous 2-ethylhexanoate ($Sn(Oct)_2$) (Sigma-Aldrich) was used without further purification. All the other reagents used in this work were of analytic reagent grade and used as received.

The mPEG–PCL diblock copolymers were synthesized by ring-opening polymerization of ε-CL with mPEG as a macroinitiator and stannous 2-ethylhexanoate as a catalyst. A predetermined amount of ε-CL, mPEG, and $Sn(Oct)_2$ (0.1% of ε-CL in molar amount) were weighed into a three-necked glass bottle equipped with a magnetic stirring bar. The bottle was sealed under dry nitrogen and was immersed in an oil bath at 130°C for 12 hours. The resulting copolymer was cooled to room temperature, and then they were precipitated in excess of cold diethyl ether from toluene solution. The obtained copolymers were purified by dissolving them in dichloromethane (DCM) and then precipitated in excess of cold diethyl ether. Finally the mixture was filtered and dried at room temperature under vacuum for 24 hours.

The molar ratio of ε-CL to mPEG was varied to obtain copolymers with different PCL block lengths. The degree of polymerization of PCL block was then calculated from nuclear magnetic resonance (^{1}H NMR) spectra.

In this article, mPEG–PCL diblock copolymers are denoted as mPEG*x*–PCL*y*, where *x* and *y* represent the number average molecular weight M_n $\left[M_n = \sum c_i / \sum (c_i / M_i)\right]$ of mPEG and PCL block, respectively. The obtained copolymers are listed in Table 1.

Characterization of mPEG–PCL diblock copolymers

Fourier transform infrared spectroscopy

Fourier transform infrared spectra were obtained using the KBr technique in the range of 4500–400 cm^{-1} and an infrared spectrophotometer (Unicam Mattson 5000; Argenteuil, France) at room temperature.

Nuclear magnetic resonance analysis

^{1}H NMR spectra were recorded by using a Brucker (DRX 300; Fremont, CA, USA) spectrometer operating at 300 MHz using the deuterated chloroform ($CDCl_3$) as a solvent. Chemical shifts (δ) were measured in ppm using tetramethylsilane as an internal reference standard.

Size exclusion chromatography

Average molecular weights were determined on a size exclusion chromatography (SEC) system (Waters, Milford, MA, USA) equipped with an isocratic pump (Waters 515) operated at a flow rate of 1 mL/min with tetrahydrofuran (THF) (Sigma-Aldrich), an autosampler (Waters 717 plus), a column oven, and a refractive-index (RI) detector (Waters 410) with integrated temperature controller maintained at 30°C.

Data collection and data process were performed with the software Empower Pro version 5.0 from Waters Corporation. For molecular mass separation a guard column (PL gel 5 μm), three Polymer Laboratories columns [2 × PLgel 5 μm Mixed C (300 × 7.5 mm), and 1 × PLgel 5 μm 500 A (300 × 7.5 mm)] (Shropshire, UK) were used in series at 30°C.

Calibration was carried out using narrow distributed polystyrene standards. The mobile phase was THF [high-performance liquid chromatography (HPLC) grade] stabilized with dieter butyl-2,6 methyl-4 phenol (Acros Organics). Polymer samples were dissolved in THF to form a homogeneous solution. Chromatography was carried out after sample filtration through a 0.45-μm cellulose membrane filter.

Absolute molar mass determination by SEC–multiangle laser light scattering/refractive index

Absolute molecular weights of copolymer were determined on a Waters Size Exclusion Chromatography system coupled with

Table 1. The synthesis of mPEG–PCL diblock copolymers with different PCL block lengths.

Copolymer	[ε-CL]/[EO] in feed	[ε-CL]/[EO] calculated from ^{1}HNMR spectra	M_w[a]	M_{NMR}[b]	M_{nSEC}[c]	PI[d]	PD[e]	Solubility in water
mPEG 5K–PCL 1.6K CP1	0.17	0.12	7.3×10^3	6.6×10^3	9.9×10^3	1.10	14	Soluble
mPEG 5K–PCL 2.5K CP2	0.26	0.19	8.4×10^3	7.5×10^3	11.5×10^3	1.14	22	Not soluble
mPEG 5K–PCL 3.4K CP3	0.30	0.25	9×10^3	8.4×10^3	12.6×10^3	1.15	30	Not soluble
mPEG 5K–PCL 3.6K CP4	0.35	0.27	9.5×10^3	8.6×10^3	12.8×10^3	1.23	32	Not soluble
mPEG 5K–PCL 7.4K CP5	0.61	0.57	13×10^3	12.4×10^3	17.3×10^3	1.34	65	Not soluble
mPEG 5K–PCL 11K CP6	0.88	0.81	16.4×0^3	16.1×10^3	22.4×10^3	1.45	97	Not soluble

[a]Theoretical molecular weight as calculated according to the feed ratio.
[b]The molecular weight as calculated according to the integrated area ratio of the resonance peaks because of the PCL block at 4.07 ppm and because of the mPEG block at 3.65 ppm.
[c]The number average molecular weight as measured by SEC analysis (calibrated with polystyrene standards).
[d]Polydispersity index as measured by the SEC analysis.
[e]Polymerization degree as calculated from the ^{1}H NMR spectra.

- an RI detector Model (Waters 410) with integrated temperature controller maintained at 30°C,
- a triple-angle light scattering (LS) detector (MiniDAWN Tristar; Wyatt Technology, Santa Barbara, CA, USA).

The two signals were measured simultaneously because of the online multiangle laser light scattering/refractive index (SEC—MALLS/RI) arrangement; so the absolute molecular weight of the copolymers could be deduced.

Data collection and processing were performed using two softwares; ASTRA® version 4.5 from Wyatt Technology and the software Empower Pro version 5.0 from Waters Corporation.

Preparation of PCL/mPEG–PCL microparticles

Different batches of microparticles have been prepared by a double emulsion–solvent evaporation method, as described by Rawat et al.[27], with some modifications (Table 2). The double emulsion was prepared from three phases as follows:

- Internal aqueous phase: 25 mg of Ara-C (HalloChem Pharma, Chongqing, China) was dissolved in aqueous solution of PVA (M_w = 31 kDa, hydrolyzation degree = 88%; Aldrich). PVA was used at 5%.
- Organic phase: the polymer (PCL, M_w = 80 kDa; Aldrich) and one of the synthesized diblock copolymers (mPEG–PCL) that have been dissolved in a nonmiscible organic solvent, the DCM (Laurylab, Saint Fons, France) at a concentration of 5% (w/w) and 10% (w/w), respectively.
- External aqueous phase: PVA aqueous solution at the same percentage used in the internal aqueous phase.

The primary emulsion W/O was prepared by adding the organic phase to the internal aqueous phase under mechanical stirring (Ultraturax® T25; IKA Werke GmbH, Staufen, Germany) at 13,500 rpm for 1 minute. The primary emulsion was then poured into the external aqueous phase under mechanical stirring (Ultraturax® T25; IKA Werke GmbH) at 6500 rpm for 1 minute to form the double emulsion W/O/W.

After obtaining emulsion, the DCM was evaporated by a rotative evaporator (R-144; Buchi, Flawil, Switzerland) at 100 rpm for 15 minutes. The formed microparticles were separated by ultracentrifugation (Beckman, Miami, FL, USA) at 25,000 rpm for 20 minutes. The obtained microparticles were then dried under compressed air for 24 hours at room temperature.

The selection of the preparation parameter values, including the Ara-C initial load, the volumes of emulsion phases, and the choice of the solvent evaporation rather than the solvent extraction, was based on the results of preliminary investigations.

Table 2. The different microparticle batches prepared using the synthesized diblock copolymers by the double emulsion–solvent evaporation technique and their physico-chemical characterization.

Batch	MP polymeric composition	Encapsulation efficiency (%)[a]	Size (μm)[a]	Zeta potential (mV)[a]
MP0	PCL	1.30 ± 0.18	3.5 ± 1.6	−22.2 ± 0.4
MP1	PCL + CP1	1.57 ± 0.16	4.4 ± 1.8	−20.7 ± 0.4
MP2	PCL + CP2	3.18 ± 0.58	4.3 ± 2.3	−15.6 ± 0.5
MP3	PCL + CP3	8.15 ± 0.11	8.5 ± 4.7	−13.7 ± 0.1
MP4	PCL + CP4	8.94 ± 1.26	9.6 ± 5.1	−13.1 ± 0.7
MP5	PCL + CP5	12.63 ± 1.34	13 ± 5.2	−12.5 ± 0.1
MP6	PCL + CP6	9.32 ± 1.14	13.5 ± 5.7	−13.4 ± 0.7

[a]The data were expressed as means ± SD (n = 3).

Encapsulation efficiency determination

Ara-C EE in the microparticles was assessed by HPLC. Briefly, 15 mg of dried loaded microparticles was added to 5 mL DCM under magnetic stirring at 50°C water bath until complete dissolution of microparticles. Then 5 mL of distilled water was added and vortexed for 15 minutes. DCM evaporation was accelerated by a short sonication (around 10 minutes) in an ultrasonic bath at 40°C. After a clear solution has been obtained, the sample volume was made to 10 mL by adding distilled water. All the samples were filtrated (0.45 μm cellulose membrane filter) before being analyzed by HPLC. The drug extraction from different microparticle batches, of the same preparation formula, was performed in triplicate.

The HPLC unit (Thermosystems, Inc., Lombard, IL, USA) consisted in a set of a Spectra System P1000XR pump, a Spectra System AS 300 autosampler, and a Spectra System UV 6000LP diode array detector. The data were recorded and analyzed with the Chromquest® PC software over the Spectra System SN4000 unit. Chromatographic separations were performed at 25°C using a modified method of that employed by[28]. Twenty microliters of samples or calibration standards were injected directly into the column and were eluted under isocratic conditions through a Spherisorb ODS-2, C18, 5 μm (250 cm × 4.6 mm) (MZ-Analysentechnik GmbH, Mainz, Germany). The mobile phase was 5 mM monobasic potassium phosphate in distilled water containing 5% (v/v) methanol. It was filtered through a 0.45-μm pore size cellulose membrane filter and degassed with helium flow before use. The flow rate was set at 1 mL/min, the total run time was 10 minutes, and the wavelength detector was 272 nm. Each determination was carried out in triplicate.

A calibration curve was performed for Ara-C standards in deionized water, with concentrations ranging from 10 to 100 µg/mL. Ara-C EE in microparticles was then determined by the linear calibration curve obtained from the area under the Ara-C peak in the HPLC chromatogram. A correlation coefficient of 0.9998 was obtained. The sample chromatograms showed a clear single peak (retention time 5 ± 0.4 minutes) belonging to Ara-C.

The drug EE was expressed as the percentage of the encapsulated amount measured in microparticles to the total amount initially used in the formulation as follows:

$$EE = \frac{\text{encapsulated}_{\text{cytarabine}}}{\text{total}_{\text{cytarabine}}} \times 100\%$$

Microparticle size and zeta potential

The size distribution of microparticles was determined using laser diffraction technique (Beckman Coulter LS 230, Fullerton, CA, USA). Microparticle size was expressed as a volume diameter.

Zeta potential was determined in diluted particles suspensions using Zetasizer 3000 HSa (Malvern, England) at 25°C. Each measurement (size or zeta potential) was performed in triplicate.

Transmission electron microscopy

Microparticle suspensions (MP5 formula) were imaged using a transmission electron microscope (TEM) (Philips CM120, Eindhoven, the Netherlands). The suspensions were placed on a carbon-coated copper TEM grid and then dried under atmosphere conditions.

Wet scanning transmission electron microscopy

Wet scanning transmission electron microscopy (Wet-STEM) observations of Ara-C microparticles (MPs) (MP5 formula) were carried out by using environment scanning electronic microscope-field emission gun (Philips XL30, Eindhoven, the Netherlands). A specific device developed for the imaging of wet samples in transmission mode[29] was used. We employed holey carbon-coated TEM copper grids, with the carbon layer down to use copper squares as retention basins. The pressure and temperature were adjusted to evaporate a small amount of water from the microparticle suspension droplet. It allows keeping a water layer thin enough so that electrons both transmitted and scattered pass through it and can be collected to contribute to the formation of the STEM image. The signal was collected by a detector, usually used for the collection of backscattered electrons, but in our case located below the sample.

Confocal laser scanning microscopy

Drug distribution within microparticles was investigated using a hydrophilic molecule model, Fluorescein isothiocyanate-dextran (FD40; Sigma-Aldrich), by a confocal laser scanning microscope (Leica TCS SP2, Bensheim, Germany) with a regular 63× numerical aperture 1.32 oil-immersion objective lens.

Fluorescent microparticles were prepared according to MP5 formula by substituting the Ara-C by the FD40. Then they were re-dispersed in distilled water and placed onto a glass slide before the observations. FD40 was detected using an argon laser with an excitation wavelength of 488 and a 507–567 nm band-pass emission filter. All the images were obtained under the same resolution.

Residual solvent measurement by gas chromatography

Twenty milligrams of Ara-C MPs (MP5 formula) was dissolved in 2 mL of dimethyl sulfoxide (Laurylab) in a 5 mL vial and an appropriate amount of toluene was added as an internal standard. The vial was airtight and kept at 4°C before gas chromatography (GC) analysis to avoid DCM evaporation.

Analysis of the residual solvents was carried out on a gas chromatograph (Model 4890; Agilent Technologies, Santa Clara, CA, USA) equipped with a split/splitless inlet port and a flame ionization detector. Separations were performed on a Bonded FSOT Capillary column [30 m × 0.53 mm (i.d.); Superox-FA; polyethylene glycol ester; Alltech Associates Inc., IL, USA].

The following conditions were used:

- inlet temperature, 250°C
- detector temperature, 280°C
- oven temperature set at 70°C, then increased at a rate of 10°C/min until 220°C. It remains at this final temperature for 2 min
- nitrogen with a flow rate of 13 mL/min was used as a carrier gas
- a volume of 0.1 µL was injected in split mode (split ratio, 1/40).

GC ChemStation Rev. A.08.03 Software from Agilent Technologies was used to acquire and process the data.

A calibration curve was traced for DCM standards diluted in dimethyl sulfoxide, with concentrations ranging from 31 to 500 ppm. A concentration of 100 ppm of toluene was used as an internal standard. Residual DCM levels in MP5 were then determined by the linear calibration curve constructed from the ratio of the AUP (area under the peak in the GC-chromatogram) of DCM standards by the AUP of toluene. A correlation coefficient of 0.9951 was obtained.

Differential scanning calorimetry

Thermal characterization of Ara-C MPs (formula MP5) was performed with a differential scanning calorimeter differential scanning calorimetry (DSC) TA 125 (TA Instrument, New Castle, DE, USA). The equipment was calibrated with indium. All samples (Ara-C MPs, blank microparticles, physical mixture, and raw materials) were accurately weighed (5–10 mg) and sealed in aluminum pans[30]. Each sample was scanned at a speed of 10°C/min in the temperature range of 20–250°C. Nitrogen was used as the purge gas with the flow rate set at 50 mL/min with an empty aluminum pan as reference.

In vitro release study

In vitro release studies of Ara-C MPs (formula MP5) were performed using a dialysis bag (dialysis tubing cellulose membrane, molecular weight cutoff 7402 Da; Sigma-Aldrich Chemie GmbH PO, Taufkirchen, Germany). The dialysis bag was pre-treated during 1 hour with a phosphate-buffered saline (PBS, pH 7.4) to ensure its wetting and sealing. Microparticles containing 5 mg of micro-encapsulated Ara-C were suspended in 1 mL of the PBS (pH 7.4) and placed in the dialysis tube. The dialysis tube was then immersed into 10 mL of PBS (pH 7.4) at 37°C. The total volume of the receptor buffer solution was removed at pre-determined time intervals and replaced with 10 mL of fresh buffer medium. All tests were performed in triplicate. The Ara-C concentrations in the PBS (pH 7.4) were measured using HPLC analysis as described above.

Results and discussion

Synthesis and characterization of mPEG–PCL diblock copolymers

The mPEG–PCL diblock copolymers (shown in Table 1) with different molecular weights and compositions were obtained by changing the feed molar ratio of mPEG/ε-CL in the presence of stannous 2-ethylhexanoate as a catalyst.

Tin compounds are well known as highly effective esterification or *trans*-esterification catalysts and they are also known to be efficient initiators of ring-opening polymerizations of lactones and related heterocycles[31]. Moreover, $SnOct_2$ has been widely used in mPEG-polyester diblock copolymer synthesis for the elaboration of drug delivery systems[21,23].

Fourier transform infrared spectroscopy

The mPEG5K–PCL7.4K diblock copolymer (CP5), mPEG, and PCL infrared spectra were recorded. The major absorption peaks in the CP5 spectrum were the absorption band at 1725 cm^{-1} (ester C[#x02550]O stretching vibrations), which is ascribed to PCL blocks and the absorption band at 1110 cm^{-1} (C–O–C stretching vibrations) being attributed to $-OCH_2CH_2$ characteristic of the mPEG blocks. It is obvious that the CP5 exhibits characteristic peaks of both mPEG and PCL segments, confirming the presence of these two moieties. These results are consistent with the data published elsewhere[32].

Nuclear magnetic resonance analysis

To further confirm the formation of mPEG–PCL copolymers, ^1H NMR spectra were recorded. Results are shown in Figure 2 and the characteristic resonance peaks are indicated in this figure. Peaks at chemical shifts of 1.39 (multiplet, *f*), 1.65 (multiplet, *e*), 2.31 (multiplet, *d*), and 4.07 ppm (multiplet, *c*) are assigned to the methylene protons of $-(CH_2)_3-$, $-OCCH_2-$, and $-CH_2OOC-$, respectively, in PCL units. The sharp peak at 3.65 ppm (multiplet, *b*) is attributed to methylene protons of $-CH_2CH_2O-$ of mPEG units in the block copolymer. The very weak peaks at 4.23 and 3.82 ppm are, respectively, attributed to the methylene protons of $-O-CH_2-CH_2-$ of mPEG end unit that links with PCL blocks. The singlet (*a*) for monomethoxy in mPEG end groups (–OCH3) appears at 3.40 ppm.

The molecular weight (M_{NMR}) of mPEG–PCL copolymers was calculated from ^1H NMR spectra according to the following equations[33,34]:

$$\frac{4m+2}{3} = \frac{\text{Int.}3.65}{\text{Int.}(-OCH_3)} \quad (1)$$

$$\frac{2(n+1)}{3} = \frac{\text{Int.}4.07}{\text{Int.}(-OCH_3)}, \quad (2)$$

where Int. 3.65 is the integral of the intensity of the methylene proton peak of $-OCH_2CH_2-$ belonging to mPEG blocks at 3.65 ppm; Int. 4.07 is the integral of the intensity of the methylene proton peak of $-CH_2OCO-$ belonging to PCL blocks at 4.07 ppm; *m* and *n* are the corresponding polymerization degrees of mPEG and PCL blocks, respectively.

The molecular weight M_{NMR}, calculated according to the integrated area of the resonance peak of the PCL block at 4.07 ppm and that of the mPEG block at 3.65 ppm, is calculated as follows:

$$M_{NMR} + M_{w\,(PCL\ block)} + M_{w\,(mPEG\ block)} = 44m + 114n. \quad (3)$$

The values 44 and 114 are the molar masses of the repeating units of the mPEG and PCL blocks, respectively.

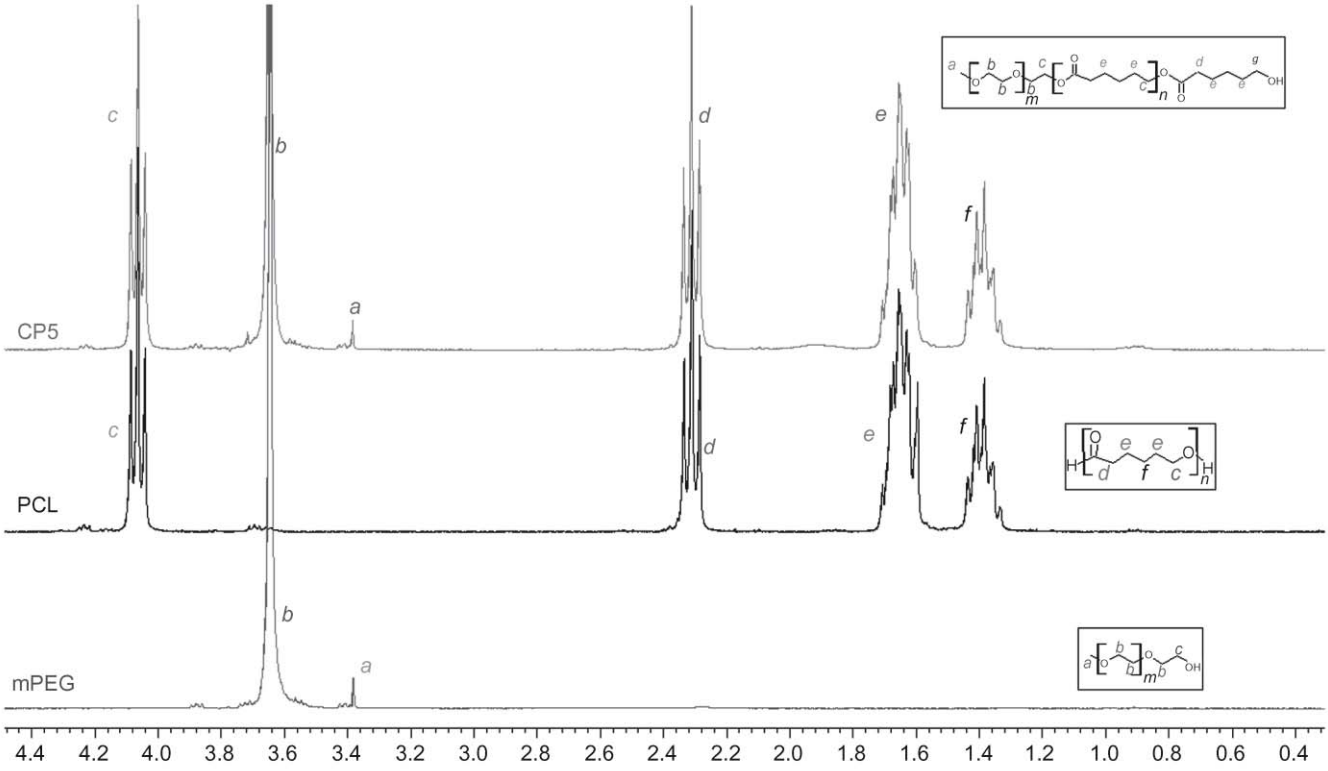

Figure 2. ^{1}H NMR spectra of CP5 (top), PCL (middle), and mPEG (bottom) in $CDCl_3$, and the assignment of the resonance peaks.

The M_{NMR}-obtained values were very close to the theoretical values M_w. In addition, the ^{1}H NMR analysis with regard to the relative contents of both blocks in the copolymer clearly indicates that the experimental data of [ε-CL]/[EO] are consistent with theoretical values.

Size exclusion chromatography

The average molecular weights and polydispersity indexes of the mPEG–PCL diblock copolymers were also measured by SEC using THF as an elution solvent and monodisperse poly(styrene) as standards. As shown in Figure 3, by increasing the ε-CL monomer amount in feed, the elution time of resultant diblock copolymers decreased, indicating the increase of copolymer molecular weights. The diblock copolymers show narrow molecular distributions with polydispersity index values around 1.10–1.45.

SEC analysis of the copolymers indicates that the observed molecular weights are higher than those of the theoretical values, especially in the case of copolymers with high PCL content (Table 1). This is explained as a result of the calibration, which was carried out with polystyrene standards. Similar observations have been reported elsewhere[35].

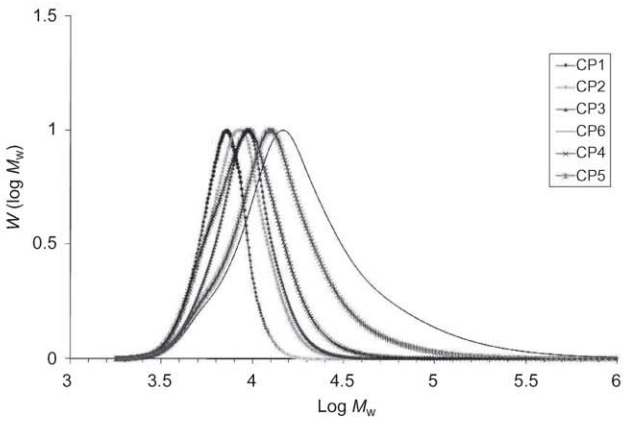

Figure 3. SEC traces of synthesized diblock copolymers. *W* represents the copolymer molar mass.

Absolute molar mass determination by SEC–MALLS/RI

The MALLS coupled with an RI detector allows the absolute molecular weight of polymers to be determined after separation by SEC, without column calibration of the respective polymer. However, this method is difficult to be applied to polymers of low molecular weight (≤30,000 g/mol) even though we tried to use it for the molar mass characterization of CP5 and CP6.

Figure 4 shows an SEC–MALLS chromatogram of CP5, with the response of the RI concentration detector and the 90° angle view of the LS detector. The vertical

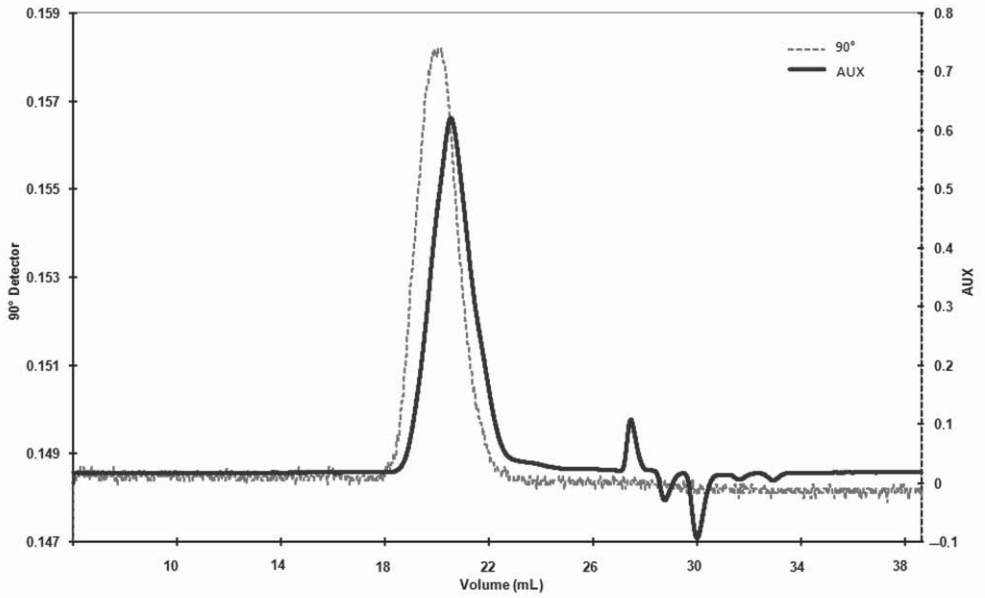

Figure 4. Elution curve of mPEG 5K–PCL7.4K (CP5), mobile phase, THF; detectors, RI (refractive index detector signal in solid line), and LS (light scattering detector signal taken at 90° in dashed line).

Table 3. Comparison of SEC–MALLS and NMR results in terms of absolute molecular weight and polymerization degree.

Copolymer	M_w[a]	$M_{w\ (SEC-MALLS)}$[b]	M_{NMR}[c]	$PD_{(SEC-MALLS)}$[d]	PD_{NMR}[e]
CP5	13×10^3	12.8×103	12.4×103	68	65
CP6	16.4×10^3	16.2×103	16.1×103	97	97

[a]Theoretical molecular weight as calculated according to the feed ratio.
[b]The absolute molecular weight as determined by SEC-MALLS method.
[c]The molecular weight as calculated according to the integrated area ratio of the resonance peaks because of the PCL block at 4.07 ppm and because of the mPEG block at 3.65 ppm.
[d]Polymerization degree as calculated from SEC–MALLS data.
[e]Polymerization degree as calculated from ^{1}H NMR data.

lines show the integration limits used in the molar mass calculation by the ASTRA® software.

Values of M_w for CP5 and CP6 determined by the two absolute methods, SEC–MALLS and ^{1}H NMR, are very close, as shown in Table 3. This suggests that the molar mass characterization of mPEG–PCL copolymers (whose M_w > 10,000 g/mol) might be achieved using SEC–MALLS, which appears to be a reliable and rapid method giving results that correlate well with those of ^{1}H NMR.

Formulation of cytarabine in PCL/mPEG–PCL microparticles

Ara-C MPs have been prepared by a modified double emulsion-solvent evaporation method. The different synthesized diblock copolymers mPEG–PCL were used as surfactant agents to stabilize the second emulsion during the microparticle preparation and then to minimize the leakage of Ara-C aqueous droplets to the external aqueous phase, being the main phenomenon leading to the poor drug EE[36]. The diblock copolymer giving rise to the optimal EE value was then selected.

The Ara-C EE, the size, and zeta potential of the microparticles prepared using the different diblock copolymers are shown in Table 2. After preliminary experiments, the preparation conditions have been fixed to study the effect of each diblock copolymer on the drug EE, size, and zeta potential of Ara-C MPs. The mPEG block length in all the copolymers was fixed while the only difference concerned the PCL block length.

Influence of the diblock copolymer molecular weight on the encapsulation efficiency

Obviously, the use of the diblock copolymers has considerably enhanced the Ara-C EE when compared to

PCL microparticles. As previously noted[37], the presence of mPEG blocks oriented toward the inner aqueous phase of the double emulsion decreases the hydrophobic character of the polymeric matrix and so increasing the affinity of the hydrophilic drug to the polymeric core, leading to an improved EE of the drug reaching approximately13% when CP5 was used (formula MP5) compared with 1.3% without adding the copolymer in the formulation (formula MP0).

It is worth noting that the longer the PCL block chain in the mPEG–PCL copolymer used in the microparticle elaboration, the higher the Ara-C EE, when all the other preparation conditions are fixed. This could be explained by the fact that a diblock copolymer with a longer anchor segment (PCL block) is more able to be adsorbed[38] or introduced in the particle polymeric matrix than a diblock with a relatively shorter PCL block.

Influence of the diblock copolymer molecular weight on the microparticle size and zeta potential

Generally speaking, using the diblock copolymers in the formulation induced a clear increase in the microparticle size. For instance, the PCL-based microparticles were around 3.5 ± 1.6 μm and increased up to 13 ± 5.2 and 13.5 ± 5.27 μm in MP5 and MP6, respectively, prepared with the longest diblock copolymers being used in our study (Table 2). This coincides well with data reported in scientific literature[39] and could be explained by the fact that the copolymer is adsorbed and/or integrated in the microparticle polymeric matrix contributing thereby to the volume of obtained microparticles.

It can be concluded that copolymers of relatively longer PCL chain may be more capable of stabilizing microparticles, as it was previously reported for nanoparticles prepared with linear or star-shaped[40] PCL/mPEG copolymers. In these works, it was found that the molecular weight of PCL block in a copolymer significantly affected the stability of nanoparticles in aqueous solution and nanoparticles with shorter PCL block length degraded faster.

Moreover, the zeta potential values of the microparticles were obviously affected by the presence of the diblock copolymers mPEG–PCL at their surfaces. Indeed, the zeta potential of obtained PCL microparticles (formula MP0) was negative (–22.2 mV). A clear decrease in the surface charge of microparticles was observed in the other formula (Table 2, e.g., –12.5 mV for MP5). This can be attributed to a shift of the shear plane position far from the particle surfaces. Similar observations have been already reported by the literature[41].

Microparticle morphology

Microparticles prepared with copolymer CP5 having the optimal EE have been selected for TEM and Wet-STEM observation to investigate their morphology. TEM micrograph (Figure 5a) shows aggregated microparticles that were almost spherical. Additionally, because of some adherence of microparticles to the copper grid, the shrinkage and collapse of particles during the drying process might cause an irregular shape of some particles. Therefore, we employed the Wet-STEM to visualize the microparticles in a thin water layer and then to address the artefact problem related to the drying process in TEM imaging. As expected, the spherical shape was confirmed by the Wet-STEM micrograph. Besides, thanks to back-scattered electron, the Wet-STEM technique informed us about the surface characteristics of the microparticles, which were found to be smooth (Figure 5b). Also, the size values obtained by laser diffraction technique correlated well with the TEM and Wet-STEM results (Figure 5c). No drug crystals were visible in the micrographs obtained in both techniques.

Confocal laser scanning microscopy

It is so far important to investigate the distribution profile of the drug inside the obtained microparticles and to check out if the drug is homogenously encapsulated inside or/and adsorbed at the microparticle surfaces. For this purpose a hydrophilic fluorescent molecule model, FD40, has been used. The main advantage of confocal laser scanning microscopy is its ability to provide visualization of images parallel to the sample surface at both internal and external levels, at multiple depths, without any mechanical sectioning. Furthermore, this technique has been already applied to determine the internal structure of microparticles[26,42–44] and thereby we applied it in our study to assess the success of microparticle preparation using our synthesized copolymers and our double emulsion–solvent evaporation method.

Figure 6 shows that microparticles are composed of homogenously distributed fluorescent aqueous vesicles in the polymer matrix where the hydrophilic molecule is dissolved in their internal aqueous medium.

According to confocal laser scanning microscopy images we suppose that Ara-C would be homogenously distributed in the internal aqueous vesicles in the microparticles, thus demonstrating the ability of the W/O/W technique to provide an adequate entrapment of hydrophilic drugs in PCL/mPEG–PCL microparticles.

Residual solvent measurement by gas chromatography

Solvents commonly used in microencapsulation, such as DCM, may be retained in microparticles as residual

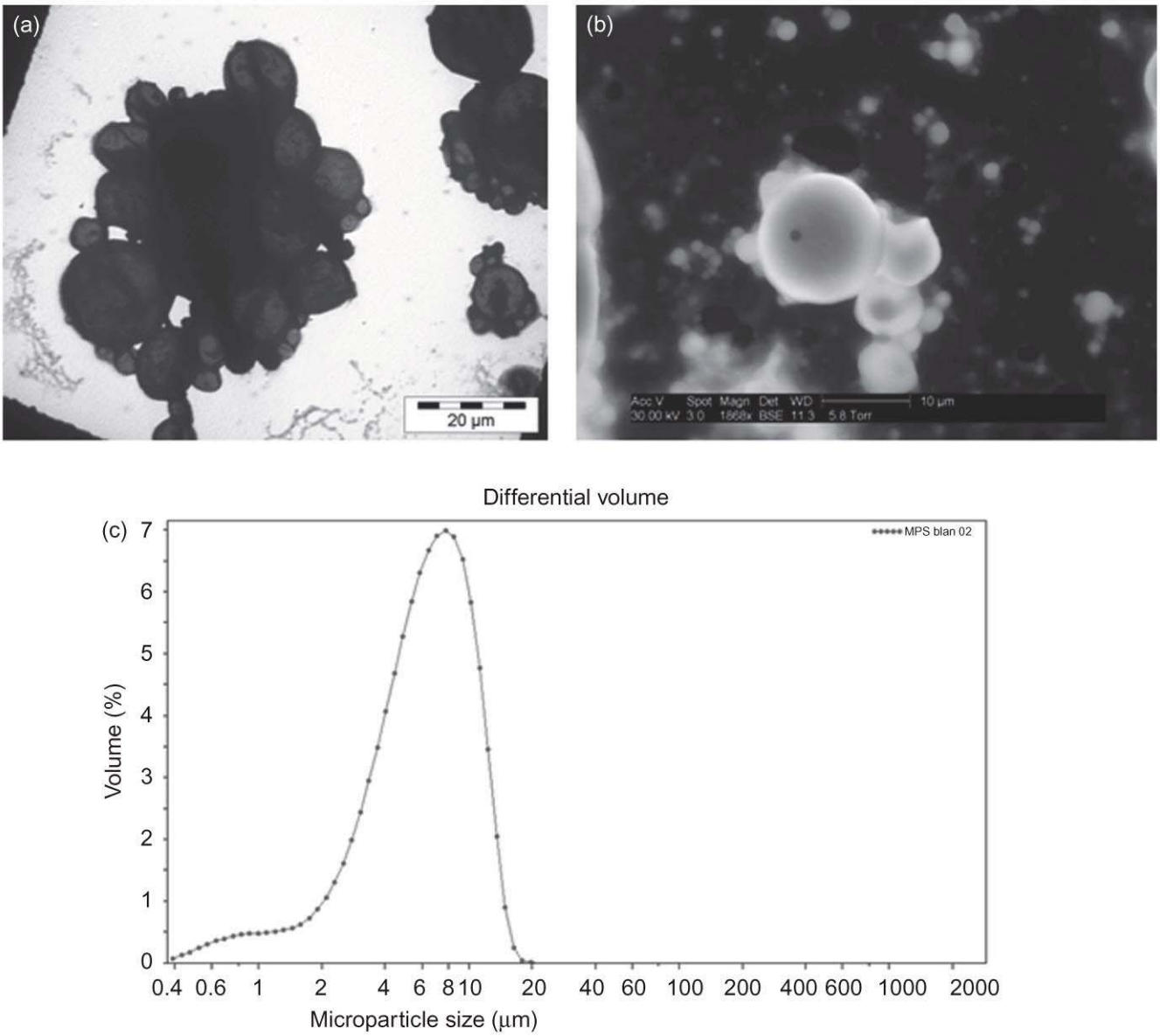

Figure 5. Morphological characteristics of the MP5 microparticles (Ara-C MPs prepared using CP5 as stabilizer), as observed by TEM imaging (a), by Wet-STEM technique (b), and the distribution of microparticle sizes (c) as determined by laser diffraction technique.

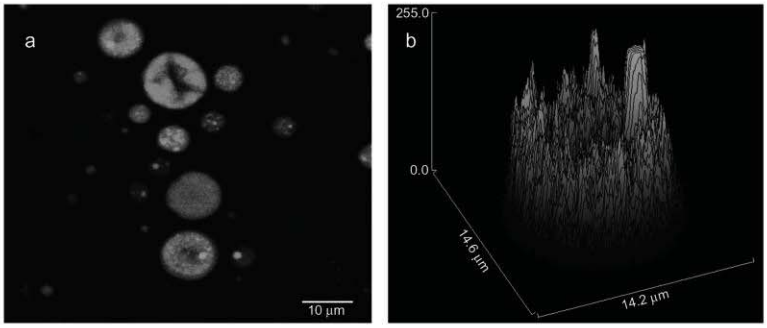

Figure 6. Distribution of FD40 in MP5 microparticles: (a) overview, (b) FD40 distribution with surface intensity plot.

organic volatile impurities. Because of the toxicological risks associated with such substances, the USP XXIII has outlined limits for these residual impurities, which is of 500 ppm for DCM.

The content of residual DCM inside the microparticles can be analyzed by GC[45–49]. It was found that the content of residual DCM in microparticles (MP5) was less than 5 ppm and well satisfied the USP XXIII regulation recommendations. This result indicates that solvent evaporation and microparticles drying can be efficiently carried out as shown in our study (under vacuum at room temperature).

Differential scanning calorimetry

The DSC technique has been widely carried out to check for the possibility of any interactions between the polymer and the loaded drugs in polymeric micro- and nanoparticulate delivery systems[50–53]. DSC analysis informs about the physical status of drugs within the polymeric matrix, which can emerge from crystalline to amorphous form[51] or molecularly dispersed and dissolved in the polymer,[54,55] influencing by consequence the relevant in vitro release properties[49,51].

The physical status of pure microparticle components and their physical mixture was determined before the microparticle preparation. Then blank microparticles and the optimized Ara-C-MPs (MP5) were also characterized with DSC (Figure 7). The pure component thermograms showed a sharp endothermic peak at 220°C and a melting peak (T_m) at 67°C, belonging to Ara-C and polymeric components (PCL and mPEG–PCL), respectively.

The DSC thermograms of the blank and drug loaded-microparticles were identical, with an endothermic peak at 58°C corresponding to the PCL T_m. Obviously, the melting point values of PCL in blank and drug-loaded microparticles were shifted to lower values after microparticle preparation. The thermal behavior of the polymer could be altered after microparticle preparation by emulsification/solvent evaporation process, as previously reported[55]. Changes of the polymer status occurred, probably because the emulsion/evaporation method causes the polymer precipitation from the previously dissolved status in DCM during microparticle formation.

Furthermore, on the drug-loaded microparticle thermogram, the endothermic peak of Ara-C has disappeared, suggesting the presence of the drug in an amorphous form.

To investigate the sensitivity of this technique to detect the drug in the concentration that was used in formula MP5, a thermogram for a physical mixture of PCL, mPEG–PCL, and Ara-C (at a ratio of 2.5/5/1, w/w, respectively) was recorded. It was found that the T_m values of the physical mixture were similar to those of the

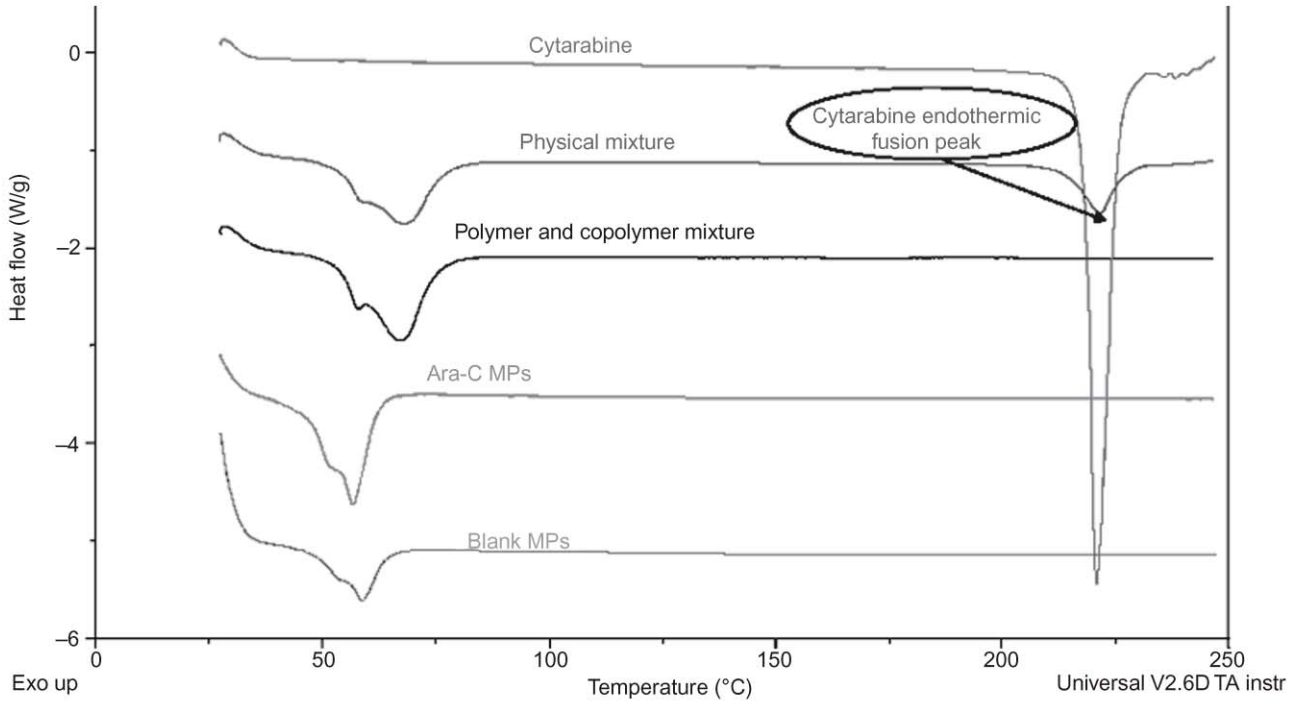

Figure 7. DSC thermograms for (from top to bottom): pure cytarabine, physical mixture of polymeric components with cytarabine, microparticle polymeric components, blank microparticles, and cytarabine-loaded microparticles (MP5).

raw materials, with a clearly observed peak for Ara-C, indicating that the Ara-C is detectable by DSC at the concentration used in microparticle preparation and the absence of its endothermic peak is actually related to the encapsulation in the polymeric matrix.

In vitro drug release study

Figure 8 shows the in vitro release profile of Ara-C MPs (MP5 formulation, with the higher EE), in pH 7.4 phosphate buffer, by representing the percentage of released Ara-C with respect to the amount of encapsulated Ara-C. The saturation concentration of Ara-C in pH 7.4 phosphate buffer is 150 mg/mL,[56] which definitely demonstrates that the sink conditions (defined as 30% of the concentration saturation) were well maintained during the whole dissolution experiment.

The release kinetics of the drug from MP5 microparticles showed a hyperbolic profile (Figure 8). A burst effect was observed in the first hour when 45% of the drug was released. We assume that this portion of drug was deposited at the regions near the PEG shell and could get access to aqueous medium without the need of long-time diffusion. Besides, the hydrophilicity of the PEG copolymers provides water uptake inside the particles[57,58] and facilitates the diffusion of the drug close to the particle surface to the release medium. The maximum drug release had taken place after 6 hours, when 81% of Ara-C was released. Afterwards, the release rate of Ara-C became steady.

Different formulations have been designed to control the release of hydrophilic molecules. Irrespective of the formulation an initial burst release profile was observed followed by a low-rate release profile. The main factors that generally influence the drug release are the polymer concentration[26], the hydrophilicity of the polymeric matrix[59], the cross-linking density of hydrophilic polymers[60], particle size, surface porosity,[61] and the preparation method[44,62].

Conclusion

In this work a series of mPEG–PCL diblock copolymers with different PCL chain lengths have been successfully synthesized to be used as surfactant agents for the Ara-C microencapsulation. This was confirmed by Fourier transform infrared spectroscopy and ^{1}H NMR data. The diblock copolymer molecular weights have been calculated by the integration of the characteristic resonance peaks in the ^{1}H NMR spectra of the synthesized copolymers. And then the calculated molecular weights of CP5

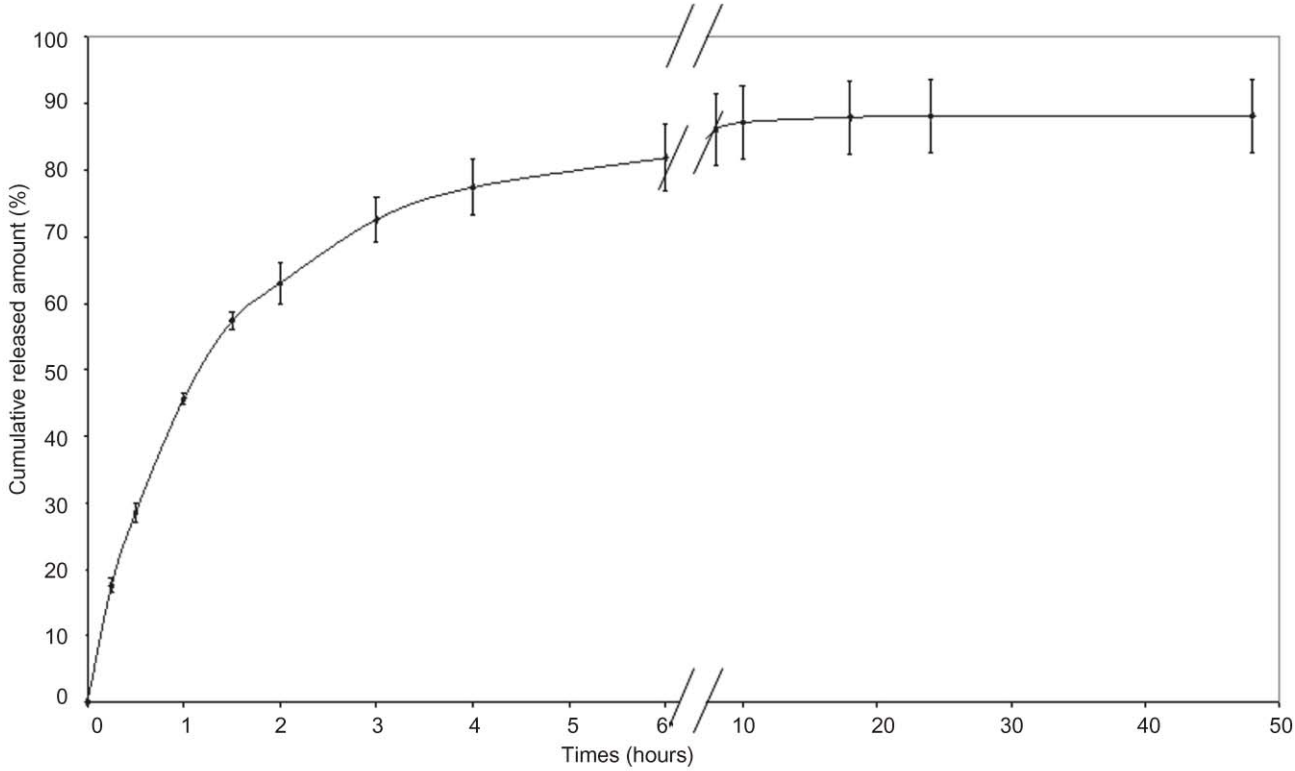

Figure 8. Cumulative percentage amount of released cytarabine from MP5 formulation in PBS (pH 7.4) at 37°C. The graph represents the mean ± SD, and each group was composed of three sets ($n = 3$).

and CP6 were verified using the SEC-MALLS/RI technique being applicable only to the polymers of relatively high molecular weight. The synthesized diblock copolymers showed narrow molecular weight distributions according to the SEC analysis.

It is found that the composition of the amphiphilic diblock copolymers, precisely the PCL block length, is influential on the particle size, Ara-C encapsulation efficiencies as well as zeta potential values of the obtained microparticles. An increase in microparticle size was observed for all the formulations prepared using the synthesized copolymers when compared to PCL microparticle size. Besides, the microparticle size increased with the increase of PCL chain length of the used copolymer. These results confirm our hypothesis about the contribution of copolymers to the microparticle polymer matrix formation. Also, an increase in the Ara-C EE was noticed, with the increase of the PCL chain length of the copolymer used in the formulation. For instance, the use of CP5 yielded the highest EE of Ara-C, increasing the latter to about 10-fold compared to PCL microparticles prepared without the copolymer.

The microparticles prepared using the CP5 showed a hyperbolic release profile of Ara-C with an initial burst release that could be attributed to the drug deposited at the region near the PEG shell. Therefore, we conclude that the use of amphiphilic diblock copolymers as surfactant agents in the encapsulation of hydrophilic molecules can largely improve the EE while keeping the known biphasic drug release profile.

Acknowledgments

The authors are grateful for the assistance of Prof. Yves Chevalier in the diblock copolymer synthesis and characterization.

Declaration of interest: The authors report no conflicts of interest.

References

1. Galmarini CM, Mackey JR, Dumontet C. (2002). Nucleosides analogues and nucleobases in cancer treatment. Lancet Oncol, 3:415-24.
2. Lindner LH, Ostermann H, Hiddemann W, Kiani A, Würfel M, Illmer T, et al. (2008). AraU accumulation in patients with renal insufficiency as a potential mechanism for cytarabine neurotoxicity. Int J Hematol, 88:381-6.
3. Mangravite LM, Badagnani I, Giacomini KM. (2003). Nucleoside transporters in the disposition and targeting of nucleoside analogs in the kidney. Eur J Pharmacol, 479:269-81.
4. Braess J, Pförtner J, Kern W, Hiddemann W, Schleyer E. (1999). Cytidine deaminase - the methodological relevance of AraC deamination for ex vivo experiments using cultured cell lines, fresh leukemic blasts, and normal bone marrow cells. Ann Hematol, 78:514-20.
5. Milano G, Chamorey AL, Thyss A. (2002). Clinical pharmacology of nucleoside analogues. Bull Cancer, 89:71-5.
6. Diab R, Degobert G, Hamoudeh M, Dumontet C, Fessi H. (2007). Nucleoside analogue delivery systems in cancer therapy. Expert Opin Drug Deliv, 4:513-31.
7. Hamoudeh M, Diab R, Fessi H, Dumontet C, Cuchet D. (2008). Paclitaxel-loaded microparticles for intratumoral administration via the TMT technique: Preparation, characterization, and preliminary antitumoral evaluation. Drug Dev Ind Pharm, 34:698-707.
8. Kang Y, Wu J, Yin G, Huang Z, Liao X, Yao Y, et al. (2008). Characterization and biological evaluation of paclitaxel-loaded poly(L-lactic acid) microparticles prepared by supercritical CO_2. Langmuir, 24:7432-41.
9. Mundargi RC, Babu VR, Rangaswamy V, Patel P, Aminabhavi TM. (2008). Nano/micro technologies for delivering macromolecular therapeutics using poly(D,L-lactide-co-glycolide) and its derivatives. J Control Release, 125:193-209.
10. Tsai M, Lu Z, Wang J, Yeh TK, Wientjes MG, Au JL. (2007). Effects of carrier on disposition and antitumor activity of intraperitoneal paclitaxel. Pharm Res, 24:1691-701.
11. Almond BA, Hadba AR, Freeman ST, Cuevas BJ, York AM, Detrisac CJ, et al. (2003). Efficacy of mitoxantrone-loaded albumin microspheres for intratumoral chemotherapy of breast cancer. J Control Release, 91:147-55.
12. Xie M, Zhou L, Hu T, Yao M. (2007). Intratumoral delivery of paclitaxel-loaded poly(lactic-co-glycolic acid) microspheres for Hep-2 laryngeal squamous cell carcinoma xenografts. Anticancer Drugs, 18:459-66.
13. Blanco MD, Gómez C, Olmo R, Muñiz E, Teijón JM. (2000). Chitosan microspheres in PLG films as devices for cytarabine release. Int J Pharm, 202:29-39.
14. Sastre RL, Olmo R, Teijón C, Muñíz E, Teijón JM, Blanco MD. (2007). 5-Fluorouracil plasma levels and biodegradation of subcutaneously injected drug-loaded microspheres prepared by spray-drying poly(D,L-lactide) and poly(D,L-lactide-co-glycolide) polymers. Int J Pharm, 338:180-90.
15. Ustariz-Peyret C. (1999). Cephradin-plaga microspheres for sustained delivery to cattle. J Microencapsul, 16:181-94.
16. Govender T, Stolnik S, Garnett MC, Illum L, Davis SS. (1999). PLGA nanoparticles prepared by nanoprecipitation: Drug loading and release studies of a water soluble drug. J Control Release, 57:171-85.
17. Pistel KF, Kissel T. (2000). Effects of salt addition on the microencapsulation of proteins using W/O/W double emulsion technique. J Microencapsul, 17:467-83.
18. Mandal TK, Shekleton M, Onyebueke E, Washington L, Penson T. (1996). Effect of formulation and processing factors on the characteristics of biodegradable microcapsules of zidovudine. J Microencapsul, 13:545-57.
19. Leo E, Brina B, Forni F, Vandelli M. (2004). In vitro evaluation of PLA nanoparticles containing a lipophilic drug in water-soluble or insoluble form. Int J Pharm, 278:133-41.
20. Tewes F, Munnier E, Antoon B, Ngaboni Okassa L, Cohen-Jonathan S, Marchais H, et al. (2007). Comparative study of doxorubicin-loaded poly(lactide-co-glycolide) nanoparticles prepared by single and double emulsion methods. Eur J Pharm Biopharm, 66:488-92.
21. Quellec P, Gref R, Perrin L, Dellacherie E, Sommer F, Verbavatz JM, et al. (1998). Protein encapsulation within polyethylene glycol-coated nanospheres. I. Physicochemical characterization. J Biomed Mater Res, 42:45-54.
22. Vangeytea P, Gautiera S, Jérôme R. (2004). About the methods of preparation of poly(ethylene oxide)-b-poly(ε-caprolactone) nanoparticles in water: Analysis by dynamic light scattering. Colloids Surf A, 242:203-11.
23. Tobio M, Gref R, Sanchez A, Langer R, Alonso MJ. (1998). Stealth PLA-PEG nanoparticles as protein carriers for nasal administration. Pharm Res, 15:270-5.
24. Ha JH, Kim SH, Han SY. (1997). Albumin release from bioerodible hydrogels based on semi-interpenetrating polymer

networks composed of poly (epsilon-caprolactone) and poly(ethylene glycol) macromer. J Control Release, 49:253–62.
25. Hachicha W, Kodjikian L, Fessi H. (2006). Preparation of vancomycin microparticles: Importance of preparation parameters. Int J Pharm, 324:176–84.
26. Coccoli V, Luciani A, Orsi S, Guarino V, Causa F, Netti PA. (2008). Engineering of poly(epsilon-caprolactone) microcarriers to modulate protein encapsulation capability and release kinetic. J Manipulative Physiol Ther, 19:1703–11.
27. Rawat A, Majumder QH, Ahsan F. (2008). Inhalable large porous microspheres of low molecular weight heparin: In vitro and in vivo evaluation. J Control Release, 128:224–32.
28. Gómez C, Blanco MD, Bernardo MV, Olmo R, Muñiz E, Teijón JM. (2004). Cytarabine release from comatrices of albumin microspheres in a poly(lactide-co-glycolide) film: In vitro and in vivo studies. Eur J Pharm Biopharm, 57:225–33.
29. Bogner A, Thollet G, Basset D, Jouneau PH, Gauthier C. (2005). Wet STEM: A new development in environmental SEM for imaging nano-objects included in a liquid phase. Ultramicroscopy, 104:290–301.
30. Hamoudeh M, Fessi H, Mehier H, Faraj AA, Canet-Soulas E. (2008). Dirhenium decacarbonyl-loaded PLLA nanoparticles: Influence of neutron irradiation and preliminary in vivo administration by the TMT technique. Int J Pharm, 348:125–36.
31. Kricheldorf HR, Kreiser-Saunders I. (2000). Polylactones 49: Bu4Sn-initiated polymerizations of 1-caprolactone. Polymer, 41:3957–63.
32. Hua C, Dong CM. (2007). Synthesis, characterization, effect of architecture on crystallization of biodegradable poly(e-caprolactone)-b-poly(ethylene oxide) copolymers with different arms and nanoparticles thereof. J Biomed Mater Res, 82:689–700.
33. Choi C, Chae SY, Kim TH, Kweon JK, Cho CS, Jang MK, et al. (2006). Synthesis and physicochemical characterization of amphiphilic block copolymer self-aggregates formed by poly(ethylene glycol)-block-poly(epsilon-caprolactone). J Appl Polym Sci, 99:3520–7.
34. Du ZX, Xu JT, Yang Y, Fan ZQ. (2007). Synthesis and characterization of poly(e-caprolactone)-bpoly(ethylene glycol) block copolymers prepared by a salicylaldimine-aluminum complex. J Appl Polym Sci, 105:771–6.
35. Huang MH, Li S, Hutmacher DW, Schantz JT, Vacanti CA, Braud C, et al. (2004). Degradation and cell culture studies on block copolymers prepared by ring opening polymerization of epsilon-caprolactone in the presence of poly(ethylene glycol). Inc J Biomed Mater Res A, 69:417–27.
36. Dinarvand R, Moghadam SH, Sheikhi A, Atyabi F. (2005). Effect of surfactant HLB and different formulation variables on the properties of poly-D,L-lactide microspheres of naltrexone prepared by double emulsion technique. J Microencapsul, 22:139–51.
37. Vila A, Sanchez A, Evora C, Soriano I, Vila Jato JL, Alonso MJ. (2004). PEG-PLA nanoparticles as carriers for nasal vaccine delivery. J Aerosol Med, 17:174–85.
38. Stolnik S, Felumb NC, Heald CR, Garnett MC, Illium L, Davis SS. (1997). Adsorption behaviour and conformation of selected poly(ethylene oxide) copolymers on the surface of a model colloidal drug carrier. Colloids Surf A Physicochem Eng Asp, 122:151–9.
39. Shen C, Guo S, Lu C. (2008). Degradation behaviors of monomethoxy poly(ethylene glycol)-b-poly(e-caprolactone) nanoparticles in aqueous solution. Polym Adv Technol, 19:66–72.
40. Shen C, Guo S, Lu C. (2007). Degradation behaviors of star-shaped poly(ethylene glycol)epoly (3-caprolactone) nanoparticles in aqueous solution. Polym Degrad Stab, 92:1891–8.
41. Li Y, Pei Y, Zhang X, Gu Z, Zhou Z, Yuan W, et al. (2001). PEGylated PLGA nanoparticles as protein carriers: Synthesis, preparation and biodistribution in rats. J Control Release, 71:203–11.
42. Morikawa MA, Yoshihara M, Endo T, Kimizuka N. (2005). Alpha-helical polypeptide microcapsules formed by emulsion-templated self-assembly. Chem Eur J, 11:1574–8.
43. Lecaroz C, Gamazo C, Renedo MJ, Blanco-Prieto MJ. (2006). Biodegradable micro- and nanoparticles as long-term delivery vehicles for gentamicin. J Microencapsul, 23:782–92.
44. Mao S, Xu J, Cai C, Germershaus O, Schaper A, Kissel T. (2007). Effect of WOW process parameters on morphology and burst release of FITC-dextran loaded PLGA microspheres. Int J Pharm, 334:137–48.
45. Bitz C, Doelker E. (1996). Influence of the preparation method on residual solvents biodegradable microspheres. Int J Pharm, 131:171–81.
46. O'Donnell PB, McGinity JW. (1997). Preparation of microspheres by the solvent evaporation technique. Adv Drug Deliv Rev, 28:25–42.
47. Sipos P, Csoka I, Srcic S, Pintye-Hodi K, Eros I. (2005). Influence of preparation conditions on the properties of Eudragit microspheres produced by a double emulsion method. Drug Dev Res, 64:41–54.
48. Xie J, Wang CH. (2007). Encapsulation of proteins in biodegradable polymeric microparticles using electrospray in the Taylor Cone-Jet mode. Biotechnol Bioeng, 97:1278–90.
49. Shah PP, Mashru RC, Rane YM, Thakkar A. (2008). Design and optimization of mefloquine hydrochloride microparticles for bitter taste masking. AAPS PharmSciTech, 9:377–89.
50. Chawla JS, Amiji MM. (2002). Biodegradable poly(o-caprolactone) nanoparticles for tumor targeted delivery of tamoxifen. Int J Pharm, 249:127–38.
51. Jeong JC, Lee J, Cho K. (2003). Effects of crystalline microstructure on drug release behavior of poly(epsilon-caprolactone) microspheres. J Control Release, 92:249–58.
52. Della Porta G, Reverchon E. (2008). Nanostructured microspheres produced by supercritical fluid extraction of emulsions. Biotechnol Bioeng, 100:1020–33.
53. Park HY, Oh KS, Koo HM, Cho SH, Chung SJ, Lim YT, et al. (2008). Heparin-immobilized pluronic/PVA composite microparticles for the sustained delivery of ionic drug. J Microencapsul, 25:106–10.
54. Hombreiro Pérez M, Zinutti C, Lamprecht A, Ubrich N, Astier A, Hoffman M, et al. (2000). The preparation and evaluation of poly(epsilon-caprolactone) microparticles containing both a lipophilic and a hydrophilic drug. J Control Release, 65:429–38.
55. Poletto FS, Jäger E, Ré MI, Guterres SS, Pohlmann AR. (2007). Rate-modulating PHBHV/PCL microparticles containing weak acid model drugs. Int J Pharm, 345:70–80.
56. Wechter WJ, Johnson MA, Hall CM, Warner DT, Berger AE, Wenzel AH, et al. (1975). Ara-cytidine acylates. Use of drug design predictors in structure-activity relationship correlation. J Med Chem, 18:339–44.
57. Sun X, Duan YR, He Q, Lu J, Zhang ZR. (2005). PELGE nanoparticles as new carriers for the delivery of plasmid DNA. Chem Pharm Bull, 53:599–603.
58. Dorati R, Genta I, Tomasi C, Modena T, Colonna C, Pavanetto F, et al. (2008). Polyethylenglycol-co-poly-D,L-lactide copolymer based microspheres: Preparation, characterization and delivery of a model protein. J Microencapsul, 25:330–8.
59. Fernández-Carballido A, Pastoriza P, Barcia E, Montejo C, Negro S. (2008). PLGA/PEG-derivative polymeric matrix for drug delivery system applications: Characterization and cell viability studies. Int J Pharm, 352:50–7.
60. Patel ZS, Ueda H, Yamamoto M, Tabata Y, Mikos AG. (2008). In vitro and in vivo release of vascular endothelial growth factor from gelatin microparticles and biodegradable composite scaffolds. Pharm Res, 25:2370–8.
61. Klose D, Siepmann F, Elkharraz K, Krenzlin S, Siepmann J. (2006). How porosity and size affect the drug release mechanisms from PLGA-based microparticles. Int J Pharm, 314:198–206.
62. Hombreiro-Pérez M, Siepmann J, Zinutti C, Lamprecht A, Ubrich N, Hoffman M, et al. (2003). Non-degradable microparticles containing a hydrophilic and/or a lipophilic drug: preparation, characterization and drug release modeling. J Control Release, 88:413–28.

Chapitre 2
Liposomes multilamellaires chargés en cytarabine et beclométhasone dipropionate

Préparation des liposomes multilamellaires par la méthode d'injection d'éthanol : application sur l'encapsulation de la cytarabine et la beclométhasone dipropionate

Les liposomes sont les plus vieux des vecteurs pharmaceutiques. Toutefois, leur utilisation en pharmacie et en médecine est en progression permanente en raison de multiples avantages que présente ce type de vecteurs. Etant composés principalement de phospholipides, les liposomes sont considérés comme les vecteurs de choix pour l'administration pulmonaire grâce, entre autre, à leur similitude avec les surfactants pulmonaires[1].

Ce chapitre a été dédié à l'évaluation des liposomes comme un système de délivrance de la cytarabine par la voie pulmonaire pour le traitement des métastases au niveau de poumons. Ces systèmes ont aussi été évalués pour l'administration pulmonaire de la beclométhasone dipropionate, agent anti-inflammatoire utilisé dans le traitement de la bronchorrhée provoquée par le cancer broncho-alvéolaire ou dans le cancer métastatique[2], en plus de son action prophylactique de la carcinogenèse des poumons[3]. L'association de ces deux vecteurs peut, alors, être d'un grand intérêt pour améliorer l'efficacité du traitement.

Les liposomes ont été préparés par la méthode d'injection d'éthanol. Une étude de formulation a été réalisée afin de sélectionner la formule permettant d'obtenir la meilleure efficacité d'encapsulation. Le test du comportement aérodynamique sur les liposomes nébulisés a donné des résultats satisfaisants concernant la fraction respirable (FPF) et le diamètre aérodynamique massique médian du nébulisat (MMAD).

---

[1] Goerke, J. (1998). Pulmonary surfactant: functions and molecular composition. *Biochimica et biophysica acta 1408*: 79-89.

[2] Hiratsuka, T., Mukae, H., Ihiboshi, H., Ashitani, J., Katoh, S., Mashimoto, H., Hirosako, S., Mizobe, T., Matsumoto, M. & Matsukura, S. (1998). Severe bronchorrhea accompanying alveolar cell carcinoma: treatment with clarithromycin and inhaled beclomethasone. *Nihon Kokyuki Gakkai zasshi = the journal of the Japanese Respiratory Society 36*: 482-7.

[3] Wattenberg, L. W., Wiedmann, T. S., Estensen, R. D., Zimmerman, C. L., Galbraith, A. R., Steele, V. E. & Kelloff, G.J. (2000). Chemoprevention of pulmonary carcinogenesis by brief exposures to aerosolized budesonide or beclomethasone dipropionate and by the combination of aerosolized budesonide and dietary myo-inositol. *Carcinogenesis 21*: 179-82.

Ethanol injection method for hydrophilic and lipophilic drug-loaded liposome preparation

Chiraz Jaafar-Maalej[a]*, Roudayna Diab[a]*, Véronique Andrieu[b], Abdelhamid Elaissari[a] and Hatem Fessi[a] †

[a] *Pharmaceutical Technology Department, Laboratoire d'Automatique et de Génie de Procédés, LAGEP, UMR CNRS 5007, Université Claude Bernard Lyon1, ISPBL-Faculté de Pharmacie de Lyon, Villeurbanne, France*

[b] *CNRS - URMITE 6236, Faculté de Médecine; Département de Pharmacie Galénique, Faculté de Pharmacie, 13385 Marseille*

*Equal contribution

†To whom correspondence should be directed

Pr. Hatem Fessi, Université Lyon 1 Claude Bernard, UMR CNRS 5007

Bat 308G, 43 Bd du 11 Novembre 1918, 69622 Villeurbanne Cedex

Tel: 0033472431893.

Fax: 0033472431882.

E-mail: fessi@lagep.univ-lyon1.fr

Accepted for publication 11th September 2009 in Journal of Liposome Research

Abstract

In this paper, a hydrophobic (beclomethasone dipropionate, BDP) and a hydrophilic (cytarabine, Ara-C) drugs have been encapsulated in liposomes in order to be administered via the pulmonary route. For this purpose, a liposome preparation method which is easy to scale up: the ethanol injection method has been selected. The effects of critical process and formulation parameters have been investigated. The drug loaded liposomes were prepared and characterized in terms of size, zeta-potential, encapsulation efficiency, release study, cell uptake and aerodynamic behaviour. Small multilamellar vesicles with sizes ranging from about 80 to 170 nm were successfully obtained. Results indicated a significant influence of phospholipid and cholesterol amounts on liposome size and encapsulation efficiency. The higher encapsulation efficiencies were about 100 % for the hydrophobic drug (BDP) and about 16 % for the hydrophilic one (Ara-C). *In vitro* release study showed a prolonged release profile for BDP, in contrast with Ara-C which was released more rapidly. Cell uptake test revealed that fluorescent liposomes have been well internalized into the cytoplasm of SW-1573 human lung carcinoma cells, confirming the possibility to use liposomes for lung cell-targeting. Nebulized Ara-C and BDP liposomes presented aerodynamic diameters compatible with deep lung deposition. In conclusion, the elaborated liposomes seem to be promising carriers for both Ara-C and BDP pulmonary delivery.

Keywords: *liposomes, ethanol injection method, nanoprecipitation, beclomethasone dipropionate, cytarabine, pulmonary, nebulization.*

1. Introduction

Pulmonary drug delivery has been considered as a promising route that enables the delivery of therapeutic agents for the treatment of both local pulmonary diseases (e.g. asthma) and systemic disorders (e.g. diabetes) (Karathanasis *et al.*, 2005). The development of liposomal formulations for aerosol delivery has expanded the potential for more effective utilization of drugs (Desai *et al.*, 2002). Liposomes offer an excellent opportunity to selective drug targeting which is expected to optimize the pharmacokinetic parameters, the pharmacological effect, prevent local irritation and reduce the toxicity of encapsulated drugs (Budai *et al.*, 2001), (Barenholz, 2003). The tolerability and safety of inhaled liposome aerosols has been previously verified in animals as well as in human volunteers (Waldrep *et al.*, 1997), (Saari *et al.*, 1998). No untoward effects have been recognized. Furthermore, the closed vesicular structures consisting of one or more lipid bilayers surrounding an inner aqueous compartment allow both hydrophilic and lipophilic drugs to be effectively encapsulated. Water-soluble drugs can be encapsulated into the inner aqueous compartment, whereas lipid-soluble drugs can be embedded within the liposome bilayers (Massing *et al.*, 2000).

Since their first report and definition by Bangham (Bangham *et al.*, 1965), numerous processes have been developed in order to prepare lipid vesicles: thin-film hydration (Bangham *et al.*, 1965), organic solvent injection method (Batzri *et al.*, 1973), reverse-phase evaporation (Szoka *et al.*, 1978) and dehydratation–rehydratation (Kirby *et al.*, 1984).

The thin-film hydration process was the most widely used technique (Liu *et al.*, 2000), (Yang *et al.*, 2009). Despite its feasibility for preparing liposomes on a laboratory scale, this technique is not suitable for a large-scale manufacturing. Moreover, yielding heterogeneous multi-lamellar vesicles (MLV) sizing over 1 µm in diameter, thin-film hydration method requires additional preparation steps such as sonication or extrusion in order to reduce and

homogenize the vesicle size (Güven *et al.*, 2009). These problems constitute a major limitation for liposomes industrial production.

Ethanol injection (Wagner *et al.*, 2002), microfluidization (Vemuri *et al.*, 1990) and micro-emulsification (Carneiro *et al.*, 2004) are commonly used methods for liposome production scale-up. The main relevance of the ethanol injection method lies on the possibility to obtain small liposomes with narrow distribution by simply injecting an ethanolic lipid solution in water (i.e. in one step, without extrusion or sonication) (Sonar *et al.*, 2008), (Justo *et al.*, 2005). The advantages of the ethanol injection method have partly been recognized in the literature. Following the original paper of Batzri (Batzri *et al.*, 1973), several reports on the injection method have been published (Kremer *et al.*, 1977), (Campbell, 1995), (Maitani *et al.*, 2001), (Dass *et al.*, 2002) and (Stano *et al.*, 2004) including some works related to the industrial preparation (Naeff, 1996).

In this paper, we aimed to demonstrate that the ethanol injection method could be of a great interest for drug-loaded liposome preparation, regardless the drug solubility. For this purpose, a water soluble (cytarabine) and a lipid-soluble (Beclomethasone dipropionate) drugs have been selected.

Beclomethasone dipropionate (BDP) is considered as the most effective anti-inflammatory agent for the treatment of asthma and other inflammatory lung diseases (Vidgren *et al.*, 1995). This glucocorticoid, although beneficial, may produce serious systemic side effects due to the swallowed drug-fraction and local *Candida* overgrowth or irritation of the vocal chords (Darwis *et al.*, 2001). Moreover, most inhaled corticoids are rapidly cleared from the lungs which explains the relatively short therapeutic effect of aerosols, the necessity for frequent administrations and the occurrence of unwanted side effects (Darwis *et al.*, 2001). The encapsulation of BDP in liposomes allows overcoming these drawbacks by sequestering the drug molecules within the phospholipid bilayers and therefore decreasing undesirable effects.

Cytarabine (cytosine arabinoside, Ara-C) is an effective chemotherapeutic agent for the treatment of acute myelogenous leukaemia and lymphocytic leukaemia (Diab *et al.*, 2007). However due to the short half-live of the drug, repeated injections are required. In order to find a non invasive way of administration, many efforts have been devoted to investigate the possibility to use an alternative administration route, such as the pulmonary one (Juliano *et al.*, 1980). Liposome-mediated pulmonary drug delivery may increase drug retention-time in the lungs, and more importantly reduce side-effects resulting in enhanced therapeutic efficacies (McCullough *et al.*, 1979), especially that the lungs are the major site of metastatic invasion.

In this work, the ethanol injection method was studied in order to be used for the encapsulation of Ara-C and BDP in liposomes. Different liposome batches have been prepared by varying the process and formulation parameters and then characterized in terms of size, zeta-potential, morphology, encapsulation efficiency and *in vitro* drug release. Afterwards, *in vitro* aerodynamic aerosol assessment and fluorescent liposome cell uptake study have been conducted in order to verify the suitability of elaborated liposomes for the pulmonary delivery.

2. Materials and methods

2.1. Materials

Cytarabine (Ara-C) was purchased from HalloChem Pharma (Chongqing, China). Beclomethasone dipropionate (BDP) was obtained as a kind gift sample from BUFA B.V. pharmaceutical products (UITGEEST-Holland). Lipoïd® E80 (Egg Yolk lecithin at 80% of phosphatidylcholine and 9% phosphatidylethanolamine) were purchased from Lipoïd GmbH (Ludwigshafen, DE). Cholesterol (CH), phosphotungstic acid, sodium dodecyl sulphate SDS, fluorescein isothiocyanate-dextran (FD4) and Nile red (NR) were purchased from Sigma-

Aldrich, (Saint Quentin Fallavier, France). Water was purified on a Milli-Q system obtained from Millipore® synergy system. All solvents (Ethanol and Methanol) used were of analytical grade (Carlo Erba Reagenti) and used as such.

2.2. Methods

2.2.1. Drug-free liposome preparation by ethanol injection method

Liposomes were prepared by a modified ethanol injection method (Batzri *et al.*, 1973). The required amounts of phospholipids and cholesterol were dissolved in ethanol. The resulting organic phase was injected by means of a syringe pump in a defined volume of distilled water under magnetic stirring. Spontaneous liposome formation occurred as soon as ethanolic solution was in contact with the aqueous phase. The liposome suspension was then kept under stirring for 15 min at room temperature. Finally the ethanol and a part of water were removed by rotary evaporation (Rotavapor R-144, Buchi, Flawil, Switzerland) under reduced pressure.

2.2.2. Drug- loaded liposome preparation

2.2.2.1. Ethanol injection method

Dug-loaded liposomes were prepared as described above. The hydrophilic drug was added to the aqueous phase (table 1) while the lipophilic drug was added to the organic one (table 2). Unloaded drug was removed by ultracentrifugation of liposome suspension (Beckman, Miami, FL, USA) at 60,000 rpm for 1 hour. The obtained pellet were dispersed in a phosphate-buffered saline PBS and stored at +4°C.

2.2.2.2. Modified nanoprecipitation method

Nanoprecipitation method adapted from (Fessi *et al.*, 1988) was optimized for the preparation of Ara-C loaded liposomes (table 3). Phospholipids and cholesterol were dissolved in ethanol. Ara-C was dissolved in a defined volume of water. The organic phase was then added to the aqueous phase and the mixture was stirred using high speed homogenizer (Ultraturax® T25, IKA Werke GmbH, Staufen, Germany) for 2 min. Afterwards, the ethanol and a part of water

were removed by rotary evaporation (Rotavapor R-144, Buchi, Flawil, Switzerland) under reduced pressure. Unloaded Ara-C was removed by ultracentrifugation of liposome suspension (Beckman, Miami, FL, USA) at 60,000 rpm for 1 hour. The obtained pellet were dispersed in a phosphate-buffered saline PBS and stored at +4°C.

2.2.3. Vesicle size and zeta potential analysis

Mean vesicle size of drug-free and drug-loaded liposomes were determined by photon correlation spectroscopy (PCS) using Malvern Zetasizer Nano-series (Malvern Instruments Zen 3600, Malvern,UK) after sample dilution in water. Zeta potential was measured by *Smoluchowski's* equation (Sze *et al.*, 2003) from electrophoretic mobility of liposomes. All measures were performed in triplicate at 25°C.

2.2.4. Determination of encapsulation efficiency

Liposome encapsulation efficiency was measured by determining the amount of entrapped drugs using the ultracentrifugation technique (Lopez-Pinto *et al.*, 2005). Briefly, a defined volume of the drug-loaded liposome sample was centrifuged in order to separate the unloaded drug. The pellet was then dissolved in ethanol in order to release the encapsulated drug (E_{drug}). An equal volume of the liposome suspension has been used in order to assess the total amount of the drug (T_{drug}) present in the suspension. T_{drug} was measured after having dissolved and disrupted the liposomes in ethanol using an ultrasound bath for few minutes. All the samples were filtred (0.45 µm cellulose membrane filter). The drug encapsulation efficiency (EE %) was expressed as the percentage of the encapsulated amount (E_{drug}) to the total amount (T_{drug}), as follows: $EE\% = \frac{E_{drug}}{T_{drug}} \times 100$

Total and encapsulated drug amounts determination was carried out using HPLC (Thermo Separation Products, Spectra system, Japan) equipped with an UV detector (UV6000LP). The data were recorded and analyzed with the Chromquest® PC software over the Spectra System SN4000 unit.

A modified method of that used by (Saari *et al.*, 1998) has been employed for BDP EE % determination . Drug was eluted at 35°C using a methanol- water (80:20, v/v) mobile phase at a flow rate of 1 ml/min and an injected volume of 20 µl. A Kromasil® column 0.5 µm, C18 (25 cm × 4.6 mm) (Peeke scientific, USA) was used as the stationary phase. The wavelength detection was set at 238 nm and the total run time was 10 min. A calibration curve of BDP standards was performed with concentrations ranging from 10 to 100 µg/ml. Correlation coefficient of 0.9995 was obtained.

Chromatographic Analysis of Ara-C were performed at 25°C using a modified method of that employed by (Gómez *et al.*, 2004). Twenty microlitters of samples or calibration standards were eluted under isocratic conditions through a Spherisorb ODS-2 column, C18, 5 µm (25 cm × 4.6 mm) (MZ-Analysentechnik GmbH, Mainz, Germany). The mobile phase was 5 mM monobasic potassium phosphate in distilled water containing 5% v/v methanol. The flow rate was set at 1 ml/min and the wavelength detector was 272 nm. Each determination was carried out in triplicate. A calibration curve was performed for Ara-C standards with concentrations ranging from 10 to 100 µg/ml. A correlation coefficient of 0.9998 was obtained. The sample chromatograms showed a clear single peak at a retention time of 5 ± 0.4 min.

2.2.5. Morphological study by Transmission Electron Microscopy

Liposome suspensions were imaged using a transmission electron microscope (TEM) (Philips CM120, Eindhoven, The Netherlands). A drop of the liposome suspension was placed onto a carbon-coated copper grid, forming a thin liquid film. The films were negatively stained with 2% phosphotungstic acid solution (w/w), pH 7.1 for 1 min. The excess of phosphotungstic solution was removed with a filter paper and stained samples were characterized using an accelerating voltage of 80 kV.

2.2.6. *In vitro* release study

In vitro release studies of liposomes loaded either with Ara-C or BDP were performed with respect to the sink conditions, using a dialysis tube (Dialysis tubing cellulose membrane, molecular weight cut-off 7402 Da, Sigma-Aldrich Chemie GmbH PO, Taufkirchen, Germany). The dialysis tube was pre-treated during 1 h with a phosphate-buffered saline (PBS, pH 7.4), to ensure its wetting and sealing. One millilitre of liposome suspension in PBS (pH 7.4) was placed in the dialysis tube. This latter was immersed into 30 ml of PBS (pH 7.4) or 1 mM SDS for Ara-C and BDP release studies, respectively. The liposome suspension in the dialysis tube and the release medium were slowly stirred with a magnetic stirrer (75 rpm), at 37°C. At pre-determined time intervals, aliquot samples of the release medium were withdrawn and replaced with equal volume of fresh release medium. All tests were performed in triplicate. The drug concentrations in the release medium were measured using HPLC analysis, as described above.

2.2.7. Stability study

Stability study has been performed on five drug-free liposome formulations in which phospholipid and cholesterol amounts have been varied. Liposomes were stored under static conditions at +4°C over a period of 28 days. Results were expressed in terms of vesicle size and morphology.

2.2.8. *In vitro* cell uptake

Cell uptake was investigated using fluorescent liposomes by means of a confocal laser scanning microscope (Leica TCS SP2, Bensheim, Germany) with regular 63x/1.32 numerical aperture oil-immersion objective lens. Towards this aim, some liposome suspensions were prepared by adding a lipophilic fluorescent probe, i.e. nile red (NR), to the organic phase or a hydrophilic one, i.e. fluorescein isothiocyanate-dextran (FD4), to the aqueous phase, according to the ethanol injection method.

SW-1573 human lung carcinoma adherent cells were grown on two glass coverslips in six-well plastic dishes at a density of 0.2 x 10^5 cells/well for 24h at 37°C. Cells were cultivated in a RPMI culture medium (RPMI, Roswell Park Memorial Institute, Gibco, Invitrogen), supplemented with 10% foetal bovine serum (FBS, Cambrex, Cergy Pontoise, France), penicillin (100 U/ml), and streptomycin (100 µg/ml) (Invitrogen).

Afterwards, the cells were incubated in the presence of liposomes labeled either with FD4, or with NR. Two controls; cells without any treatment and cells treated with an aqueous solution/dispersion of the fluorescent agent (at the same concentration as in the liposome suspensions) were used.

After 24 h of incubation in the presence of the fluorescent liposomes, the SW-1573 cells were rinsed with PBS (pH 7.4) twice and then were treated with picric acid-formaldehyde (PAF, 4% v/v in PBS) in the dark at room temperature for 10 min. The cells were washed again with PBS at least three times and then they were treated by Di Aminido Phenyl lndol (DAPI, Vector Laboratories, Burlingame, CA, USA) for 10 min in the dark at room temperature. Finally, cells were washed with distillated water, dried at room temperature and conserved in the dark at +4°C.

2.2.9. Aerodynamic assessment of liposomes

The aerodynamic behavior of the drug-loaded liposomes was assessed using a Next Generation Impactor (NGI, Copley Scientific, Nottingham, UK) at a flow rate of 30 L/min. Liposomal suspensions (5 ml) were nebulized using PARI LC SPRINT® (Pari GmbH, Starnberg, Germany) jet nebulizers driven by a PARIBOY® SX compressor (Pari GmbH, Starnberg, Germany). Nebulizer was operated to dryness. After nebulization the drug deposited in the throat and each NGI plates was extracted by methanol and then assayed by HPLC, as described above. All measurements were performed in triplicate.

The mass median aerodynamic diameter (MMAD) and geometric standard deviation (GSD) of aerosol droplets were determined from the curve of the cumulative mass distribution versus aerodynamique diameters (AED) (Majoral *et al.*, 2006). Respirable fraction or (fine particle fraction, FPF) was determined as the cumulative drug mass fraction corresponding to nebulized droplets with a mean size ≤ 5 µm (Bridges *et al.*, 2000), (Jaafar-Maalej *et al.*, 2009). The nebulization efficiency (NE%) was calculated considering the cumulative drug mass collected on the NGI plates and expressed as a percentage of the initial drug mass submitted to nebulization (Zaru *et al.*, 2007):

NE% = 100 X [Nebulized drug mass (collected on plates) / Initial drug mass (placed in the nebulizer)]

3. Results and discussion

3.1. Systematic study of drug-free liposome preparation method

3.1.1. Solvent screening

Numerous water-miscible solvents have been used for the preparation of liposomes: acetone, ethanol, chloroform, and methanol (Domazou *et al.*, 2002), (Kikuchi *et al.*, 1987), (Isele *et al.*, 1994). When organic solvents are used in drug formulation, some criteria have to be taken into account, such as toxicity, water-solubility, viscosity and dissolving powers toward the lipids and the drug.

In this work, alcohols, and chloroform were suitable solvents, with respect to phospholipid (E 80) and drugs solubility. Although usually removed by evaporation, solvents may remain as traces in the final formulation representing a possible risk for human health and affecting the stability of vesicles. Methanol and chloroform were not selected due to the higher toxicity. Then the ethanol was used with the aim of reducing the toxic problems in the final liposome formulation.

3.1.2. Ethanol injection method: influence of process and formulation parameters on vesicle size

3.1.2.1. Influence of solvent/non solvent volume ratio

A systematic study was carried in order to point out the influence of solvent/ non solvent (S/NS) volume ratio on liposome formation. The ratio of S/NS was varied from 0.1 to 2 while the phospholipid concentration and cholesterol percentages were kept constant at 20 mg/ml and 20% (w/w), respectively. It should be mentioned that when S/NS volume ratio was 0.1 or above 2, the liposome formation does not take place. Results are shown in figure 1. Vesicle size remains nearly constant for S/NS volume ratio ranging from 0.1 to 1 (108 ± 7 nm). As the volume ratio reached 2, the mean vesicle size notably increased (804 nm). These findings suggest that the S/NS volume ratio has a minor influence with respect to the vesicle size as long as the critical value (S/NS = 1) is not exceeded. When ratio was above 2, the phospholipid solubility in ethanol/water mixture increased preventing liposome formation. According to these results, the ratio was fixed at 0.5 for the following experiments.

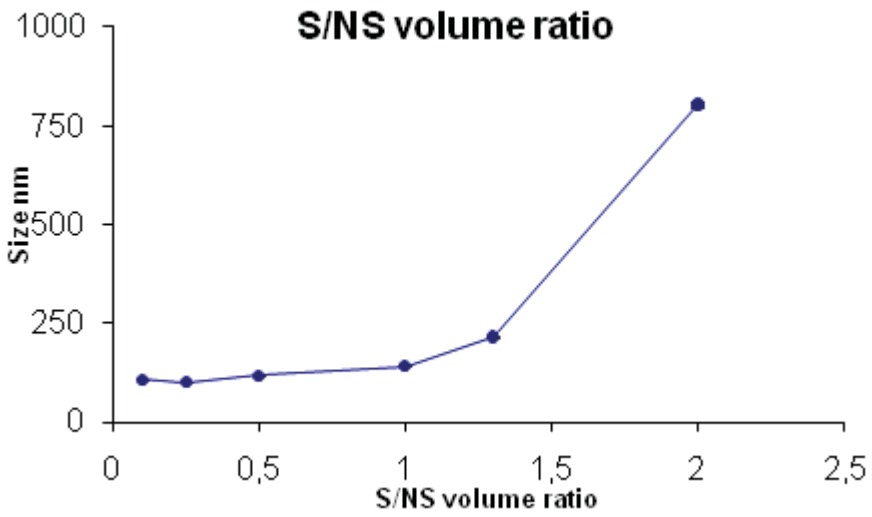

Figure 1. The impact of solvent / non solvent volume ratio effect on drug-free liposome size.

3.1.2.2. Influence of injection velocity

The ethanol injection velocity was controlled by the mean of a syringe pump. The injection rate was varied from 600 µl/min to 1800 µl/m for 3 different S/NS volume ratio. Lipid concentration and cholesterol percentage were kept constant.

According to figure 2a, the injection velocity has no significant effect on the mean vesicle size, whatever is the used S/NS volume ratio. It has been established that the solvent injection technique is based on lipid precipitation and the rapid diffusion of the solvent across the solvent-lipid interface with the aqueous phase, independently of the organic solvent injection velocity (Schubert *et al.*, 2003). Similar results have been reported in previous studies (Kremer *et al.*, 1977), (Pons *et al.*, 1993).

It is noteworthy that an injection rate inferior to 600 µl/min, resulted in diluted liposome suspension which may lower the encapsulation efficiency of the water soluble agent, as it has been observed elsewhere (Pons *et al.*, 1993).

3.1.2.3. Influence of stirring rate

Stirring rate of aqueous phase during solvent injection has been varied from 400 to 800 rpm for two injection velocity values (900 and 1800 µl/min). It can be clearly seen in figure 2b that the vesicle size decreased from 129 to 73 nm with increasing the stirring rate for both used injection velocities, indicating a negative influence of the stirring rate on the mean liposome size.

The decrease of the vesicle size can be explained by the intensification of the micromixing between the two phases with increasing the stirring rate. High micromixing efficiency may enhance the mass transfer and the rate of diffusion between the organic and aqueous phases. Hence high homogenous supersaturation may occur in short time leading to rapid self arrangement of phospholipid and small vesicle formation (Zhang et al., 2006).

3.1.2.4. Influence of phospholipid concentration

The influence of phospholipid concentration on liposome size was investigated (figure 2c). For phospholipid concentration ranging from 10 to 60 mg/ml, a vesicle size increase from 92 ± 4 nm to 163 ± 4 nm was observed. It should be mentioned that phospholipid concentration above 60 mg/ml results in large aggregates of phospholipid due to exceeding phospholipid solubility limit.

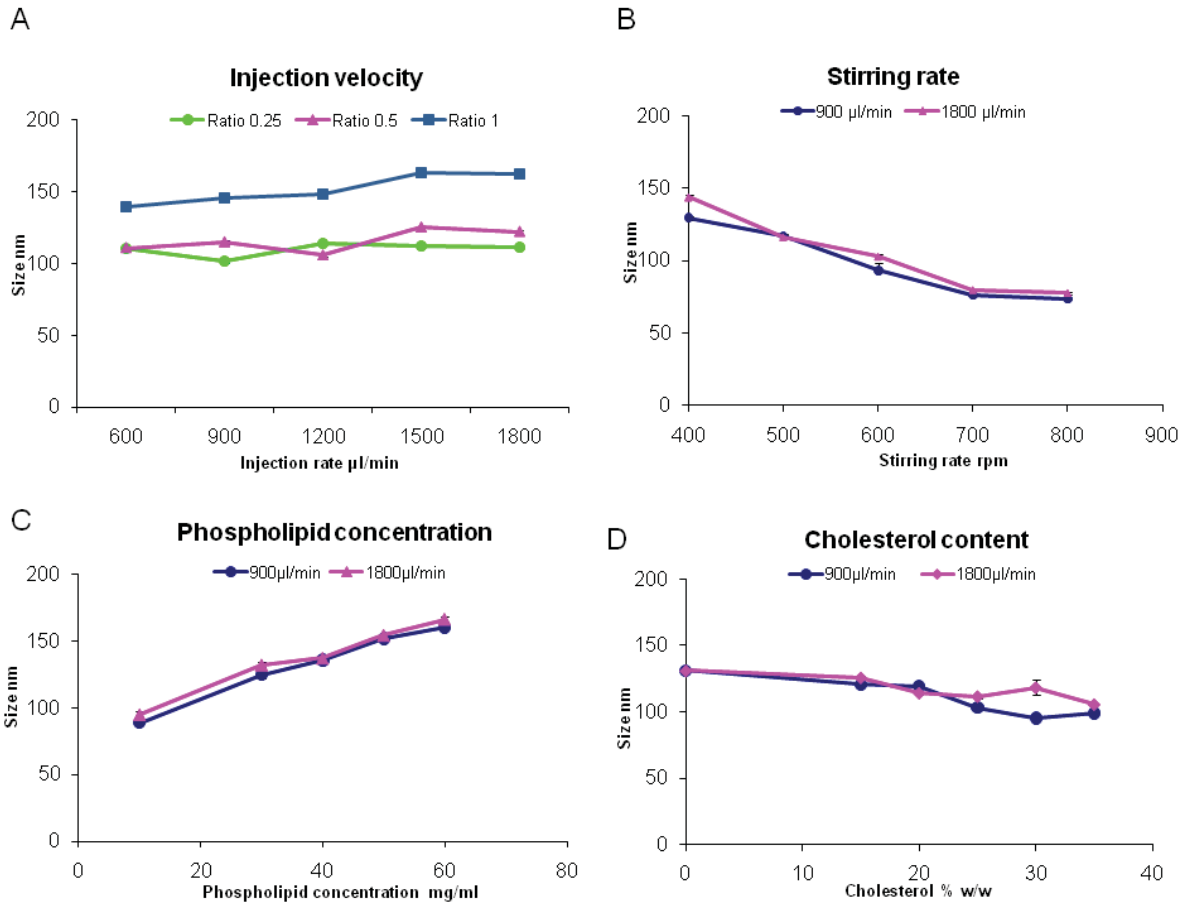

Figure 2. The impact of injection velocity (A), stirring rate (B), phospholipid concentration (C) and cholesterol content (D) effects on drug-free liposome size.

3.1.2.5. Influence of cholesterol content

A series of experiments were conducted in order to investigate the effect of the liposome cholesterol content on vesicle size. As shown in figure 2d, when liposomes were prepared with increasing cholesterol content no significant increase in the vesicle size was observed. This result was obtained for both injection velocities (900 and 1800 µl/min).

Cholesterol is one of the common additives included in the liposome formulation in order to improve their bilayer characteristics (i.e., the fluidity of the bilayer membrane or its stability). However, it may not induce vesicle size variations, as it has been previously reported (Mohammed *et al.*, 2004), (Yan *et al.*, 2000).

According to Kremer (Kremer *et al.*, 1977), liposome characteristics produced by the ethanol injection method, may depend on the injection velocity, the alcohol concentration and the lipid concentration. Also, the stirring rate during alcohol injection could be of high importance. Our results revealed that the stirring rate and lipid concentration were the main factors influencing the mean liposomes size. Liposome formation mechanism has been explained by the bilayer planar fragments (BPFs) theory (Lasic, 1988). According to this concept the phospholipids dissolved in ethanol precipitate at the phase boundary water/organic solvent resulting in BPFs formation. Upon complete diffusion of organic solvent to the external aqueous phase, BPFs self assembly results in vesicle formation (Lasic, 1988) (figure 3). Hence, the phospholipid concentration is the major factor influencing liposome size.

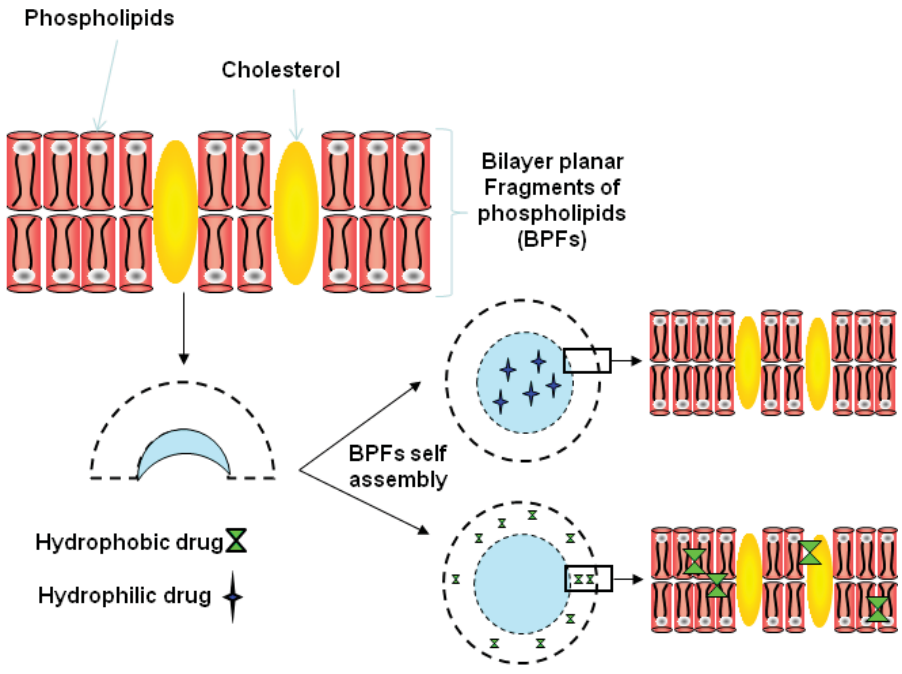

Figure 3. Schematic illustration of Bilayer Planar Fragments (BPFs) theory of lipid vesicle formation.

3.2. Encapsulation of cytarabine

Being a small highly hydrophilic molecule, Ara-C encapsulation into lipid or polymeric nanoparticles is a major challenge because of its rapid efflux or diffusion across liposome fluid membrane or due to its low affinity to constitutive polymers during nanoparticle preparation. Numerous attempts to encapsulate Ara-C in conventional liposomes (i.e. multilamellar vesicles MLV or small unilamellar vesicle SUV) have been reported in the literature (Hunt *et al.*, 1979), (Juliano *et al.*, 1980), (Mayhew *et al.*, 1979), (McCullough *et al.*, 1979), (Patel *et al.*, 1984), (Rustum *et al.*, 1979). Nevertheless, the achieved encapsulation efficiency values have never been mentioned in any of these published works, to the best of our knowledge.

In this work, two encapsulation methods; the nanoprecipitation as well as the ethanol injection techniques; have been evaluated and the impact of the different preparation parameters on the vesicle size and Ara-C entrapment have been studied.

3.2.1. Influence of the preparation method on the vesicle size and encapsulation efficiency

It has been found that using the same formulation parameters, ethanol injection and modified nanoprecipitation methods have produced Ara-C loaded liposomes with slight differences in sizes and encapsulation efficiencies. However, higher Ara-C encapsulation efficiencies (reaching a value of 15.6% for EI7) and smaller vesicle sizes were achieved using ethanol injection method (figure 4).

3.2.2. Influence of solvent/non solvent volume ratio on the vesicle size and encapsulation efficiency

The influence of the S/NS volume ratio on the encapsulation efficiency of Ara-C loaded liposomes has been studied. As expected, the S/NS volume ratio significantly affected the encapsulation efficiency in both preparation methods (table 1 and 3).

Table 1. Physico-chemical characterization of different batches of Ara-C-loaded liposomes prepared using ethanol injection method.

Injection velocity 900 µl/min, Stirring rate 700 rpm							
Batch	**Ara-C concentration (mg/ml)**	**Solvent/non solvent volume ratio**	**Phospholipid concentration (mg/ml)**	**Cholesterol concentration (mg/ml)**	**Cholesterol % w/w [a]**	**Encapsulation efficiency (% w/w) [b]**	**Size (nm) [c]**
EI 1	5	0.5	20	4	20	8.6 ± 0.2	137 ± 1.1
EI 2	2.5	0.25	20	4	20	3.2 ± 0.1	109 ± 0.3
EI 3	10	0.5	20	4	20	5.8 ± 0.03	108 ± 1.4
EI 4	5	0.25	20	4	20	3.9 ± 0.7	82 ± 0.6
EI 11	5	0.25	20	7	35	1.9 ± 0.02	85 ± 0.9
EI 0	5	0.25	20	0	0	3.8 ± 1.7	83 ± 0.7
EI 5	10	0.5	40	8	20	7.6 ± 0.3	128 ± 0.7
EI 6	5	0.25	40	8	20	5.8 ± 0.4	113 ± 1.6
EI 7	5	0.25	60	12	20	15.6 ± 2.3	142 ± 1.9

[a] *Cholesterol percentage with respect to phospholipid mass used in the formulation.*
[b] *Encapsulation efficiencies are expressed as mean values ± standard deviations (n=3).*
[c] *The liposome sizes are expressed as mean values ± standard deviations (n=3).*

Table 3. Physico-chemical characterization of different batches of Ara-C-loaded liposomes prepared using modified nanoprecipitation method.

Batch	Ara-C concentration (mg/ml)	Solvent/non solvent volume ratio	Phospholipid concentration (mg/ml)	Cholesterol concentration (mg/ml)	Cholesterol % w/w [a]	Stirring rate (rpm)	Encapsulation efficiency (% w/w) [b]	Size (nm) [c]
NP 1	5	0.5	20	4	20	13500	6.3 ± 0.2	139 ± 1.5
NP 2	2.5	0.25	20	4	20	13500	5.0 ± 0.1	116 ± 0.9
NP 3	10	0.5	20	4	20	13500	5.4 ± 0.3	125 ± 0.3
NP 4	5	0.25	20	4	20	13500	3.3 ± 0.2	117 ± 0.5
NP 5	5	0.5	20	4	20	6500	5.9 ± 0.1	130 ± 1.3
NP 6	2.5	0.25	20	4	20	6500	6.3 ± 0.2	113 ± 0.4
NP 7	10	0.5	20	4	20	6500	2.8 ± 0.1	130 ± 0.3
NP 8	5	0.25	20	4	20	6500	2.1 ± 0.5	136 ± 0.7
NP 9	5	0.25	40	8	20	6500	5.6 ± 0.2	141 ± 2.6
NP 10	5	0.25	60	12	20	6500	10.1 ± 1.2	161 ± 2.7

[a] *Cholesterol percentage with respect to phospholipid mass used in the formulation.*
[b] *Encapsulation efficiencies are expressed as mean values ± standard deviations (n=3).*
[c] *The liposome sizes are expressed as mean values ± standard deviations (n=3).*

Using the ethanol injection method, a clear decrease in Ara-C encapsulation efficiency has been noticed (from 8.6 to 3.9% for EI1 and EI4, respectively), as the aqueous phase volume has been doubled (table 1). Similarly, the same effect of S/NS volume ratio on the encapsulation efficiency has been found for the liposomes prepared by modified nanoprecipitation method. Accordingly, NP4 and NP8 showed lower encapsulation efficiency values (3.3 and 2.1%) when compared to those of NP1 and NP5 (6.3 and 5.9%), respectively (table 3).

Vesicle size has been positively affected by the S/NS volume ratio in both preparation methods (table 1 and 3). Batches having an S/NS volume ratio of 0.5 showed higher vesicle sizes than liposome batches produced using S/NS ratio value of 0.25.

These results may be attributed to the more rapid ethanol diffusion in the volume-increased aqueous phase leading to the formation of smaller-sized liposomes because of the more rapid phospholipid self-assembly. Accordingly, the smaller vesicle sizes the smaller aqueous core volume and the lower obtained encapsulation efficiencies, knowing that the hydrophilic drug is mainly encapsulated in the liposome aqueous core (Pons *et al.*, 1993).

3.2.3. Influence of phospholipid concentration on the vesicle size and encapsulation efficiency

Phospholipid concentration showed a positive effect on liposome encapsulation efficiencies and sizes for both preparation methods (figure 4). When phospholipids concentration was increased from 40 to 60 mg/ml, Ara-C encapsulation efficiencies have been nearly tripled (5.8 to 15.6%) using ethanol injection method and doubled (from 5.6 to 10.1%) using modified nanoprecipitation technique. Similar encapsulation results have been obtained for 5-fluorouracil loaded-liposomes (a pyrimidine analogue molecule like cytarabine) (Tomoko *et al.*, 2005). Moreover, a slight increase in vesicle sizes was observed with phospholipid concentration increasing from 40 to 60 mg/ml, using either ethanol injection method (from

113 to 142 nm, table 1) or modified nanoprecipitation (from 141 to 161 nm, table 3). The positive effect of phospholipid concentration on the encapsulation efficiency of hydrophilic drugs has been previously reported (Kesisoglou *et al.*, 2005).

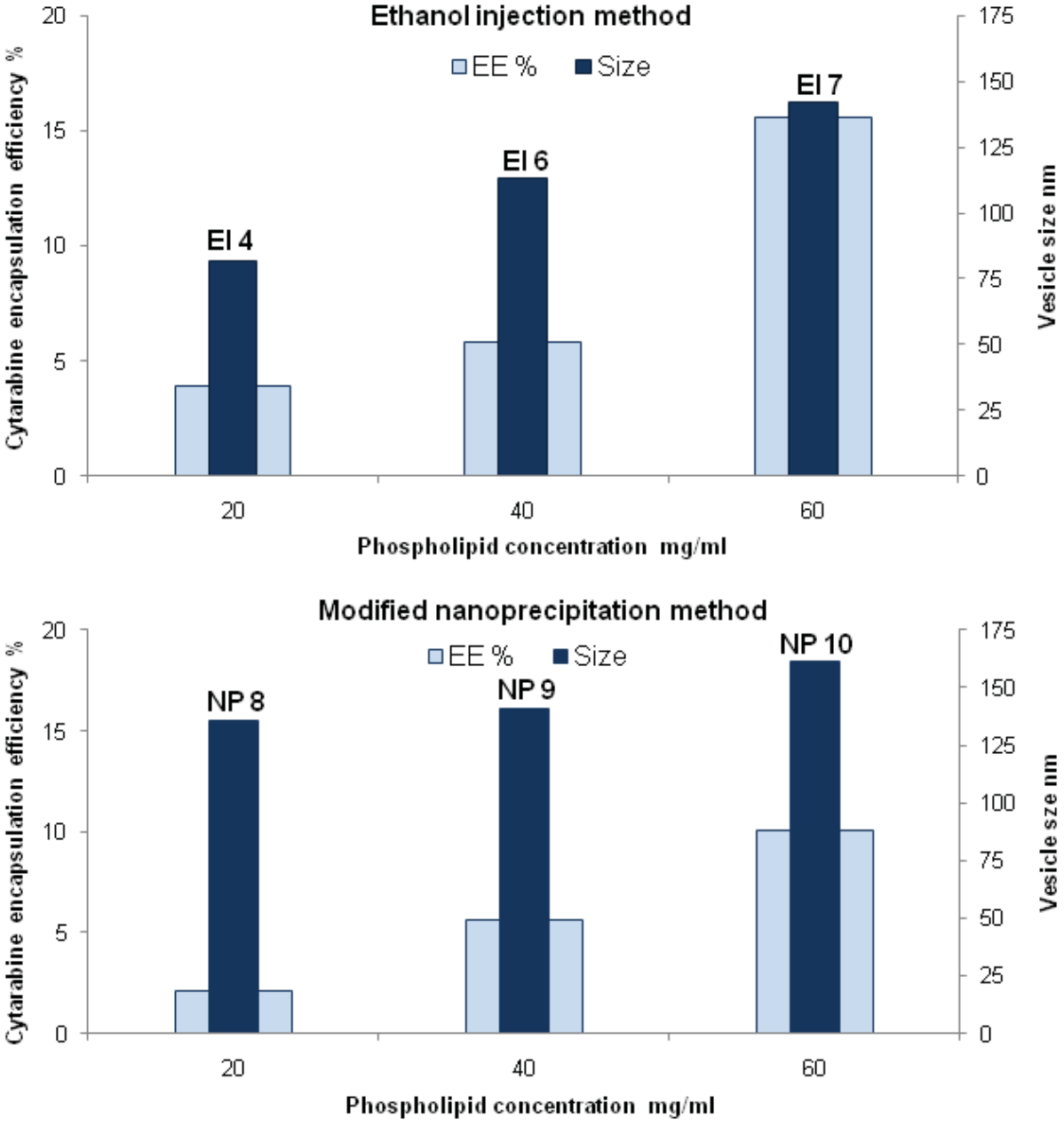

Figure 4. Vesicle size and encapsulation efficiency (EE%) of Ara-C loaded liposomes prepared using ethanol injection (EI 4, EI 6 and EI 7) or modified nanoprecipitation method (NP 8, NP 9 and NP 10), with different phospholipid concentrations. Cholesterol content, drug concentration and solvent/non solvent volume ratio were kept constant at 20% (w/w), 5 mg/ml and 0.25, respectively.

3.2.4. Influence of cholesterol content on the vesicle size and encapsulation efficiency

As it was observed for drug-free liposomes, cholesterol percentage with respect to phospholipid mass had no significant increase in Ara-C loaded vesicle sizes (EI0, EI4 and EI11, table 1). However, the encapsulation efficiency was clearly affected by the cholesterol content in the Ara-C loaded liposomes. Increasing cholesterol concentration from 4 to 7 mg/ml (20 and 35% w/w with respect to phospholipid mass, respectively) was accompanied with a clear decrease in Ara-C encapsulation efficiencies (from 3.9 to 1.9%, for EI4 and EI11, table 1). The cholesterol effect can be explained by the increased lipophilic character of liposome wall (when higher amount of cholesterol was introduced) and consequently lowering the affinity of the hydrophilic drug to lipid vesicles.

On the other hand, the absence of cholesterol in the liposome composition (EI0) had no effect on Ara-C entrapment when compared to EI4 (prepared using a cholesterol percentage of 20% w/w with respect to lipid mass). This confirms that the cholesterol does not compete with Ara-C (which is mainly entrapped in the aqueous core) to be in the phospholipid bilayer.

3.3. Encapsulation of beclomethasone

Liposome suspensions with increasing BDP concentration were prepared by ethanol injection method and examined using cross polarisation microscopy. It is found that the highest BDP concentration achievable in the liposomal formulation was 400 µg/ml. When higher BDP concentration was used in formulation, non liposome-entrapped fraction precipitated in the suspension being microscopically perceptible as crystals. This can be attributed to the high BDP hydrophobicity (water-solubility is lower than 0.1 µg/ml).

3.3.1. Influence of phospholipids concentration on the vesicle size and encapsulation efficiency

The influence of the phospholipid concentration on BDP encapsulation efficiency and vesicle size has been studied. As indicated in figure 5a, both liposome size and encapsulation

efficiency increased as phospholipid concentration in the formulation has been increased. The encapsulation efficiency of BDP-loaded liposomes was found to be in the range of 87 – 100% whereas their mean vesicle size ranged from 117 to 166 nm (figure 5a). Encapsulation results may indicate the high association of drug with phospholipid bilayers of liposomes with the increase of lipid surface and bilayer number. It has been reported that the thickness of the lipid surface of liposome increases with the increasing amount of phospholipid used in formulation (Sezer *et al.*, 2007). Similar results have been obtained for BDP-loaded liposomes preparaed by thin-film hydration method (Waldrep *et al.*, 1994), (Waldrep *et al.*, 1997) and for other lipophilic agents (Fang *et al.*, 2001).

Table 2. Physico-chemical characterization of different batches of BDP-loaded liposomes prepared using ethanol injection method.

Injection velocity 900 µl/min, Stirring rate 700 rpm, S/NS volume ratio 0.5						
Sample	**BDP concentration µg/ml**	**Phospholipid concentration (mg/ml)**	**Cholesterol concentration (mg/ml)**	**Cholesterol % (w/w) [a]**	**Encapsulation efficiency % (w/w) [b]**	**Size (nm) [c]**
BDP1	400	20	4	20	87.4 ± 3.9	117 ± 2.3
BDP2	400	40	8	20	93.3 ± 2.2	122 ± 1.9
BDP3	400	60	12	20	100.0 ± 2.1	166 ± 1.4
BDP- C0	400	40	0	0	96.0 ± 2.4	137 ± 2.9
BDP- C30	400	40	7	35	93.9 ± 2.1	132.6 ± 3.3

[a] *Cholesterol percentage with respect to phospholipid mass used in the formulation.*
[b] *Encapsulation efficiencies are expressed as mean values ± standard deviations (n=3).*
[c] *The liposome sizes are expressed as mean values ± standard deviations (n=3).*

3.3.2. Influence of cholesterol content on the vesicle size and encapsulation efficiency

Cholesterol was added to the liposome formulations for its three recognized effects: increasing fluidity or micro-viscosity of the phospholipid bilayer; reducing the permeability of the liposome membrane; and stabilizing liposomes in the presence of biological fluids (Sezer *et al.*, 2007), (Gregoriadis *et al.*, 1979).

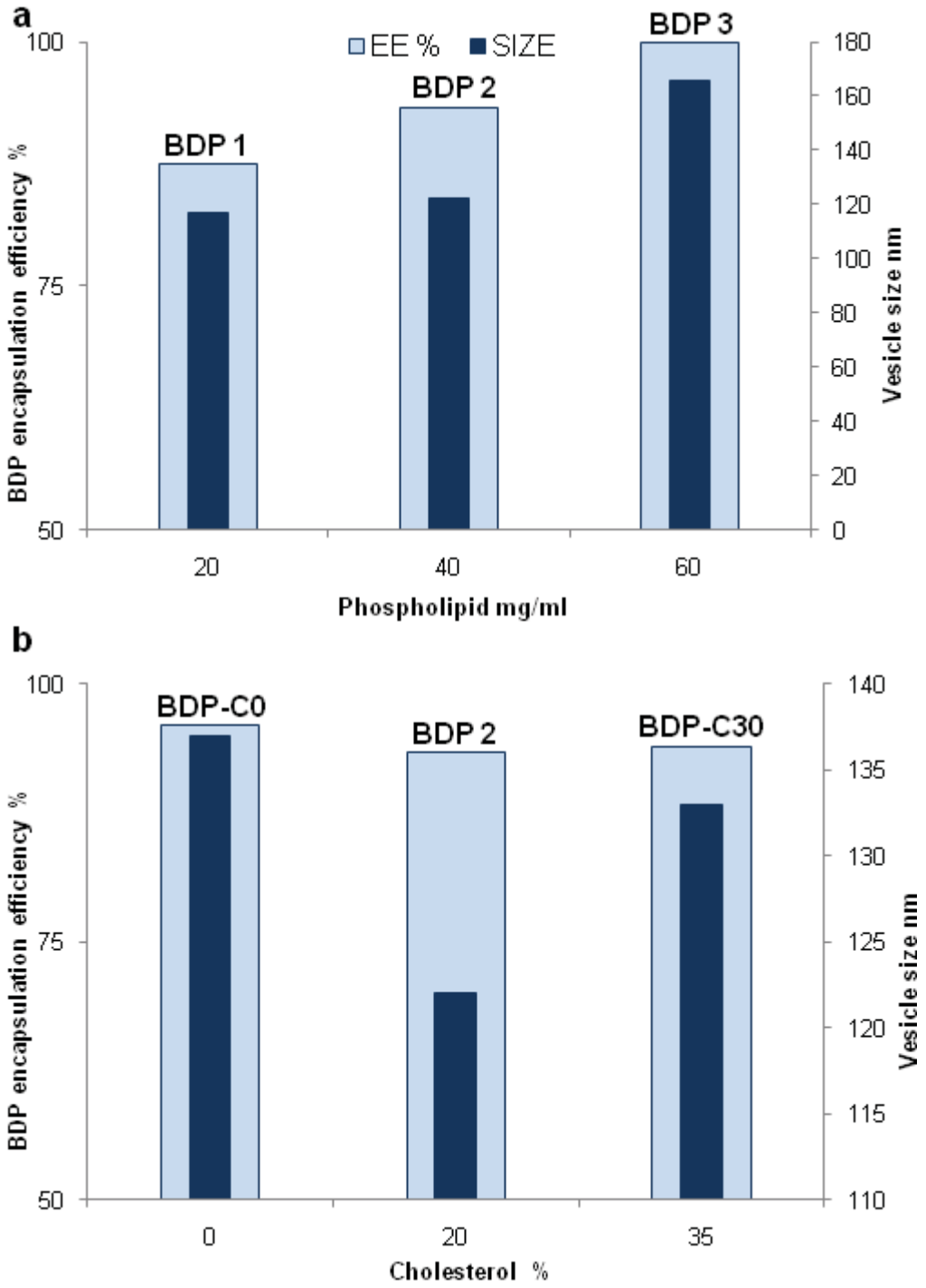

Figure 5. BDP encapsulation efficiency (EE%) as a function of (a) phospholipid concentration (BDP1, BDP2 and BDP3) or (b) amount of cholesterol in liposomes (BDP-C0, BDP2 and BDP-C30).

(a) Cholesterol content and drug concentration were kept constant at 20% (w/w) and 400µg/ml, respectively.

(b) Phospholipid and drug concentrations were kept constant at 40 mg/ml and 400 µg/ml, respectively.

As shown in figure 5b, the presence of cholesterol within the liposomes bilayer resulted in a slight reduction in EE % when liposome contained 20% cholesterol compared to 0% (93.3% versus 96% respectively). Since cholesterol might lower the partitioning of drug molecules to

the bilayer membrane, inclusion of cholesterol within lipid bilayers, generally results in a decrease in the lipophilic drug entrapment efficiencies (Zaru *et al.*, 2007). This could be explained by the fact that the lipophilic molecules compete with cholesterol molecules for the lipophilic space in the lipid bilayer and drug may be displaced by cholesterol (Fang *et al.*, 2001). The more the cholesterol molecules in liposomes of the same vesicle size, the less the space they leave in the lipid bilayer to be occupied by drug molecules. Moreover, the inclusion of cholesterol in liposomes also restricted the flexibility of the lipid hydrocarbon chains, and hence hindered drug penetration into lipid bilayer (Mohammed *et al.*, 2004). However, increasing the cholesterol content to 35% (figure 5b) had no effect on BDP incorporation. This observation may be explained by the fact that the competition between BDP and cholesterol molecules to be introduced in the phospholipid bilayers has reached a stable balance, in our experimental conditions.

In term of size, the incorporation of cholesterol in liposomes had no significant effects, which is in accordance with size results found for drug free-liposomes.

Factors affecting drug encapsulation efficiency within liposomes are various and mainly rely on liposome composition (i.e. phospholipid and cholesterol) and encapsulated drug properties. Concerning the encapsulated drugs, the encapsulation efficiency are commonly affected by the hydrophilic/lipophilic drug character (Barenholz, 2003), (Kulkarni *et al.*, 1995). The water-insoluble drug encapsulation efficiencies are usually high, reaching values up to 100%. However, water-soluble drug encapsulation efficiencies are limited by liposome aqueous core volume since they are mostly entrapped in the aqueous cavities (Kulkarni *et al.*, 1995).

3.4. Zeta potential

As surface charge is chiefly generated by liposome-constituting phospholipids, which were the same in all formulas, no significant difference has been found between the different drug-loaded batches (detailed data are not given). All liposomes were negatively charged and zeta-

potential values varied between -22 and -30 mV which is considered as an optimal potential assuring particle stability (Epstein *et al.*, 2008).

3.5. Morphological characterization

Liposome morphology was studied by transmission electron microscopy (TEM) (figure 6). Negative-stain TEM images showed that liposomes obtained using both preparation methods (ethanol injection and modified nanoprecipitation), were spherical-shaped and composed of several phospholipid bilayers (multilamellar vesicles), which could have an impact on the drug release and the cell uptake behaviour. According to TEM images, liposomes were ranged in size from 80 to 160 nm. Indeed, microscopic size results correlated well with the size values obtained by PCS.

No notable differences were found in morphology between Ara-C (figure 6 A, 6B, 6E and 6F) and BDP (figure 6 C and 6D) loaded liposomes. Moreover, the employed method showed no impact on liposome morphological characteristics. No drug crystals were visible in TEM-images regardless the preparation technique or the loaded drug.

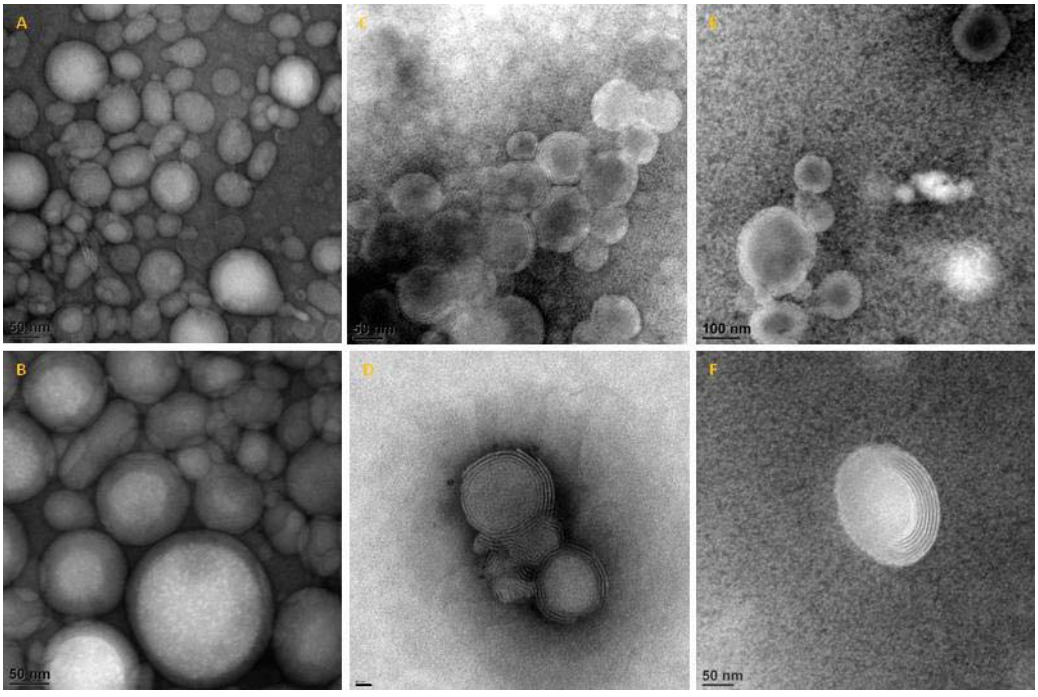

Figure 6. TEM micrographs of Ara-C loaded liposomes prepared by modified nanoprecipitation (A, B) or ethanol injection method (E, F) and BDP-loaded liposomes (C, D).

3.6. Stability study

Stability study has been carried out on free-drug liposomes over a period of four weeks. Five different formulations were selected in order to follow vesicle size and morphology evolution during storage (table 4). In term of size, small differences of about few nanometers (5–10 nm) were observed over the storage time (figure 7). Figure 8 shows the morphological changes of drug-free liposomes during storage. According to TEM images, liposome size and morphology (multilamellar spherical shape) remain nearly unchanged during one month.

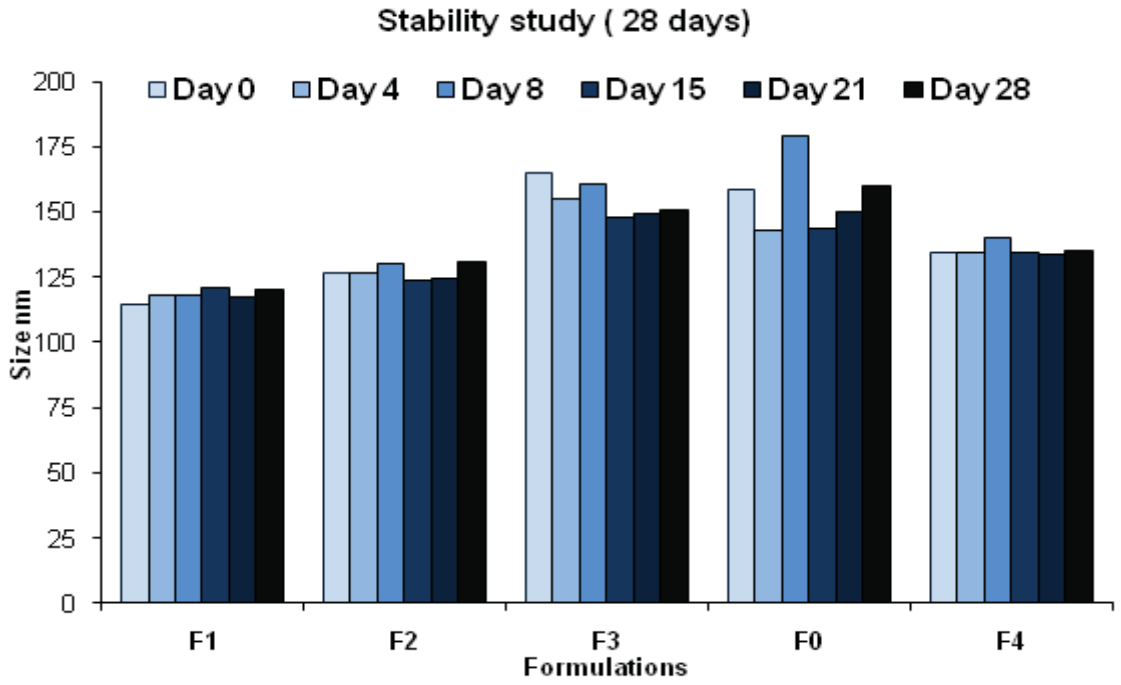

Injection velocity 900 µl/min, Stirring rate 700 rpm, S/NS volume ratio 0.5			
Sample	Phospholipid concentration (mg/ml)	Cholesterol concentration (mg/ml)	Cholesterol % (w/w)
F1	20	4	20
F2	40	8	20
F3	60	12	20
F0	40	0	0
F4	40	7	35

Figure 7. Stability study of five different drug-free liposomes batches in PBS at +4 °C over a period of 28 days.

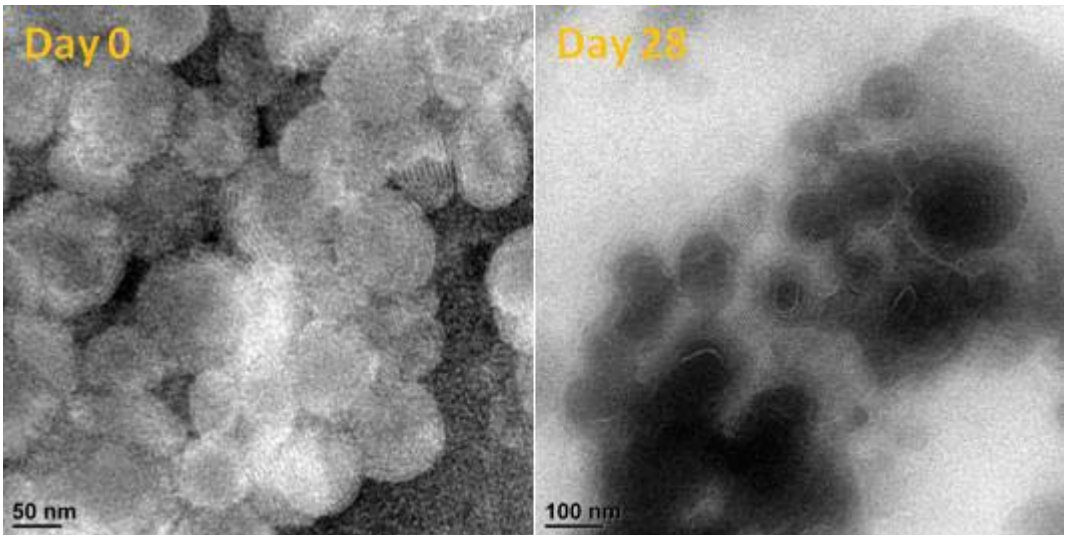

Figure 8. TEM micrographs of drug-free liposomes (F3) at day 0 and 28 days later.

3.7. *In vitro* release study

In vitro release study has been performed on five different formulas of drug-loaded liposomes (figure 9 and 10). The studied formulas have been selected in order to investigate the phospholipid concentration and cholesterol content impact on drug release profile, being the main parameters that influenced size and encapsulation efficiencies.

No significant difference in Ara-C release kinetics has been noticed between the different formulas. In all the studied cases, initial rapid release has been observed and lasted during the first three hours. Then it was followed by a steady release state. A maximum drug release had taken place after 7 hours, when about 80% of Ara-C was released. Consequently, modifying phospholipid and cholesterol amounts showed no influence on Ara-C release profile. Similar results have been reported for 5-fluorouracil (a pyrimidine analogue molecule like cytarabine) (Hitzman *et al.*, 2006) and other hydrophilic drug loaded liposomes (Betageri *et al.*, 1992), (Bard *et al.*, 1982). The relatively rapid release of Ara-C can be explained by its main location in liposome aqueous core and therefore by its rapid efflux to the external release medium.

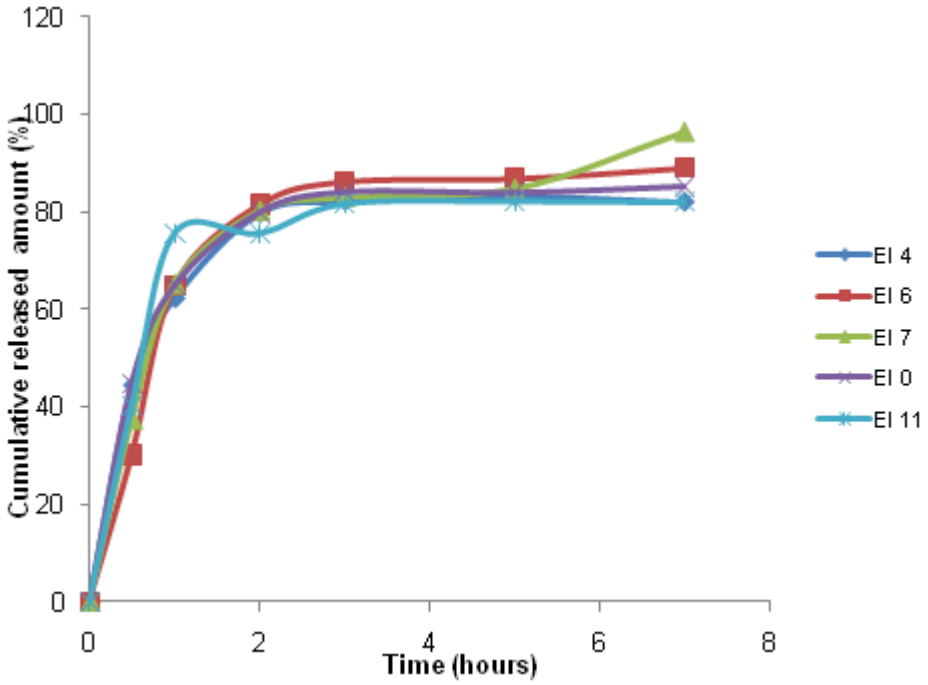

Figure 9. Ara-C release profile from five different liposome formulas.

However, the phospholipid concentration and cholesterol content markedly affected BDP release profile (figure 10). As the concentration of phospholipids was increased from 20 to 60 mg/ml, using the same cholesterol percentage with respect to phospholipid amount (20%), cumulative BDP released amount decreased. The same effect has been noticed with increasing the cholesterol percentage. For all the evaluated formulations, triphasic release kinetics was observed. During the first 6 days, all the studied formulas showed a slight release (< 10%) followed by a fairly rapid leakage reaching a maximum over 14 days. Afterwards, the release rate became steady for all the formulas. Being a highly lipophilic drug, BDP should be entrapped within the phospholipid bilayers. Hence, the release mechanism involves slow diffusion through the liposome wall (Gulati *et al.*, 1998). The triphasic release feature may be attributed to the multilamellarity of liposome membrane. No sudden release has occurred during the release study, indicating that no liposome disintegration had taken place. These results are consistent with stability data.

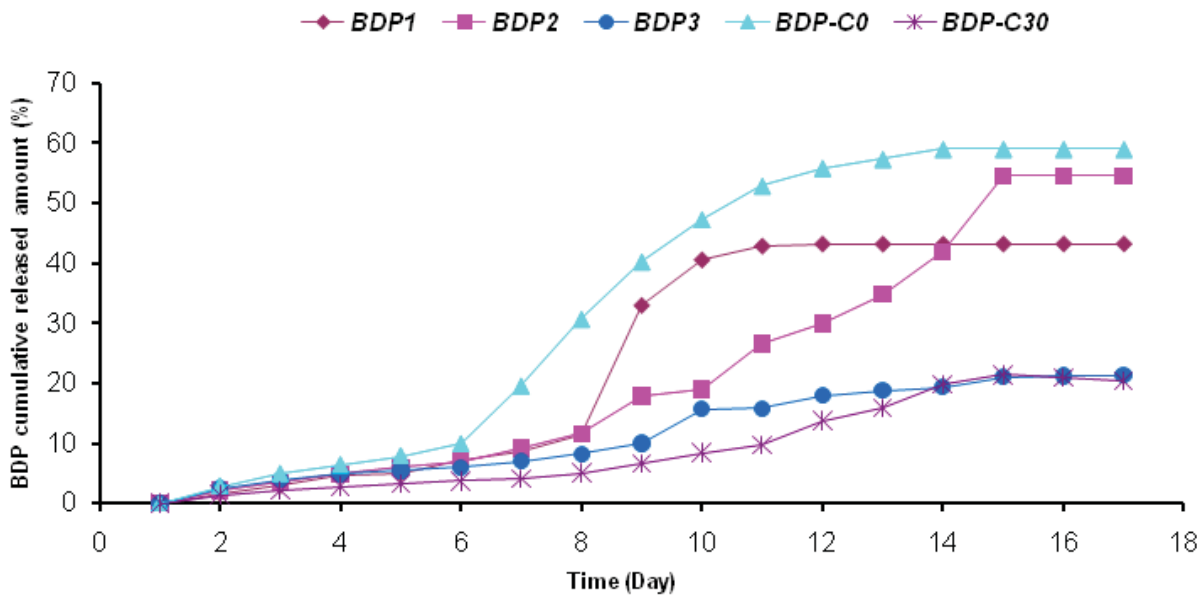

Figure 10. BDP release profile from five different liposome formulas.

It has been stated in the literature (Juliano *et al.*, 1978) that the release of lipophilic agents from liposomes is delayed because of their location within the lipid bilayers. However, water soluble drugs show relatively fast leakage out of the lipid vesicles resulting in immediate release.

3.8. *In vitro* cell uptake

The cell uptake of two types of fluorescent liposomes has been visualized by confocal laser scanning microscopy CLSM (figure 11). Nuclei were labelled by DAPI (appeared in blue), allowing fluorescent liposomes to be localized in the intracellular compartments.

The results show that the two types of fluorescent liposomes have been internalized into the cytoplasm of SW cells (figure 11 A [1-4] and B [1-4]). No internalization in nuclei could be detected. These results were compared with controls in which cells were incubated for 24 h in presence of the aqueous suspension/solution of the free fluorescent molecules (NR and FD4) (figure 11C [1-4] and 11D [1-4], respectively). Figure 11 C1 shows a detection of NR traces into SW-cells. This could be explained by its lipophilic character enabling it to passively diffuse across the cell membrane (Xu *et al.*, 2009). However, its small solubility in culture medium resulted in crystal formation and prevented a big fraction of NR to diffuse into the

cells. In contrast to NR, FD4 molecules slightly diffuse across the cell membrane despite of their solubility in the culture medium, as it was observed elsewhere (Schipper *et al.*, 1997) (figure 11 D1). Moreover, treated SW-cells morphology in the four previous cases seems to be similar to that of non treated cells (figure 11 E [1-4]), indicating that the interaction of fluorescent liposomes or free fluorescent molecules with cells did not cause any damage in cell membranes. Consequently, the cytoplasmic delivery of fluorescent liposomes could not be explained by a disruption in the cell membrane. A fusion between the liposomal membrane and the cell one is the most likely probable mechanism (Knoll *et al.*, 1988).

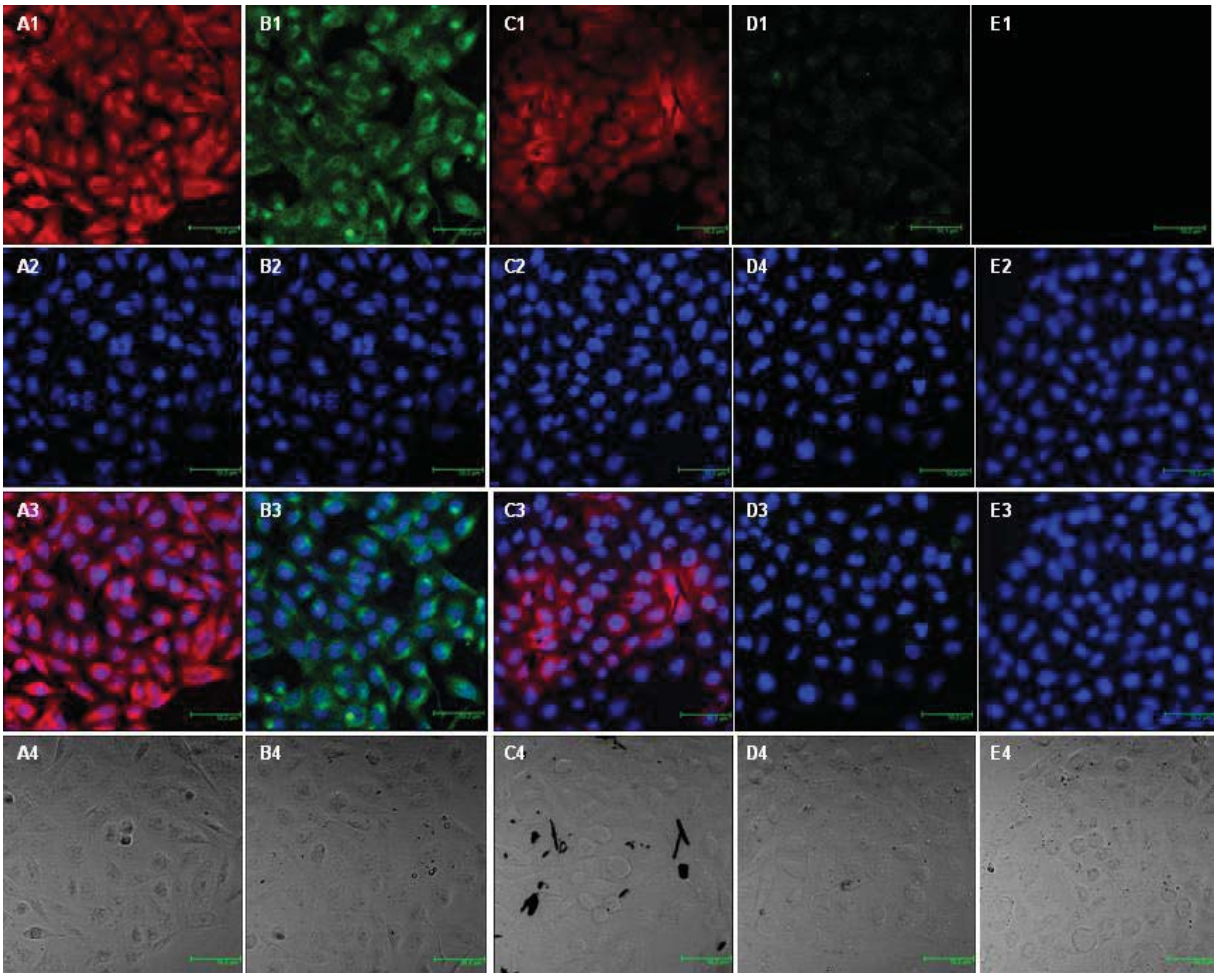

Figure 11. Fluorescence and optic microscopy images of the fluorescent-liposome cell uptake. SW- 1573 cells were incubated for 24 h with (A) liposomes loaded with red nile, (B) liposomes loaded with FD4, (C) free red nile and (D) free FD4. (E) represents non treated SW- 1573 cells. DAPI was used to visualize nuclei (blue) and overlay images are presented in the third column (from left to right). Optic microscopy images of cells are presented in the fourth column (from left to right), as controls. Scale bar represents 50.2 µm.

3.9. Aerodynamic assessment of liposomes

In order to evaluate the suitability of Ara-C and BDP-loaded liposomes for pulmonary administration, *in vitro* aerosol characterizations have been performed. For this aim, EI 7 and BDP3 formulas were selected, as they showed the most efficient drug entrapment.

Aerosol characteristics for the liposomal suspension of Ara-C and BDP are shown in Table 4. For both Ara-C and BDP formulas MMAD values were lower than 5 µm (figure 12). Indeed, the MMAD is a key factor influencing the aerosol deposition pattern. Generally speaking, aerosolized particle of a diameter < 5 µm could be of therapeutic interest for deep lung delivery (Suarez *et al.*, 2000). By the same way, FPF informs about respirable fraction which is considered to be directly proportional to the amount of drug able to reach the deep lung. Hence, the higher the FPF value, the deeper the estimated drug lung deposition (Sebti *et al.*, 2006). The FPF values were of 55% and 62% for nebulized BDP and Ara-C liposomes, respectively. Taking into account the nebulizer dead volume (≈ 1 ml), the found values of FPF were acceptable. According to these data, Ara-C and BDP liposomal suspensions have been successfully nebulized with air-jet nebulizers resulting in droplet size ranges compatible with deep lung deposition.

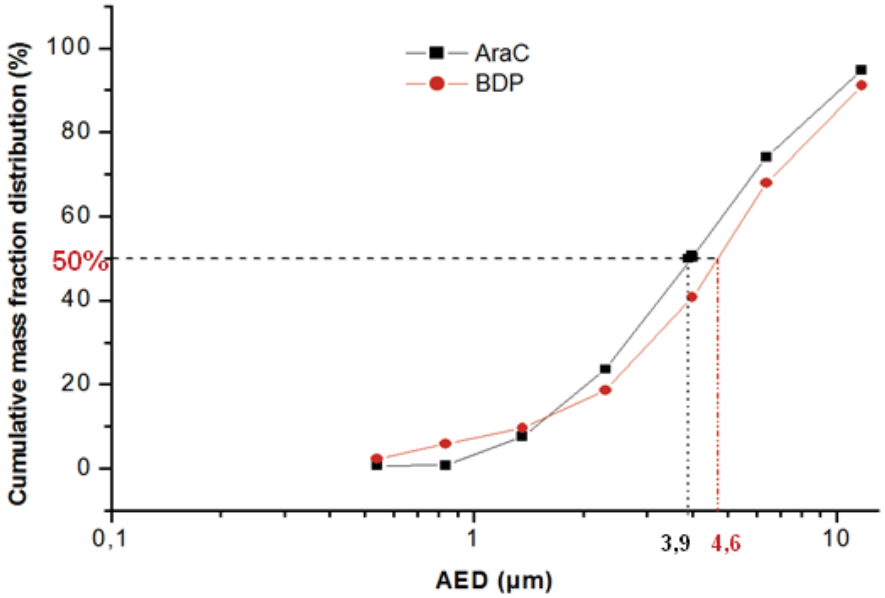

Figure 12. Cumulative mass fraction distributions versus aerodynamic diameters for nebulized liposomal Ara-C (IE 7) and liposomal BDP (BDP 3).

Table 4. Mass median aerodynamic diameter (MMAD), geometric standard deviation (GSD), fine particle fraction (FPF) and nebulization efficiency (NE) of liposomal BDP and Ara-C aerosols, expressed as mean values ± standard deviation (n = 3).

	MMAD (µm)	GSD	FPF (%)	NE (%)
BDP liposomal suspension	4.63 ± 0.21	2.23 ± 0.11	55.2 ± 2.27	43 ± 0.80
Ara-C liposomal suspension	3.91 ± 0.22	2.20 ± 0.12	61.9 ± 1.85	52 ± 0.77

4. Conclusion

In this paper, the ethanol injection method has been studied and the different influencing parameters have been evidenced. This technique offers the advantages of being fast, one step-based process and reproducible. According to found results, the stirring rate of the aqueous phase and the phospholipid concentration in the organic phase were the key parameters affecting free-drug liposome size.

A hydrophilic (Ara-C) and a lipophilic (BDP) drug have been successfully entrapped in small-sized liposomes using the ethanol injection method. Besides, a modified nanoprecipitation method has been tested for Ara-C encapsulation. Obtained results indicated that this latter do not enhance liposome characteristics (size and encapsulation efficiency). Ethanol injection method seems to be more suitable for hydrophilic drug encapsulation, as smaller vesicles and higher encapsulation efficiencies have been achieved. Multi-lamellar structure of liposome membrane has been evidenced by TEM, irrespective of the preparation method.

In vitro release study has been performed on several formulations in which different cholesterol and phospholipid amounts have been introduced. Ara-C loaded liposomes showed similar hyperbolic release profiles, regardless of liposome formulation. While, triphasic prolonged release profiles have been observed for BDP loaded liposomes and were significantly different according to the cholesterol and phospholipid amounts used in the formulation. Further release studies, in simulated physiological pulmonary conditions, will be interesting to perform, in order to predict Ara-C and BDP loaded-liposome behaviour in the respiratory tract.

Cell uptake test revealed that fluorescent liposomes have been well internalized into the cytoplasm of SW-1573 human lung carcinoma cells, confirming the suitability of the elaborated liposomes for lung cell-targeting which could be of great interest for pulmonary metastasis treatment. Furthermore, aerodynamic assessment indicated the convenience of the elaborated liposomes to nebulization as generated aerosols showed appropriate FPF and MMAD values.

In conclusion, the ethanol injection method successfully achieved stable and nano-sized liposomes with suitable encapsulation efficiencies. The elaborated liposomes seem to be promising carriers for both Ara-C and BDP pulmonary delivery. This study will be completed by *in vivo* assessment studies of the nebulized liposomes.

Acknowledgment

SW-1573 carcinoma lung cells were kindly given by Dr. Lars-Peter Jordheim (INSERM U590, Faculté de Médecine Rockefeller, Univesité lyon 1). The authors are grateful to Mr. Serge Buathier for his helpful assistance in performing transmission electron microscopy characterization.

References

Bangham, A. D., Standish, M. M. & Watkins, J.C. (1965). Diffusion of univalent ions across the lamellae of swollen phospholipids. *J Mol Biol* 13: 238-52.

Bard, D. R., Knight, C. G. & Page-Thomas, D.P. (1982). Toxicity of liposomal N–acyl daunorubicins to L929 cells in culture. *Brit J Cancer* 45: 783–785.

Barenholz, Y. (2003). Relevancy of drug loading to liposomal formulation therapeutic efficacy. *J Liposome Res* 13: 1-8.

Batzri, S. & Korn, E.D. (1973). Single bilayer liposomes prepared without sonication. *Biochim Biophys Acta* 298: 1015-9.

Betageri, G. V. & Parsons, D.L. (1992). Drug encapsulation and release from multilamellar and unilamellar liposomes. *Int J Pharm* 81: 235-241.

Bridges, P. A. & Taylor, K.M. (2000). An investigation of some of the factors influencing the jet nebulisation of liposomes. *Int J Pharm* 204: 69-79.

Budai, M. & Szógyi, M. (2001). Liposomes as drug carrier systems. Preparation, classification and therapeutic advantages of liposomes. *Acta Pharm Hung* 71: 114-8.

Campbell, M. J. (1995). Lipofection reagents prepared by a simple ethanol injection technique. *Biotechniques* 18: 1027-32.

Carneiro, A. & Santana, M. (2004). Production of liposomes in a multitubular system useful for scaling up of processes.. *Progr Colloid Polym Sci* 128: 273–277.

Darwis, Y. & Kellaway, I.W. (2001). Nebulisation of rehydrated freeze-dried beclomethasone dipropionate liposomes. *Int J Pharm* 215: 113-21.

Dass, C. R., Walker, T. L. & Burton, M.A. (2002). Liposomes containing cationic dimethyl dioctadecyl ammonium bromide: formulation, quality control, and lipofection efficiency. *Drug Deliv* 9: 11-8.

Desai, T. R., Hancock, R. E. W. & Finlay, W.H. (2002). A facile method of delivery of liposomes by nebulization. *J Control Release* 84: 69-78.

Diab, R., Degobert, G., Hamoudeh, M., Dumontet, C. & Fessi, H. (2007). Nucleoside analogue delivery systems in cancer therapy. *Expert Opin Drug Deliv* 4: 513-31.

Domazou, A. & Luisi, P. (2002). Size distribution of spontaneously formed liposomes by the alcohol injection method. *J Liposome Res* 12: 205–220.

Epstein, H., Gutman, D., Cohen-Sela, E., Haber, E., Elmalak, O., Koroukhov, N., Danenberg, H. D. & Golomb, G. (2008). Preparation of alendronate liposomes for enhanced stability and bioactivity: in vitro and in vivo characterization. *AAPS J* 10: 505-15.

Fang, J. Y., Hong, C. T., Chiu, W. T. & Wang, Y.Y. (2001). Effect of liposomes and niosomes on skin permeation of enoxacin. *Int J Pharm* 219: 61-72.

Fessi, H., Puissieux, F., Devissaguet, J. & Thies, C. (1988). Process for the preparation of dispersible colloidal systems of a substance in the form of nanoparticles. *US Patent no*: 5118528.

Gregoriadis, G. & Davis, C. (1979). Stability of liposomes in vivo and in vitro is promoted by their cholesterol content and the presence of blood cells. *Biochem Bioph Res Co* 89: 1287-93.

Gulati, M., Grover, M., Singh, S. & Singh, M. (1998). Lipophilic drug derivatives in liposomes. *Int J Pharm* 165: 129-168.

Gómez, C., Blanco, M. D., Bernardo, M. V., Olmo, R., Muñiz, E. & Teijón, J.M. (2004). Cytarabine release from comatrices of albumin microspheres in a poly(lactide-co-glycolide) film: in vitro and in vivo studies. *Eur J Pharm Biopharm* 57: 225-33.

Güven, A., Ortiz, M., Constanti, M. & O'Sullivan, C.K. (2009). Rapid and efficient method for the size separation of homogeneous fluorescein-encapsulating liposomes. *J Liposome Res* 19: 148-54.

Hitzman, C. J., Elmquist, W. F., Wattenberg, L. W. & Wiedmann, T.S. (2006). Development of a respirable, sustained release microcarrier for 5-fluorouracil I: In vitro assessment of liposomes, microspheres, and lipid coated nanoparticles. *J Pharm Sci* 95: 1114-26.

Hunt, C. A., Rustum, Y. M., Mayhew, E. & Papahadjopoulos, D. (1979). Retention of cytosine arabinoside in mouse lung following intravenous administration in liposomes of different size. *Drug Metab Dispos* 7: 124-8.

Isele, U., van Hoogevest, P., Hilfiker, R., Capraro, H. G., Schieweck, K. & Leuenberger, H. (1994). Large-scale production of liposomes containing monomeric zinc phthalocyanine by controlled dilution of organic solvents. *J Pharm Sci* 83: 1608-16.

Jaafar-Maalej, C., Andrieu, V., Elaissari, A. & Fessi, H. (2009). Assessment methods of inhaled aerosols: technical aspects and applications. *Expert Opin Drug Deliv*. [Epub ahead of print].

Juliano, R. L. & MucCullough, H.N. (1980). Controlled deivery of an antitumor drug: localized action of liposome encapsulated cytosine arabinoside administered via the respiratory system. *J Pharmacol Exp Ther* 214: 381-7.

Juliano, R. L., Stamp, D. & McCullogh, N. (1978). Pharmacokinetics of liposomes encapsulated antitumor drugs and implications for therapy.. *Ann N Y Acad Sci 308*: 411–423.

Justo, O. R. & Moraes, A.M. (2005). Kanamycin incorporation in lipid vesicles prepared by ethanol injection designed for tuberculosis treatment. *J Pharm Pharmacol* 57: 23-30.

Karathanasis, E., Ayyagari, A. L., Bhavane, R., Bellamkonda, R. V. & Annapragada, A.V. (2005). Preparation of in vivo cleavable agglomerated liposomes suitable for modulated pulmonary drug delivery. *J Control Release* 103: 159-75.

Kesisoglou, F., Zhou, S. Y., Niemiec, S., Lee, J. W., Zimmermann, E. M. & Fleisher, D. (2005). Liposomal formulations of inflammatory bowel disease drugs: local versus systemic drug delivery in a rat model. *Pharm Res* 22: 1320-30.

Kikuchi, H. & Yamauchi, H. (1987). Method for Producing Liposomes. *US Patent no*: 4687661.

Kirby, C. J. & Gregoriadis, G. (1984). Preparation of liposomes containing factor VIII for oral treatment of haemophilia. *J Microencapsul* 1: 33-45.

Knoll, G., Burger, K. N., Bron, R., van Meer, G. & Verkleij, A.J. (1988). Fusion of liposomes with the plasma membrane of epithelial cells: fate of incorporated lipids as followed by freeze fracture and autoradiography of plastic sections. *J Cell Biol* 107: 2511-21.

Kremer, J. M., Esker, M. W., Pathmamanoharan, C. & Wiersema, P.H. (1977). Vesicles of variable diameter prepared by a modified injection method. *Biochemistry* 16: 3932-5.

Kulkarni, S. B., Betageri, G. V. & Singh, M. (1995). Factors affecting microencapsulation of drugs in liposomes. *J Microencapsul* 12: 229-46.

Lasic, D. D. (1988). The mechanism of vesicle formation. *Biochem J* 256: 1-11.

Liu, D. Z., Chen, W. Y., Tasi, L. M. & Yang, S.P. (2000). Microcalorimetric and shear studies on the effects of cholesterol on the physical stability of lipid vesicles. *Colloids Surf A* 172: 57-67.

Lopez-Pinto, J. M., Gonzalez-Rodriguez, M. L. & Rabasco, A.M. (2005). Effect of cholesterol and ethanol on dermal delivery from DPPC liposomes. *Int J Pharm* 298: 1–12.

Maitani, Y., Soeda, H., Junping, W. & Takayama, K. (2001). Modified ethanol injection method for liposomes containing beta-sitosterol beta-d-glucoside. *J Liposome Res* 11: 115-25.

Majoral, C., Le Pape, A., Diot, P. & Vecellio, L. (2006). Comparaison of various Methods for processing cascade impactor data. *Aerosol Sci Tech* 40: 672-682.

Massing, U. & Fuxius, S. (2000). Liposomal formulations of anticancer drugs: selectivity and effectiveness. *Drug Resist Update* 3: 171-177.

Mayhew, E., Rustum, Y. M., Szoka, F. & Papahadjopoulos, D. (1979). Role of cholesterol in enhancing the antitumor activity of cytosine arabinoside entrapped in liposomes. *Cancer Treat Rep* 63: 1923-8.

McCullough, H. N. & Juliano, R.L. (1979). Organ-selective action of an antitumor drug: pharmacologic studies of liposomes-encapsulated beta-cytosine arabinoside administered via the respiratory system of the rat. *J Natl Cancer I* 63: 727-31.

Mohammed, A. R., Weston, N., Coombes, A. G. A., Fitzgerald, M. & Perrie, Y. (2004). Liposome formulation of poorly water soluble drugs: optimisation of drug loading and ESEM analysis of stability. *Int J Pharm* 285: 23-34.

Naeff, R. (1996). Feasibility of topical liposome drugs produced on an industrial scale. *Adv Drug Deliver Rev* 18: 343–347.

Patel, K. R. & Baldeschwieler, J.D. (1984). Treatment of intravenously implanted Lewis lung carcinoma with liposome-encapsulated cytosine arabinoside and non-specific immunotherapy. *J Int Cancer* 34: 415-20.

Pons, M., Foradada, M. & Estelrich, J. (1993). Liposomes obtained by the ethanol injection method. *Int J Pharm* 95: 51-56.

Rustum, Y. M., Dave, C., Mayhew, E. & Papahadjopoulos, D. (1979). Role of liposome type and route of administration in the antitumor activity of liposome-entrapped 1-beta-D-arabinofuranosylcytosine against mouse L1210 leukemia. *Cancer Res* 39: 1390-5.

Saari, S. M., Vidgren, M. T., Koskinen, M. O., Turjanmaa, V. M., Waldrep, J. C. & Nieminen, M.M. (1998). Regional lung deposition and clearance of 99mTc-labeled beclomethasone-DLPC liposomes in mild and severe asthma. *Chest* 113: 1573-9.

Schipper, N. G., Olsson, S., Hoogstraate, J. A., deBoer, A. G., Vårum, K. M. & Artursson, P. (1997). Chitosans as absorption enhancers for poorly absorbable drugs 2: mechanism of absorption enhancement. *Pharm Res* 14: 923-9.

Schubert, M. A. & Müller-Goymann, C.C. (2003). Solvent injection as a new approach for manufacturing lipid nanoparticles--evaluation of the method and process parameters. *Eur J Pharm Biopharm* 55: 125-31.

Sebti, T. & Amighi, K. (2006). Preparation and in vitro evaluation of lipidic carriers and fillers for inhalation. *Eur J Pharm Biopharm* 63: 51-8.

Sezer, A. D., Akbuğa, J. & Baş, A.L. (2007). In vitro evaluation of enrofloxacin-loaded MLV liposomes. *Drug Deliver* 14: 47-53.

Sonar, S., D' Souza, S. E. & Mishra K P (2008). A simple one-step protocol for preparing small-sized doxorubicin-loaded liposomes. *J Environ Pathol Tox* 27: 181-9.

Stano, P., Bufali, S., Pisano, C., Bucci, F., Barbarino, M., Santaniello, M., Carminati, P. & Luisi, P.L. (2004). Novel camptothecin analogue (gimatecan)-containing liposomes prepared by the ethanol injection method. *J Liposome Res* 14: 87-109.

Suarez, S. & Hickey, A.J. (2000). Drug properties affecting aerosol behavior. *Respir Care* 45: 652-66.

Sze, A., Erickson, D., Ren, L. & Li, D. (2003). Zeta-potential measurement using the Smoluchowski equation and the slope of the current-time relationship in electroosmotic flow. *J Colloid Interface Sci* 261: 402-10.

Szoka, F. J. & Papahadjopoulos, D. (1978). Procedure for preparation of liposomes with large internal aqueous space and high capture by reverse-phase evaporation. *Proceedings of the National Academy of Sciences of the United States of America 75*: 4194-8.

Tomoko, N. & Fumiyoshi, I. (2005). Encapsulation efficiency of water-soluble and insoluble drugs in liposomes prepared by the microencapsulation vesicle method. *Int J Pharm* 298: 198-205.

Vemuri, S., Yu, C. D., Wangsatorntanakun, V. & Roosdorp, N. (1990). Large-Scale Production of Liposomes by A Microfluidizer. *Drug Dev Ind Pharm* 16: 2243-2256.

Vidgren, M., Silvasti, M., Korhonen, P., Kinkelin, A., Frischer, B. & Stern, K. (1995). Clinical equivalence of a novel multiple dose powder inhaler versus a conventional metered dose inhaler on bronchodilating effects of salbutamol. *Arzneimittel-Forschung* 45: 44-7.

Wagner, A., Vorauer-Uhl, K. & Katinger, H. (2002). Liposomes produced in a pilot scale: production, purification and efficiency aspects. *Eur J Pharm Biopharm* 54: 213-9.

Waldrep, J. C., Gilbert, B. E., Knight, C. M., Black, M. B., Scherer, P. W., Knight, V. & Eschenbacher, W. (1997). Pulmonary delivery of beclomethasone liposome aerosol in volunteers : Tolerance and safety. *Chest* 111: 316–23.

Waldrep, J. C., Keyhani, K., Black, M. & Knight, V. (1994). Operating characteristics of 18 different continuous-flow jet nebulizers with beclomethasone dipropionate liposome aerosol. *Chest* 105: 106-10.

Xu, P., Gullotti, E., Tong, L., Highley, C. B., Errabelli, D. R., Hasan, T., Cheng, J., Kohane, D. S. & Yeo, Y. (2009). Intracellular drug delivery by poly(lactic-co-glycolic acid) nanoparticles, revisited. *Mol Pharmaceut* 6: 190-201.

Yan, E. C. & Eisenthal, K.B. (2000). Effect of cholesterol on molecular transport of organic cations across liposome bilayers probed by second harmonic generation. *Biophys J* 79: 898-903.

Yang, X., Zhao, X., Phelps, M. A., Piao, L., Rozewski, D. M., Liu, Q., Lee, L. J., Marcucci, G., Grever, M. R., Byrd, J. C., Dalton, J. T. & Lee, R.J. (2009). A novel liposomal formulation of flavopiridol. *Int J Pharm* 365: 170-4.

Zaru, M., Mourtas, S., Klepetsanis, P., Fadda, A. M. & Antimisiaris, S.G. (2007). Liposomes for drug delivery to the lungs by nebulization. *Eur J Pharm Biopharm* 67: 655-66.

Chapitre 3
Complexe d'inclusion de cyclodextrine d'une nouvelle prodrogue de la cytarabine

Préparation et caractérisation des complexes d'inclusion d'une nouvelle prodrogue de la cytarabine

Dans ce chapitre nous avons couplé deux stratégies de vectorisation ; la préparation d'une prodrogue de la cytarabine (Ara-C) et l'inclusion moléculaire de ce dernier dans l'hydroxypropyle *β*-cyclodextrine (HP-*β*-CD). La première approche dénommée (*tumour-activated prodrug*) consiste à la préparation de prodrogues non (ou peu) cytotoxiques et activables au sein des tumeurs[1, 2].

La prodrogue de cytarabine synthétisée consiste en un dérivé monophosphate portant un groupement biolabile, le *t*Bu-*S*-acyl-thioethyl, protégeant le groupement phosphate, qu'on a appelé le bis(*t*butyl-*S*-acyl-2-thioethyl)-cytidine monophosphate (AraC-SATE) [3].

L'activation de l'AraC-SATE est réalisée par des enzymes déjà présentes au sein de la tumeur [4], les groupements phosphates étant camouflés par un groupement biolabile, pour libérer le groupement phosphate au niveau intracellulaire et donner naissance à la molécule active qui consiste en un analogue du nucléoside monophosphate (figure 1).

Cette prodrogue élargit le spectre thérapeutique de l'Ara-C envers certains types de cellules tumorales résistantes au traitement. D'autre part, elle protège l'Ara-C de la dégradation par les désaminases. Toutefois, la faible solubilité aqueuse de cette prodrogue peut diminuer l'activité biologique *in vivo* en raison de sa précipitation dans les milieux biologiques. Ainsi, nous avons fait appel aux cyclodextrines pour préparer des vecteurs

---

[1] Denny, W. A. (2001). Prodrug strategies in cancer therapy. *European Journal of Medicinal Chemistry 36*: 577–595.

[2] Denny, W. A. (2004). Tumor-activated Prodrugs - A New Approach to Cancer Therapy. *Cancer Investigation 22* : 604-619.

[3] Galmarini, C., Clarke, M., Santos, C., Jordheim, L., Perigaud, C., Gosselin, G., Cros, E., Mackey, J. & Dumontet, C. (2003). Sensitization of ara-C-resistant lymphoma cells by a pronucleotide analogue. *International Journal of Cancer 107*: 149–154.

[4] Bazzanini, R., Gouy, M., Peyrottes, S., Gosselin, G. & Périgaud, C. (2005). Synthetic approaches to a mononucleotide prodrug of cytarabine. *Nucleosides, Nucleotides and Nucleic Acids 24*: 1635-1649.

moléculaires dont la solubilité aqueuse et aussi la stabilité et la biodisponibilité de la molécule incluse sont reconnues d'être meilleures[5, 6].

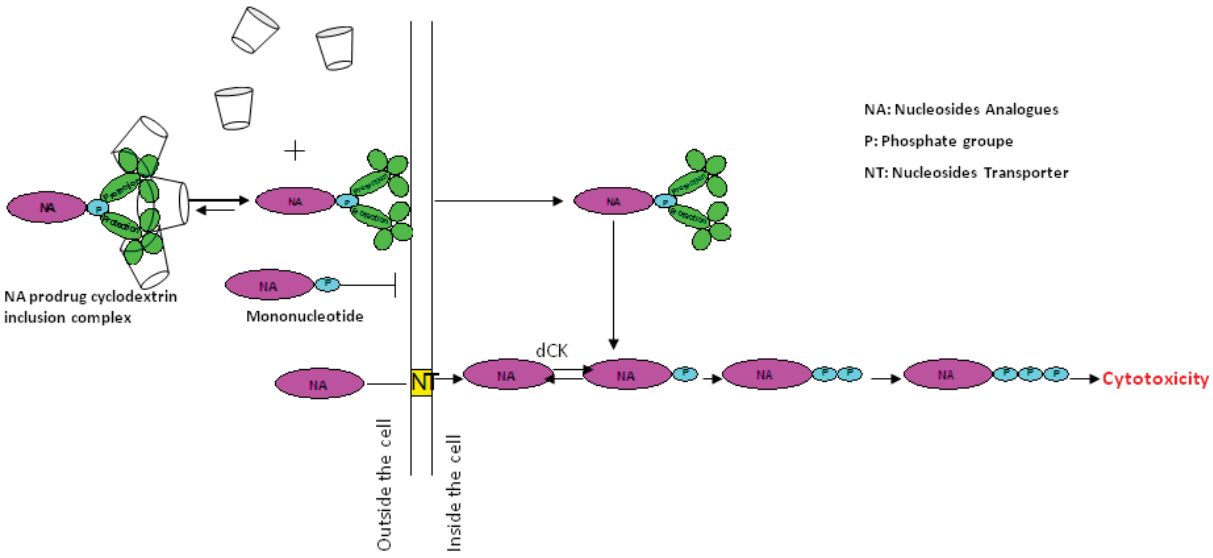

Figure 1. Mécanisme d'action des analogues de nucléosides, celui de la prodrogue des analogues de mononucléotides et celui supposé du complexe d'inclusion prodrogue - HP-β-CD.

L'activité cytotoxique de l'Ara-C, l'AraC-SATE et du complexe a été évaluée sur deux lignées de cellules leucémiques murines: la lignée sauvage sensible au traitement (L1210) et la lignée résistante au traitement (L1210 10K). Les résultats obtenus ont montré que la prodrogue est beaucoup plus active sur la lignée résistante que l'Ara-C, contrairement à l'Ara-C qu'elle est plus active que l'AraC-SATE sur la lignée sauvage. Par ailleurs, aucune différence significative d'activité cytotoxique n'a été trouvée entre la prodrogue et son complexe d'inclusion, ce qui indique que le phénomène d'inclusion ne modifie pas l'activité cytotoxique de la prodrogue.

[5] Connors, K. A. (1997). The Stability of Cyclodextrin Complexes in Solution. *Chemical reviews 97*: 1325-1358.

[6] Mallick, S., Pattnaik, S., Swain, K. & De, P.K. (2007). Current perspectives of solubilization: potential for improved bioavailability. *Drug development and industrial pharmacy 33*: 865-73.

Journal of
Nanoscience and Nanotechnology
Vol. 8, 1–6, 2008

Preparation, Characterization and *In Vitro* Evaluation of a New Nucleotide Analogue Prodrug Cyclodextrin Inclusion Complexes

Roudayna Diab[1,†], Lars P. Jordheim[2,†], Ghania Degobert[1], Suzanne Peyrottes[3], Christian Périgaud[3], Charles Dumontet[2], and Hatem Fessi[1,*]

[1] *Laboratoire d'Automatique et de Génie des Procédés, LAGEP, UMR CNRS 5007, Université Lyon 1 Claude Bernard, 43 Boulevard du 11 Novembre 1918, 69622 Villeurbanne Cedex, France*
[2] *Laboratoire de Cytologie Analytique, INSERM U590, Université Lyon 1 Claude Bernard, 8 Avenue Rockefeller, 69008 Lyon, France*
[3] *UMR 5625 CNRS-UM II, Université Montpellier II, Case Courier 008, Place E. Bataillon, 34095 Montpellier Cedex 5, France*

Bis(*t*butyl-*S*-acyl-2-thioethyl)-cytidine monophosphate is a new cytotoxic mononucleotide prodrug which have been developed to reverse the cellular resistance to nucleoside analogues. Unfortunately, its *in vivo* utilisation was hampered by its poor water solubility, raising the need of a molecular vector capable to mask its physicochemical characteristics although without affecting its cytotoxic activity. Hydroxypropyl-β-cyclodextrin was used to prepare the prodrug inclusion complexes, allowing it to be solubilized in water and hence to be used for *in vitro* and *in vivo* experiments. A molar ratio of the cyclodextrin: prodrug of 3 was sufficient to obtain complete solubilization of the prodrug. The inclusion complex was characterized by differential scanning calorimetry, which revealed the disappearance of the melting peak of the prodrug suggesting the formation of inclusion complex. Proton Nuclear Magnetic Resonance spectroscopy provided a definitive proof of the inclusion complex formation, which was evidenced by the large chemical shift displacements observed for protons located in the interior of the hydrophobic cyclodextrin cavity. The complex retained its cytotoxic activity as shown by *in vitro* cell survival assays on murine leukemia cells. These results provided a basis for potential therapeutic applications of co-formulation of this new nucleotide analogue with hydroxypropyl-β-CD in cancer therapy.

Keywords: Mononucleotide Prodrug, Hydroxypropyl-β-Cyclodextrin, Inclusion Complex, Solubilization.

RESEARCH ARTICLE

1. INTRODUCTION

Nucleosides analogues (NAs) are critical components of anticancer, antiviral and immunosuppressive therapy. They are antimetabolites, a class of drugs that inhibit DNA synthesis either directly or through inhibition of DNA precursor synthesis on the de novo or salvage pathways.[1,2] NAs are inactive prodrugs that are dependent on intracellular phosphorylation to their pharmacologically active triphosphate form.[3] Their intracellular activation depends on enzymes involved in the metabolism of endogenous nucleosides, and in particular deoxycytidine kinase (dCK) which catalyses the rate-limiting step. The clinical use of these molecules is limited by the emergence of pharmacological resistance such as decreased dCK activity,[4] rapid deactivation by cytidine deaminase, a very low lipophilicity, and quick excretion. To overcome theses limitations, a mononucleotide prodrug of cytarabine (AraC) have been developed by Galmarini et al.,[5] bearing *t*Bu-*S*-acyl-thioethyl (*t*Bu-SATE) group, as biolabile phosphate protection and hence capable of releasing intracellularly the monophosphorylated nucleoside analogue (Fig. 1). This molecule broaden the therapeutic spectrum of AraC toward kinase-deficient tumour cells,[5] protect AraC from deamination since the major substrate requirement of cytidine deaminase is a free 5′-hydroxyl group and increase the lipophilicity of the parent AraC.

The poor water solubility of the developed nucleotide analogue, i.e., bis(*t*butyl-*S*-acyl-2-thioethyl)-cytidine monophosphate (AraC-SATE), however, may cause low biological activity *in vivo*, because of its precipitation in water solutions. Modification of the AraC-SATE

*Author to whom correspondence should be addressed.
†Equal contribution.

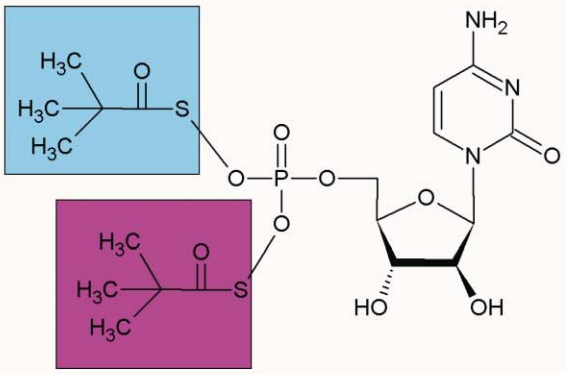

Fig. 1. Chemical structure of Bis(*tert*-butyl-*S*-acyl-thioethyl) phosphotriester derivative of ara-CMP (AraC-SATE), a prodrug-C.

physicochemical properties can be achieved by the preparation of cyclodextrin inclusion complexes.

Cyclodextrins (CDs) are natural products. They constitute a family of cyclic oligosaccharides comprising repetitive 6, 7, or 8 glucose units (α-, β-, γ-CD, respectively). The inside of the molecule forms a hydrophobic cavity, while the outer surface is hydrophilic, enabling it to act as a host for a wide variety of hydrophobic drugs and components.[6] By complexation, cyclodextrins can increase the solubility, stability and bioavailability of the guest molecule.[7] In this work, hydroxypropyl-β-CD (HP-β-CD), a derivative of natural β-CD, was used to prepare AraC-SATE cyclodextrin inclusion complexes because of its higher water solubility and lower toxicity via intravenous injections than those of the natural CD.[8]

In this paper, HP-β-CD: AraC-SATE inclusion complex was prepared and characterized by DSC and ^{1}H RMN and then its biological activity was tested *in vitro* on sensitive and resistant murine leukemic cells.

2. MATERIALS AND METHODS

2.1. Materials

Methylthiazoletetrazolium (MTT), isopropanol, ethanol and HP-β-CD were purchased from Sigma Aldrich (Saint-Quentin, France), HCl from Merck (Strasbourg, France), RPMI 1640 cell culture media from Invitrogen (Cergy Pontoise, France), L-glutamine and penicillin-streptomycin from Gibco (Cergy Pontoise, France), and fetal bovine sera from PAN Biotech GmbH (Aidenbach, Germany). AraC-SATE was obtained by adaptation of a published procedure,[9] and AraC (Aracytine®) was from Pharmacia (Saint-Quentin-en-Yvelines, France).

2.2. Preparation of Inclusion Complexes

To generate drug–cyclodextrin complexes, AraC-SATE (10 mM) and (60 mM) and HP-β-CD were completely dissolved in a mixed solution of ethanol and water (1:5 v/v) at a molar ratio of 3:1 (HP-β-CD:AraC-SATE) and stirred for 15 min at 37 °C. After evaporating the ethanol from the mixed solution, the resulted solution was lyophilized.

2.3. Differential Scanning Calorimetry (DSC) of the Inclusion Complexes

The characterization of HP-β-CD, AraC-SATE and the inclusion complex (HP-β-CD:AraC-SATE) was carried out with a differential scanning calorimeter (DSC), TA instruments DSC 2920 Modulated DSC, (New Castle, DE, USA). Each sample was scanned at a speed of 10 °C/min, in the temperature range of 20 to 250 °C.

2.4. Proton Nuclear Magnetic Resonance (^{1}H RMN) Spectroscopy

The inclusion complex (HP-β-CD:AraC-SATE) was characterized in deuterated water by ^{1}H RMN. The spectrum was obtained in a DRX 500 MHz Brucker spectrophotometer, at 298 K. Chemical shift displacements HP-β-CD protons and those of the inclusion complex were measured in order to prove inclusion of AraC-SATE in the cyclodextrin cavity.

2.5. Cell Culture

Nucleoside analogue sensitive (wt) and resistant (10 K) L1210 murine leukemic cells were cultured in RPMI 1640 media containing L-glutamine, penicillin (200 UI/ml), streptomycin (200 μg/ml) and fetal bovine serum (10%) at 37 °C in presence of CO_2 5%.

2.6. Cytotoxicity Studies

L1210 cells (20,000 cells per well) were incubated in 24 well plates (Becton Dickinson, NJ, USA) in a final volume of 1 ml containing different drug concentrations at 37 °C for 72 hours. MTT (500 μg) was added and after 2 hours of incubation at 37 °C, the supernatant was replaced with 300 μl isopropanol/HCl/H20 (v/v/v 90/9/1) to solubilize the formazan crystals. Spectrophotometrical determination of optical density was performed using a microplate reader (Labsystem Multiskanner RC). Inhibitory concentration 50 (IC_{50}) was defined as the concentration inhibiting proliferation to a level equal to 50% of that of controls and the resistance ratio (RR) was the ratio between the IC_{50} of the gemcitabine-resistant L1210 10 K cell line and the IC_{50} of the sensitive parental cell line L1210 wt. IC_{50} values were determined from concentration-effect curves generated using Microsoft® Excel.

3. RESULTS AND DISCUSSION

3.1. Inclusion Complex Formation

Different molar ratios of AraC-SATE and HP-β-CD were used to prepare the inclusion complex. A complete

solubilization was only possible with a molar ratio (HP-β-CD:AraC-SATE) of three or more. The inclusion complex was formed in 15 minutes, which is a very short time, compared to periods usually needed (3–7 days) for the complexation reaction.[10] This could be justified by the fact that the methyl short hydrophobic chains in the *ter*-butyl extremity of AraC-SATE can easily fulfil the hydrophobic cavities of HP-β-CD molecules.

3.2. Differential Scanning Calorimetry (DSC) of the Inclusion Complex

A complete dissolution of AraC-SATE in the presence of HP-β-CD was obtained with (HP-β-CD:AraC-SATE) ratios of 3 or higher. The highest AraC-SATE concentration tested was 60 mM. In order to verify the formation of the inclusion complex (HP-β-CD:AraC-SATE), the pure products and the complex were analyzed by DSC as shown by the thermograms in Figure 2. The active substance AraC-SATE showed a characteristic sharp peak at 168 °C indicating the drug melting point (Fig. 2(a)). Pure HP-β-CD had a broad peak, which reached a maximum around 90 °C. This phenomenon might be attributed to the loss of water corresponding to cyclodextrin dehydration (Fig. 2(b)). The thermal analysis of the complex (HP-β-CD:AraC-SATE) revealed the disappearance of the melting phenomenon described for the drug (Fig. 2(c)) indicating the interaction of AraC-SATE and the HP-β-CD cavity.

DSC analysis can be used to inform about the structural modifications in the internal cavity of cyclodextrin induced by inclusion phenomenon.[11,12] In fact, if this cavity contains only guest molecules, we shouldn't have any dehydration peak in the DSC spectrum of the final mixture. However, experimental results show generally the persistence of this peak with a more or less significant modification of its characteristics.[13] According to the literature, it is well known that if the guest molecule forms an inclusion complex with cyclodextrin, there is no crystalline structure to absorb energy, and then the inclusion complex formation can be confirmed by the disappearance of the endothermic melting peak in complex thermogram.[14]

3.3. Proton Nuclear Magnetic Resonance (^{1}H RMN) Spectroscopy

To provide a definitive proof of inclusion complex formation, we realized ^{1}HNMR spectroscopy study, since chemical and electronic environments of protons are affected during complexation, which is reflected by chemical shift displacements ($\Delta\delta = \delta_{(complex)} - \delta_{(free)}$).

In HP-β-CD spectrum in the presence of AraC-SATE, appreciable chemical shift displacements were observed with respect to the spectrum of free compound, due to some conformational changes occurred via the complexation (Table I). The protons H5, H3, H6 located within or near the internal cavity were markedly affected with $\Delta\delta$ of −0.070, −0.028, and −0.028 ppm, respectively, while the signals of H2 and H4 protons on the outer surface of HP-β-CD changed only slightly except the proton H1, whose $\Delta\delta$ is of −0.046. So, we can suppose that a part of the molecule AraC-SATE is included within the HP-β-CD cavity and the other part interacts with its outer surface and especially

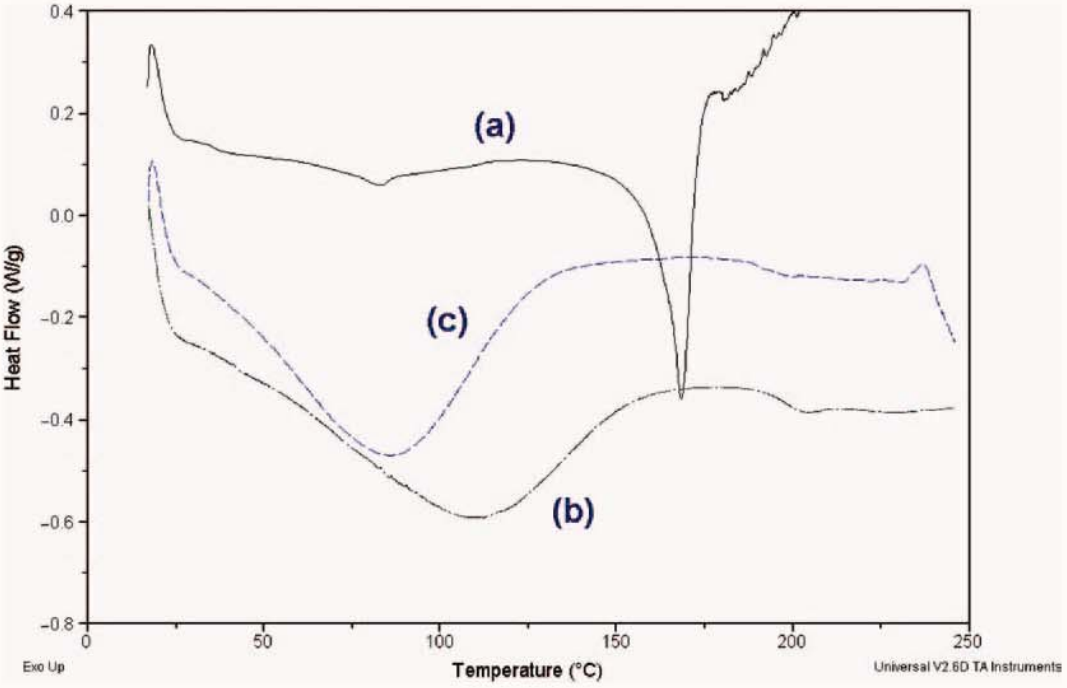

Fig. 2. DSC thermograms of: (a) AraC-SATE, (b) HP-β-CD and (c) inclusion complex (HP-β-CD:AraC-SATE).

RESEARCH ARTICLE

Table I. ^{1}HNMR chemical shifts displacements (ppm) of HP-β-CD in D2O at 298 K, in the free and complexed states at 3:1 molar ratio of HP-β-CD:AraC-SATE.

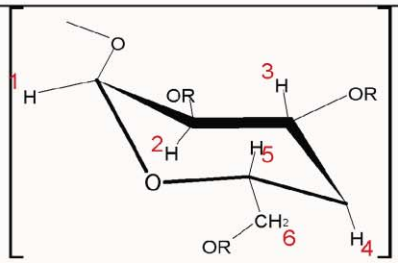

R = $[CH_2CH(CH_3)O]_n$ H

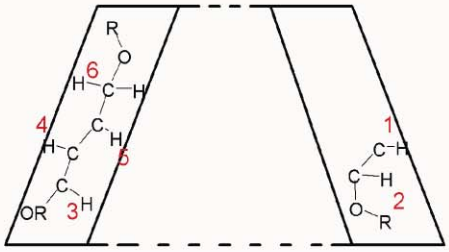

HP-β-CD protons	δ HP-β-CD	δ AraC-SATE	$\Delta\delta^a$
H3	3.945	3.917	−0.028
H6	3.788	3.760	−0.028
H5	3.646	3.576	−0.070
H2	3.531	3.546	0.015
H4	3.409	3.403	−0.006
H1	5.184	5.138	−0.046
-CH3	*b*	*b*	*b*

[a]Chemical shift displacements were expressed as $\Delta\delta = \delta$ HP-β-CD-δ HP-β-CD-AraC-SATE. [b]Could not be determined due to the overlapping with other signals.

with the proton H1. Chemical shifts of protons other than those listed in Table I could not be accurately measured because of the overlapping and broadening of signals.

As reported in the literature, for cyclodextrin we generally observe displacements in the chemical shifts of the protons located within the internal cavity (H3, H5) because only this part is in contact with the guest molecule.[15] In certain cases, chemical shifts displacements of external protons (H1, H2, and H4) can be observed. This occurs when the encapsulated molecule has a big size and when it presents one or more aliphatic chains which can remain outside the cavity and interact with the external faces of cyclodextrin.[16]

3.4. Cell Culture and Cytotoxicity Studies

The inclusion complexes were tested on nucleoside analogue sensitive (wt) and resistant (10 K) L1210 *in vitro*-cultured cells (Fig. 4). Furthermore, the influence of dilution on the inclusion complex cytotoxic activity has been studied using two bulk solutions at two different AraC-Sate concentrations (10 μM and 60 μM). This study was conducted to know whether the prodrug inclusion into HP-β-CD cavity would alter or mask the cytotoxic effect of the included drug.

The concentrations inhibiting cell growth by 50% (IC_{50}) were found to be 0.008 ± 0.001 μM (AraC), 0.077 ± 0.0021 μM (AraC-SATE in DMSO), 0.123 ± 0.068 μM (ratio 3:1 10 mM) and 0.063 ± 0.047 (ratio 3:1 60 mM) for L1210 wt cells, 73.33 ± 25.17 μM (AraC), 8.33 ± 2.89 μM (AraC-SATE in DMSO), 20.00 ± 10.00 μM (ratio 3:1 10 mM) and 11.67 ± 7.64 (ratio 3:1 60 mM) for nucleoside analogue resistant L1210 cells. These results showed that HP-β-CD did not modify the AraC-SATE cytotoxicity on L1210 wt and 10 K cells.

IC_{50} represents the anticancer drug efficacy and its value is inversely proportional to the drug cytotoxic activity. In this study, we found that AraC-SATE (the prodrug) and its inclusion complex were less cytotoxic to wild cells than AraC; exhibiting IC_{50} values 10 fold higher than the AraC IC_{50} value. However, they were more cytotoxic to resistant cells, when compared to AraC, with IC_{50} values inferior to that of AraC (the parent drug). Moreover, the prodrug and its inclusion complex showed no significant differences in their IC_{50} values. So, we can conclude that the presence of HP-β-CD did not alter the biological activity of the prodrug, and that we were successfully able to substitute the toxic organic solvent by a safe aqueous solution of the prodrug, which can be used for intravenous administration.

Table II. IC_{50} values and resistance ratios in L1210 wt (the wild strain) and L1210 10 K (the resistant strain) cells as determined by methylthiazoletetrazolium assay.

	IC_{50} (μM)			
	L1210 wt	L1210 10 K	RR	Pt
Arac	0.00767 ± 0.00116	73.3 ± 25.2	9947 ± 4365	0.0072[a]
AraC-SATE	0.0767 ± 0.0208	8.33 ± 2.89	112 ± 48.9	0.0077[a]
(HPβCD: AraC-SATE)	0.123 ± 0.0681	20.0 ± 10.0	180 ± 105	0.026[a]
(HPβCD: AraC-SATE)	0.0633 ± 0.0473	11.7 ± 7.64	283 ± 202	0.058[a]

Note. Data are mean values of four independent single experiments.
RR: is the resistance ratio which is calculated as IC_{50} for L1210 wt/IC_{50} for L1210 10 K.
Pt is the value of P calculated by Student test.
[a]Statistically significant.

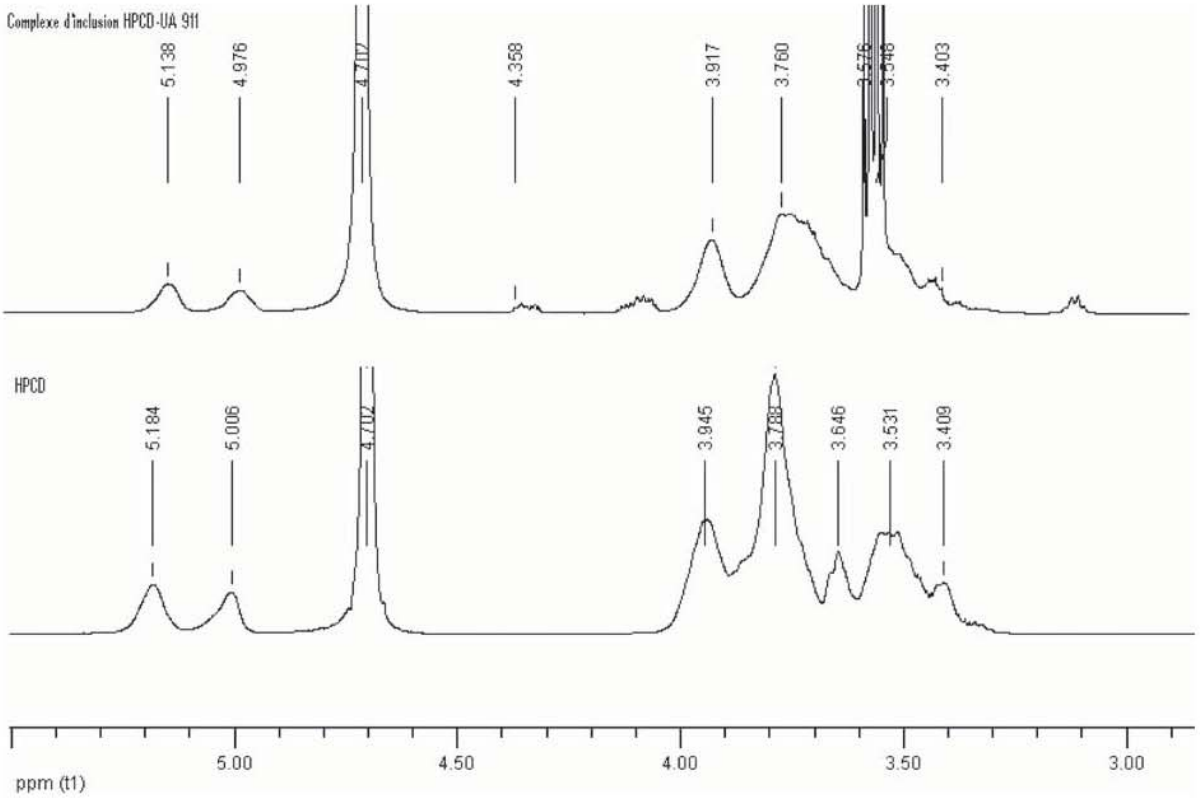

Fig. 3. ^{1}HNMR partial spectra of free HP-β-CD (top) and inclusion complex HP-β-CD:AraC-SATE at molar ratio of 3:1 (bottom).

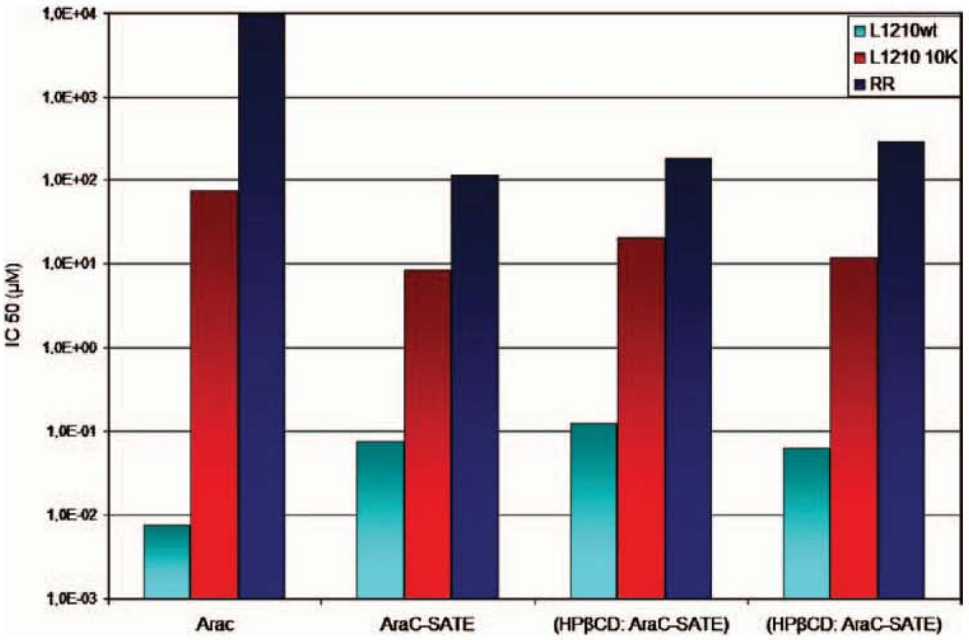

Fig. 4. IC_{50} (in μM) for L1210 wt and 10 K cells using AraC, AraC-SATE in DMSO, and solutions of HP-β-CD:AraC-SATE (ratio 3:1) at 10 and 60 mM. RR is the resistance ratio which is calculated as IC_{50} for L1210 wt/IC_{50} for L1210 10 K.

4. CONCLUSION

In summary, the present study proposes the use of HP-β-CD to overcome the problem associated with the use of AraC-SATE, i.e., the poor water solubility, by the formation of the complex inclusion HP-β-CD:AraC-SATE. Thereby, we were able to prepare AraC-SATE water solutions at adequate concentrations for *in vitro* AraC-SATE

RESEARCH ARTICLE

biological activity studies. The formation of inclusion complex was confirmed by the DSC and ^{1}HNMR findings. Furthermore, the cytotoxic activity of the prodrug was not masked by the presence of HP-β-CD, so we can suppose that the prodrug molecules in cell culture are released from the cyclodextrine hydrophobic cavity, and then diffuse through cellular membranes before reaching its site of action. These results provided a basis for the potential therapeutic application of co-formulation of AraC-SATE with HP-β-CD in cancer therapy.

References and Notes

1. C. M. Galmarini, J. R. Mackey, and C. Dumontet, *Lancet Oncol.* 3, 415 **(2002)**.
2. S. A. Hunsucker, B. S. Mitchell, and J. Spychala, *Pharmacol. Therapeut.* 107, 1 **(2005)**.
3. A. R. Van Rompy, M. Johansson, and A. Karlsson, *Pharmacol. Therapeut.* 100, 119 **(2003)**.
4. L. Jordheim, C. M. Galmarini, and C. Dumontet, *Curr. Cancer Drug Tar.* 4, 443 **(2003)**.
5. C. M. Galmarini, M. L. Clarke, C. L. Santos, L. Jordheim, C. Perigaud, G. Gosselin, E. Cros, J. R. Mackey, and C. Dumontet, *Int. J. Cancer* 107, 149 **(2003)**.
6. T. Loftsson and M. E. Brewster, *J. Pharm. Sci.* 85, 1017 **(1996)**.
7. E. M. Martin Del Valle, *Process Biochem.* 39, 1033 **(2004)**.
8. F. Leroy-Lechat, D. Wouessidjewe, J.-P. Andreux, F. Puisieux, and D. Duchêne, *Int. J. Pharm.* 101, 97 **(1994)**.
9. I. Lefebvre, C. Perigaud, A. Pompon, A. M. Aubertin, J. L. Girardet, A. Kirn, G. Gosselin, and J. L. Imbach, *J. Med. Chem.* 38, 3941 **(1995)**.
10. T. Loftsson and D. Duchêne, *Int. J. Pharm.* 329, 1 **(2007)**.
11. R. Ficarra, P. Ficarra, M. R. Di Bella, D. Raneri, S. Tommasini, M. L. Calabro, M. C. Gamberini, and C. Rustichelli, *J. Pharmaceut. Biomed.* 23, 33 **(2000)**.
12. M. M. Meier, M. Luiz, B. Scponganicz, and V. Soldi, *Thermochim. Acta* 375, 153 **(2001)**.
13. M. M. Meier, M. Marilde, T. B. Luiz, B. Szpoganicz, and V. Soldi, *Thermochim. Acta* 375, 153 **(2001)**.
14. F. Giordano, C. Novak, and J. R. Moyano, *Thermochim. Acta* 380, 123 **(2001)**.
15. H. Boudad, P. Legrand, G. Lebas, M. Cheron, D. Duchêne, and G. Ponchel, *Int. J. Pharm.* 218, 113 **(2001)**.
16. R. Ficarra, S. Tommasini, D. Raneri, M. L. Calabro, M. R. Di Bella, C. Rustichelli, M. C. Gamberini, and P. Ficarra, *J. Pharmaceut. Biomed.* 29, 1005 **(2002)**.

Received: 25 October 2007. Accepted: 26 November 2007.

RESEARCH ARTICLE

Discussion générale

Discussion générale

Malgré la découverte de nombreux nouveaux agents cytotoxiques qui peuvent être des candidats potentiels pour le traitement du cancer, cette maladie mortelle reste encore à l'origine de plus de six millions de décès chaque année dans le monde, et le nombre est en augmentation. Les analogues de nucléosides et nucléobases (AN) ont été parmi les premiers agents thérapeutiques à être introduits dans la chimiothérapie du cancer, ayant une activité cytotoxique importante sur les tumeurs solides et les hémopathies malignes (Galmarini *et al.*, 2002 a). En effet, ces molécules agissent sur les cellules cancéreuses après avoir subi au niveau intracellulaire trois étapes de phosphorylation pour se transformer en leur forme active tri-phosphatée. C'est cette dernière forme qui va inhiber la synthèse des acides nucléiques, soit directement en s'incorporant dans le brin croissant de l'acide nucléique, soit indirectement en inhibant les précurseurs de synthèse et/ou les enzymes des voies de synthèse de l'ADN (Van Rompy *et al.*, 2003). Leur activation dépend donc des concentrations intracellulaires des enzymes kinases et notamment les déoxyribonucléoside kinases, qui catalysent la réaction de phosphorylation des nucléosides en mononucléotides (nucléosides monophosphates) (Mansson et al., 2003).

Aujourd'hui, de nombreux problèmes restent à surmonter concernant la chimiothérapie par les AN. Le problème principal réside dans le manque de sélectivité et le grand volume de distribution des AN. En effet, les AN ne sont pas naturellement spécifiques des cellules tumorales, en conséquence, elles vont s'accumuler non seulement dans les tumeurs, mais aussi dans les tissus sains. En outre, la plupart des AN ont des demi-vies courtes en raison leur dégradation enzymatique rapide, notamment par les désaminases au niveau du foie et des reins (Song *et al.*, 2005). Pour toutes ces raisons, les doses thérapeutiques sont particulièrement élevées et doivent être régulièrement augmentées, entraînant une toxicité aiguë et un index thérapeutique trop faible. S'ajoutent à cela l'émergence des résistances cellulaires au traitement, qui sont attribuées, entre autres, à la faible expression des enzymes kinases dans les cellules résistantes (Galmarini *et al.*, 2002 b). Par ailleurs, les AN sont des molécules hydrophiles ayant une faible perméabilité membranaire et elles nécessitent des transporteurs pour traverser la membrane cellulaire (Song *et al.*, 2005). L'abondance de ces transporteurs va donc jouer un rôle important dans la sensibilité des cellules au traitement.

La plupart des difficultés rencontrées en vue d'une utilisation clinique efficace des AN consiste à administrer des concentrations thérapeutiques adéquates aux tissus cibles. Dans ce contexte, le développement des micro- ou nano-transporteurs pour réaliser une administration ciblée des AN aux tumeurs s'avère indispensable pour améliorer leur index thérapeutique.

Dans presque tous les vecteurs développés et reportés dans la littérature, les chercheurs ont été généralement confrontés aux problèmes de faible rendement d'encapsulation et de libération presque immédiate des AN (à l'exception de particules de DepoFoam^{TM}) (Diab *et al.*, 2007). De notre point de vue, le vecteur idéal des AN doit satisfaire aux critères suivants: une encapsulation facile et efficace du médicament ; une biocompatibilité et une innocuité assurée en excluant de la formulation l'usage des produits toxiques, tels que les monomères et les agents de réticulation ; une protection fiable des principes actifs contre la dégradation dans les milieux biologiques ; et une libération intracellulaire du médicament.

Dans ce contexte, nous pensons que les vecteurs particulaires à base de polymères biodégradables tels que le PCL, PLA ou PLGA pourraient constituer des véhicules convenables pour l'administration ciblée des AN, si les problèmes d'encapsulation sont résolus. Notre choix a porté sur le PCL en raison de sa vitesse de dégradation *in vivo* qui est plus lente par rapport à celle des autres polyesters (Ali *et al.*, 1993) et en conséquence les profils de libération des systèmes particulaires à base de PCL le sont aussi.

En général, les problèmes d'encapsulation des AN sont liés à leur affinité faible pour les polymères hydrophobes. En effet, il s'agit des molécules hydrophiles de faible poids moléculaire pouvant migrer facilement lors du procédé d'encapsulation vers le milieu aqueux externe. Nous avons, donc, opté d'introduire un deuxième polymère (un copolymère à bloc), composé d'un bloc hydrophobe apte à s'ancrer dans les particules et d'un bloc hydrophile qui confère à la structure un caractère hydrophile, dans le but d'améliorer l'affinité et, par conséquence, le taux d'encapsulation de la molécule hydrophile dans le système particulaire développé. Pour ce faire, une série de copolymères diblocs mPEG-PCL avec des blocs PCL de différents poids moléculaires ont été synthétisés. La synthèse s'est effectuée par polymérisation coordinative anionique en présence d'un catalyseur, le 2-éthyle hexanoate d'étain $Sn(Oct)_2$, par ouverture de cycle de l' ε-caprolactone (ε-CL) à partir de la fonction hydroxyle disponible aux extrémités terminales du PEG (figure 1).

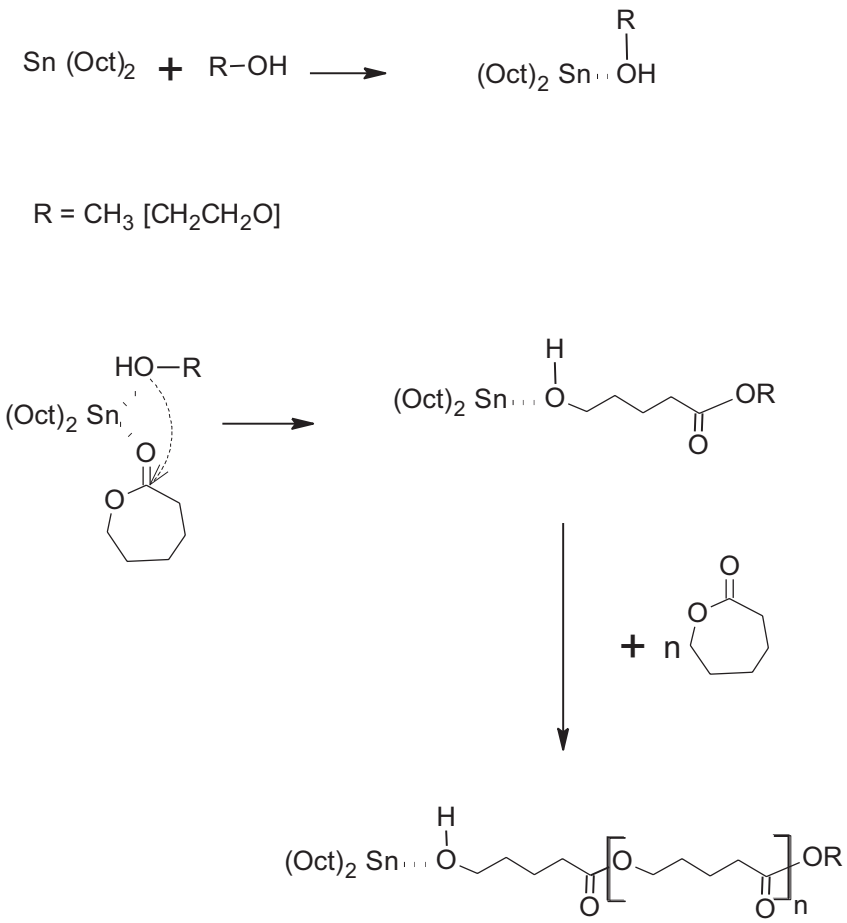

Figure 1. Mécanisme supposé de la polymérisation de l' ε-CL en présence de $Sn(Oct)_2$ comme catalyseur et mPEG comme co-initiateur.

Les copolymères obtenus ont été caractérisés par spectroscopie infrarouge (IRTF), résonance magnétique nucléaire du proton (^{1}H RMN) et chromatographie d'exclusion stérique à multi-détection (SEC-MALLS). La spectroscopie infrarouge a confirmé que les copolymères ont été synthétisés avec succès. En effet, les spectres IRTF des copolymères ont montré d'une part, des pics d'absorption caractéristiques des blocs mPEG, notamment la bande d'absorption à 1110 cm^{-1} (vibrations stretching C—O—C) qui est attribué au groupement —OCH_2CH_2 des blocs mPEG et d'autre part des pics d'absorption à 1725 cm^{-1} du groupement ester C═O (vibrations stretching) caractéristique des blocs de PCL.

Pour apporter une preuve supplémentaire à la formation des copolymères et procéder, le cas échéant, au calcul des poids moléculaires des produits de synthèse, nous avons fait appel à la spectroscopie ^{1}H RMN. Le poids moléculaire des copolymères synthétisés a été calculé par intégration des pics de résonance caractéristiques dans les spectres ^{1}H RMN des copolymères. En outre, il a été trouvé que les valeurs déterminées à partir des spectres ^{1}H RMN étaient très

proches des valeurs théoriques calculées à partir des masses des réactifs introduits au départ dans le milieu réactionnel.

La SEC-MALLS à multi-détection permet, à l'aide d'un réfractomètre et un détecteur de diffusion de lumière multi-angle, une détermination absolue de la masse moléculaire sans calibration préalable de la colonne avec le polymère étudié. Cette technique a été utilisée pour vérifier les masses moléculaires pour les deux copolymères ayant les chaînes de PCL les plus longues, étant applicable pour les polymères dont le poids moléculaire est relativement haut. Les résultats trouvés étaient en corrélation avec ceux de la ^{1}H RMN. Par ailleurs, l'analyse de SEC a montré que les copolymères synthétisés avaient une distribution de masse étroite avec des valeurs d'indice de polydispersité comprise entre 1.10 et 1.45.

Les différents copolymères synthétisés et caractérisés ont été utilisés avec le PCL pour préparer des différents lots de microparticules en utilisant la méthode de double émulsion-évaporation de solvant. Il a été constaté que la composition du copolymère, précisément la longueur de blocs de PCL, influe sur la taille, l'efficacité d'encapsulation ainsi que sur les valeurs du potentiel zêta des microparticules obtenues.

Conformément à nos attentes, une efficacité d'encapsulation de plus en plus importante a été obtenue, suite à l'introduction des copolymères mPEG-PCL ayant des chaînes PCL de plus en plus longues. L'utilisation de mPEG 5K - PCL 7.4K dans la formulation a donné la plus grande efficacité d'encapsulation d'Ara-C (≈13%) et qui était 10 fois plus grande par rapport à celle des microparticules préparées à base de PCL seul (1.3%).

Par ailleurs, une augmentation de la taille des microparticules a été observée pour toutes les formulations préparées en utilisant les copolymères comparées aux microparticles à base du PCL seul. Et la taille des particules a augmenté avec l'augmentation de la longueur de la chaîne PCL dans le copolymère. Contrairement à la taille des particules, les valeurs du potentiel zêta des microparticules ont nettement baissées après l'introduction des copolymères dans la formulation, ce qui peut être attribué aux chaînes mPEG (neutres) qui tapissent la surface des particules. Ces résultats confirment notre hypothèse sur la contribution des copolymères à la formation de la matrice polymérique des particules.

En outre, les microparticules préparées en utilisant le mPEG 5K - PCL 7.4K ont montré un profil de libération d'Ara-C hyperbolique, avec une libération initiale brusque (*burst effect*) qui peut être attribuée aux molécules d'Ara-C déposées à proximité de la chevelure formée par les chaînes de PEG à la surface des particules.

Les compartiments aqueux internes et par conséquence la distribution de l'Ara-C à l'intérieur des microparticules, ont été visualisés grâce à la microscopie confocale à balayage laser (CLSM) et à l'utilisation d'une molécule hydrophile modèle fluorescente, la fluorescéine isothiocyanate-dextran. Selon les images de CLSM, les microparticules se sont avérées composées des vésicules aqueuses fluorescentes, distribuées d'une manière homogène à l'intérieur de la matrice polymérique, ce qui nous amène à en déduire que la méthode de double émulsion-évaporation de solvant est une technique adéquate pour séquestrer dans les microparticules, une partie de la phase aqueuse interne et par conséquence une partie de l'Ara-C qui y est dissoute.

Le dichlorométhane résiduel dans les particules a été dosé par chromatographie phase gazeuse (GC) afin de valider l'innocuité des microparticules. La quantité trouvée était bien au dessous du seuil fixé par la pharmacopée américaine et européenne. Par ailleurs, les résultats de DSC ont bien montré que l'Ara-C se trouve dans les particules sous forme amorphe, ce qui peut contribuer, entre autres, à sa libération rapide.

Les microparticules à base de PCL et mPEG-PCL semblent être des vecteurs prometteurs pouvant être convenablement chargées en Ara-C sans l'utilisation de monomères ou d'agents réticulants qui sont extrêmement toxiques et dont les traces persistent malgré les multiples étapes de lavage qui suivent la préparation des particules. Par ailleurs, les microparticules préparées avaient des tailles moyennes compatibles avec de nombreuses voies d'administration, comme la voie sous-cutanée, intratumorale, intra-péritonéale ou intramusculaire.

Toutefois, il serait intéressant de faire une étude de plan d'expérience (*screening*) pour optimiser les paramètres de formulation et ceux du procédé pour avoir une meilleure réponse en termes d'efficacité d'encapsulation et profil de libération, à savoir : la concentration du principe actif, la concentration du PVA, le volume de la phase aqueuse interne et celui de la phase aqueuse externe, et la concentration du PCL, la concentration du mPEG-PCL, les vitesses d'agitation en émulsification primaire et en émulsification secondaire...etc.

Une alternative aux polymères biodégradables, dans le souci de l'innocuité et la biocompatibilité du vecteur développé, est d'utiliser les liposomes. Les phospholipides, composés amphiphiles naturels, sont des matériaux potentiels pour l'encapsulation des petites molécules hydrophiles. Les liposomes étaient, donc, les seconds vecteurs testés pour la délivrance de l'Ara-C, ainsi qu'une molécule lipophile, le beclométhasone dipropionate BDP, ayant une action prophylactique reconnue de la carcinogenèse des poumons (Wattenberg *et al.*, 2000).

La méthode d'injection d'éthanol a été choisie pour préparer les liposomes. En effet, cette technique présente plusieurs avantages ; étant rapide, simple (effectuée en une seule étape) et reproductible (Sonar *et al.*, 2008). Le procédé de préparation a été étudié et les paramètres primordiaux du procédé ont été mis en évidence. Selon les résultats trouvés, la vitesse d'agitation de la phase aqueuse et la concentration de phospholipides dans la phase organique ont été les principaux paramètres affectant la taille des liposomes blancs (non chargées en principe actif).

L'Ara-C et le BDP ont bien été encapsulés dans des liposomes de petite taille en utilisant la méthode d'injection d'éthanol. Par ailleurs, la nanoprecipitation (modifiée) a été évaluée pour l'encapsulation de l'Ara-C. Les résultats obtenus indiquent que cette dernière n'améliore en rien les caractéristiques des liposomes (taille et efficacité d'encapsulation). En revanche, la méthode d'injection d'éthanol semble être plus adaptée à l'encapsulation des molécules hydrophiles, permettant d'atteindre une efficacité d'encapsulation plus élevée et une taille plus petite des vésicules. Une structure multi-lamellaire de la membrane des liposomes a été mise en évidence par la microscopie électronique à transmission, quelle que soit la méthode de préparation.

L'étude de libération in vitro a été effectuée sur plusieurs formulations dans lesquelles des masses différentes de cholestérol et de phospholipides ont été introduites. Les différents lots de liposomes chargés en Ara-C ont donné des profils de libération hyperbolique similaires, indépendamment de la formulation. Alors que des profils triphasiques de libération prolongée, ont été observés pour les liposomes chargés en BDP et ils étaient sensiblement différents selon le taux de cholestérol et de phospholipides utilisés dans la formulation.

Le test d'internalisation cellulaire a révélé que les liposomes fluorescents ont été bien internalisés dans le cytoplasme des cellules humaines du cancer broncho-pulmonaire SW-

1573, confirmant la pertinence des liposomes élaborés pour le ciblage des cellules pulmonaires et qui pourrait être d'un grand intérêt pour le traitement des métastases au niveau des poumons.

Par ailleurs, le test du comportement aérodynamique a montré une bonne aptitude des liposomes préparés à la nébulisation, étant donné les valeurs obtenus de l'efficacité de nébulisation (52% pour l'Ara-C et 43% pour le BDP). En outre, la possibilité d'utiliser les liposomes d'Ara-C et de BDP pour une administration pulmonaire profonde, a été confirmée, vu les résultats obtenus de la fraction respirable (FPF) (62% pour l'Ara-C et 55% pour le BDP) et le diamètre aérodynamique massique médian (MMAD) (3.9 µm pour l'Ara-C et 4.6 µm pour le BDP) pour les aérosols générés par ces liposomes.

En conclusion, la méthode d'injection d'éthanol a donné avec succès des liposomes d'une taille nanométrique, stables et avec des rendements d'encapsulation appropriés. Les liposomes élaborés semblent être des transporteurs prometteurs pour les deux principes actifs (l'Ara-C et le BDP) pour la voie pulmonaire.

Les vecteurs particulaires sont des candidats prometteurs pouvant remédier aux problèmes liés au grand volume de distribution des AN et le manque de sélectivité de ces agents anticancéreux. En revanche, pour faire face aux problèmes de résistance au traitement, notamment ceux qui sont en rapport avec des faibles concentrations d'enzymes de phosphorylation, une autre approche de la vectorisation semble être indispensable. La formation d'une prodrogue de la cytarabine capable de donner naissance à un analogue de la cytidine monophosphate au niveau intracellulaire s'avère une solution adéquate de ce type de résistance à la chimiothérapie par les AN.

Pour ce faire, l'équipe de Pr. Christian Périgaud a développé une prodrogue de la cytarabine monophosphate portant un groupement biolabile, le *t*Bu-*S*-acyl-thioethyl, protégeant le groupement phosphate, qu'on a appelé le bis(*t*butyl-*S*-acyl-2-thioethyl)-cytidine monophosphate (AraC-SATE) (Galmarini *et al.*, 2003). Cette prodrogue est active sur les cellules résistantes à l'Ara-C ayant un faible taux de déoxycytidine kinase (dCK) (Galmarini *et al.*, 2003), puisque la prodrogue est capable de libérer le groupement phosphate au niveau intracellulaire et donner naissance à la molécule monophosphorylée sans passer par la mono-phosphorylation catalysée par le dCK, étape primaire et décisive de l'activation des AN. De plus, contrairement à l'Ara-C, l'AraC-SATE résiste à la dégradation par les désaminases.

La faible solubilité aqueuse de la prodrogue peut, néanmoins, diminuer l'activité biologique in vivo en raison de sa précipitation dans les milieux biologiques et présente un obstacle à son utilisation clinique. Ainsi, pour modifier les propriétés physico-chimiques de cette prodrogue, nous avons fait appel à l'HP-*β*-CD.

Il s'agit d'un oligosaccharide cyclique semi-synthétique, composé de 7 molécules de glucose dont certains atomes d'hydrogène ont été substitués par des groupements hydroxypropyles pour augmenter la solubilité aqueuse de la molécule native (la *β*-cyclodextrine). La surface externe des ces composés est hydrophile puisqu'elle est tapissée par les groupements hydroxyles et hydroxypropyles. La cavité interne, composé par le squelette carbonique, est hydrophobe pouvant inclure des molécules hydrophobes, appelés « molécules invitées », pour former des complexes d'inclusion. La complexation entraîne l'augmentation de la solubilité, la stabilité et la biodisponibilité de la molécule incluse (Martin Del Valle, 2004).

Des preuves sur l'inclusion moléculaire de l'AraC-SATE, ont été apportées en utilisant deux techniques analytiques ; l'analyse thermique différentielle (*DSC*) et la résonance magnétique nucléaire du proton (^1H *NMR*). En effet, la première technique permet de visualiser et d'étudier tous les phénomènes température-dépendants qui peuvent avoir lieu pour un composé donné : fusion, évaporation, transition vitreuse, dégradation. Ces phénomènes dépendent étroitement de la structure moléculaire et en particulier des interactions intermoléculaires qui ont lieu au sein du composé. Dans les thermogrammes de l'HP-*β*-CD pur et l'AraC-SATE pur, un large pic endothermique qui correspond à la déshydratation des molécules de l'HP-*β*-CD et un pic trop étroit qui correspond à la fusion cristalline de l'AraC-SATE, ont été identifiés, respectivement. Par contre, dans le thermogramme du complexe d'inclusion, seul le pic de déshydratation de la cyclodextrine est apparu. La disparition du pic de fusion de l'AraC-SATE dans ce dernier, indique que l'AraC-SATE est dispersé à l'état amorphe dans une matrice constituée par les molécules de cyclodextrine.

En outre, la preuve directe de la formation du complexe d'inclusion a été apportée par la deuxième technique (^1H *NMR*). Cette technique fournit des informations sur la structure de la molécule et donne une idée sur l'environnement immédiat de chaque proton ou carbone. L'inclusion de la molécule invitée dans la cavité de la cyclodextrine est systématiquement accompagnée d'une variation des pics de résonance de plusieurs protons de cyclodextrine et

notamment les protons H3 et H5 qui sont orientés vers la cavité interne, en raison de l'anisotropie magnétique exercée par la molécule invitée. Ceci se traduit par une variation de la valeur du déplacement chimique de ces protons. Les spectres de résonnance magnétique de l'HP-*β*-CD et du complexe d'inclusion, ont bien montré une variation dans les valeurs du déplacement chimique pour les protons H3 et H5 du complexe par rapport à leurs valeurs initiales dans la cyclodextrine pure.

Le test de MTT de l'Ara-C, l'AraC-SATE et de son complexe d'inclusion à deux concentrations différentes en AraC-SATE 10 et 60 µM (pour voir l'effet de dilution) a été effectué sur deux lignées de cellules leucémiques murines: la lignée sauvage sensible au traitement (L1210) et la lignée résistante au traitement (L1210 10K). Nous avons trouvé que l'IC 50 (inhibiting cell growth by 50%) pour la prodrogue était 10 fois plus importante que celle de l'Ara-C pour la lignée sauvage, ce qui indique que la prodrogue est moins cytotoxique que l'Ara-C pour la lignée sauvage. En revanche, pour la lignée résistante, la prodrogue est apparue beaucoup plus cytotoxique que l'Ara-C, avec une valeur IC 50 nettement inférieure. Par ailleurs, aucune différence significative d'activité cytotoxique n'a été trouvée entre la prodrogue et son complexe d'inclusion, ce qui indique que le phénomène d'inclusion ne modifie pas l'activité cytotoxique de la prodrogue.

L'utilisation de l'HP-*β*-CD a permis de résoudre le problème de solubilité de la prodrogue sans affecter son activité cytotoxique. Cependant, il serait intéressant de tester d'autres types de vecteurs, comme les nanosphères et les nanocapsules, qui pourront permettre, en plus de l'amélioration de la solubilité apparente, de renforcer la protection de la prodrogue et probablement assurer sa libération intracellulaire. Malheureusement, la faible quantité, dont nous disposons, de la prodrogue ne nous a pas permis d'élaborer des nanoparticules de l'AraC-SATE.

Références

Ali, S. A., Zhong, S. P., Doherty, P. J. & Williams, D.F. (1993). Mechanisms of polymer degradation in implantable devices. I. Poly(caprolactone). *Biomaterials 14*: 648-56.

Diab, R., Degobert, G., Hamoudeh, M., Dumontet, C. & Fessi, H. (2007). Nucleoside analogue delivery systems in cancer therapy. *Expert opinion on drug delivery 4*: 513-31.

Galmarini, C. M., Mackey, J. & Dumontet, C. (2002 a). Nucleosides analogues and nucleobases in cancer treatment. *Lancet of Oncology 3*: 415 -424.

Galmarini, C. M., Thomas, X., Calvo, F., Rousselot, P., El Jafaari, A., Cros, E. & Dumontet, C. (2002 b). Potential mechanisms of resistance to cytarabine in AML patients. *Leukemia Research 26*: 621-629.

Galmarini, C., Clarke, M., Santos, C., Jordheim, L., Perigaud, C., Gosselin, G., Cros, E., Mackey, J. & Dumontet, C. (2003). Sensitization of ara-C-resistant lymphoma cells by a pronucleotide analogue. *International Journal of Cancer 107*: 149–154.

Mansson, E., Flordal, E., Liliemark, J., Spasokoukotskaja, T., Elford, H., Lagercrantz, S. & Albertioni, F. (2003). Down-regulation of deoxycytidine kinase in human leukemic cell lines resistant to cladribine and clofarabine and increased ribonucleotides reductases activity contributes to fludarabine resistance. *Biochemical Pharmacology 65*: 237-247.

Martin Del Valle, E. (2004). Cyclodextrins and their uses: a review. *Process Biochemistry 39*: 1033-46.

Sonar, S., D' Souza, S. E. & Mishra K P (2008). A simple one-step protocol for preparing small-sized doxorubicin-loaded liposomes. *Journal of environmental pathology, toxicology and oncology : official organ of the International Society for Environmental Toxicology and Cancer 27*: 181-9.

Song, X., Lorenzi, P. L., Landowski, C. P., Vig, B. S., Hilfinger, J. M. & Amidon, G.L. (2005). Amino acid ester prodrugs of the anticancer agent gemcitabine: synthesis,

Bioconversion, metabolic bioevasion, and hPEPT1-mediated transport. *Molecular Pharmaceutics 2*: 157-167.

Van Rompy, A. R., Johansson, M. & Karlsson, A. (2003). Substrate specificity and phosphorylation of antiviral and anticancer nucleosides analogues by human deoxyribonucleoside kinanses and ribonucleoside kinases. *Pharmacology and Therapeutics 100*: 119-139.

Wattenberg, L. W., Wiedmann, T. S., Estensen, R. D., Zimmerman, C. L., Galbraith, A. R., Steele, V. E. & Kelloff, G.J. (2000). Chemoprevention of pulmonary carcinogenesis by brief exposures to aerosolized budesonide or beclomethasone dipropionate and by the combination of aerosolized budesonide and dietary myo-inositol. *Carcinogenesis 21*: 179-82.

Conclusion générale et perspectives

Conclusion générale et perspectives

Nos travaux de thèse ont permis d'ouvrir la voie vers l'utilisation de trois types de vecteurs de l'Ara-C en chimiothérapie des cancers hématologiques et leurs métastases : les microparticules polymériques à base de PCL et mPEG-PCL, les liposomes multilamellaires et les complexes d'inclusion de la prodrogue de l'Ara-C, qui est active sur certaines lignées cellulaires résistantes à l'Ara-C, l'AraC-SATE.

Les microparticules d'Ara-C ont été préparées par la méthode de double émulsion pour éviter au maximum l'emploi de monomères ou d'agents réticulants qui sont généralement utilisés dans les techniques de préparation des microparticules chargées en principes actifs hydrophiles. Grâce à l'utilisation du copolymère mPEG 5K- PCL 7.4K, nous avons réussi à améliorer l'efficacité d'encapsulation de l'Ara-C d'un facteur de 10, comparée à celle des microparticules à base de PCL seul. Cependant, de meilleurs taux d'encapsulation de l'Ara-C peuvent être atteints, en optimisant les paramètres du procédé et la formulation. D'où la nécessité d'effectuer une étude de plan d'expérience « *factorial design* ». Par ailleurs, d'autres types de copolymères à blocs peuvent être testés pour l'élaboration des microparticules chargées en Ara-C, notamment le dibloc mPEG-PLGA et le tribloc PLGA-PEG-PLGA, qui peuvent donner des meilleurs taux d'encapsulation, ayant des blocs de PLGA dont le caractère hydrophile est supérieur à celui du PCL.

En ce qui concerne les liposomes à membrane multilamellaire chargées en Ara-C ou en BDP et préparées par la méthode d'injection d'éthanol, ces derniers ont montré des caractéristiques physico-chimiques satisfaisantes en termes de taille, d'efficacité d'encapsulation et de stabilité. Les liposomes élaborés semblent être des transporteurs prometteurs pour les deux principes actifs (l'Ara-C et le BDP) pour la voie pulmonaire, étant donné les valeurs obtenus de la FPF et le MMAD pour les aérosols générés par ces liposomes. L'association des deux vecteurs pourrait être d'un grand intérêt pour le traitement des métastases au niveau des poumons, étant donné l'action du BDP comme un agent anti-inflammatoire dans le traitement de la bronchorrhée provoquée par le cancer métastatique ou le cancer broncho-alvéolaire.

Enfin, la préparation des complexes d'inclusion de la prodrogue de l'Ara-C, l'AraC-SATE, en utilisant le HP-β-CD, a permis d'améliorer la solubilité apparente de la prodrogue

et par conséquence de pouvoir l'administrer *in vivo* à des concentrations adéquates, sans que l'inclusion dans la cyclodextrine affecte son activité cytotoxique. Par ailleurs, d'autres types de vecteurs seront intéressants à tester pour véhiculer l'AraC-SATE, comme les nanoparticules ou les liposomes. En effet, ces vecteurs pourront à la fois, améliorer la solubilité apparente de l'AraC-SATE, renforcer sa protection *in vitro et in vivo* et probablement assurer sa libération intracellulaire.

Résumé
Les analogues de nucléosides (AN), sont des agents importants dans le traitement d'hémopathies malignes et de certaines tumeurs solides. Le catabolisme rapide, la résistance cellulaire au traitement et le grand volume de distribution dans le corps limitent potentiellement l'efficacité thérapeutique des AN. Notre objectif est de concevoir un vecteur permettant un ciblage de ces molécules vers les tissus cancéreux, assurant son internalisation cellulaire et sa protection dans les milieux biologiques. Trois types de vecteurs de taille micronique, submicronique et moléculaire ont été élaborés et caractérisés : microparticules polymériques à base de poly(ε-caprolactone) (PCL), liposomes multilamellaires et complexes d'inclusion de la prodrogue de la cytarabine (Ara-C), qui est active sur certaines lignées cellulaires résistantes à l'Ara-C, l'AraC-SATE (bis(tbutyl-S-acyl-2-thioethyl)-cytidine monophosphate).
Les microparticules ont été préparées par la méthode de « double émulsion - évaporation de solvant » en utilisant comme surfactants des copolymères amphiphiles composés de blocs biodégradables de PCL et de blocs bio-éliminables de polyéthylène glycol (PEG). Une série de copolymères mPEG-PCL avec des blocs PCL de différents poids moléculaires a été synthétisée et l'effet de la longueur de chaînes de PCL sur les caractéristiques physico-chimiques des particules a été étudié. Une efficacité d'encapsulation satisfaisante a pu être obtenue, qui a été dix fois plus importante que celle des microparticules à base de PCL seul.
Les liposomes ont été préparés par la méthode d'injection d'éthanol. Une étude de formulation a été réalisée afin de sélectionner la formule permettant d'obtenir la meilleure efficacité d'encapsulation. Le test d'internalisation cellulaire et du comportement aérodynamique des liposomes nébulisés ont montré la pertinence des liposomes élaborés pour le ciblage des cellules pulmonaires qui pourrait être d'un grand intérêt pour le traitement des métastases au niveau des poumons.
L'encapsulation moléculaire de l'AraC-SATE dans l'hydroxyporpyl-β-cyclodextrine a été réalisée pour augmenter la solubilité apparente de la prodrogue. L'évaluation des complexes sur des cultures de cellules leucémiques murines a montré une activité cytotoxique comparable à celle de la prodrogue indiquant que l'inclusion moléculaire ne modifie pas l'activité biologique de la prodrogue.

Mots clés : *Cyclodextrines, complexes d'inclusion, cytarabine, liposomes, microparticules.*

Abstract
Nucleoside analogues (NA) are important agents in the treatment of haematological malignancies and solid tumours. Their rapid catabolism, cell resistance and overdistribution in the body jeopardize the NA chemotherapy. Our objective is to design a vector for these molecules targeting cancerous tissue and ensuring its cellular internalization and protection in the biological media. Micro-sized, nano-sized and molecular vectors were developed and characterized: polymeric microparticles of poly (ε-caprolactone) (PCL), multilamellar liposomes and inclusion complexes of the prodrug of cytarabine (Ara-C), which is active on some cell types resistant to treatment, the AraC-SATE (bis(tbutyl-S-acyl-2-thioethyl)-cytidine monophosphate).
The microparticles were prepared by the "double emulsion - solvent evaporation" method using as surfactants, amphiphilic copolymers consisting of biodegradable blocks (PCL) and bio-removable blocks (polyethylene glycol, PEG). A series of copolymers mPEG-PCL with PCL blocks of different molecular weights was synthesized and the effect of PCL chain length on the particle physico-chemical properties was studied. Satisfactory encapsulation efficiency could be obtained, which was 10 times greater than that of microparticles prepared with PCL alone.
Liposomes were prepared by the ethanol injection method. A formulation study was conducted in order to select the formula having the optimal encapsulation efficiency. Investigations about the cell internalization and the aerodynamic behaviour of the nebulized liposomes showed the relevance of developed liposomes for targeting lung cells that could be of great interest for the treatment of metastases in the lungs.
The molecular encapsulation of the AraC-SATE in the hydroxyporpyl-β-cyclodextrin was carried out in order to increase the apparent solubility of the prodrug. The evaluation of inclusion complexes on murine leukemic cell cultures showed a cytotoxic activity comparable to that of the prodrug indicating that the molecular inclusion does not alter the biological activity of the prodrug.

Key words: *Cyclodextrins, cytarabine, inclusion complexes, liposomes, microparticles.*

DISCIPLINE: PHARMACIE GALÉNIQUE ET PHARMACOTECHNIE

Laboratoire d'Automatique et de Génie des Procédés (LAGEP), UMR CNRS 5007,
Université Claude Bernard Lyon 1,
43 bd du 11 Novembre 1918, 69622 Villeurbanne cedex, France